

**DEVELOPMENT OF NANOPARTICLES AND FILMS
OF POLYHYDROXYALKANOATES FROM
MARINE BACTERIA**

Thesis submitted to
Cochin University of Science and Technology
in Partial Fulfilment of the Requirements for
the Award of the Degree of
Doctor of Philosophy
in
Environmental Microbiology and Biotechnology
Under the Faculty of Environmental Studies

By

Sowmya P Mohandas

Reg. No. 4954



National Centre for Aquatic Animal Health
Cochin University of Science and Technology
Kochi 682016, Kerala, India

September 2019

Development of nanoparticles and films of polyhydroxyalkanoates from marine bacteria

Ph.D. Thesis under the Faculty of Environmental Studies

Author

Sowmya P Mohandas
Research Scholar
National Centre for Aquatic Animal Health
School of Environmental Studies
Cochin University of Science and Technology
Kerala, India

Supervising Guide

Prof. (Dr) I.S. Bright Singh, FNAAS
KSCSTE Emeritus Scientist
National Centre for Aquatic Animal Health
Cochin University of Science and Technology
Kerala, India.

National Centre for Aquatic Animal Health
Cochin University of Science and Technology
Kochi – 682016, Kerala, India

September 2019

**NATIONAL CENTRE FOR AQUATIC ANIMAL HEALTH
COCHIN UNIVERSITY OF SCIENCE AND TECHNOLOGY**

Prof. (Dr) I. S. Bright Singh, FNAAS
KSCSTE Emeritus Scientist

Lakeside Campus, Fine Arts Avenue
Kochi-682016, Kerala, India

Certificate

This is to certify that research work presented in the thesis entitled **“Development of nanoparticles and films of polyhydroxyalkanoates from marine bacteria”** is an authentic record of research work carried out by **Ms. Sowmya P Mohandas** under my guidance at National Centre for Aquatic Animal Health, Cochin University of Science and Technology, Cochin- 682016, in partial fulfillment of the requirements for the Degree of Doctor of Philosophy and that no part of this work has previously formed the basis for the award of any degree, diploma, associateship, fellowship or any other similar title or recognition. All the relevant corrections and modifications suggested by the audience and recommended by the doctoral committee of the candidate during the pre-synopsis seminar have been incorporated in the thesis.

Kochi - 682016
September 2019

Prof. (Dr) I. S. Bright Singh
(Supervising Guide)

Declaration

I hereby do declare that the work presented in this thesis entitled **“Development of nanoparticles and films of polyhydroxyalkanoates from marine bacteria”** is based on the original work done by me under the guidance of Dr. I. S. Bright Singh, KSCSTE Emeritus Scientist, National Centre for Aquatic Animal Health, Cochin University of Science and Technology, Kochi- 682016, in partial fulfillment of the requirements for the award of the Degree of Doctor of Philosophy and that no part of this work has previously formed the basis for the award of any degree, diploma, associateship, fellowship or any other similar title or recognition.

Kochi - 682016
September 2019

Sowmya P Mohandas

Acknowledgement

I would like to gratefully acknowledge all those who have motivated, encouraged and supported me throughout this wonderful journey.

First and foremost, I want to express my heartfelt gratitude and deep regards to my supervising guide Prof. (Dr) I.S. Bright Singh, FNAAS, KSCSTE Emeritus Scientist, for his time, immense support, scientific guidance, thoughtful discussions and encouragement throughout my research. I owe him a lot for his patience, contributions and fatherly care that helped me during the work. He has always given me freedom to work independently and helped me publish manuscripts from time to time. It would have not been possible to complete this work without his continuous inspiration.

I gratefully acknowledge my subject expert Dr. T. P. Sajeewan, Assistant Professor, National Centre for Aquatic Animal Health, for his immense support and valuable suggestions during my research.

I convey my sincere thanks to Dr. Valsamma Joseph, Director, National Centre for Aquatic Animal Health for her good advice and constant encouragement throughout the period of work.

I take this occasion to express my thanks to Prof. (Dr) Mohandas, Emeritus Scientist, for his kind support, motivation and critical views during my research time.

I owe deep gratitude to Prof. (Dr). Rosamma Philip, UGC-BSR Faculty, Department of Marine Biology, Microbiology and Biochemistry for her supervision, love and care during my research work.

I thankfully acknowledge Dr. Sivanandan Achari, Director, School of Environmental Studies and all other esteemed faculty members for their crucial suggestions and assistance offered.

I would like to thank the administrative staff of School of Environmental Studies and Mr. Jaison Joseph, Assistant Section Officer of NCAAH for their timely support and cooperation.

I gratefully acknowledge the financial support from the Ministry of Earth Sciences, Government of India, through the project MoES/CMLRE/10-MLR-TD/09/2012 dated 09/10/2012 "Polyhydroxybutyrate from marine microorganisms for biomedical and aquaculture applications". I thank Cochin University of Science and Technology for providing me the UJRF fellowship. I also thank the Department of Science and Technology, Government of India, for providing the Purse fellowship.

My special gratitude and appreciation to Mr. Linu Balan, my research partner who always supported and helped me in my work. I thank him for spending his valuable time for scientific discussions and encouraging and criticizing me during my research.

I am indebted to my NCAAH colleagues Mr. Boobal R, Ms. Lekshmi N, Dr. Sanyo Sabu, Ms. Jisha Kumaran, Dr. Dhaneesha Mohandas, Ms. Deepa G, Ms. Ramya R Nair, Dr. Preena P G, Ms. Ajitha, Mr. Anoop B S, Mr. Devassy Christo, Ms. Indira, Dr. Asha P, Ms. Limmy T P, Ms. Vinusree K P, Dr. Salini S, Dr. Arun Augustine, Ms. Krishna Priya, Ms. Pramada Prasad, Ms. Merlin T P and Mr. Umar for their true friendship, love and support.

Sincere thanks to all my beloved seniors Dr. Jayesh. P, who is currently working as Assistant Professor, NCAAH, Ms. Deepa G D, Dr. Riya George, Dr. Vrinda Sukumaran, Dr. Sunitha Poullose, Dr. Rose Mary Jose, Dr. Haseeb, Dr. Prem Gopinath, Dr. Ammu Thomas, Dr. Sareen Sara John, Dr. Priyaja and Dr. Sudheer N S, for their advices and wholehearted support.

I express my thanks to Dr. Gopalakrishnan Menon, DSK-PDF, for his generous care, advice and encouragement given to me all the time.

I wish to extend my warm regards to the new members of NCAAH Ms. Ahna, Ms. Gopika, Ms. Saranya, Ms. Sreevidya, Ms. Thasreefa, Mr. Kannan and Ms. Soumya Balakrishnan for their assistance and friendship.

I deeply appreciate all NCAAH staffs, Mr. Soman, Mrs. Surya, Mrs. Blessy Jose, Kusumam chechi and Parisa chechi who always helped and supported me during the research.

I am extremely thankful to Ms. Bhavya K, Ms. Manomi Sarasan, Mr. Solly Solomon, Dr. Sruthy K.S, Dr. Aishwarya Nair, Dr. Neema Job, Ms. Anju M V, Ms. Dhanya Keshavan and Dr. Ramya K D, Department of Marine Biology, Microbiology and Biochemistry, CUSAT, for their assistance and valuable suggestions.

I also express my thanks to STIC – CUSAT, Department of Applied Chemistry, CUSAT, Sree Chitra Tirunal Institute for Medical Sciences and Technology, Thiruvananthapuram and All India Institute of Medical Sciences, Delhi for the great help provided in the structural analyses of the polymer and microscopic examinations of bacteria.

I take this opportunity to acknowledge Prof. Sabu Thomas, Vice-Chancellor and Founder Director, International and Inter University Centre for Nanoscience and Nanotechnology (IIUCNN), Mahatma Gandhi University, Kottayam for the help provided in the characterisation of the polymer films and nanoparticles.

And most of all, I thank my father, mother and my brother for their support, patience and trust that helped me to pursue my dreams. My father always provided persistent inspiration for my journey in this life. My mother has always prayed for getting good results in my studies and research work. On this occasion I remember my grandparents for their love, care and support. I deeply thank my family for their unconditional love and sacrifices during this period. I am blessed to have them in my life and dedicate my thesis to them.

I have no words to express my gratitude to my life partner, Mr. Jayanath G, who has supported me all through my research. His patience and caring has helped me during the hard times of my research. His words showered immense strength and confidence for me during my lifetime. On this occasion, I would also thank my little daughter, Srinika, who was just 3 months when I started writing my thesis. Special thanks to my mother-in-law for being so loving and helping for carrying out my research.

I thank you all from the bottom of my heart.

Soumya P Mohandas

Contents

Chapter 1

| | |
|--|----------------|
| GENERAL INTRODUCTION..... | 01 - 45 |
| 1.1 Biodegradable polymers | 01 |
| 1.2 Polyhydroxyalkanoates | 03 |
| 1.2.1 Structure of PHA..... | 05 |
| 1.2.2 Properties of PHA | 08 |
| 1.3 PHA biosynthetic pathway | 09 |
| 1.4 Microbial fermentation of PHA | 14 |
| 1.5 PHA production in marine bacteria..... | 18 |
| 1.6 PHA production from renewable sources..... | 19 |
| 1.7 Statistical designs for PHA optimization | 22 |
| 1.8 Downstream processing | 23 |
| 1.8.1 Solvent extraction..... | 23 |
| 1.8.2 Chemical digestion..... | 25 |
| 1.8.3 Enzymatic digestion | 27 |
| 1.8.4 Mechanical disruption..... | 27 |
| 1.8.5 Supercritical fluids | 28 |
| 1.8.6 Cell fragility | 28 |
| 1.8.7 Aqueous two phase system | 29 |
| 1.9 PHA market | 29 |
| 1.10 Applications of PHAs..... | 32 |
| 1.10.1 Drug carriers..... | 32 |
| 1.10.2 Tissue engineering..... | 35 |
| 1.10.3 Medical devices..... | 38 |
| 1.10.4 Aquaculture applications..... | 40 |
| 1.11 Future perspective..... | 44 |
| 1.12 Objectives of the study..... | 45 |

Chapter 2

| | |
|---|----------------|
| ISOLATION, SCREENING AND IDENTIFICATION OF POLYHYDROXYALKANOATE PRODUCING BACTERIA FROM MARINE ENVIRONMENTS..... | 47 - 72 |
| 2.1 Introduction..... | 47 |
| 2.2 Materials and methods | 51 |
| 2.2.1 Sample collection | 51 |
| 2.2.2 Isolation and sub-culturing of bacteria from marine environment..... | 52 |
| 2.2.3 Screening of PHA producing bacteria..... | 52 |

| | | |
|-----------|---|----|
| 2.2.3.1 | <i>Nile red fluorescence assay</i> | 52 |
| 2.2.3.2 | <i>Nile red staining</i> | 54 |
| 2.2.4 | PHA production | 54 |
| 2.2.5 | PHA estimation | 55 |
| 2.2.6 | Identification of PHA producing bacteria | 55 |
| 2.2.6.1 | <i>Biochemical characterization</i> | 55 |
| 2.2.6.2 | <i>16S rRNA gene sequencing</i> | 59 |
| 2.2.6.2.1 | <i>Genomic DNA extraction</i> | 59 |
| 2.2.6.2.2 | <i>PCR amplification of genomic DNA</i> | 60 |
| 2.2.6.2.3 | <i>DNA sequencing and phylogenetic analysis</i> | 61 |
| 2.2.7 | Bacterial growth curve of selected isolates | 61 |
| 2.3 | Results and discussion..... | 62 |
| 2.3.1 | Isolation and screening of PHA producing bacteria..... | 62 |
| 2.3.2 | PHA production | 63 |
| 2.3.3 | Biochemical characterization | 64 |
| 2.3.4 | Identification of bacteria by 16S rRNA gene sequencing and Phylogenetic analysis | 66 |
| 2.3.5 | Bacterial growth curve of selected isolates | 71 |
| 2.4 | Conclusion | 72 |

Chapter 3

PRODUCTION AND CHARACTERIZATION OF POLYHYDROXYBUTYRATE FROM *VIBRIO HARVEYI* MCCB 284 UTILISING GLYCEROL AS CARBON SOURCE 73 - 102

| | | |
|---------|--|----|
| 3.1 | Introduction..... | 73 |
| 3.2 | Materials and methods | 77 |
| 3.2.1 | PHB production | 77 |
| 3.2.2 | Transmission Electron Microscopy | 78 |
| 3.2.3 | Optimization for PHB production..... | 79 |
| 3.2.4 | PHB extraction..... | 79 |
| 3.2.5 | Polymer characterization..... | 80 |
| 3.2.5.1 | <i>FTIR</i> | 80 |
| 3.2.5.2 | <i>DSC</i> | 80 |
| 3.2.5.3 | <i>TGA</i> | 80 |
| 3.2.5.4 | <i>NMR</i> | 81 |
| 3.2.5.5 | <i>GPC</i> | 81 |
| 3.2.6 | Statistical analysis | 82 |
| 3.3 | Results and discussion..... | 82 |
| 3.3.1 | PHB production | 82 |
| 3.3.2 | TEM | 83 |
| 3.3.3 | Optimization of PHB production | 84 |
| 3.3.3.1 | <i>Effect of initial pH</i> | 84 |

| | | |
|---------|--|-----|
| 3.3.3.2 | <i>Effect of sodium chloride concentration</i> | 84 |
| 3.3.3.3 | <i>Effect of carbon sources</i> | 86 |
| 3.3.3.4 | <i>Effect of incubation time</i> | 89 |
| 3.3.3.5 | <i>Effect of inoculum size</i> | 91 |
| 3.3.3.6 | <i>Effect of temperature</i> | 92 |
| 3.3.4 | Polymer characterization..... | 93 |
| 3.3.4.1 | <i>FTIR</i> | 93 |
| 3.3.4.2 | <i>DSC</i> | 95 |
| 3.3.4.3 | <i>TGA</i> | 96 |
| 3.3.4.4 | <i>NMR</i> | 97 |
| 3.3.4.5 | <i>GPC</i> | 100 |
| 3.4 | Conclusion | 102 |

Chapter 4

BIOSYNTHESIS AND CHARACTERIZATION OF POLYHYDROXYALKANOATE FROM MARINE BACILLUS CEREUS MCCB 281 UTILISING GLYCEROL

AS CARBON SOURCE 103 -143

| | | |
|---------|--|-----|
| 4.1 | Introduction..... | 103 |
| 4.2 | Materials and methods | 107 |
| 4.2.1 | PHA production and quantification..... | 107 |
| 4.2.2 | Identification of phaC gene | 108 |
| 4.2.3 | Transmission Electron Microscopy | 109 |
| 4.2.4 | Effect of initial pH, temperature and substrates on PHA production | 109 |
| 4.2.5 | Statistical optimization of PHA production | 110 |
| 4.2.5.1 | <i>Plackett-Burman design for screening of significant variables</i> | 110 |
| 4.2.5.2 | <i>Response Surface Methodology</i> | 111 |
| 4.2.5.3 | <i>Validation of the model</i> | 112 |
| 4.2.6 | Fermenter level production | 112 |
| 4.2.7 | PHA extraction..... | 112 |
| 4.2.8 | Polymer characterization..... | 112 |
| 4.2.8.1 | <i>FTIR</i> | 112 |
| 4.2.8.2 | <i>XRD</i> | 113 |
| 4.2.8.3 | <i>GC-MS</i> | 113 |
| 4.2.8.4 | <i>NMR</i> | 114 |
| 4.2.8.5 | <i>GPC</i> | 114 |
| 4.3 | Results and discussion..... | 114 |
| 4.3.1 | PHA production | 114 |
| 4.3.2 | Identification of phaC gene | 115 |

| | | |
|-------|--|-----|
| 4.3.3 | TEM | 118 |
| 4.3.4 | Effect of initial pH, temperature and substrates on PHA production | 118 |
| | 4.3.4.1 <i>Effect of initial pH</i> | 119 |
| | 4.3.4.2 <i>Effect of temperature</i> | 119 |
| | 4.3.4.3 <i>Effect of carbon sources</i> | 120 |
| | 4.3.4.4 <i>Effect of precursor</i> | 122 |
| 4.3.5 | Statistical optimization of PHA production | 123 |
| | 4.3.5.1 <i>Plackett-Burman design for screening of significant variables</i> | 123 |
| | 4.3.5.2 <i>Response Surface Methodology</i> | 125 |
| | 4.3.5.3 <i>Validation of the model</i> | 133 |
| 4.3.6 | Fermenter level studies..... | 134 |
| 4.3.7 | Polymer characterization | 135 |
| | 4.3.7.1 <i>FTIR</i> | 135 |
| | 4.3.7.2 <i>XRD</i> | 135 |
| | 4.3.7.3 <i>GC-MS</i> | 137 |
| | 4.3.7.4 <i>NMR</i> | 138 |
| | 4.3.7.5 <i>GPC</i> | 142 |
| 4.4 | Conclusion | 143 |

Chapter 5

BIOCOMPATIBILITY OF POLYHYDROXYBUTYRATE- CO-HYDROXYVALERATE FROM *BACILLUS CEREUS*

| | | |
|--|---|-----|
| MCCB 281 FOR MEDICAL APPLICATIONS | 145 - 175 | |
| 5.1 | Introduction..... | 145 |
| 5.2 | Materials and methods | 150 |
| | 5.2.1 Nanoparticle synthesis and characterization | 151 |
| | 5.2.2 <i>In vitro</i> biocompatibility assay..... | 152 |
| | 5.2.3 Film synthesis and characterization | 153 |
| | 5.2.4 Cell proliferation | 155 |
| | 5.2.5 Cell staining | 156 |
| | 5.2.6 Haemocompatibility studies | 156 |
| | 5.2.7 Statistical analysis | 157 |
| 5.3 | Results and discussion..... | 157 |
| | 5.3.1 Nanoparticle synthesis and characterization | 157 |
| | 5.3.2 Biocompatibility of nanoparticles | 161 |
| | 5.3.3 Film synthesis and characterization | 162 |
| | 5.3.4 Cell attachment and proliferation | 168 |
| | 5.3.5 Haemocompatibility studies | 171 |
| 5.4 | Conclusion | 174 |

Chapter 6

| | |
|---|------------------|
| SUMMARY AND CONCLUSION..... | 177 - 186 |
| References | 187 - 226 |
| GenBank Submission | 227 - 230 |
| List of Publications | 231 - 232 |
| Reprint of Paper Published | 233 - 255 |

List of Tables

| | | |
|-----------|--|-----|
| Table 1.1 | Range of typical properties of PHAs | 09 |
| Table 1.2 | Enzymes involved in the various biosynthetic pathways for PHA production..... | 13 |
| Table 1.3 | Batch fermentation for PHA production | 15 |
| Table 1.4 | Fed-batch fermentation for PHA production | 16 |
| Table 1.5 | Continuous fermentation for PHA production..... | 17 |
| Table 1.6 | Some of the pilot and industrial scale PHA manufacturers currently active worldwide | 31 |
| Table 2.1 | The details of sampling location along the southwest coast of India..... | 53 |
| Table 2.2 | PHA production based on cell dry weight from different bacterial isolates obtained from tunicates and water samples..... | 64 |
| Table 2.3 | Biochemical tests of the selected PHA producing bacterial isolates..... | 65 |
| Table 2.4 | Identification of PHA producers isolated from tunicate and water samples | 68 |
| Table 4.1 | Range of independent variables selected for Plackett-Burman design for PHA production | 110 |
| Table 4.2 | Range of independent variables selected for the response surface central composite design for PHA production | 111 |
| Table 4.3 | Effect of different concentrations of propionic acid on PHA production | 123 |
| Table 4.4 | Results of the experimental Plackett - Burman design for PHA production from <i>B. cereus</i> MCCB 281 | 124 |
| Table 4.5 | ANOVA for cell dry weight and PHA yield of selected factorial model under Plackett-Burman design..... | 125 |
| Table 4.6 | Results of central composite design for PHA production from <i>B. cereus</i> MCCB 281 | 126 |
| Table 4.7 | ANOVA for response surface model of cell dry weight from <i>B. cereus</i> MCCB 281 | 127 |

| | | |
|-----------|---|-----|
| Table 4.8 | ANOVA for response surface model of PHA yield from <i>B. cereus</i> MCCB 281 | 130 |
| Table 5.1 | Static contact angle and surface free energy measurements of PHBV and PHB films | 163 |
| Table 5.2 | Surface roughness of PHBV and PHB films | 165 |
| Table 5.3 | Thermal properties of PHBV and PHB films | 166 |
| Table 5.4 | Mechanical properties of PHBV and PHB films | 168 |
| Table 5.5 | Blood coagulation analysis of PHBV and PHB films..... | 174 |

List of Figures

| | | |
|------------|---|----|
| Figure 1.1 | Classification of biodegradable polymers..... | 02 |
| Figure 1.2 | General structure of PHAs (R1/R2 = alkyl groups C ₁ -C ₁₃ , x=1-4, n=100-30,000) | 04 |
| Figure 1.3 | Chemical structure of PHAs, PHB: poly(3- hydroxybutyrate); PHBV: poly(3-hydroxybutyrate-co-3- hydroxyvalerate); P3HB4HB: poly(3-hydroxybutyrate- co-4-hydroxybutyrate); PHO: poly(3-hydroxyoctanoate); PHBHHx: poly(3-hydroxybutyrate-co-3- hydroxyhexanoate) | 05 |
| Figure 1.4 | Structure of PHA granule..... | 07 |
| Figure 1.5 | Biosynthetic pathways for PHA production in different species of bacteria. Numbers representing detailed enzymes (or genes) involved in the PHA synthesis are tabulated in Table 1.2 | 11 |
| Figure 2.1 | (a) Fluorescence of PHA producing bacteria in ZoBell's marine agar supplemented with Nile red dye and glucose as carbon source during primary screening (b) Secondary screening of PHA producing bacteria by Nile red staining..... | 62 |
| Figure 2.2 | Genomic DNA isolated from PHA producing bacteria according to Cheng and Jiang method. Lane 2- 1 kb DNA ladder; Lane 1, 3 to 11- genomic DNA of isolates..... | 67 |
| Figure 2.3 | PCR product of 16S rRNA gene amplified using universal primers. Lane 3- 1 kb DNA ladder; Lane 1, 2, 4 to 7- 1500 bp size PCR product | 67 |
| Figure 2.4 | Phylogenetic analysis of (a) <i>V. harveyi</i> MCCB 284 (b) <i>B. cereus</i> MCCB 281 with its closely related species based on 16S rRNA gene sequences. The tree was constructed with MEGA 6.0 software using Neighbour- joining method. The evolutionary distance was computed using the Kimura 2- parameter method. Bootstrap values indicated at the nodes..... | 70 |
| Figure 2.5 | Growth curve of <i>V. harveyi</i> MCCB 284. Data shown are mean standard deviations of triplicate | 71 |

| | | |
|-------------|---|----|
| Figure 2.6 | Growth curve of <i>B. cereus</i> MCCB 281. Data shown are mean standard deviations of triplicate..... | 71 |
| Figure 3.1 | TEM of <i>V. harveyi</i> showing the presence of PHA granules | 83 |
| Figure 3.2 | Effect of pH on the growth and PHB production of <i>V. harveyi</i> MCCB 284 using glucose 20 g L ⁻¹ as carbon source. Data shown are mean standard deviations of triplicate..... | 85 |
| Figure 3.3 | Effect of sodium chloride concentration on the growth and PHB production of <i>V. harveyi</i> MCCB 284 using glucose 20 g L ⁻¹ as carbon source. Data shown are mean standard deviations of triplicate..... | 86 |
| Figure 3.4 | Effect of different carbon sources on the growth and PHB production of <i>V. harveyi</i> MCCB 284 after 72 h incubation at 28°C and 150 rpm. Data shown are mean standard deviations of triplicate | 88 |
| Figure 3.5 | Effect of different concentration of glycerol on the growth and PHB production of <i>V.harveyi</i> MCCB 284. Data shown are mean standard deviations of triplicate..... | 88 |
| Figure 3.6 | Effect of incubation time on growth and PHB production of <i>V. harveyi</i> MCCB 284 with glycerol 20 g L ⁻¹ as carbon source. Data shown are mean standard deviations of triplicate..... | 90 |
| Figure 3.7 | Effect of initial inoculum size on the growth and PHB production of <i>V. harveyi</i> MCCB 284 after 72 h incubation at 28 °C and 150 rpm. Glycerol 20 g L ⁻¹ was used as carbon source. Data shown are mean standard deviations of triplicate. | 91 |
| Figure 3.8 | Effect of incubation temperature on the growth and PHB production of <i>V. harveyi</i> MCCB 284. Glycerol 20 g L ⁻¹ was used as carbon source. Data shown are mean standard deviations of triplicate..... | 93 |
| Figure 3.9 | Infrared spectra of (A) purified polymer from <i>V. harveyi</i> MCCB 284; (B) commercial PHB..... | 94 |
| Figure 3.10 | Differential scanning calorimetry curve of polymer extracted from <i>V. harveyi</i> MCCB 284 | 95 |
| Figure 3.11 | Thermogravimetric (TGA - DTG) plot of PHB obtained from <i>V. harveyi</i> MCCB 284 | 97 |

| | | |
|-------------|--|-----|
| Figure 3.12 | ¹ H Nuclear magnetic resonance spectra of (A) purified polymer from <i>V. harveyi</i> MCCB 284; (B) commercial PHB..... | 99 |
| Figure 3.13 | ¹³ C Nuclear magnetic resonance spectra of (A) purified polymer from <i>V. harveyi</i> MCCB 284; (B) commercial PHB..... | 101 |
| Figure 3.14 | Gel permeation chromatogram of purified polymer produced by <i>V. harveyi</i> MCCB 284..... | 102 |
| Figure 4.1 | PCR amplification of <i>phaC</i> synthase gene of <i>B. cereus</i> MCCB 281 using gene specific primers. Lane 1- 100 bp DNA ladder; Lane 2, 3- 750 bp amplified product..... | 115 |
| Figure 4.2 | Phylogenetic tree of <i>pha C</i> synthase gene of <i>B. cereus</i> MCCB 281 with its closely related species based on amino acid sequences from GenBank. Bootstrap values are denoted at the nodes. | 116 |
| Figure 4.3 | Multiple sequence alignment of amino acid sequences of <i>phaC</i> gene of <i>B. cereus</i> MCCB 281 with other related species obtained from NCBI database | 117 |
| Figure 4.4 | TEM of <i>B. cereus</i> MCCB 281 showing the presence of PHA granules..... | 118 |
| Figure 4.5 | Effect of pH on PHA production in <i>B. cereus</i> MCCB 281 using glucose 20 g L ⁻¹ as carbon source. Data shown are mean standard deviations of triplicate | 119 |
| Figure 4.6 | Effect of temperature on PHA production in <i>B. cereus</i> MCCB 281 using glucose 20 g L ⁻¹ as carbon source. Data shown are mean standard deviations of triplicate..... | 120 |
| Figure 4.7 | Effect of carbon sources on PHA production in <i>B. cereus</i> MCCB 281. Data shown are mean standard deviations of triplicate..... | 121 |
| Figure 4.8 | Response surface 3D plots showing interactive effect of process variables for cell dry weight (a) salt concentration and glycerol (b) salt concentration and incubation time (c) glycerol and inoculum size (d) inoculum size and incubation time on PHA production from <i>B. cereus</i> MCCB 281 | 129 |

| | | |
|-------------|---|-----|
| Figure 4.9 | Response surface 3D plots showing interactive effect of process variables for PHA yield (a) glycerol and inoculum size (b) inoculum size and incubation time on PHA production from <i>B. cereus</i> MCCB 281 | 132 |
| Figure 4.10 | Scale up of PHA production in 5L fermenter in the optimized culture conditions..... | 134 |
| Figure 4.11 | FTIR spectra of (a) purified polymer from <i>B. cereus</i> MCCB 281; (b) commercial PHBV (12mol% 3-HV) | 136 |
| Figure 4.12 | X-ray diffraction pattern of PHA produced by MCCB 281 and commercial PHBV (12mol% 3-HV)..... | 137 |
| Figure 4.13 | GC-MS spectrum of purified PHA produced by MCCB 281 | 138 |
| Figure 4.14 | ¹ H NMR spectra of (a) purified polymer from MCCB 281; (b) commercial PHBV (12mol% 3-HV); ¹³ C NMR spectra of (c) purified polymer from MCCB 281; (d) commercial PHBV (12mol% 3-HV)..... | 141 |
| Figure 4.15 | Gel permeation chromatogram of purified polymer produced by <i>B. cereus</i> MCCB 281 | 142 |
| Figure 5.1 | Particle size micrograph of PHBV nanoparticles produced using oil-in-water-emulsion technique..... | 159 |
| Figure 5.2 | Zeta potential micrograph of PHBV nanoparticles produced using oil-in-water-emulsion technique | 159 |
| Figure 5.3 | Transmission electron micrograph of PHBV nanoparticles | 160 |
| Figure 5.4 | Scanning electron micrograph of PHBV nanoparticles | 160 |
| Figure 5.5 | Cytotoxicity results of MTT assay with PHBV nanoparticles using L929 mouse fibroblast cells. Data shown as mean ± SD (n=6)..... | 161 |
| Figure 5.6 | Film synthesis using solvent casting method..... | 162 |
| Figure 5.7 | Scanning electron micrograph of (a) PHBV, (b) PHB film obtained by solvent casting technique..... | 162 |
| Figure 5.8 | Water contact angle images of (a) PHBV (b) PHB films | 164 |
| Figure 5.9 | Atomic force micrograph of rough surface of (a) PHBV (b) PHB films | 165 |

| | | |
|-------------|--|-----|
| Figure 5.10 | TGA thermograms of (a) PHBV and (b) PHB films | 167 |
| Figure 5.11 | Cell viability of L929 cells grown on PHB and PHBV films after 48 h incubation at 37 °C. Cells grown on tissue culture plate (without film) were used as 100 % control. Data shown as mean ± SD (n=4)..... | 169 |
| Figure 5.12 | Scanning electron micrograph of morphology of L929 cells adhered to (a) PHBV (b) PHB film surface after 48 h incubation at 37 °C. | 170 |
| Figure 5.13 | Microscopic images of L929 cells on (a) PHBV and (c) PHB films after 48 h incubation. Fluorescent microscopic images of L929 cells after staining with Hoechst 33258 dye on (b) PHBV and (d) PHB films after 48 h incubation | 170 |
| Figure 5.14 | Haemolysis assay of polymer films (a) positive control (b) negative control (c) PHBV film (d) PHB film..... | 172 |
| Figure 5.15 | Scanning electron micrograph of morphology of platelets adhered to (a) PHBV (b) PHB film surface after incubation with PRP for 2 h at 37 °C | 173 |

GENERAL INTRODUCTION

| | | |
|------------------------|------|---|
| <i>C o n t e n t s</i> | 1.1 | <i>Biodegradable polymers</i> |
| | 1.2 | <i>Polyhydroxyalkanoates</i> |
| | 1.3 | <i>PHA biosynthetic pathway</i> |
| | 1.4 | <i>Microbial Fermentation of PHA</i> |
| | 1.5 | <i>PHA production in marine bacteria</i> |
| | 1.6 | <i>PHA production from renewable sources</i> |
| | 1.7 | <i>Statistical designs for PHA optimization</i> |
| | 1.8 | <i>Downstream processing</i> |
| | 1.9 | <i>PHA market</i> |
| | 1.10 | <i>Applications of PHAs</i> |
| | 1.11 | <i>Future perspective</i> |
| | 1.12 | <i>Objectives of the study</i> |

1.1 Biodegradable polymers

Biodegradable polymers are polymers recycled naturally by biological processes of bacteria or other living organisms to carbon dioxide, methane, water and biomass. These are non-toxic polymers produced from renewable resources such as sugarcane bagasse, corn sugar, vegetable oils, coconut pulp, cane molasses, whey, ligno-cellulosic biomass, oil palm etc. The carbon flux during synthesis and degradation of these polymers are balanced and thus, do not contribute to global warming. Biodegradable polymers are mainly divided into three

categories (Fig. 1.1); bio-polyesters from renewable sources such as polyhydroxyalkanoates (PHAs), poly lactic acid (PLA), polyglycolic acid (PGA), synthetic materials that are biodegradable or compostable such as polybutylene adipate terephthalate (PBAT), poly ϵ -caprolactone (PCL) and biomass products based polymers (cellulose, starch, chitosan, modified natural polymers). PGA, PHA, PCL and PLA are the most important and popular biodegradable polymers. These polymers have now become an emerging area for applied research and technology, due to their potential to overcome environmental concerns caused by synthetic plastics and unique properties that allow their applications in human health care. The peculiar properties of these polymers could make them substitutes of synthetic plastics for most of the industrial, house-hold and health care applications. It is predicted that the global capacity of bio-based polymer production will triple from 5.1 million tonnes in 2013 to 17 million tonnes in 2020 (Aeschelmann and Carus, 2015).

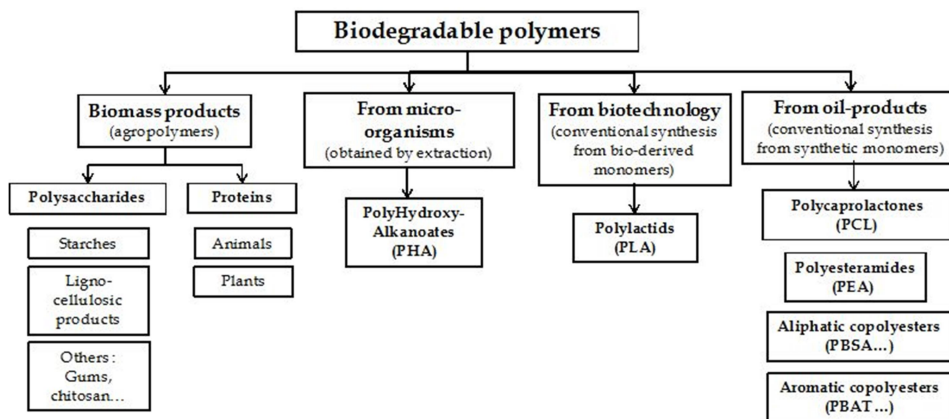


Fig. 1.1 Classification of biodegradable polymers (Dinesh, 2016)

1.2 Polyhydroxyalkanoates

PHAs are a class of bio-based polymers consisting of long chain hydroxy acid (HA) monomers linked together by an ester bond. This bond is formed between the carboxylic group of one monomer with the hydroxyl group of another monomer unit (Philip et al., 2007). They are accumulated in bacteria as storage granules when carbon source is found excess with limited nitrogen, phosphorous or oxygen. The polymer is primarily a product of carbon assimilation (from glucose or starch) and is utilized by microorganisms as an energy storage molecule to be metabolized when other common energy sources are not available (Bugnicourt et al., 2014). Depending upon the number of carbon atoms in the monomers, PHAs are classified into 3 distinct groups: scl-PHAs (short chain length PHAs), mcl-PHAs (medium chain length PHAs) and lcl-PHAs (long chain length PHAs). Scl-PHAs consists of 3–5 carbon atoms and are synthesized by a wide range of bacteria such as *Cupriavidus necator*, *Azohydromonas lata*, *Azotobacter vinelandii*, *Bacillus cereus*, recombinant *Escherichia coli* etc. Mcl-PHAs are composed of monomers having 6–14 carbon atoms and are accumulated mainly by *Pseudomonas* species. Mcl-PHA was first identified in *Pseudomonas putida* grown on octane (de Smet et al., 1983). Other examples include *P. resinovorans*, *P. citronellolis*, *P. oleovorans* and *P. chlororaphis* which produce mcl-PHA with different monomer compositions (Pereira et al., 2019). Lcl-PHAs has more than 14 carbon atoms (Anderson and Dawes, 1990). These monomers can form homopolymers or co-polymers with different physical properties. In all PHAs characterized so far, the hydroxyl substituted carbon atom is in the

R configuration. Also, the alkyl group that vary from methyl to decyl is in C3 position (Fig. 1.2).

Polyhydroxybutyrate (PHB) is the most well characterized and widely studied scl- PHA of D (-)-3-hydroxybutyric acid first discovered in *Bacillus megaterium* by French microbiologist Lemoigne in 1926 (Lemoigne, 1926). Scl- PHAs are crystalline polymers that are stiff, brittle with high melting point and low glass transition temperature whereas mcl-PHAs are thermoplastic elastomers with low crystallinity and tensile strength but high elongation to break. They also have low melting point and glass transition temperature. Scl-PHAs include homopolymers and co-polymers having monomers of 3-HB (3-hydroxybutyrate), 4-HB (4-hydroxybutyrate), 3-HV (3-hydroxyvalerate) etc, while mcl-PHAs include co-polymers having monomers of 3-HO (3-hydroxyoctanoate), 3-HHx (3-hydroxyhexanoate), 3-HDD (3-hydroxydodecanoate) and 3-HTD (3-hydroxytetradecanoate) (Fig 1.3).

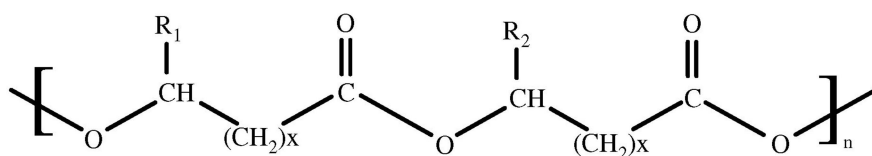


Fig. 1.2 General structure of PHAs (R1/R2 = alkyl groups C₁-C₁₃, x=1-4, n=100-30,000) (Philip et al., 2007)

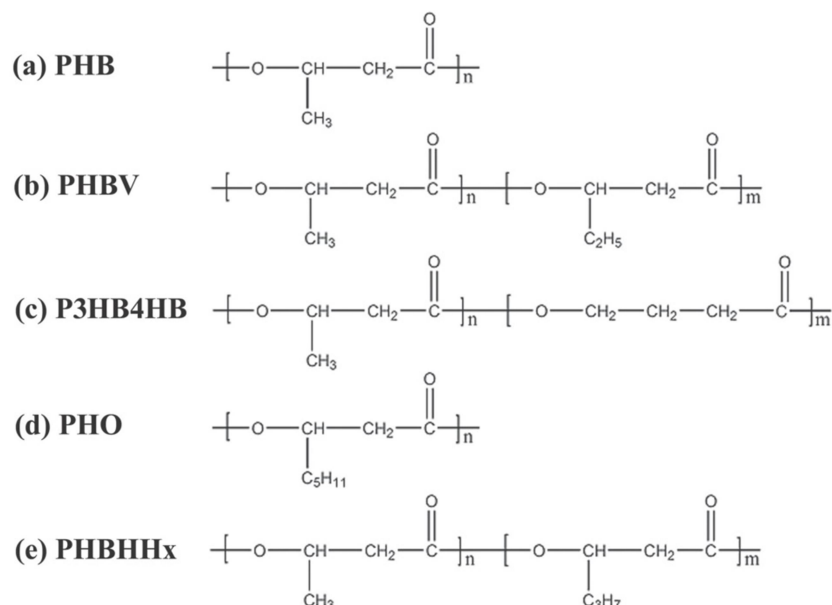


Fig. 1.3 Chemical structure of PHAs, PHB: poly(3-hydroxybutyrate); PHBV: poly(3-hydroxybutyrate-co-3-hydroxyvalerate); P3HB4HB: poly(3-hydroxybutyrate-co-4-hydroxybutyrate); PHO: poly(3-hydroxyoctanoate); PHBHHx: poly(3-hydroxybutyrate-co-3-hydroxyhexanoate (Ke et al., 2017)

1.2.1 Structure of PHA

PHAs are highly amorphous hydrophobic granules surrounded by a phospholipid membrane with embedded or attached proteins. Chemical analyses have shown that granules contain approximately 97.5% PHA, 2% protein and 0.5% lipid (Pötter and Steinbüchel, 2005). PHA granule-associated proteins (PGAPs) in bacteria consists of the intracellular PHA depolymerase (*PhaZ*), amphiphilic phasin proteins (*PhaP*), PHA synthase (*PhaC*), PHA-specific regulatory proteins (*PhaR*) and additional proteins with unknown functions (Fig. 1.4). The intracellular depolymerase is required for the mobilization of reserve polyester. Phasins (*PhaP*) are non-catalytic proteins with a hydrophobic domain which is associated with

PHA granule surface and a hydrophilic domain exposed to the cytoplasm of the cell (Grage et al., 2009). They function as structural proteins that promote PHA biosynthesis and their copy number has an impact on PHA granule size. These proteins are synthesized in very large quantities under storage conditions, representing 5% of the total protein (Pötter and Steinbüchel, 2005). Phasins stabilize PHA granules and prevent coalescence of separated granules. Kinetic simulation of the self-assembly process revealed that phasins have an impact on the kinetics of granule formation by reducing the lag phase (Rehm, 2003). Two distinct phasin-like proteins, PhaM and PhaF have been identified and characterized as being crucial for segregation and granule distribution during cell division (Galán et al., 2011; Pfeiffer et al., 2011). Among the proteins associated with the granule surface, only the PHA synthase is required for PHA granule formation, in the presence of a suitable substrate. The regulatory proteins (PhaR) are responsible for the formation of PHA granules by influencing the expression of both PhaP and themselves (Cai et al., 2015). PhaR binds to the promoter of PhaP as well as its own promoter to repress the transcription. When cells start accumulating PHA, PhaR attaches to the PHA granules, which results in a lower cytoplasmic PhaR level that can no longer repress transcription of PhaP. PhaP is then synthesized and binds subsequently to the PHA granules. PhaP is usually more abundant than PhaR and possesses a higher hydrophobic affinity to PHA granules. When the PHA granules reach a maximum possible size, the entire surface will be covered by PhaP proteins that displace PhaR proteins from the PHA granules. The cytoplasmic PhaR concentration returns to a higher level which will repress the transcription of both PhaP and PhaR.

This tight regulation by PhaR ensures a well-organized granule formation process, in which sufficient PhaP proteins are produced to coat the newly synthesized PHAs, with few free PhaP present in the cytoplasm (Pötter and Steinbüchel, 2005).

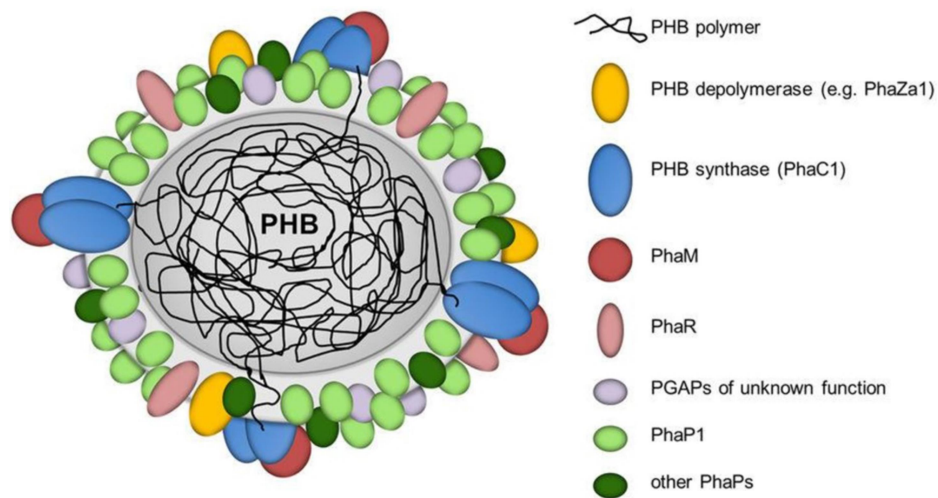


Fig. 1.4 Structure of PHA granule (Butt et al., 2018)

The structural composition of PHAs depends on the carbon source, the type of PHA synthase and the microorganism used for polymer production. The monomers are polymerized into high molecular weight polymers in the range of 200,000 to 3,000,000 Da. PHA exist as discrete inclusions that are typically $0.2 \pm 0.5 \mu\text{m}$ in diameter localized in the cell cytoplasm and may be visualized with a phase contrast light microscope due to their high refractivity (Sudesh et al., 2000). *In vivo*, the hydrophobic polyester core is largely amorphous, with water acting as a plasticizer to prevent crystallization. This is the mobile state of PHA, which is, subjected to the action of synthesizing and degrading enzymes. During extraction of granules from the bacterial cell, the phospholipid and protein layer is damaged. After

isolation, extracellular PHA granule is often crystalline with 50-80% crystallinity (Grage et al., 2009). The densities of crystalline and amorphous PHB are 1.26 and 1.18 g cm⁻³ respectively.

1.2.2 Properties of PHA

PHAs are semi-crystalline, isotactic, non-toxic, biodegradable, biocompatible, UV-resistant, aliphatic polyesters that are optically active with the chiral center of the monomer unit always in the R- configuration. PHA also shows piezo electric effect. Other properties of PHAs include resistance to hydrolytic degradation, poor resistance to acids and bases, water insoluble but soluble in chloroform and other chlorinated hydrocarbons, gas impermeable, sinks in water facilitating its anaerobic biodegradation in sediments and less sticky than traditional polymers when melted (Bugnicourt et al., 2014). The melting point of PHB is 175-179 °C and it decomposes at 200 °C. It has a glass transition temperature (T_g) of 2-4 °C (Table 1.1). PHB have physical properties similar to synthetic plastic polypropylene (PP) (Akaraonye et al., 2010). They both have a compact helical configuration and a melting point near 180 °C. PHB and PP display similar degrees of crystallinity and glass transition temperature, even though their chemical properties are completely different. PHB is stiffer and more brittle than PP.

When a co-polymer is formed with 3-HV monomer units, there is a decrease in crystallinity, melting point and stiffness (Young's modulus) with increase in toughness that enhances the desirable properties for commercial applications. The incorporation of 3-HV units into PHB had a profound effect on crystallization behaviour, influencing the nucleation

rates, growth rates, degree of crystallinity and subsequent aging effects which may result from particular crystallization conditions (Anderson and Dawes, 1990). Introduction of co-monomers other than 3-HV such as 3-HHx and 4-HB into PHB chain also gives rise to co-polymers of improved mechanical properties (Khanna and Srivastava, 2005).

Table 1.1 Range of typical properties of PHAs (Bugnicourt et al., 2014)

| Properties* (units) | Values |
|---------------------|---------|
| T _g (°C) | 2-4 |
| T _m (°C) | 175-180 |
| X _c (%) | 50-80 |
| E (GPa) | 1-2 |
| σ (MPa) | 15-40 |
| ε (%) | 1-15 |

*T_g: glass transition temperature, T_m: melting temperature,
X_c: crystallinity degree, E: Young's modulus,
σ : tensile strength, ε: elongation at break

1.3 PHA biosynthetic pathway

PHA biosynthetic pathways are intricately linked with the bacterial central metabolic pathways including glycolysis, Krebs cycle, β-oxidation, de novo fatty acids synthesis, amino acid catabolism, Calvin cycle and serine pathway. The most common intermediate shared between PHA and the above metabolic pathways is acetyl-coenzymeA (acetyl-CoA). In some PHA-producing microorganisms such as *C. necator*, *Chromatium vinosum* and *P. aeruginosa*, the metabolic flux from acetyl-CoA to PHA is greatly dependent on nutrient conditions. Under nutrient rich conditions, the production of high amounts of coenzyme A from Krebs cycle blocks PHA synthesis by inhibiting an enzyme β-ketothiolase (encoded by *PhaA* gene)

involved in PHA pathway, so that acetyl-CoA is channelled into the Krebs cycle for energy production and cell growth. Conversely, under unbalanced nutrient conditions (i.e., nutrient limiting in the presence of excess carbon), coenzyme A levels are non-inhibitory allowing acetyl-CoA to be directed towards PHA accumulation. This metabolic regulation strategy in turn enables the PHA accumulating microorganisms to maximize nutrient resources in their adaptation to environmental conditions (Tan et al., 2014).

The most common PHA biosynthetic pathway (pathway I) was studied in detail in *C. necator* (Fig. 1.5, Table 1.2). The biosynthetic pathway of PHB consists of three enzymatic reactions catalyzed by three different enzymes which constitute the *PhaCAB* operon. The first reaction consists of the condensation of two acetyl-CoA molecules into acetoacetyl-CoA by β -ketothiolase (encoded by *PhaA*). The second reaction is the reduction of acetoacetyl-CoA to (R)-3-hydroxybutyryl-CoA by an NADPH-dependent acetoacetyl-CoA dehydrogenase (encoded by *PhaB*). Finally, the (R)-3-hydroxybutyryl-CoA monomers are polymerized into PHB by PHA synthase (encoded by *PhaC*) (Madison and Huisman, 1999). The second PHA biosynthetic pathway (pathway II) is related to fatty acid uptake by microorganisms. Some bacteria such as *P. putida*, *P. aeruginosa* and *Aeromonas hydrophila* are able to use pathway II to synthesize mcl-PHA or copolymers of 3-HB and 3-HHx. After fatty acid β -oxidation, acyl-CoA enters the PHA biosynthesis process. Enzymes including 3-ketoacyl-CoA reductase, epimerase, (R)-enoyl-CoA hydratase/enoyl-CoA hydratase I, acyl-CoA oxidase (putative), and enoyl-CoA hydratase I (putative) were found to be involved in supplying the PHA precursor 3-hydroxyacyl-CoA which in turn is polymerized into PHA by PHA synthases (Chen, 2010).

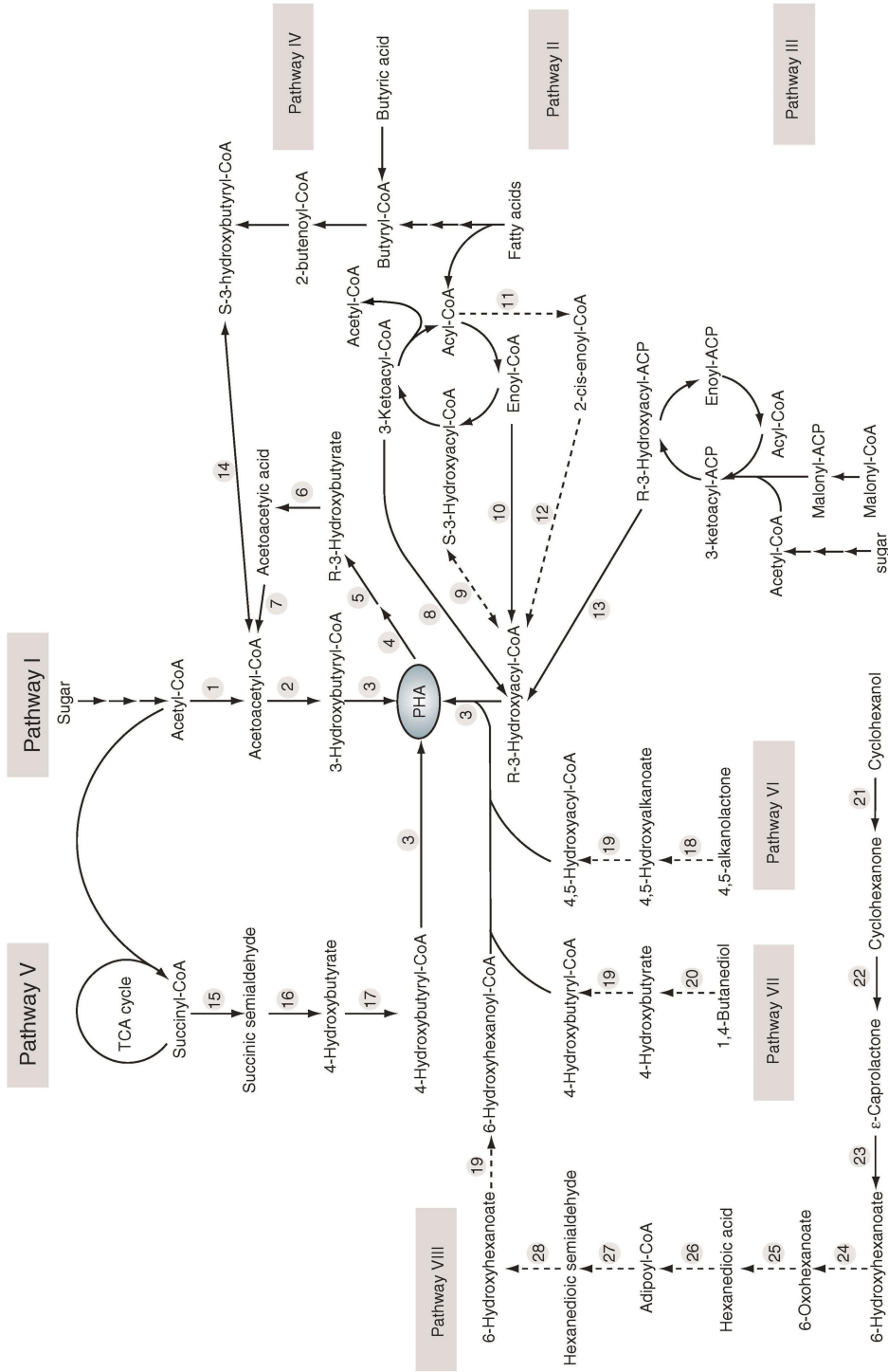


Fig. 1.5 Biosynthetic pathways for PHA production in different species of bacteria. Numbers representing detailed enzymes (or genes) involved in the PHA synthesis are tabulated in Table 1.2 (Chen, 2010)

PHA synthases are enzymes involved in the polymerization of PHAs. They are mainly divided into 4 classes based on their primary sequences, substrate specificity and subunit composition: class I and class II PHA synthases comprise of only one type of subunit (PhaC) with molecular masses between 61 kDa and 73 kDa. According to their *in vivo* and *in vitro* substrate specificity, class I PHA synthases (e.g. *C. necator*) preferentially utilize CoA thioesters of various (R)-3- hydroxy acids of 3 to 5 carbon atoms, whereas class II PHA synthases (e.g. *P. aeruginosa*) preferentially utilize CoA thioester of various (R)-3-hydroxy acids of 6 to 14 carbon atoms. Class III PHA synthases (e.g. *Allochromatium vinosum*) comprise enzymes consisting of two different types of subunits (i) the PhaC subunit (molecular mass of approx. 40 kDa) exhibiting amino acid sequence similarity of 21–28% to class I and II PHA synthases and (ii) the PhaE subunit (molecular mass of approx. 40 kDa) with no similarity to PHA synthases. These PHA synthases prefer CoA thioesters of (R)-3-hydroxy acids of 3 to 5 carbon atoms. Class IV PHA synthases (e.g. *B. megaterium*) resemble the class III PHA synthases, but PhaE subunit is replaced by PhaR (molecular mass of approx. 20 kDa). All PHA synthases share a conserved cysteine residue at the catalytic active site to which the growing PHA chain is covalently attached. The active-site cysteine, along with other conserved amino acids (histidine and aspartate) constitutes the catalytic triad of PHA synthase which is similar to that of esterases. PHA synthases have structural similarities with esterases and has a α/β -hydrolase fold (Rehm, 2003).

Table 1.2 Enzymes involved in the various biosynthetic pathways for PHA production (Chen, 2010)

| No. | Pathway | Abbreviation | Enzyme | Species |
|-----|----------------|--------------|---|---|
| 1 | Pathway I | PhaA | β -Ketothiolase | <i>Ralstonia eutropha</i> |
| 2 | | PhaB | NADPH dependent acetoacetyl-CoA reductase | |
| 3 | | PhaC | PHA synthase | |
| 4 | Associated way | PhaZ | PHA depolymerase | <i>Aeromonas hydrophila</i> 4AK4 |
| 5 | | | Dimer hydrolase | <i>Pseudomonas stutzeri</i> 1317 |
| 6 | | | (R)-3-Hydroxybutyrate dehydrogenase | <i>R. eutropha</i> |
| 7 | | | Acetoacetyl-CoA synthetase | <i>Pseudomonas oleovorans</i> |
| 8 | Pathway II | FabG | 3-Ketoacetyl-CoA reductase | <i>Pseudomonas putida</i> KT2442, |
| 9 | | | Epimerase | <i>A. hydrophila</i> 4AK4, |
| 10 | | PhaJ | (R)-Enoyl-CoA hydratase/enoyl-CoA hydratase I | <i>Pseudomonas aeruginosa</i> |
| 11 | | | Acyl-CoA oxidase, putative | |
| 12 | | | Enoyl-CoA hydratase I, putative | |
| 13 | Pathway III | PhaG FabD | 3-Hydroxyacyl-ACP-CoA transferase Malonyl-CoA-ACP transacylase | <i>Pseudomonas mendocina</i> , recombinant <i>Escherichia coli</i> |
| 14 | Pathway IV | | NADH-dependent acetoacetyl-CoA reductase | <i>Rhizobium</i> (Cicer) sp. CC 1192 |
| 15 | | SucD | Succinic semialdehyde dehydrogenase | <i>Clostridium kluyveri</i> |
| 16 | Pathway V | 4hbD | 4-Hydroxybutyrate dehydrogenase | |
| 17 | | OrfZ | 4-Hydroxybutyrate-CoA:CoA transferase | |
| 18 | Pathway VI | | Lactonase, putative | Mutants and recombinant of |
| 19 | | | Hydroxyacyl-CoA synthase, putative | <i>Alcaligenes eutrophus</i> |
| 20 | Pathway VII | | Alcohol dehydrogenase, putative | <i>A. hydrophila</i> 4AK4 |
| 21 | Pathway VIII | ChnA | Cyclohexanol dehydrogenase | <i>Acinetobacter</i> sp. SE19, |
| 22 | | ChnB | Cyclohexanone monooxygenases | <i>Brevibacterium epidermidis</i> |
| 23 | | ChnC | Caprolactone hydrolase | HCU |
| 24 | | ChnD | 6-Hydroxyhexanoate dehydrogenase | |
| 25 | | ChnE | 6-Oxohexanoate dehydrogenase | |
| 26 | | | Semialdehyde dehydrogenase, putative | |
| 27 | | | 6-Hydroxyhexanoate dehydrogenase, putative | |
| 28 | | | Hydroxyacyl-CoA synthase, putative | |

1.4 Microbial fermentation of PHA

Selection of microorganism for PHA production is based on several factors including the cell's ability to utilize an inexpensive carbon source, growth rate, polymer synthesis rate and maximum extent of polymer accumulation (Khanna and Srivastava, 2005). Depending on the culture conditions that favour PHA accumulation, bacteria used for the PHA production can be classified into two groups. The first group of bacteria requires limitation of essential nutrients such as nitrogen, oxygen and presence of excess carbon source for the efficient synthesis of PHA. The representative bacteria belonging to this group are *C. necator*, *P. extorquens* and *P. oleovorans*. This condition requires a two stage fermentation system where high growth rate of bacteria is achieved in first stage followed by high rate of product accumulation in second stage. This strategy utilizes different types of media, one for biomass production and another with nutrient limitation for PHA accumulation. Batch, fed-batch and continuous fermentation strategies can be adopted for this group of microorganisms. On the other hand, the second group of bacteria does not require nutrient limitation for PHA synthesis and can accumulate PHA during exponential growth phase and a single stage fermentation strategy is adopted (Khanna and Srivastava, 2005). Some of the bacteria included in this group are *A. lata*, a mutant strain of *A. vinelandii* and recombinant *E. coli* harbouring the PHA biosynthetic operon of *C. necator*.

Batch and fed-batch fermentations are the widely used strategies in the industrial fermentation processes. Batch fermentation for PHA production is a popular method due to its flexibility, ease to perform and

low operational costs (Table 1.3). However, batch cultures have the disadvantage of low yield and PHA productivity as carbon sources are readily utilized in batch culture and the cells degrade the accumulated PHA (Zinn et al., 2001). The harvesting time of biomass is critical in batch cultures due to increased chance of PHA degradation.

Table 1.3 Batch fermentation for PHA production

| Microorganism | Substrate | Cell dry weight (CDW) (g L ⁻¹) | PHA yield (g L ⁻¹) | PHA content (% CDW) | Reference |
|---------------------------|------------------------|--|--------------------------------|---------------------|-------------------------------|
| <i>A. lata</i> | Sucrose | 8.71 | 6.2 | 71.2 | Gahlawat and Srivastava, 2012 |
| <i>B. firmus</i> NII 0830 | Rice straw hydrolysate | 1.9 | 1.7 | 89 | Sindhu et al., 2013 |
| <i>B. mycoidea</i> DFC1 | Sucrose | 4.35 | 3.32 | 76.3 | Narayanan and Ramana, 2012 |
| <i>Alcaligenes</i> sp. | Cane molasses | 11.8 | 8.8 | 74.6 | Tripathi et al., 2013 |

Fed-batch cultivation is more efficient than batch cultivation in terms of achieving high product and cell concentration because the medium composition can be controlled by substrate inhibition (Table 1.4). Therefore, high initial concentration of substrates fed can be avoided. The limitations of fed-batch are the long downtime between two batches which results in high operational costs. In fed-batch fermentation, an initial batch step is carried out to achieve high cell density, followed by a

continuous step which limits growth nutrients except carbon source. Different feeding strategies such as pulse feed of substrate, constant feed rate, increasing or decreasing feed rate, high feed rate are performed for maximum productivity. In general, fed-batch fermentations usually involve the control of nutrient feed through dissolved oxygen (DO), regulation of pH and concentration of specific medium component (e.g. substrate) in the medium (Kaur, 2015). However, high concentrations of the substrate may lead to the production of more than one product of interest, thus, reducing the efficacy of the carbon flux towards PHA production (Akaraonye et al., 2010).

Table 1.4 Fed-batch fermentation for PHA production

| Microorganism | Substrate | Cell dry weight (CDW) (g L ⁻¹) | PHA yield (g L ⁻¹) | PHA content (% CDW) | Reference |
|------------------------------|-------------|--|--------------------------------|---------------------|-------------------------------|
| <i>A. lata</i> | Sucrose | 29.7 | 22.6 | 76 | Gahlawat and Srivastava, 2013 |
| <i>B. megaterium</i> MSBN17 | Pulp waste | 26.7 | 19.1 | 71.5 | G.Sathiyarayanan et al., 2013 |
| <i>C. necator</i> DSM 545 | Glycerol | 104.7 | 65.6 | 62.7 | Mozumder et al., 2014 |
| <i>B. sacchari</i> DSM 17165 | Wheat straw | 144.5 | 105 | 72 | Cesário et al., 2014 |

Continuous fermentation strategy has the advantage of maintaining constant nutrient environment and is useful to study the effect of nutrient limitation on the bacterial growth and productivity in a quick and real time manner (Table 1.5) (Hoskisson and Hobbs, 2005). A continuous production process is of greater commercial interest due to its high productivity, especially for strains with a high maximum specific growth rate (Braunegg et al., 1995; Ramsay et al., 1991). Continuous fermentation may be performed in single, two stage or multi stage operations and the chemostat continuous cultivation processes for PHA biosynthesis was found to be more efficient in terms of productivity, product quality and increased efficiency of the downstream processing (Koller and Braunegg, 2015). In single-stage fermentation, the biomass increase while PHA content decrease with increase in dilution rate. Therefore, a compromise between PHA content, cell concentration and productivity is required in a single-stage process for attaining reasonable PHA content (Akaraonye et al., 2010). The main disadvantage of continuous fermentation is microbial contamination due to long operational runs.

Table 1.5 Continuous fermentation for PHA production

| Microorganism | Substrate | Cell dry weight (CDW) (g L ⁻¹) | PHA yield (g L ⁻¹) | PHA content (% CDW) | Reference |
|-----------------------|-----------|--|--------------------------------|---------------------|--------------------|
| <i>Halomonas</i> TD01 | Glucose | 40 | 24 | 60 | Tan et al., 2011 |
| <i>C. necator</i> | Glucose | 81 | 63 | 77 | Atlić et al., 2011 |

1.5 PHA production in marine bacteria

Marine bacteria are a good resource for PHA production due to their adaptability to thrive in extreme conditions of physical and chemical factors affecting growth. Marine bacteria are potent PHA producers having the potential to utilize a wide range of carbon sources including pure sugars, renewable sources and industrial waste products. Bacterial genus *Vibrio* has been found to be first reported potent PHA producer isolated from marine sediments (Baumann et al., 1971). Some haloarchaeal species belonging to genera such as *Haloferax*, *Haloarcula*, *Natrialba*, *Haloterrigena*, *Halococcus*, *Haloquadratum*, *Halorubrum*, *Natronobacterium*, *Natronococcus* and *Halobacterium* are also found to be efficient PHA producers (Poli et al., 2011). Some potent marine isolates, their PHA cultivation strategies and polymer yield are discussed here in detail. PHB production from marine bacterium *Vibrio natriegens* showed 40% PHB accumulation with glycerol as carbon source (Chien et al., 2007). Another *Vibrio* sp. showed a high biomass yield of 9.1 g L⁻¹ with a PHB content of 4.2 g L⁻¹ in batch fermentation with glucose as carbon source (Arun et al., 2009). *Vibrio azureus* BTKB33 isolated from marine sediments showed a maximum PHA production of 0.48 g L⁻¹ and PHA content of 426.88 mg g⁻¹ of cell dry weight in presence of glucose (Sasidharan et al., 2014). In another study, *Vibrio* sp. BM-1 showed a PHB yield of 0.81 g L⁻¹ and PHB content 24% in presence of glycerol as carbon source (Wei et al., 2011). A marine isolate of *B. megaterium* MSBN04 isolated from sponge *Spongia officinalis* accumulated 8.637 mg g⁻¹ of substrate PHB from biomass 15.2 mg g⁻¹ of substrate with 56% PHB content in solid state fermentation with industrial waste palm jaggery and

tapioca starch as substrates (Sathiyarayanan et al., 2013). In a similar study, a cell dry weight of 26 g L⁻¹ and PHB yield of 19 g L⁻¹ was obtained in fed batch cultivation of *Bacillus subtilis* MSBN17 isolated from sponge *Callyspongia diffusa* with pulp industry waste as substrate. The overall productivity was calculated as 0.477 g L⁻¹ h⁻¹ which was relatively higher than active PHA producer *C. necator* under fed-batch process using different culture medium (Sathiyarayanan et al., 2013). *B. megaterium* H16, isolated from the solar salterns of Ribandar, Goa accumulated 40% PHA in the presence (5% w/v) or absence of sodium chloride using glucose as carbon (Salgaonkar et al., 2013). In another study, a mangrove isolate *Bacillus* sp. accumulated 2 g L⁻¹ PHA co-polymer with 73% PHA content in presence of glucose (Moorkoth and Nampoothiri, 2016). *Halomonas* TD01, a moderate halophile produced 80 g L⁻¹ cell dry weight with 80% PHB on glucose salt medium in a 56 h fed-batch process (Tan et al., 2011). The demand to isolate and identify novel marine bacteria capable of utilizing renewable resources as potent PHA producers opens a new avenue for the effective polymer production thereby reducing the production costs.

1.6 PHA production from renewable sources

Microbial PHA production would be more economical and sustainable, if, it can be produced from cheap renewable substrates or industrial by products. It is important to note that the selection of carbon sources should not only focus on the market prices but also on the availability and on the global price (Chanprateep, 2010). Some of the cheap and surplus renewable sources commonly used for PHA production

include cheese whey, molasses, fats and oils, starch residues of cassava or corn, lignocellulosic residues and waste glycerol. Different bacteria utilize different types of carbon sources for PHA accumulation. An isolate of *Methylobacterium* sp. ZP24, was able to utilize whole whey for PHA production giving 5.1 g L⁻¹ cell dry weight with 1.1 g L⁻¹ PHA yield in 48 h (Yellore and Desai, 1998). The use of whey as substrate studied in recombinant *E. coli* cells harboring *A. lata* genes showed a cell dry weight of 6.6 g L⁻¹, PHA yield of 5 g L⁻¹ and PHA content of 76% after 96 h incubation (Ahn et al., 2000). When *Thermus thermophilus* HB8 was grown in culture medium containing 24% (v/v) whey, a cell dry weight of 1.6 g L⁻¹ and PHA content of 35% (w/w) was obtained after 24 h of cultivation. The PHA produced in presence of whey was a novel heteropolymer consisting of 38mol% 3-hydroxyvalerate, 9.89mol% 3-hydroxyheptanoate, 16.59mol% 3-hydroxynanoate and 35.42mol% 3-hydroxyundecanoate (Pantazaki et al., 2009). PHA production in *C. necator* H16 using soyabean oil as carbon source reported a cell dry weight yield of 126 g L⁻¹ and PHA content of 76% after 96 h incubation (Kahar et al., 2004). PHA production by *B. megaterium* using cane molasses as substrate showed a cell dry weight of 3.6 g L⁻¹ and PHA yield of 2.2 g L⁻¹ from 2% molasses carried out in a 10 L fermentor with 4 L working volume (Gouda et al., 2001). PHA production from cassava starch hydrolysate by *Cupriavidus* sp K KU38 showed a cell dry weight of 5.97 g L⁻¹, PHA yield of 2.43 g L⁻¹ and PHA content of 61.6% under the optimum conditions (Poomipuk et al., 2014). PHA production by *H. boliviensis* using cassava starch hydrolysate showed a cell dry weight of 9.2 g L⁻¹ and PHA content of 56% after 30 h incubation (Rivera-Terceros

et al., 2015). *B. firmus* NII 0830 utilized acid pre-treated rice straw hydrolysate as the sole carbon source without any detoxification and accumulated 1.9 g L⁻¹ cell dry weight, 1.69 g L⁻¹ PHA and 89% PHA content in the cell (Sindhu et al., 2013). PHA production from wheat straw hydrolysate using *B. sacchari* DSM 17165 showed a maximum polymer concentration of 105 g L⁻¹ after 61 h incubation with polymer productivity of 1.6 g L⁻¹ h⁻¹ and polymer accumulation of 72% in fed batch conditions (Cesário et al., 2014). Biodiesel by-product glycerol when used as the sole carbon source for PHA production in *B. cepacia* resulted in a cell dry weight yield of 5.8 g L⁻¹ and PHA content of 81.9% with 3% (v/v) glycerol as a feedstock over 96 h of growth (Zhu et al., 2009). *Zobellella denitrificans* MW1 used glycerol as the sole carbon source for PHA production by fed-batch fermentation showed a PHA accumulation of 87% and polymer yield of 4.25 g L⁻¹ (Ibrahim and Steinbüchel, 2009). *Halomonas* sp. KM-1 utilized pure glycerol and produced PHA of 2.3 g L⁻¹ with 44.8% PHA content. It was noted that the isolate could effectively utilize pure glycerol than waste glycerol for PHA production (Kawata and Aiba, 2010). Marine isolates *B. sonorensis* and *H. hydrothermalis* utilized Jatropha biodiesel by-product crude glycerol for PHA production and were found to accumulate PHA up to 71.8% and 75% cell dry weight respectively. The use of cheap and inexpensive Jatropha biodiesel product without any pre-treatment as sole carbon source may be a good alternative for cost effective PHA production (Shrivastav et al., 2010). PHA production by *B. thuringiensis* EGU45 showed a cell dry weight 4.9 g L⁻¹, PHA yield 3.5 g L⁻¹ and PHA content 72% in presence of nutrient broth supplemented with 5% (v/v) crude glycerol in 48 h (Kumar et al., 2015).

1.7 Statistical designs for PHA optimization

For most multivariable processes, it is difficult to determine which of the factors are the most important when a number of them are involved. Hence, it is necessary to submit the process to an initial screening design prior to optimization. The methodology of Plackett–Burman (PB) is a tool for this initial screening, as it is possible to determine the influence of various factors with only a small number of trials, instead of using more extensive factorial designs, which will furnish more complete information, but which involves unfeasible complexity (Kalil et al., 2000). The conventional method of optimization primarily used was one-factor-at-a-time approach (OFAT) in which, one factor influencing the process is varied when all others are kept constant. Factorial design is advantageous in relation to this conventional method; as such an approach is time consuming and fails to identify optimal conditions for the process due to its failure to study the interactions between the various factors. The limitation of such method can be avoided by using statistical experimental design, a powerful tool, which allows analysing the interactions between the different variables and decreasing the process variability (Aramvash et al., 2015).

The primary purpose of the experimental design technique is to understand the interactions among the factors, which could help in the optimization of selected factors and provide statistical models. Response surface methodology (RSM) is a collection of statistical and mathematical techniques useful for developing, improving and optimizing processes. It has important applications in the design, development and formulation of

new products, as well as in the improvement of existing product designs (Myers et al., 2009). RSM is often used to refine models that have been determined as important factors using screening designs or factorial designs. The 2 main types of response surface designs are Central Composite Design (CCD) and Box-Behnken Design (BBD). BBD have less design points when compared to axial points of CCD, hence the numbers of experiments are more in CCD. CCD also tests at extreme conditions and hence gives better quadratic models. CCD is suitable to optimize the effective factors with minimum number of experiments and also to analyse the interaction between them (Anupam et al., 2011). Optimization of PHA production using CCD has been carried out in different bacteria using various renewable and inexpensive carbon sources (Aramvash et al., 2015; Pandian et al., 2010; Ramadas et al., 2010; Sathiyarayanan et al., 2013).

1.8 Downstream processing

PHAs are intracellular granules and need to be separated from other biomass components of the cell. The common methods used for biomass separation is centrifugation, cross flow filtration and flocculation. There are different methods used for recovery of PHA from the bacterial biomass.

1.8.1 Solvent extraction

Solvent extraction is the most common method to recover PHA from the cell biomass. This method is also used routinely in the laboratory because of its simplicity and rapidity. In this process, the modification of

cell membrane permeability takes place that allow the release and solubilization of PHA, followed by non-solvent precipitation. This method also removes bacterial endotoxin and causes negligible degradation to the polymers. Solvent extraction has several advantages over the other extraction methods in terms of efficiency (Jacquel et al., 2008). Extraction of PHA with chlorinated hydrocarbons such as chloroform, 1, 2-dichloroethane (Ramsay et al., 1994) or ethylene carbonate and 1, 2-propylene carbonate (Fiorese et al., 2009) are commonly practiced. Lower chain ketone such as acetone is the most prominent solvent especially for the extraction of mcl-PHA. Precipitation of PHA is commonly induced by polar solvents such as methanol and ethanol (Ramsay et al., 1994). So, it is possible to obtain very pure PHA with high molecular weights. Unfortunately, the large scale application of solvent extraction can cause environmental problems. The use of 1, 2 propylene carbonate is an alternative to halogenated solvents in the recovery of PHA. Hot (120 to 150°C) ethylene carbonate or 1, 2-propylene carbonate is used for PHA extraction from moist or dry fermentation processes. These solvents have the advantage that PHA is precipitated in good yield from them on cooling. In addition, they may be recycled without the need for a solvent regeneration step. Extraction with ethylene carbonate resulted in greater degree of de-polymerization than the use of 1, 2-propylene carbonate. The biomass is suspended in ethylene carbonate and/or 1, 2-propylene carbonate and the suspension is then heated with stirring and extracted biomass is centrifuged. The highest yield of 95% and purity of 84% was obtained with the combination of a temperature of 130 °C and a contact time of 30 min, with a precipitation period of 48 h for *C. necator* (Fiorese

et al., 2009). This is comparable with the values obtained from chloroform extraction (94% yield and 98% purity).

1.8.2 Chemical digestion

This method includes the use of chemicals such as sodium hypochlorite and surfactants like SDS, Triton X-100 and EDTA for PHA recovery. Sodium hypochlorite has strong oxidizing properties and its non-selectivity can be manipulated to digest non-PHA cellular mass (NPCM) and facilitate PHA recovery (Yu and Chen, 2006). The use of sodium hypochlorite causes severe degradation of molecular weight of PHA and hence mostly used in combination with surfactants or organic solvents. Berger et al., 1989 have optimized the conditions of sodium hypochlorite treatment along with biomass concentration and digestion time. PHA of 95% purity was obtained with 50% reduction in its molecular weight. The use of sodium hypochlorite with chloroform as dispersion method was studied by Hahn et al., 1994 and PHA of above 97% purity was obtained. By this method, three separate phases are obtained; an upper phase of hypochlorite solution, a middle phase accumulated with non-PHA cell materials and undisturbed cells, and the lower chloroform phase containing dissolved PHA. The polymer is then recovered by precipitation using a non-solvent and filtration. When the hypochlorite concentration was above 3%, the purity was higher than 97%. The hydrophobic nature of PHA and hydrophilic nature of lyophilized cells is exploited for recovery of PHA in dispersions of sodium hypochlorite solution and chloroform. The PHA granules recovered by this method was reported to be highly crystalline (Kunasundari and Sudesh, 2011) .

Anion detergent sodium dodecyl sulfate (SDS) disrupt cells by incorporating itself into the lipid bilayer membrane and at higher concentration, it breaks the membrane to produce micelles of surfactant and membrane phospholipids, which leads to the release of PHA into the solution surrounded by the cellular debris (Ramsay et al., 1990). Also SDS solubilizes protein and non-PHA cellular materials (Chen et al., 1999). A high surfactant dose (5%) increases the recovery cost and causes problems in wastewater treatment. The use of surfactant alone cannot give a high PHA purity hence, a combination with other agents such as hypochlorite and sodium hydroxide is needed. The treatment of PHA containing biomass with 1% surfactant each of SDS or Triton X-100 followed by hypochlorite wash produced PHA of 97% purity with molecular weight slightly higher when compared to PHA obtained by only hypochlorite treatment (Ramsay et al., 1990). SDS with chelating agent EDTA was used for the recovery of PHA from *C. necator* and the polymer of 98.7% purity and a recovery yield of 93.3% was obtained. The chelating agents destabilize the outer membrane of Gram negative bacteria by forming complexes with divalent cations (Chen et al., 1999). Incubation of *C. necator* and *E. coli* cells with 5% (w/v) SDS for 3 to 6 h allowed recovery of 95% of the intracellular PHA (Yang et al., 2011) but the purity of the recovered polymer was improved by extending the detergent treatment for longer than 6 h.

1.8.3 Enzymatic digestion

The use of enzymes leads to good recovery levels but high cost of enzymes is a major drawback. The enzymatic recovery and purification of PHA produced in *C. necator* has been investigated in detail (Kapritchkoff et al., 2006). PHA purity of 88.8% was achieved with 2% bromelain at 50 °C and pH 9.0. To improve the process efficiency and reduce the enzyme cost, experiments with pancreatin, an enzymatic commercial preparation with protease activity was performed. A polymer purity of 90% was obtained at pH 8 and temperature 50 °C. The efficiency of enzymatic treatment may be improved by combining with chemical methods.

1.8.4 Mechanical disruption

This method includes the use bead mill, high pressure homogenizer and sonication for PHA recovery. A method that combines a high pressure homogenizer in the presence of 5% SDS was used in the PHA recovery from *Methylobacterium* sp.V49. The maximum yield of 98% and purity of 95% was obtained (Ghatnekar et al., 2002). The combined use of sonication and chloroform treatment was carried out for PHA extraction and recovery in *A. lata* DSM1123 (Penloglou et al., 2012). Unlike other recovery methods, mechanical disruption is favoured mainly due to low cost and the method causes only mild damage to the products (Tamer et al., 1998).

1.8.5 Supercritical fluids

Supercritical fluids (SCF) have unique physicochemical properties such as high densities and low viscosities that make them a suitable extraction solvent. Supercritical carbon dioxide is the predominantly used SCF due to its low toxicity and reactivity, moderate critical temperature and pressure, availability, low cost and non-flammability. PHA extraction using SCF showed a recovery of 89% from *C. necator* at 200 atmosphere pressure, 40 °C with 0.2 mL methanol as modifier (Hejazi et al., 2003). To further improve the purity of PHA, chemical pre-treatment with 0.4% (w/w) sodium hydroxide was done. This recovery process of PHA is more economical as the costly freeze drying step can be avoided (Kunasundari and Sudesh, 2011).

1.8.6 Cell fragility

Bacteria like *A. vinelandii* and recombinant *E. coli* become fragile after the accumulation of large amount of PHA. Cell fragility mechanism is present in both Gram positive and Gram negative bacteria. The addition of fish peptone to the cultivation medium of *A. vinelandii* UWD led to the formation of large, pleomorphic, osmotically sensitive cells while high molecular weight PHA synthesis was enhanced. The cells were treated with 1N aqueous ammonia (pH 11.4) at 45 °C for 10 min. This treatment removed about 10% of the non-PHA biomass from the pellet, of which 60–77% was protein. The final product consisted of 94% PHA, 2% protein and 4% non- protein residual mass (Page and Cornish, 1993). In another method using the fragility in recombinant *E. coli* cells, a PHA content of 77% was obtained. The cells were treated with 0.2N NaOH at

30 °C for 1 h and the polymer was recovered with a purity of 98.5% (Choi and Lee, 1999).

1.8.7 Aqueous two phase system

An aqueous two-phase system (ATPS) is an aqueous, liquid-liquid, biphasic system which is obtained either by mixture of aqueous solution of two polymers, or a polymer and a salt such that two immiscible phases coexist. Polyethylene glycol (12% w/v) and potassium phosphate (9.7%, pH 8.0) containing enzymatic cell hydrolyzed *B. flexus* biomass was incubated at 37 °C for 2 h, which partitioned PHA into top PEG phase and residual cell materials into bottom phase (Divyashree et al., 2009). ATPS is not being used in industrial scale due to the absence of commercial kits to evaluate ATPS at bench scale as well as poor understanding of the mechanism (Ritopalomares, 2004).

1.9 PHA market

The extensive research carried out in the area of PHAs to develop its properties and applications have made them a potentially emerging and eco-friendly biomaterial of the future generation. Industrial-scale production of PHA depends on a number of critical factors such as the cost of substrates, microbial content of the PHA, its yield and downstream process (Kaur, 2015). In the scale up studies, the carbon source accounts up to 50% of the total cost (Choi and Lee, 1999) and hence the economic feasibility of mass production requires the development of efficient biotechnological processes with the use of inexpensive carbon sources and selection of high yield microorganisms.

C. necator has been the most extensively studied and commonly used bacterium for PHA production. In the 1980s, a glucose-utilizing mutant of *C. necator* was employed by Imperial Chemical Industries (UK) for the industrial production of poly (3- hydroxybutyrate-co-3-hydroxyvalerate) (abbreviated as PHBV) which was sold under the trade name BiopolTM. Among PHA manufacturing companies, the main company with a large production is the U.S. biotech company Metabolix, Inc. in Cambridge, Massachusetts. Metabolix is the largest market player, with an annual production capacity of 50,000 tons of PHA and have manufacturing facilities located at Iowa (U.S.A) and Leon (Spain). The company markets the PHA intended for injection molding, thermoforming, cast film and sheet applications in food and beverage, agriculture and healthcare sector. In 2010, Telles, a joint venture company formed by the Archer Daniels Midland Company (ADM) and Metabolix, Inc. opened the first commercial-scale plant to produce a corn syrup-based PHA resin, MirelTM, in Clinton, U.S.A. NodaxTM, another class of PHA co-polymers consisting of medium chain length PHAs commercially available from Danimer Scientific, USA has been used as additives, aqueous coatings, fibers, filaments, films, hot-melt adhesives and injection-molded articles (Noda et al., 2010). Table 1.6 details the worldwide commercial PHA manufacturers.

Table 1.6 Some of the pilot and industrial scale PHA manufacturers currently active worldwide (Kourmentza et al., 2017)

| Name of Company | Product (Trademark) | Substrate | Biocatalyst | Production Capacity |
|---|---|--|--|--------------------------------|
| Biomatera, Canada | PHA resins (Biomatera) | Renewable raw materials | Non-pathogenic, non-transgenic bacteria isolated from soil | |
| Bio-On Srl, Italy | PHB, PHBV spheres (minerv®-PHA) | Sugar beets | <i>C. necator</i> | 10,000 t/a |
| Kaneka Corporation, Japan | PHB-PHHx (AONILEX®) | Japan plant oils | | 3500 t/a |
| PHB Industrial S.A., Brazil | PHB, PHBV (BIOCYCLE®) | Sucrose | <i>Alcaligenes</i> sp. | 3000 t/a |
| TianAn Biologic Materials Co. Ltd., China | PHB, PHBV (ENMAT™) | Dextrose from corn or cassava grown in China | <i>C. necator</i> | 10,000 t/a, 50,000 t/a by 2020 |
| Tianjin GreenBio Material Co., China | P (3, 4HB) films, pellets/foam pellets (Sogreen®) | Sugar | | 10,000 t/a |

PHB: poly (3-hydroxybutyrate); PHBV: poly (3-hydroxybutyrate-co-3-hydroxyvalerate); PHBHHx:poly (3-hydroxybutyrate-co-3-hydroxyhexanoate); P(3,4HB):poly (3-hydroxybutyrate-co-4-hydroxybutyrate)

The global use and industrialization of PHA is limited due to high production costs of approximately US \$2.25–2.75/lb (Johnston et al., 2018). The increasing availability of renewable raw materials, increasing demand and use of biodegradable polymers for bio-medical, packaging and food applications along with favourable green procurement policies are expected to benefit the PHA market growth (Kourmentza et al., 2017).

1.10 Applications of PHAs

The use of PHAs as bio-based polymers has gained much attention due to their biological origin and non-toxic nature.

1.10.1 Drug carriers

PHAs have been recognized as excellent biomaterials with desirable material properties and high biocompatibility. PHAs are potential candidates as drug carriers for controlled and targeted delivery of antibiotics, anticancer drugs, growth factors, hormones and pain relievers due to their unique properties and non-toxic nature. Controlled drug delivery systems aim to deliver drugs at predetermined rates and predefined periods of time for curing diseases in a sustained manner. The advantage of PHA in controlled drug delivery is the availability of PHA in chemically pure form and their low degradation rate in biological system (Gürsel and Hasirci, 1995). Targeted delivery involves the delivery of mainly chemotherapeutic drugs with high toxicity as well as the high activity peptides and proteins to targets or ligands that specifically bind them. In addition to the passive targeting, the easy functionalization of cell-specific ligands such as folate, peptides and

sugars onto the surface of polymeric nanocarriers enables to enhance the therapeutic efficiency and disease specificity in drug delivery. PHAs fabricated in the form of nanoparticles with sizes ranging from 50 to 150 nm can be internalized by cancer cells at higher rates than normal cells due to enhanced permeability and retention (EPR) effect (Li and Loh, 2017). PHB microspheres loaded with rifampicin were studied for use as a chemoembolizing agent. The amount of drug released from the microspheres was found approximately 90% in 24 h. The encapsulation (52–65% w/w) was more efficient in the neutral form, but the drug was quickly released without any particle degradation in both the acidic and neutral forms (Kassab et al., 1997). The controlled release of gentamycin antibiotic from PHA/gentamicin complexes was found to reduce the number of *Staphylococcus aureus* within 48 h after exposure in the treatment of orthopaedic infections (Rossi et al., 2004). PHA/hydroxyapatite (HA) composite microspheres encapsulating gentamycin was developed as a long-term drug delivery system. The rate of drug diffusion was substantially higher than that of polymer degradation, so the release profile was more dependent on drug diffusion rather than on polymer degradation. The hybrid structure of the microspheres allows the drug to impregnate in the polymer matrices, rather than on the surface of the microspheres. Though the initial burst was so low, the drug diffused slowly through the interspaces of the polymer matrices during 70 days (Wang et al., 2007). PHA conjugated with folic acid nanoparticles was effective for the selective delivery of anticancer drug doxorubicin to folate receptor-overexpressed HeLa cancer cells. The *in vivo* anti-tumor activity also showed a much better therapeutic efficacy in inhibiting

tumour growth (Zhang et al., 2010). PHA attached with folic acid and loaded with antineoplastic drug, etoposide seems to be a promising candidate for the targeted cancer therapy. The cytotoxicity of the folic acid conjugated and etoposide loaded PHA nanoparticles to cancer cells was much higher than free etoposide or etoposide loaded PHA nanoparticles without folic acid. In addition, the cytotoxicity of folic acid conjugated and etoposide loaded PHA nanoparticles to HeLa cancer cells was found to be higher than that of L929 normal fibroblast cells, demonstrating that the folic acid conjugated PHA nanoparticles has the ability to selectively target cancer cells (Kılıçay et al., 2011). PHA nanoparticles were developed for the sustained release of phosphoinositide-3-kinases (PI3K) inhibitor (TGX221) to block the proliferation of cancer cell lines. PI3K inhibitors are anticancer drugs used in targeted therapy. TGX221 was gradually released from PHA nanoparticles and growth of PC3 cancer cell line was significantly reduced in presence of nanoparticles entrapped with the inhibitor (Lu et al., 2011). PHA nanoparticles were fabricated and used as drug carrier for the release of hydrophobic anticancer drug ellipticine. The *in vitro* drug release studies showed 2 fold higher % inhibitions of A549 cancer cells on treating with ellipticine loaded PHBV nanoparticles in comparison to ellipticine alone. This drug delivery system offers exciting possibilities for cancer therapy by increasing the bioavailability of antineoplastic drug to the tumor site (Masood et al., 2013). PHA micro/nanoparticles were found to have the potential to serve as topical and transdermal drug delivery carriers for the delivery of skin therapeutics on aged or damaged skin or in cases of skin diseases such as psoriasis.

The aim of transdermal delivery systems is to deliver low molecular weight agents safely and effectively without irritating the stratum corneum or the deeper tissue layers of skin (Eke et al., 2014). PHA nanoparticles formulated as carriers of a hydrophobic photosensitizer 5, 10,15,20-Tetrakis(4-hydroxy-phenyl)- 21*H*,23*H*-porphine (pTHPP) for photodynamic therapy (PDT) demonstrated time and concentration dependent cell death with a gradual release pattern of pTHPP and high photocytotoxicity against human colon adenocarcinoma cell line HT-29 especially after longer incubation time. PHA nanoparticles act as promising vehicles for delivery of hydrophobic photosensitizer drugs with potential application in PDT. PDT is an attractive and selective cancer treatment modality which is an alternative approach to conventional cancer treatments (Pramual et al., 2016).

1.10.2 Tissue engineering

PHAs are well suited for tissue engineering applications due to their inherent biocompatibility, biodegradability and diverse set of physical properties exhibited among PHA and its co-polymers. PHAs with necessary modifications have great potential to contribute to tissue engineering, developing tissue products for medical and therapeutic applications such as vascular grafts, heart valves, nerve tissue engineering etc. PHAs can be used to produce scaffolds, which have higher mechanical strength. These scaffolds promote growth of the cells by supplying nutrition (Ray and Kalia, 2017). PHA based porous trileaflet heart valve scaffold was fabricated and were seeded with vascular cells and implanted in lambs. The tissue-engineered constructs were covered with tissue and

there was no thrombus formation. PHAs could be used for implantation in the pulmonary position with an appropriate function for 120 days in lambs. Hence, PHA scaffold was suitable for the fabrication of a functional trileaflet tissue-engineered heart valve (Sodian et al., 2000). Matrices of collagen containing calcium phosphate and PHA were produced to create a cartilage via tissue engineering. The matrices allowed sufficient adhesion and proliferation of chondrocytes under *in vitro* conditions. Also these scaffolds supported the differentiated chondrocyte phenotype and induced the production of cartilage matrix. *In vivo* histological studies revealed that chondrocytes in the matrices remained adherent and actively participated in neocartilage formation in the whole phase of repair process. This study also showed that PHA matrices permitted appropriate gradual degradation and allowed tissue remodelling to occur. PHA matrices also showed the early cartilage formation resembling normal articular cartilage (Köse et al., 2005). The attachment, proliferation and differentiation of smooth muscle cells from rabbit aorta (RaSMCs) on PHA films showed strong cell attachment, proliferation and differentiation. The results revealed the potential of PHAs for the construction of SMCs related graft scaffolds for tissue engineering application (Qu et al., 2006). PHA nanofibre matrices were found to support cell attachment and viability of human keratinocyte cell line, HaCat and hence, could be used for applications in skin tissue engineering (Li et al., 2008). The effects of PHA films and PHA nanofibre scaffolds on neural stem cells (NSC) growth and differentiation showed that PHA nanofibre scaffolds, structurally similar to natural extracellular matrix could support growth of NSCs and showed stronger

cellular adhesion, better connection and higher viability. PHA nanofibre scaffold serves as NSCs matrix and promotes differentiation of NSCs to neurons which is beneficial for central nervous system repair (Xu et al., 2010). PHA and PHA/Bioglass foams were prepared to evaluate the material bioactivity and biocompatibility *in vitro* using MG-63 osteoblasts and *in vivo* in a rat model. The results showed *in vitro* cell proliferation as well as allowed vascularization when applied subcutaneously in rats for up to 7 days. The interconnected porous microstructure in these foams proved to be suitable for MG-63 osteoblast cell attachment and proliferation. The results from the study also showed the potential of using PHA functional composites for bone tissue engineering with sensing properties (Misra et al., 2010). Terpolyester PHBVHHX (poly (3-hydroxybutyrate-co-3-hydroxyvalerate-co-3-hydroxyhexanoate) scaffolds were fabricated to study their ability to favour differentiation of human bone marrow stromal cells (hBMSC) into nerve cells. Terpolyester PHBVHHX films showed stronger cell adhesion, proliferation and differentiation for hBMSC compared with that of PLA and PHBHHX. PHBVHHx 3 D scaffolds immersed in nerve differentiation medium were able to promote hBMSC differentiation into nerve cells compared with their 2D films. Smaller pore sizes of scaffolds increased differentiation of hBMSC into nerve cells, whereas decreased cell proliferation. The microenvironment of PHBVHHx scaffolds with suitable pore sizes promoted generation of more neurons and less astrocytes, which is useful to avoid gliar scar formation resulted from astrocytes during spinal cord injury (Wang et al., 2010). PHBVHHx scaffolds loaded with umbilical cord-derived mesenchymal stem cells (UC-MSCs) and hepatocyte-like

cells differentiated from UC-MSCs were transplanted into liver-injured mice. Liver morphology on day 28 post-transplantation of scaffolds loaded with UC-MSCs or hepatocyte-like cells differentiated from UC-MSCs significantly improved and looked similar to the normal liver. UC-MSCs contained in scaffolds secreted various cytokines and growth factors, which in turn stimulated native hepatocytes or hepatocyte-like cells to initiate the hepatic regeneration process. The results demonstrated that PHBVHHx scaffolds loaded with UC-MSCs or differentiated UC-MSCs had the similar effect on injured livers and significantly promoted the recovery of injured livers (Su et al., 2014).

1.10.3 Medical devices

PHA reinforced with hydroxyapatite showed favourable bone tissue adaptation response with no evidence of an undesirable chronic inflammatory response after an implantation period up to 12 months in white rabbits. Bone was rapidly formed close to the material and subsequently becomes highly organized, with up to 80% of the implant surface lying in direct apposition to new bone. The material showed no conclusive evidence of extensive structural breakdown *in vivo* during the implantation period of the study. PHA has favourable characteristics for the potential construction of temporary scaffold for regeneration of bone tissue (Doyle et al., 1991). Absorbable, nonwoven patches made from PHA were implanted as transannular patches into the right ventricular outflow tract and pulmonary artery in weanling sheep. Regeneration of a neointima and a neomedial, comparable to native arterial tissue was observed in the test group. In the control group, a neointimal layer was

present but no neomedia comparable to native arterial tissue. The regenerated vessel had structural and biochemical qualities in common with the native pulmonary artery (Malm et al., 1994). A vascular autograft made of PGA/PHA blend with the outer part of the conduit made of three layers of nonporous PHA and the inner part with randomly arrayed fibres of nonwoven PGA mesh was introduced in lambs to evaluate whether the conduit withstand systemic pressure and can be used to create a vascular autograft for use in the aortic position. Morphological examination demonstrated no early thrombosis in these grafts and tissue formation was noted as early as 10 days after implantation. The increased cell density and collagen formation associated with changes in mechanical properties suggested that favourable biological events are on-going within the graft maintained by the polymeric scaffold (Shum-Tim et al., 1999). PHA conduits were used to bridge a 10-mm gap in the rat sciatic nerve. The growth of Schwann cells enhanced the axonal regeneration distance and no deleterious immune response was observed. The study demonstrated that cultured Schwann cells retain their capacity to enhance axonal regeneration following transplantation to peripheral nerve defect. Transplantation of Schwann cells may be an alternative for nerve gap reconstruction, as they are essential for nerve development and regeneration (Mosahebi et al., 2002). PHA monofilament sutures were used to test healing of muscle-fascial wounds in Wistar rats. The tissue reaction to the implantation of PHA sutures was similar to that occurs during wound process and foreign-body reaction. The reaction of tissues to PHA implants exhibited a transient post-traumatic inflammation (up to four weeks) and the formation of a fibrous capsule less than 200 μm

thick, which became as thin as 40-60 μm after 16 weeks, in the course of reverse development. PHA sutures implanted intramuscularly for a period of one year did not cause any acute vascular reaction at the site of implantation or any adverse events, such as suppurative inflammation, necrosis, calcification of the fibrous capsule or malignant tumor formation (Shishatskaya et al., 2004). A 3D microfibrinous mat of PHA, poly(L-D,L-lactic acid) (P(L-D,L) LA) and poly(glycerol sebacate) (PGS) that allow growth of mesenchymal stem cells (MSCs) from human umbilical cord matrix aligned parallel to each other was prepared mimicking the cell organization in the native myocardium. The micron-sized parallel fibres of the polymer blends were effective in cell alignment and cells have penetrated deep within the mat through the fibre spaces, occupying the whole structure; 8–9 cell layers were obtained. It was shown that biodegradable macroporous tubing was possible to create a thick myocardial patch to replace myocardial infarctions and improve long-term heart function (Kenar et al., 2010).

1.10.4 Aquaculture applications

PHA was studied for its immunostimulatory and dietary efficiency as feed for variety of fishes and other invertebrates in aquaculture. A preliminary study was performed to evaluate the importance of PHA as a protecting agent against pathogenic *Vibrio campbellii* in aquaculture. The addition of PHA particles to the culture system of *Artemia franciscana* resulted in significantly prolonged survival of the shrimp. This study is the first report showing the use of bacterial storage compound PHA to control bacterial infections. The use of PHA might constitute an

ecologically and economically sustainable alternative strategy to fight infections in aquaculture. This approach increased the survival up to 73% upon infection with the pathogen *V. campbellii*. PHA particles were partially degraded in the shrimp gut and the fatty acid produced, protected the shrimp from the pathogen in two ways, i.e. by providing the shrimp with energy (resulting in a gut epithelium that is more resistant to infection) and by inhibiting the growth of the pathogen (Defoirdt et al., 2007). In another study, the use of PHA-accumulating bacteria as a bio-control strategy for aquaculture was investigated. The addition of PHA producing strain of *Brachymonas denitrificans* from the activated sludge enhanced the survival of *Artemia* challenged with *V. campbellii* LMG 21363. It was found that the addition of PHA accumulating enrichment culture was less efficient when compared to addition of PHA (amorphous) accumulating pure culture of *B. denitrificans* in enhancing the survival rates of shrimp (Halet et al., 2007). The use of PHA in fish feed of juvenile European sea bass, *Dicentrarchus labrax* increased fish weight and growth performance. The supplementation of PHA in the feed at 2% and 5% (w/w) was observed to have a positive influence on the average weight gain of the sea bass juveniles. During the rearing period of 6 weeks, the average fish weight gained to 243% and 271% respectively, relative to 216% for the 0% PHA treatment group (De Schryver et al., 2010). The effect of PHA on the culture performance of larvae of the giant freshwater prawn *Macrobrachium rosenbergii* was studied. PHA particles were fed to *A. nauplii* which were used as feed for larvae of *M. rosenbergii*. From the experiment, it was found that larvae with PHA-containing *A. nauplii* significantly improved larval survival.

Feeding larvae with crystalline PHA containing *A. nauplii* resulted in significantly lower levels of total bacteria and *Vibrio* count. When the combination of PHA and a lipid emulsion rich in highly unsaturated fatty acids was studied, the highest larval survival was noted in the treatment with addition of both PHA and the emulsion. The treatments with PHA only and lipid emulsion only also significantly increased the survival of the larvae, though less pronounced than in the treatment with both additives. The application of PHA in aquaculture larval rearing, or more specifically in prawn larval production, may be constrained due to the current high cost of commercial PHA products (Nhan et al., 2010). In a study to investigate the immunostimulatory efficacy of poly3-hydroxybutyrate -co-3-hydroxyvalerate ([P (3-HB-co-3-HV)]), a class of short chain co-polymer produced by *B. thuringiensis* A102 strain on the immune system of *Oreochromis mossambicus* against virulent *Aeromonas hydrophila*, showed an overall stimulation of all the immune mechanisms tested and was protective against disease challenge as well. The specific immune response was measured in terms of antibody response to sheep red blood cells and the nonspecific immune mechanisms were analysed in terms of serum lysozyme activity, total peroxidases activity and antiprotease activity. The efficacy of PHA supplemented diet as a potential immunostimulant was determined by the ability of the fish to survive the experimental challenge with live virulent *A. hydrophila*. The bacterial challenge experiment showed that highest dose of 5% PHA supplementation was more effective than 1% and 3% doses. All the doses tested were found to stimulate both specific and non-specific immune mechanisms. The study concluded that PHA can be used as a potential

immunostimulant in finfish aquaculture (Suguna et al., 2014). A study of PHA producing bacterium *Brevibacterium casei* MSI04 isolated from a marine sponge *Dendrilla nigra* as anti-biofilm or anti-adhesive agent against shrimp pathogenic vibrios –*V. harveyi*, *V. alginolyticus*, *V. vulnificus*, *V. fischeri* and *V. parahaemolyticus* was evaluated. This is a first report on anti-adhesive activity of PHA against prominent *Vibrio* pathogens in shrimp aquaculture. The effect of PHA on biofilm formation of *Vibrios* was studied using microtitre plate assay, light microscopic and phase contrast microscopic observation. The highest anti-adhesive activity up to 96% was recorded against *V. vulnificus* and *V. fischeri*, followed by 92% against *V. parahaemolyticus* and *V. alginolyticus* and 88% against *V. harveyi*. The highest reduction of adhesion (88-96%) was observed with 600 µg of PHA. Results of microtitre plate assay suggested that when the surface was covered by PHA, the adhesion was inhibited effectively. Hence PHA can be coated on shrimp feed to reduce the colonization capacity of *Vibrio* on the farmed shrimp as well as in the farm environment (Kiran et al., 2014). To assess the beneficial effects of amorphous PHA supplied through the live feed *Artemia* on *M. rosenbergii* larvae, a non-challenged growth test and a challenge test using *V. harveyi* was performed. Supplying PHA-accumulated bacteria through live feed to *M. rosenbergii* larvae resulted in positive effects in terms of growth and survival as well as in terms of protection against pathogenic infections against *Vibrio*. This particular study has provided the first practical information on the application of amorphous PHA supplied through live feed for crustacean larviculture (Thai et al., 2014). The effect of PHA delivery on the survival, growth and metamorphosis of blue mussel larvae

was studied. PHA was supplied in crystalline and amorphous form at different concentrations to the culture water of blue mussel larvae. The supplementation of amorphous PHA at a concentration of 1 mg L^{-1} showed a positive effect on the larval survival. This is because amorphous PHA is more biodegradable than its crystalline form (Van Hung et al., 2015).

1.11 Future perspective

PHAs symbolize a future sustainable bio-based plastic because of their favourable properties. The selection of wild type bacteria that can utilize inexpensive carbon source and PHA optimization can result in cost-effective polymer production. PHAs have a diverse structural composition which provides thermo processibility, flexible mechanical property, biodegradability and biocompatibility that can be used to fulfil wide range of applications in medical, industrial, aquaculture and health care. In medical field, *in vivo* PHA implantation has not shown any carcinogenicity and their degradation products can be rapidly removed by β -oxidation. Several attempts had been made to improve various physico-mechanical properties of PHAs to augment their applications such as by blending with hydroxyapatite for improved strength for bone tissue engineering, by random co-polymerization to improve flexibility for soft tissue engineering, by block co-polymerization or chemical modification to improve cell attachment and proliferation for various tissue engineering applications. Chemical modifications of PHAs alter their mechanical properties, surface structure, amphiphilic character and rate of degradation thereby reforming the polymer as functional PHAs, which are more

suitable for a wide range of commercial applications. Chemical modifications allow the incorporation of specific functional groups to PHAs that are not easily achievable through biological routes. In future, increasing investigations will be directed towards the improvement of PHA production and their functional modifications to transform this microbial storage granule to multifunctional biomaterial.

1.12 Objectives of the study

In view of the attempts to identify novel PHA producing bacteria from marine environments and to optimize process factors for cost-effective PHA production, the following objectives were undertaken:

- 1) Isolation, screening and identification of polyhydroxyalkanoate producing bacteria from marine environments.
- 2) Production and characterization of polyhydroxybutyrate from *Vibrio harveyi* MCCB 284 utilizing glycerol as carbon source.
- 3) Biosynthesis and characterization of polyhydroxyalkanoate from marine *Bacillus cereus* MCCB 281 utilizing glycerol as carbon source.
- 4) Biocompatibility of polyhydroxybutyrate-co-hydroxyvalerate from *Bacillus cereus* MCCB 281 for medical applications.

.....❧.....

ISOLATION, SCREENING AND IDENTIFICATION OF POLYHYDROXYALKANOATE PRODUCING BACTERIA FROM MARINE ENVIRONMENTS

- 2.1 *Introduction*
- 2.2 *Materials and methods*
- 2.3 *Results and discussion*
- 2.4 *Conclusion*

2.1 Introduction

Over the past few years, good progress has been made in the marine microbial research due to the rich biodiversity and potential of marine microbes to produce various bioactive compounds which have high value in pharmaceutical and biotechnological applications. Marine microorganisms occur in vast numbers and represent a huge genetic diversity as ocean water contains up to one million microorganisms per millilitre and several thousand microbial types. Microbes are higher in magnitude in coastal waters with their higher productivity and higher load of organic matter and nutrients. Marine microorganisms plays crucial role in all biochemical cycles and functioning of different marine ecosystems. They are responsible for the degradation of organic matter in the ocean and for maintaining the balance between produced and fixed carbon dioxide. Marine phototrophic microorganisms such as cyanobacteria, diatoms and phytoplankton are

responsible for more than 50% of the oxygen production on Earth. Because of the complex nature of marine environment, marine microorganisms, such as bacteria, fungi, microalgae etc. have developed complex biochemical and physiological capabilities with which they can adapt to extreme and unfavourable conditions of marine environment, and also possess the potential for the production of metabolites that could not be seen in their terrestrial counterparts. They live in a biologically competitive environment with unique conditions of salinity, pressure, temperature, light, oxygen, pH and nutrients (Biswas et al., 2016). That is why most bacteria isolated from seawater are Gram negative rods, as it is assumed that the outer membrane structure of these bacteria is evolutionarily adapted to aquatic environmental constituents (Soliev et al., 2011).

Marine bacteria have now become an important area of study in the search for novel microbial products. Cultivation of these microbes in the laboratory can be challenging due to the inability of different growth media to adequately mimic the natural environments. In addition, many species are not viable, or may require long incubation period for sufficient growth. Previous studies have successfully cultured novel microbes using encapsulation method, diffusion growth chambers, casein and microorganism specific agars and media enriched with selective antibiotics (Zengler et al., 2002). The incorporation of seawater in various agar media and the development of other specialized growth media have been successful in establishing the growth of fastidious microorganisms (Christensen and Martin, 2017). However, conventional serial dilution method followed by standard plating techniques is still being used for the

isolation of culturable marine bacteria. ZoBell's marine agar formulated by ZoBell (ZoBell, 1941) was found to have a composition that mimics seawater and thus enables the growth of marine bacteria abundantly. This medium has been mostly used for the growth and enumeration of marine bacteria (Arun et al., 2009; Kiran et al., 2014; Shrivastav et al., 2010; Wecker et al., 2015).

Identification of bacteria using molecular method of 16S rRNA gene sequencing is based on the presence of bacterial species-specific variable regions. The 16S rRNA gene sequence is about 1,550 bp long and is composed of hypervariable region flanked by conserved segments. These hypervariable regions are used to identify phylogenetic characteristics of microorganisms and thus, the 16S rRNA gene sequence is the most widely used marker gene for profiling bacterial communities (Tringe and Hugenholtz, 2008). The gene is large enough with sufficient interspecific polymorphisms to provide distinguishing and statistically valid measurements. Universal primers are usually chosen as complementary to the conserved regions at the beginning of the gene and at either the 540-bp region or at the end of the whole sequence and the sequence of the variable region in between is used for the comparative taxonomy (Chen et al., 1989). The comparison of 16S rRNA gene sequences has been recognized as an invaluable tool for confirming bacterial species identity but not for strain differentiation as the sequences show limited intraspecific variations (Drancourt et al., 2000).

There are different methods adopted for screening of PHA producing bacteria. The methods most widely used for detecting PHAs are staining

techniques using Nile red (Spiekermann et al., 1999), Nile blue A (Ostle and Holt, 1982) and Sudan Black (Burdon, 1946). A viable colony staining method based on the direct inclusion of the lipophilic dye Nile red in the agar medium such that the growth of the cells are not affected and the presence of PHA granules in the bacterial colonies can be directly monitored was developed. Nile red dye could diffuse into the cytoplasm of the bacteria during growth and subsequently into the PHA inclusions. PHA producing bacteria showed fluorescence under UV radiation when cultivated under PHA accumulating conditions. Therefore, the direct addition of dye to the medium provided a tool to discriminate between PHA producers and non-producers without killing the cells (Spiekermann et al., 1999). In Nile blue A and Sudan black staining methods, the bacteria grown under PHA accumulating conditions are heat fixed and stained to visualize the presence of PHA granules inside the cells. Sudan black is non-specific to PHA as it also stains other lipid granules inside the cells whereas Nile blue A and Nile red are more specific than Sudan black for PHA detection (Shamala et al., 2003). The other methods used for identifying PHA producing bacteria is the PCR amplification of PHA synthase gene using degenerate primers (Shamala et al., 2003; Sheu et al., 2000). This technique is a rapid and accurate detection system for screening large numbers of environmental isolates. However, this technique leads to formation of non-specific PCR amplified products and absence of PCR products due to the use of degenerate primers (Higuchi-Takeuchi et al., 2016).

In this study, PHA producing bacteria were isolated from marine samples using ZoBell's marine agar medium by standard plating techniques.

Screening of PHA producers was done using Nile red staining techniques. The morphological characteristics and 16S rRNA gene sequencing was performed for the identification of PHA producing isolates. PHA production was studied with glucose as carbon source. The selected isolates were studied for optimization of PHA production and the extracted polymer was characterized using different techniques in the later chapters.

2.2 Materials and methods

2.2.1 Sample collection

- 1) Tunicate samples (*Acsidia nigra*) were collected from Vizhinjam Bay, Thiruvananthapuram, Kerala (8°22'N, 76°59'E) by SCUBA diving, washed with sterile sea water and stored in polythene cover immersed in ice for analysis.
- 2) Water samples were collected on-board on Fishery Oceanographic Research Vessel (FORV) Sagar Sampada (Cruise No.321), Ministry of Earth Sciences, Government of India using conductivity temperature depth sensors (CTD) from 16 stations at various depths along the south west coast of India. The details of sampling locations were provided in Table 2.1. The samples were collected in sterile tubes and added sterile glycerol to reach 20% (v/v) and stored in -20 °C for analysis.

2.2.2 Isolation and sub-culturing of bacteria from marine environment

The surface of the tunicate samples was washed with sterile sea water and body of the tunicate was cut into small pieces and homogenized using mortar and pestle. The resultant homogenate was serially diluted in sterile sea water and dilutions 10^{-2} , 10^{-3} and 10^{-4} were spread on ZoBell's marine agar 2216 E plates (HiMedia, India) and incubated at 28 °C for 7 days.

The water samples were serially diluted in sterile sea water and dilutions 10^{-2} , 10^{-3} , 10^{-4} and 10^{-5} were spread on ZoBell's marine agar plates and incubated at 28 °C for 7 days. Morphologically distinct colonies were picked with the help of sterile loop, streaked on ZoBell's plates and incubated at 28 °C for 48 h to obtain pure colonies of the isolates. All the isolates were stored in ZoBell's agar slants at room temperature.

2.2.3 Screening of PHA producing bacteria

2.2.3.1 Nile red fluorescence assay

The fluorescence plate assay is a primary screening method used for detecting PHA production. This was a sensitive and viable colony staining method used for the detection of PHAs at any time during the growth of bacteria. For this, pure culture isolates were streaked on ZoBell's agar plates supplemented with Nile red dye and carbon source (20 g L⁻¹ glucose) and incubated at 28 °C for 48 h. Nile red dye (HiMedia, India) was dissolved at a stock concentration of 0.25 mg mL⁻¹ in DMSO and added at a final concentration of 0.5 µg mL⁻¹ in the agar medium (Spiekermann et al., 1999). The plates were then exposed to UV light (312 nm in UV transilluminator) to detect the accumulation of PHAs and other lipid storage granules inside the

bacterial cells. The intensity of fluorescence produced was directly proportional to the amount of PHA accumulated.

Table 2.1 The details of sampling location along the southwest coast of India

| Sl. No. | Latitude (N) | Longitude (E) | Station depth (m) | Sample depth (m) | Temperature (°C) | Salinity (ppt) |
|---------|--------------|---------------|-------------------|------------------|------------------|----------------|
| 1 | 9 57.701 | 75 59.904 | 34 | 2 | 29.03 | 32.65 |
| | | | | 29 | 29.23 | 34.37 |
| 2 | 9 57.656 | 75 50.472 | 52 | 2 | 28.99 | 32.85 |
| | | | | 46 | 28.86 | 35.19 |
| 3 | 9 57.990 | 75 38.664 | 102 | 2 | 29.00 | 33.62 |
| | | | | 97 | 26.01 | 35.54 |
| 4 | 9 58.448 | 75 35.357 | 228 | 2 | 29.00 | 33.74 |
| | | | | 97 | 26.01 | 35.82 |
| 5 | 9 58.177 | 75 28.985 | 1070 | 2 | 29.10 | 34.85 |
| 6 | 9 58.215 | 75 28.999 | 2523 | 2 | 29.41 | 35.46 |
| | | | | 35 | 29.29 | 35.50 |
| | | | | 70 | 26.99 | 35.51 |
| | | | | 205 | 15.10 | 35.16 |
| 7 | 7 59.914 | 75 00.538 | 2847 | 2 | 28.97 | 34.97 |
| | | | | 35 | 28.35 | 35.34 |
| | | | | 225 | 14.91 | 35.14 |
| 8 | 7 53.198 | 75 68.464 | 1654 | 2 | 29.04 | 32.62 |
| | | | | 40 | 29.27 | 35.30 |
| | | | | 215 | 15.09 | 35.09 |
| 9 | 7 53.198 | 75 08.464 | 1819 | 4 | 28.70 | 31.81 |
| | | | | 28 | 28.58 | 32.06 |
| | | | | 103 | 27.98 | 35.69 |
| | | | | 200 | 15.01 | 35.07 |
| 10 | 7 13.858 | 76 32.312 | 1817 | 4 | 28.57 | 31.87 |
| 11 | 7 26.443 | 76 54.754 | 124 | 4 | 28.83 | 30.44 |
| | | | | 10 | 28.83 | 31.99 |
| | | | | 20 | 28.62 | 32.22 |
| | | | | 56 | 29.16 | 34.41 |
| | | | | 96 | 27.48 | 35.43 |
| | | | | 100 | 24.44 | 35.30 |
| 12 | 7 59.373 | 77 18.765 | 48 | 3 | 28.83 | 33.77 |
| | | | | 44 | 28.71 | 32.05 |
| 13 | 7 58.688 | 76 44.809 | 144 | 4 | 28.92 | 33.73 |
| | | | | 120 | 18.81 | 35.03 |
| 14 | 8 03.240 | 76 23.660 | 1153 | 4 | 28.95 | 34.40 |
| | | | | 60 | 28.50 | 35.62 |
| | | | | 195 | 15.18 | 35.06 |
| 15 | 8 11.430 | 75 54.931 | 1460 | 4 | 29.17 | 34.96 |
| 16 | 9 15.100 | 75 45.700 | 368 | 2 | 28.97 | 32.30 |

2.2.3.2 Nile red staining

Secondary screening was done by Nile red staining. The pure cultures were grown in ZoBell's plates supplemented with carbon source (20 g L⁻¹ glucose) and incubated at 28 °C for 48 h for PHA accumulation. Cells were heat fixed and stained with Nile red dye (10 µg mL⁻¹ in acetone) for 30 min at 80 °C and then de-stained with 8% acetic acid, washed with distilled water and dried (Ostle and Holt, 1982). The cells were observed in fluorescence microscope under oil immersion (Olympus, Japan). All the PHA positive isolates were stored as glycerol stocks in -80°C and as agar slants overlaid with sterile liquid paraffin at room temperature.

2.2.4 PHA production

For PHA production, inoculum was prepared by growing the cultures on ZoBell's marine agar slants at 28 °C. Cells were dislodged from the slant using sterile inoculation loop, suspended in 2 mL sterile medium and absorbance measured in UV-Visible spectrophotometer (Shimadzu UV-1601, Japan) at a wavelength of 600 nm. The optical density of the isolates was adjusted to 1.0 using sterile medium prior to inoculation. A two stage fermentation strategy was employed for PHA production studies, in which the isolate was allowed to grow in the production medium for 24 h at 28 °C for biomass formation and then carbon source at a concentration of 2% (w/v) was added and further incubated for 48 h at 28 °C for PHA accumulation. An aliquot of 50 mL production medium (composition: Peptone- 5 g L⁻¹, Yeast extract- 1 g L⁻¹ in 30 ppt sea water, pH 7.5) was inoculated with 0.1% (v/v) of each

isolate and incubated at 28 °C for 24 h at 150 rpm for biomass production. Carbon source (20 g L⁻¹ glucose) was added to medium and incubated for 48 h for PHA accumulation. The optical density (OD 600) was measured every 24 h to monitor the growth of the isolates.

To determine cell dry weight (CDW in g L⁻¹), 10 mL culture was centrifuged at 8000 g for 10 min at 28 °C and cell pellet was washed twice with distilled water to remove salt and media components. The cell pellet was transferred to pre-weighed tube and lyophilized. The experiment was carried out in triplicate. The PHA content was measured as percentage based on cell dry weight.

2.2.5 PHA estimation

For PHA estimation, 1 mL of conc.H₂SO₄ was added to lyophilized cell pellet and incubated at 100 °C for 15 min. The polymer was converted into crotonic acid which turned into brown colour after the addition of acid. The absorbance of crotonic acid was measured at 235 nm using UV-Visible spectrophotometer (Shimadzu, Japan) and the amount of PHA produced was calculated from crotonic acid standard curve (Law and Slepecky, 1961).

2.2.6 Identification of PHA producing bacteria

2.2.6.1 Biochemical characterization

The biochemical characterization of the bacterial isolates that exhibited more than 50 % PHA production based on cell dry weight was performed as described in *Bergey's Manual of Determinative Bacteriology*.

Morphological identification of the isolates was done by Gram staining. The various biochemical tests performed were described in detail.

(a) Kovac's oxidase test

This test was used to determine the presence of cytochrome c oxidases capable of using oxygen as the terminal electron acceptor. Fresh cultures of bacteria grown on ZoBell's marine agar slant were used. A platinum loop was used to transfer a loop full of inoculum and make a smear on a filter paper pre-moistened with 2 -3 drops of freshly prepared 1% (v/v) tetramethyl-*p* phenylenediamine dichloride (TMPD). A positive reaction was indicated by the presence of purple colour within 10 s, indicating the formation of indophenol.

(b) Catalase test

Catalase mediates the breakdown of hydrogen peroxide (H_2O_2) into oxygen and water thereby, neutralizing toxic forms of oxygen metabolites. Catalase production was demonstrated by adding 1-2 drops of 3% H_2O_2 to fresh culture of test organisms in ZoBell's broth placed on a clean and dry glass slide. The rapid evolution of oxygen in the form of gas bubbles indicates a positive result.

(c) Nitrate reduction test

This test was done to detect the presence of nitrate reductase enzyme which causes the reduction of nitrate (NO_3) to nitrite (NO_2). The isolates were inoculated in nitrate broth (composition: Peptone- 5 g L⁻¹, Yeast extract-3 g L⁻¹, Beef extract-1 g L⁻¹, Potassium

nitrate-1 g L⁻¹, pH 7.5) and incubated at 28 °C for 48 h. The presence of nitrite was determined by the addition 0.5 mL of reagent A (Sulphanilic acid- 1% in 5N acetic acid), followed by 0.5 mL of reagent B (α -naphthylamine- 0.6% in 5N acetic acid) to 5 mL of the culture. The development of red colour indicated that the nitrate had been reduced to nitrite.

(d) Indole production test

Bacteria produce indole by decomposition of tryptophan, which was present in tryptone broth. The isolates were inoculated in tryptone broth (composition: Tryptone-1.5 g L⁻¹, NaCl-5 g L⁻¹, pH-7.5), incubated at 28 °C for 48 h and 0.5 mL of Kovac's reagent (ρ -dimethyl amino benzaldehyde- 5 g, amyl alcohol -75 mL, con. HCl- 25 mL) was added to each tube. The liberated indole reacts with Kovac's reagent to produce red colour on top of the medium.

(e) Methyl red and Voges Proskauer test

The isolates were inoculated in MR-VP broth (HiMedia, India) and incubated for 24 h at 28 °C. Methyl red test detects the production of acid during the glucose fermentation. A few drops of methyl red indicator were added to the culture and a resultant red colour was considered positive. The indicator was prepared by dissolving 0.1 g methyl red in 300 mL 95% ethyl alcohol, which was then diluted to 500 mL with distilled water.

In Voges Proskauer test, the ability of bacteria to produce acetylmethyl carbinol from glucose fermentation was determined. If present,

acetylmethyl carbinol was converted to diacetyl in the presence of α -naphthol, strong alkali (40% KOH) and atmospheric oxygen, which in turn reacts with the peptone constituents in medium to produce a pink colour. An aliquot of 0.6 mL of 5% α -naphthol in absolute ethanol was added to the culture, followed by 0.2 mL of 40% KOH and mixed well. A positive reaction was indicated by the presence of pink colour in 2-5 min.

(f) Citrate utilization test

The ability of isolates to utilise citrate as the sole source of carbon was tested using Simmon's citrate agar medium (HiMedia, India). The bacterial isolates were streaked on Simmon's citrate agar slants and incubated for 48 h at 28 °C. Utilization of citrate results in an alkaline reaction, which changes the colour of the medium from green to blue in presence of bromothymol blue as indicator.

(g) Starch hydrolysis

ZoBell's marine agar containing 1% (w/v) soluble starch was used for testing starch hydrolysis. The bacterial isolates to be tested were spotted on agar plates and incubated at 28 °C for 48 h. The plates were flooded with Gram's iodine solution (1% iodine and 2% KI in distilled water). Presence of halo around the colonies indicated positive result.

(h) Gelatin hydrolysis

ZoBell's marine agar incorporated with 2% (w/v) gelatin was used for demonstration of gelatinase activity. The bacterial isolates were

spot inoculated on agar plates and incubated at 28 °C for 24-48 h. The plates were flooded with mercuric chloride solution (5% HgCl₂ in 20% conc. HCl). Presence of clear zone around the colonies indicated positive result.

(i) Acid production from sugars

Hugh and Leifson's basal medium (composition: Peptone- 2 g L⁻¹, NaCl- 5 g L⁻¹, K₂HPO₄- 0.3 g L⁻¹, 30 mL phenol red 1% aqueous solution at pH 7.3) was used for testing acid production from various sugars. The basal medium was autoclaved at 15 lbs for 15 min at 121 °C and the sugars (glucose, sucrose, fructose, maltose, lactose, xylose, arabinose, mannitol, galactose, trehalose, rhamnose, glycerol and erythritol) were autoclaved separately at 10 lbs for 10 min and added to the basal medium at a final concentration of 0.1% (w/v). The tubes were inoculated and incubated at 28 °C for 72 h. The production of acid results in change of pink colour of phenol red indicator to yellow.

2.2.6.2 16S rRNA gene sequencing

2.2.6.2.1 Genomic DNA extraction

Genomic DNA of the selected PHA producing isolates was extracted following (Cheng and Jiang, 2006) method. Briefly, 2 mL of overnight culture was centrifuged at 8000 g for 2 min at 4 °C to pellet cells. The supernatant was removed, the cells were washed twice with 400 µL STE buffer (100 mM NaCl, 10 mM Tris-HCl, 1 mM EDTA, pH 8.0) and centrifuged at 8000 g for 2 min. The pellet was resuspended in

200 μL milliq and 100 μL Tris-saturated phenol (pH 8.0) was added and vortexed for 60 s for cell lysis. The sample was subsequently centrifuged at 13,000 g for 5 min at 4 °C to separate the aqueous phase from the organic phase. An aliquot of 160 μL upper aqueous phase was transferred to a clean 1.5 mL tube, 40 μL milliq was added to make up to 200 μL , mixed with 100 μL chloroform and centrifuged at 13,000 g for 5 min at 4 °C. This step was repeated 2-3 times to remove proteins. To the clear aqueous phase, 5 μL RNase (10 mg mL⁻¹) was added and incubated at 37 °C for 10 min for RNA digestion. Then 100 μL chloroform was added to the tube, mixed well and centrifuged at 13,000 g for 5 min at 4 °C. Aliquots of 100-150 μL upper aqueous phase was transferred to a clean 1.5 mL tube which have the purified DNA. The genomic DNA was separated on 1% agarose gel prepared in 1X TAE buffer and stained with ethidium bromide. Gel electrophoresis was carried out at 70 V in an electrophoresis apparatus. The gel was visualized under UV light in Gel documentation system (BIORAD Gel Doc™ XR+, USA) with Image lab™ software.

2.2.6.2.2 PCR amplification of genomic DNA

16S rRNA bacterial marker gene was amplified by PCR using universal primers (27F- GAGTTTGATCCTGGCTCA-) and (1492R-ACGGCTACCTTGTTACGACTT-). PCR reaction mixture (25 μL) contain 1 μL genomic DNA, 12.5 μL emerald mix (Takara, Japan), 1.25 μL each of 27F and 1492R primers and the remaining volume was made up with sterile milliq. PCR condition for gene amplification was initial denaturation at 94 °C for 3 min, followed by 29 cycles of denaturation at

94 °C for 30 s, annealing at 58 °C for 40 s, extension at 72 °C for 1 min and final extension at 72 °C for 5 min. The PCR product was separated on 1% agarose gel prepared in 1X TAE buffer, stained with ethidium bromide and visualized using gel documentation system.

2.2.6.2.3 DNA sequencing and phylogenetic analysis

The amplified products were sequenced based on Sanger sequencing method using ABI 3730xl DNA Analyzer at SciGenom Labs, Cochin, Kerala. The partial 16S rRNA forward and reverse sequences were aligned using software Gene Tool and the nucleotide sequences were compared within nucleotide collection database (nr/nt) available in NCBI using BLASTn. The bacterial species showing the highest similarity with query sequence was identified and the nucleotide sequences were deposited in GenBank database. Phylogenetic analysis was performed using Neighbour – Joining method (Saitou and Nei, 1987) with bootstrapping for 1000 replicates to assess the stability of tree topology (Felsenstein, 1985) with MEGA 6.0 software (Tamura et al., 2013). For this, a set of homologous sequences that showed highest similarity with the query sequence was obtained from NCBI database and were aligned using CLUSTAL W algorithm.

2.2.7 Bacterial growth curve of selected isolates

The selected isolates were grown in ZoBell's marine broth to analyse the growth phases. The growth was observed for 48 h. Samples were withdrawn at regular intervals of time and optical density (OD) was measured at 600 nm using UV-visible spectrophotometer. The growth curve was plotted with OD at 600 nm against incubation time. All the

experiments were carried out in triplicates. From the growth curve, the generation time (t_d) and specific growth rate (μ) of the isolates was calculated.

2.3 Results and discussion

2.3.1 Isolation and screening of PHA producing bacteria

A total of 25 bacterial isolates were obtained from the tunicate samples, of which, three exhibited fluorescence under UV light when grown in ZoBell's medium supplemented with Nile red dye and glucose as carbon source indicating PHA production. A total of 150 bacterial isolates were obtained from water samples from various stations along the south west coast of India, of which, 30 showed fluorescence indicating PHA accumulation in presence of glucose (Fig. 2.1a). All the isolates selected after primary screening showed fluorescence in Nile red staining, thereby confirming PHA accumulation (Fig. 2.1b). During Nile red staining, PHA granules appeared as bright orange individual granules.

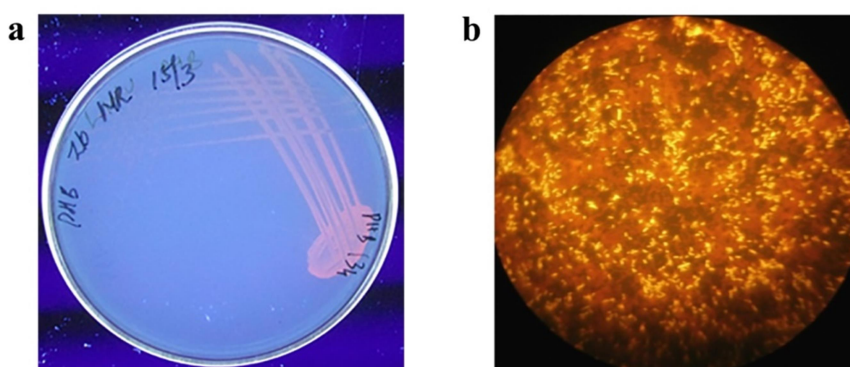


Fig. 2.1 (a) Fluorescence of PHA producing bacteria in ZoBell's marine agar supplemented with Nile red dye and glucose as carbon source during primary screening (b) Secondary screening of PHA producing bacteria by Nile red staining

2.3.2 PHA production

Only 3 isolates obtained from tunicate samples showed PHA production in presence of glucose as carbon source. From the water samples, 16 out of 30 isolates were selected for PHA production in presence of glucose and the remaining isolates lost viability after sub-culturing. The isolates were incubated at 28 °C, 150 rpm and PHA production was determined after 72 h incubation. PHA content based on CDW, expressed in %, was calculated from crotonic acid assay method. PHA accumulation of the isolates, their CDW and PHA content after 72 h incubation with glucose as carbon source were represented in Table 2.2. A maximum CDW of 2 g L⁻¹ was produced by isolate PHB 339 with 54% PHA content and a minimum CDW of 0.69 g L⁻¹ was produced by isolate PHB 340 with 29% PHA content.

Three isolates PHB 345, 346 and 347 designated as MCCB 283, 284 and 285 respectively isolated from the tunicate samples and four isolates PHB 334, 337, 339 and 342 designated as MCCB 278, 279, 281 and 282 respectively from water samples showed more than 50 % PHA production based on CDW. These isolates were selected for further phenotypic and genotypic characterization.

Table 2.2 PHA production based on cell dry weight from different bacterial isolates obtained from tunicates and water samples

| Isolates | Cell dry weight (CDW) g L ⁻¹ | PHA content based on CDW (% w/w) |
|----------|---|----------------------------------|
| PHB 329 | 1.22 ± 0.4 | 45.32 ± 1.3 |
| PHB 330 | 1.40 ± 1.2 | 32.54 ± 1.5 |
| PHB 331 | 1.02 ± 0.3 | 47.77 ± 2.1 |
| PHB 332 | 1.41 ± 0.2 | 48.67 ± 1.9 |
| PHB 333 | 1.99 ± 0.5 | 42.69 ± 1.8 |
| PHB 334 | 1.71 ± 0.7 | 54.28 ± 2.3 |
| PHB 335 | 1.67 ± 0.6 | 39.57 ± 2.5 |
| PHB 336 | 0.83 ± 0.3 | 46.43 ± 1.5 |
| PHB 337 | 1.91 ± 1.3 | 51.35 ± 3.3 |
| PHB 338 | 0.43 ± 0.5 | 45.21 ± 1.7 |
| PHB 339 | 2.02 ± 0.3 | 54.32 ± 1.8 |
| PHB 340 | 0.69 ± 0.4 | 29.53 ± 1.5 |
| PHB 341 | 1.10 ± 0.2 | 49.21 ± 2.2 |
| PHB 342 | 1.72 ± 0.2 | 53.40 ± 2.5 |
| PHB 343 | 0.93 ± 0.7 | 43.76 ± 2.4 |
| PHB 344 | 1.04 ± 0.5 | 47.53 ± 1.5 |
| PHB 345 | 1.21 ± 0.8 | 55.43 ± 2.7 |
| PHB 346 | 1.28 ± 0.5 | 58.30 ± 0.6 |
| PHB 347 | 1.71 ± 0.4 | 51.34 ± 1.5 |

Data shown as mean ± SD (n=3)

2.3.3 Biochemical characterization

The results of different biochemical tests performed to study the phenotypic characteristics of the seven potent PHA producing bacteria were summarised in Table 2.3.

Table 2.3 Biochemical tests of the selected PHA producing bacterial isolates

| Tests | MCCB | | | | | | |
|-----------------------------|------|-----|-----|-----|-----|-----|-----|
| | 278 | 279 | 281 | 282 | 283 | 284 | 285 |
| Gram staining | - | + | + | - | - | - | - |
| Catalase | + | + | + | + | + | + | + |
| Oxidase | + | + | + | + | + | + | + |
| Indole | - | - | - | - | + | + | + |
| Methyl red | - | + | + | - | + | + | + |
| Voges-Proskauer | - | - | - | - | - | - | - |
| Citrate utilization | - | + | + | - | + | + | + |
| Nitrate reduction | - | + | + | + | + | + | + |
| Starch hydrolysis | + | + | + | - | + | + | + |
| Gelatin hydrolysis | + | + | + | - | + | + | + |
| Acid production from sugars | | | | | | | |
| Glucose | + | + | + | + | + | + | + |
| Sucrose | + | - | + | + | - | + | - |
| Fructose | + | + | + | + | + | + | + |
| Lactose | - | - | - | - | - | + | - |
| Maltose | + | + | + | + | - | + | - |
| Xylose | - | - | - | - | - | + | - |
| Arabinose | - | - | - | - | - | - | - |
| Mannitol | + | - | - | + | - | + | + |
| Galactose | - | - | - | - | - | + | + |
| Trehalose | - | + | + | + | + | + | + |
| Rhamnose | - | - | - | - | - | - | - |
| Glycerol | + | + | + | + | + | + | + |
| Erythritol | - | - | - | - | - | - | - |

All the isolates were rod shaped bacteria. Isolates MCCB 279 and 281 was Gram positive spore forming bacteria and remaining five isolates were Gram negative non-spore forming. All isolates were positive for both oxidase and catalase tests. Isolates MCCB 283, 284 and 285 were positive for indole test. All isolates were positive for starch and gelatin

hydrolysis except isolate MCCB 282. Similarly, all isolates were positive for nitrate reduction except MCCB 278. All showed negative result for Voges-Proskauer test. Isolates MCCB 279, 281, 283 and 284 were positive for both methyl red and citrate utilization tests. All isolates produced acid from both glucose and glycerol whereas, none of them showed acid production from lactose, arabinose, rhamnose and erythritol.

2.3.4 Identification of bacteria by 16S rRNA gene sequencing and Phylogenetic analysis

16S rRNA sequencing is a reliable method useful in identification of bacteria providing genus and species level identification in most cases. In addition, 16S rRNA sequencing is most useful in the context of bacterial species that are often difficult to identify with phenotypic tests (Woo et al., 2008). For this, genomic DNA of the PHA positive isolates was extracted (Fig. 2.2) and 16S rRNA gene was amplified using universal primers yielding a PCR product of approximately 1500 bp (Fig. 2.3). The nucleotide sequences were compared with sequences available in NCBI database using BLAST algorithm. The sequences were deposited in GenBank database and accession numbers obtained. The bacterial identification and GenBank accession numbers of the isolates were described in Table 2.4. Based on 16S rRNA gene sequencing, the isolates MCCB 283, 284 and 285 obtained from tunicate samples were identified as *Vibrio rotiferianus*, *Vibrio harveyi* and *Vibrio jascicida* respectively. The isolates MCCB 278, 279, 281 and 282 obtained from water samples were identified as *Alteromonas macleodii*, *Bacillus cereus* (MCCB 279 and 281) and *Halomonas meridiana* respectively.

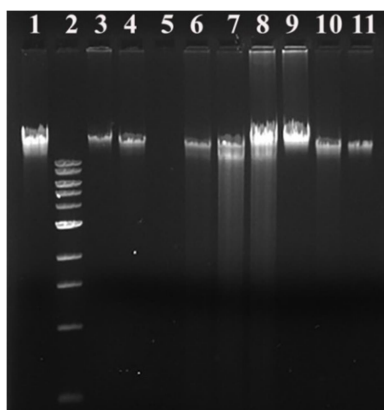


Fig. 2.2 Genomic DNA isolated from PHA producing bacteria according to Cheng and Jiang method. Lane 2- 1 kb DNA ladder; Lane 1, 3 to 11- genomic DNA of isolates

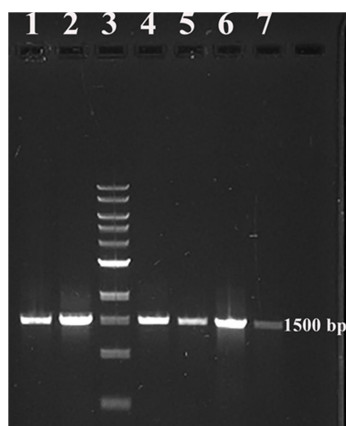


Fig. 2.3 PCR product of 16S rRNA gene amplified using universal primers. Lane 3- 1 kb DNA ladder; Lane 1, 2, 4 to 7- 1500 bp size PCR product

Isolates MCCB 284 (*V. harveyi*) from tunicate samples and MCCB 281(*B. cereus*) from water samples showed the maximum PHA accumulation and were selected for further PHA production studies. Phylogenetic analysis of these isolates was performed using MEGA 6.0 software (Fig. 2.4). *V. harveyi* MCCB 284 showed closest match with

V. harveyi strain FJXPH0612, whereas *B. cereus* MCCB 281 showed 100% similarity to a number of *B. cereus* strains obtained from NCBI.

Table 2.4 Identification of PHA producers isolated from tunicate and water samples

| Isolate numbers | Name of Isolates | % similarity from NCBI database | GenBank Accession Number |
|-----------------|---------------------------------------|---------------------------------|--------------------------|
| 334 | <i>Alteromonas macleodii</i> MCCB 278 | 99 | KR921917 |
| 337 | <i>Bacillus cereus</i> MCCB 279 | 100 | KR921918 |
| 339 | <i>Bacillus cereus</i> MCCB 281 | 99 | KR921920 |
| 342 | <i>Halomonas meridiana</i> MCCB 282 | 99 | KR921921 |
| 345 | <i>Vibrio rotiferianus</i> MCCB 283 | 99 | KR921928 |
| 346 | <i>Vibrio harveyi</i> MCCB 284 | 100 | KR921929 |
| 347 | <i>Vibrio jascicida</i> MCCB 285 | 100 | KR921930 |

Vibrios are highly abundant in aquatic environments, including estuaries, marine coastal waters and sediments (Thompson et al., 2004). *Vibrio* spp. were first among the isolates from marine sediments to be reported as potent PHA producers (Baumann et al., 1971). *V. harveyi* has been previously reported as PHA producer isolated from marine environment (Sun et al., 1994). This was the first report of PHA accumulation in *V. rotiferianus* and *V. jascicida* isolated from tunicates. Other *Vibrio* spp. such as *V. azureus*, *V. proteolyticus* and *V. natriegens* were also reported as PHA producers (Chien et al., 2007; Melba and Ananthan, 2016; Sasidharan et al., 2014). *Vibrio* sp. produces scl-PHAs especially PHB utilizing different sugars as carbon source.

PHB was first discovered in *B. megaterium* by French microbiologist Lemoigne in 1926 (Lemoigne, 1926). *Bacillus* spp. were reported to

accumulate homo-polymers and co-polymers of PHAs utilizing simple, inexpensive and structurally unrelated carbon sources in the production medium (Labuzek and Radecka, 2001). Additionally, *Bacillus* sp. possesses the ability to secrete many hydrolytic enzymes that could be exploited for cost affordable PHA production by utilising agro and industrial waste materials. Different *Bacillus* spp. such as *B. licheniformis*, *B. subtilis*, *B. thuringiensis*, *B. mycooides*, *B. cereus*, *B. sphaericus* and *B. firmus* were reported to accumulate PHAs from a variety of simple and complex carbon sources (Mohapatra et al., 2017). Another isolate obtained from water sample was *A. macleodii* which been reported as an exopolysaccharide producer isolated from marine environment (Cambon-Bonavita et al., 2002). However, no PHA production has been reported in this bacterium so far. Among the PHA producing halophiles, the genus *Halomonas* was reported to be the most diverse in PHA production and *H. boliviensis* was the most extensively studied species of this genus. PHA accumulation in these bacteria has been recognized as a useful phenotypic marker that helps to distinguish between species (Mata et al., 2002). *H. meridiana* was one among the species that was capable of accumulating PHA, but exclusive studies were not carried out in this isolate so far. More than 30 species of this genus were known to synthesize PHA, although the capability of storing PHA was not determined in several species (Quillaguamán et al., 2010). The advantage of *Halomonas* spp. for PHA production include the adaptability in high pH and NaCl containing medium, thereby reducing the risk of microbial contamination and enhancing the recovery of PHA by simple hypotonic lysis of cells (Koller, 2015).

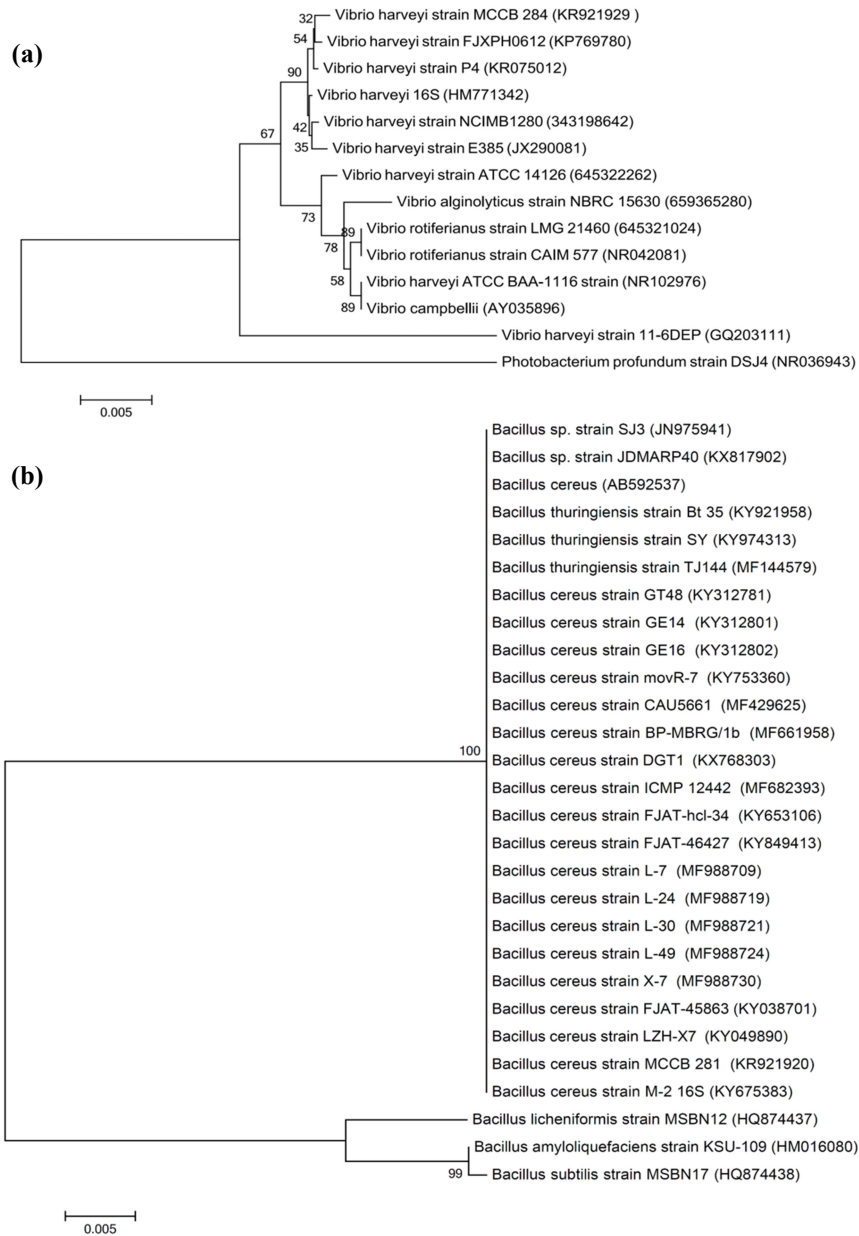


Fig. 2.4 Phylogenetic analysis of (a) *V. harveyi* MCCB 284 (b) *B. cereus* MCCB 281 with its closely related species based on 16S rRNA gene sequences. The tree was constructed with MEGA 6.0 software using Neighbour-joining method. The evolutionary distance was computed using the Kimura 2- parameter method. Bootstrap values indicated at the nodes

2.3.5 Bacterial growth curve of selected isolates

The growth curve of the selected two isolates MCCB 281 and 284 was carried out in ZoBell's marine broth to determine the generation time and specific growth rate. The specific growth rate (μ) was defined as the increase in cell mass per unit time. The generation time or doubling time (t_d) was defined as the time required for the bacteria to double in size and it was usually determined during log phase. In log phase, all bacteria are in their rapid stage of cell division and show balanced growth.

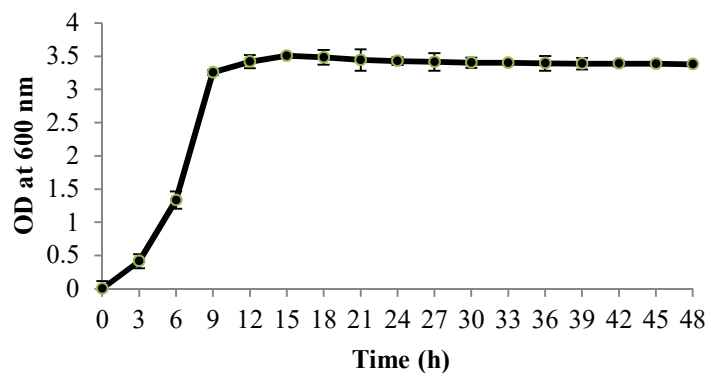


Fig. 2.5 Growth curve of *V. harveyi* MCCB 284. Data shown are mean standard deviations of triplicate

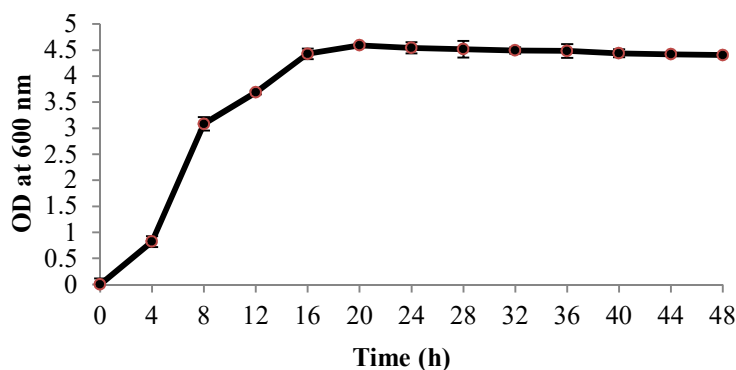


Fig. 2.6 Growth curve of *B. cereus* MCCB 281. Data shown are mean standard deviations of triplicate

In case of *V. harveyi* MCCB 284, the logarithmic phase started at 3 h after incubation and reached stationary phase at the end of 9 h (Fig. 2.5). The generation time and specific growth rate was estimated to be 0.3 h and 2.31 h^{-1} respectively. The isolate showed a short generation time indicating faster growth. For *B. cereus* MCCB 281, the logarithmic phase started at 4 h after incubation and reached stationary phase at the end of 16 h (Fig. 2.6). The generation time and specific growth rate was found to be 0.6 h and 1.15 h^{-1} respectively.

2.4 Conclusion

Marine environment is an untapped resource of microbial diversity for the isolation of novel PHA producing microorganisms. PHA producing bacteria were isolated from tunicate and water samples collected from marine environments. Nile red staining was used for screening of PHA producing bacteria with glucose as carbon source. Morphological and molecular based studies were carried out for the identification of PHA producing isolates. A total of 7 potent isolates showed more than 50% polymer production based on cell dry weight in presence of glucose after 72 h incubation. *V. harveyi* MCCB 284 from tunicate samples and *B. cereus* MCCB 281 from water samples were selected for PHA production and optimization studies.

.....❧.....

Chapter 3

PRODUCTION AND CHARACTERIZATION OF POLYHYDROXYBUTYRATE FROM *VIBRIO HARVEYI* MCCB 284 UTILISING GLYCEROL AS CARBON SOURCE

Contents

- 3.1 Introduction
- 3.2 Materials and methods
- 3.3 Results and discussion
- 3.4 Conclusion

3.1 Introduction

Polyhydroxyalkanoates (PHAs) are a class of natural polyesters produced by microorganisms as intracellular energy reserves during nutrient limiting conditions (Anderson and Dawes, 1990). PHAs are synthesized by a wide variety of Gram-positive and Gram-negative bacteria including members of the family *Halobacteriaceae*, *Archaea* and by several other marine bacteria (Grage et al., 2009). It is accumulated in bacteria as a membrane enclosed inclusion which constitutes up to 80% of the cell dry weight. PHAs are classified into 3 types as short chain length (scl-PHAs) with 3 - 5 carbon atoms, medium chain length (mcl-PHAs) with 6 - 14 carbon atoms and long chain length (lcl-PHAs) with more than 14 carbon atoms (Anderson and Dawes 1990). More than 150

different types of PHA monomers have been identified so far, which belongs to this group of linear polyesters (Steinbüchel, 1995).

Polyhydroxybutyrate (PHB) is a short chain length linear polyester of D (-)-3-hydroxybutyric acid first discovered in *Bacillus megaterium* by French microbiologist Lemoigne in 1926 (Lemoigne, 1926). PHB, the most widely studied and characterized member of PHA family is a homopolymer which is relatively stiff and brittle in nature. PHB is brittle due to the formation of large crystalline domains in the form of spherulites. The formation of large spherulites is a unique character of this polymer possibly due to its exceptional purity (Jain et al., 2010). PHB is a semi-crystalline polymer, characterized by polymorphic crystallization and exists in two crystallize forms, α and β . The α -form comprises of lamellar crystals and is the most common conformation for PHB crystals whereas; the β -form is characterized as a planar zigzag conformation present in films and fibres with high tensile strength (Pan and Inoue, 2009). Being a biodegradable and biocompatible polymer, PHB undergoes complete degradation under aerobic and anaerobic conditions (Tokiwa et al., 2009). PHB is known to be extensively used for various applications in the field of medicine, tissue engineering, drug delivery, packaging and aquaculture. PHB is used as microsphere and nanoparticle formulations for targeted and controlled delivery of anticancer drugs, as scaffolds in tissue engineering, and as surgical implants for wound healing (Gumel et al., 2013).

The major drawback that hampers the large scale production of PHB is the high cost of carbon source that accounts for 50% of the total

expenses (Choi and Lee, 1999). Most of the carbon sources used for industrial PHB production is pure carbohydrates (glucose, sucrose), alkanes and fatty acids (Cesário et al., 2014). In this context, by-products from agriculture and industry have turned out to be the promising sources of carbon which could cut down the cost of PHB production (Suwannasing et al., 2015; Valentino et al., 2015). The various cheap carbon sources that have been used for PHB production include whey (Koller et al., 2011), cassava starch (Poomipuk et al., 2014), rice bran (Huang et al., 2006), wheat straw (Cesário et al., 2014), molasses (Tripathi et al., 2013) and glycerol (Shrivastav et al., 2010). The use of glycerol, an industrial waste, has been proven an attractive feed material for the cost-effective production of PHB (Kumar et al., 2015). The production of biodiesel by the trans-esterification of oil with a short chain alcohol generates approximately 10% (w/w) glycerol as by-product (Mozumder et al., 2014). The efficient utilisation of this by-product without any pre-treatments is indispensable for the economic feasibility of the growing biodiesel industry. Moreover, glycerol can be utilised by different bacteria to produce high-value added products.

The nature of microorganisms, inherited metabolic pathways, media constituents and bioprocess strategies are the additional significant factors that govern PHB production (Grothe et al., 1999). The microbes need to possess several desirable features to be selected and regarded as promising PHB producers. Such features include their performance utilising renewable feedstocks, use of seawater instead of fresh water, possibility of PHB production under open, non-sterile conditions and their potential to develop contamination-free continuous bioprocesses

(Kourmentza et al., 2017). The optimization of media constituents and physical factors plays an important role in increasing the polymer production via, microbial fermentation process. The one-factor-at-a-time method (O-F-A-T) is a simple and common approach used to optimize culture conditions such as carbon and nitrogen sources, mineral constituents, pH, temperature and agitation by changing one factor and keeping all other parameters constant for increased microbial production of value added products. This approach can be used to optimize the effective factors for enhanced polymer production.

Marine environment, a largely unexplored source of microbial diversity, remains quite neglected towards developing industrial processes in equivalence to the terrestrial counter parts. Marine habitat constitutes an untapped source of novel microbes, their compounds and metabolic pathways which are largely exploited for biotechnological applications. Marine environment has rich biodiversity for isolation of novel PHA producing bacteria with the desired properties and diverse compositions. Marine bacteria have the unique potential to produce biopolymers with relatively new properties (Imhoff et al., 2011). Numerous studies reported that marine bacteria such as *Vibrio* spp., *Bacillus* spp. and *Halomonas* spp. could accumulate PHB nearly to 50% of their cell dry weight (Chien et al., 2007; Sathiyarayanan et al., 2013; Shrivastav et al., 2010; Wei et al., 2011). Several *Vibrio* spp such as *V. harveyi* isolated from marine environment (Sun et al., 1994), *V. natriegens* from mangrove sediment (Chien et al. 2007), *V. harveyi* from Pacific ocean (Boyandin et al., 2008), *Vibrio* sp.BM-1 from marine environment (Wei et al., 2011), *Vibrio* sp. KN01 from sea water (Numata and Doi, 2012) and *V. azureus*

from marine sediment (Subin et al., 2013) have also been identified as potent PHB producers. The advantages of using marine bacteria for industrial scale PHB synthesis include the possible reduction in contamination caused by terrestrial/aerial bacteria that lack salt resistance and the option to use filtered seawater as culture medium which can reduce the cost of production (Numata and Doi, 2012).

The present study deals with the production and optimization of factors such as pH, temperature, sodium chloride concentration, carbon sources, incubation time and inoculum size by conventional method for enhanced PHB production by *V. harveyi* MCCB 284 isolated from Vizhinjam Bay, Thiruvananthapuram, Kerala, which utilises glycerol as the sole carbon source. The polymer was extracted, purified and characterized by Fourier Transform Infrared Spectroscopy (FTIR), Nuclear Magnetic Resonance Spectroscopy (NMR), Gel Permeation Chromatography (GPC), Differential Scanning Calorimetry (DSC) and Thermogravimetric analysis (TGA) techniques.

3.2 Materials and methods

3.2.1 PHB production

PHB production studies were carried using *V. harveyi* MCCB 284 isolated from marine tunicate *Ascidia nigra* in the production medium (composition: Peptone- 5 g L⁻¹, Yeast extract- 1 g L⁻¹) prepared in sea water and pH adjusted to 7.8. For production studies, the isolate was streaked on ZoBell's marine agar slants and incubated for 24 h at 28 °C. Aliquot of 2 mL sterile production medium was added to the agar slant; cells dislodged using sterile inoculation loop and aseptically transferred

to another tube. Cell density was then measured in UV-Visible spectrophotometer (Shimadzu UV-1601, Japan) at a wavelength of 600 nm and adjusted to 1.0 with a cell density 2×10^8 CFU mL⁻¹. A two stage cultivation strategy was adapted to increase PHB accumulation. The inoculum (0.1% v/v) was added to 200 mL production medium and incubated at 28 °C for 24 h at 150 rpm in an orbital shaker. After 24 h, glucose was added to the culture medium (final concentration 20 g L⁻¹) as carbon source for the enhanced PHB accumulation and was further incubated for 48 h before cell harvesting. Cell growth was monitored every 24 h by measuring optical density at 600 nm spectrophotometrically. Cell dry weight (CDW) and PHA content were measured as explained in sections 2.2.4 and 2.2.5 of Chapter 2.

3.2.2 Transmission Electron Microscopy (TEM)

V. harveyi MCCB 284 was grown in PHB production medium with 20 g L⁻¹ glucose and incubated for 48 h at 28 °C. Cells were harvested and washed with 0.1 M sodium cacodylate buffer (pH 7.0), treated with 2.5% (v/v) glutaraldehyde overnight at 4 °C, post fixed with 2% (w/v) osmium tetroxide for 2 h at 4 °C. It was again washed with the buffer and dehydrated with a graded series of acetone and embedded in epoxy resin. The embedded specimen was cut into ultrathin sections and stained with uranyl acetate and lead citrate. TEM observations were performed using a TECNAI 200 TEM (FEI, Electron Optics, USA) at All India Institute of Medical Sciences (AIIMS), New Delhi.

3.2.3 Optimization for PHB production

The various factors that influenced the PHB production of *V. harveyi* MCCB 284 were analysed by ‘one-factor-at-a-time’ approach under shake flask culture conditions. For all experiments, the bacterial isolate was inoculated at a cell density corresponding to 2×10^8 CFU mL⁻¹ in 25 mL production medium. PHB production under the varying conditions of initial pH (5.0-10.0), sodium chloride concentration (5-100 g L⁻¹), carbon sources (glucose, fructose, sucrose, xylose, lactose, mannitol, glycerol, sodium acetate and starch), concentration of carbon source (10-50 g L⁻¹), incubation period (6-72 h), initial inoculum size (0.1-10% v/v) and temperature (20-40 °C) were investigated. The CDW and PHB content were estimated after 72 h. The PHB content was expressed as percentage based on cell dry weight. The experiment was carried out in triplicate.

3.2.4 PHB extraction

A quantity of 1 g lyophilized cell pellet was treated with 50 mL chloroform and 50 mL hypochlorite solution (4% available chlorine) for 1 h at 30 °C and the mixture was centrifuged at 8000 g for 10 min. The lower chloroform phase containing the extracted polymer was collected and the dissolved PHB was precipitated by the addition of 10 volumes of 70% (v/v) ice cold methanol. The precipitated PHB was filtered and dried at 60 °C (Hahn et al., 1994).

3.2.5 Polymer characterization

3.2.5.1 FTIR

The presence of various functional groups in the polymer was identified from the FTIR spectrum which provides the molecular fingerprint of the sample. The polymer was ground with KBr crystals to form pellet and dried. The sample was subjected to FTIR analysis using Nicolet FT-IR Spectrometer (Thermo Scientific, France). The spectrum was recorded between 4000 and 400 cm^{-1} with a resolution of 4 cm^{-1} and was compared with commercial PHB (Sigma, USA).

3.2.5.2 DSC

Differential Scanning Calorimetry (DSC) was employed to record the thermal transitions of the extracted polymer. The polymer sample was heated from 25 °C to 200 °C at a rate of 10 °C min^{-1} under nitrogen atmosphere (100 mL min^{-1}) using DSC 60 Plus (Shimadzu, Japan). The melting temperature (T_m) and the melting enthalpy (ΔH_m) of the polymer were determined from DSC endothermal peak. The crystallinity (X_c) of the extracted PHB was calculated by the following equation:

$$X_c(\%) = (\Delta H_m / \Delta H_{\text{PHB}}^0) * 100 \dots\dots\dots(3.1)$$

where ΔH_m (J/g) was the melting enthalpy of the polymer, (ΔH^0) was the melting enthalpy of 100% crystalline PHB (146 J/g) (Barham et al., 1984).

3.2.5.3 TGA

Thermogravimetric analysis (TGA) was performed to determine the thermal stability and decomposition pattern of polymer using TGA Q50

(TA Instruments, USA). Approximately 5-8 mg of the sample was heated from 30 °C to 800 °C at a rate of 10 °C min⁻¹ under nitrogen atmosphere (100 mL min⁻¹).

3.2.5.4 NMR

¹H and ¹³C Nuclear Magnetic Resonance Spectroscopy (NMR) of the extracted polymer and commercial PHB were analysed on Bruker Avance III spectrometer operated at 400 MHz. The sample was dissolved in deuterated chloroform (CDCl₃) and the spectra were recorded. The analyses were carried out at the Sophisticated Test and Instrumentation Centre (STIC), CUSAT, Kerala.

3.2.5.5 GPC

Number-average molecular weight (M_n), weight-average molecular weight (M_w) and polydispersity index (PDI) of the polymer were determined by Gel Permeation Chromatography (GPC) using Waters HPLC/GPC system with 600 Series Pump and Waters Styragel HR series HR5E/4E/2/0.5 column equipped with a 7725 Rheodyne injector and refractive index 2414 detector (Waters Corporation, USA). A quantity of 1 mg PHB was completely dissolved in 1 mL chloroform and filtered through 0.2 µm PVDF membranes. The injection volume was 20 µL. The mobile phase was chloroform at a flow rate of 1 mL min⁻¹. Polystyrene standards of molecular weight 1865000, 100000, 9130 were used for relative calibration. The analysis was performed at Sree Chitra Tirunal Institute for Medical Sciences and Technology, Trivandrum, Kerala.

3.2.6 Statistical analysis

Statistical analysis of the experimental data was carried out using one-way ANOVA followed by the Tukey-Kramer multiple comparisons test using the software GraphPad InStat version 3.0.

3.3 Results and discussion

3.3.1 PHB production

PHB production of *V. harveyi* MCCB 284 was carried out in 200 mL production medium with 0.1% (v/v) inoculum and incubated at 28 °C for 72 h at 150 rpm in an orbital shaker. The isolate MCCB 284 produced a CDW of $1.34 \pm 0.1 \text{ g L}^{-1}$ with PHB yield $0.8 \pm 0.19 \text{ g L}^{-1}$. The isolate MCCB 284 showed $60 \pm 0.63\%$ (w/w) PHB accumulation in the presence of 20 g L^{-1} glucose as carbon source. It has been previously reported that PHB synthesis and luminescence in this bacterium has a potential link on the bacterial cell density (Sun et al., 1994).

In a related study to determine PHB production in a marine benthic isolate *V. azureus* BTKB33 in presence of glucose as carbon source in the minimal medium, it was observed that maximum PHA production of 0.48 g L^{-1} with PHB content 42% (w/w) was obtained (Sasidharan et al., 2014). Another study of a marine *Vibrio* sp. showed a maximum CDW of 9.1 g L^{-1} , PHB yield of 4 g L^{-1} and PHB content of 44% (w/w) in presence of 20 g L^{-1} glucose in 72 h incubation time (Arun et al., 2009). The PHB accumulation study of *Vibrio* sp. KN01 under aerobic- anaerobic condition in presence of glucose showed a CDW of 1.6 g L^{-1} with a very low PHB content of 5% (w/w); but, the isolate produced PHB co-polymer in presence

of soybean oil as carbon source with PHA content 40% (w/w) (Numata and Doi, 2012). However, in the present study, the isolate MCCB 284 showed a higher polymer accumulation than previously reported *Vibrio*. spp.

Experiments of PHB production carried in other Gram negative bacteria such as *C. necator* ATCC 17699 showed a CDW of 5.1 g L⁻¹ with PHB yield 1.4 g L⁻¹ and PHB content of 27% based on CDW with 20 g L⁻¹ glucose as carbon source after 48 h incubation (Aramvash et al., 2015). Furthermore, PHB production in halophilic bacterium *Halomonas boliviensis* LC1 in presence of glucose showed a CDW of 2.1 g L⁻¹, with PHB yield 0.83 g L⁻¹ and PHB content of 39% w/w (Van-Thuoc et al., 2008).

3.3.2 TEM

TEM analysis showed the presence of granules in *V. harveyi* MCCB 284 grown in ZoBell's broth containing 20 g L⁻¹ glucose for 48 h (Fig. 3.1). The cells contain PHB granules that vary in size and number.

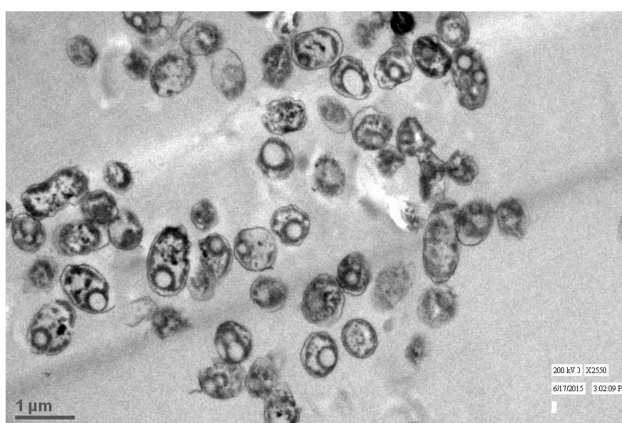


Fig. 3.1 TEM of *V. harveyi* showing the presence of PHA granules

3.3.3 Optimization of PHB production

The various factors such as initial pH, sodium chloride (NaCl) concentration, carbon sources, incubation time, initial inoculum size and incubation temperature that influence PHB production in *V. harveyi* MCCB 284 were sequentially optimized by ‘one-factor-at-a-time’ approach in shake flask conditions. The optimized value for each factor was used in subsequent stages of the optimization.

3.3.3.1 Effect of initial pH

To examine the effect of initial pH, the isolate MCCB 284 was inoculated into 25 mL production medium of varying pH 5.0-10.0 and incubated at 28 °C for 72 h. The pH was adjusted using 1 M NaOH or 1 M HCl prior to sterilization. Although the growth of the culture occurred at lower and higher pH values, maximum PHB production of $61 \pm 2.2\%$ based on CDW was observed at the pH 8.0 (Fig. 3.2). At extreme pH values 5.0 and 10.0, the isolate showed very less growth, whereas at pH ranges 6.0-9.0, MCCB 284 grew well. It was observed that the optimum pH for biomass and polymer production was 8.0. Moreover, *V. harveyi* was well known to grow at alkaline pH ranges as previously reported (Balebona et al., 1995). In most marine bacteria, PHB production was found to be favoured at pH ranges 7.0-8.0 (Arun et al., 2009; Kiran et al., 2014; Shrivastav et al., 2010).

3.3.3.2 Effect of sodium chloride concentration

The isolate MCCB 284 was inoculated into the production medium with different salt concentrations ranging from 5 g L⁻¹ to 100 g L⁻¹. The

optimum sodium chloride concentration for the PHB production of MCCB 284 was 20 g L^{-1} with a CDW and PHB content of $1.3 \pm 0.03 \text{ g L}^{-1}$ and $66 \pm 0.32\%$ (w/w) respectively at the end of 72 h (Fig. 3.3). *V. harveyi* MCCB 284 showed meagre growth and PHB production of 22% (w/w) at 100 g L^{-1} NaCl concentration. The concentration of sodium chloride in the culture medium has crucial impact on PHB production, as *Vibrio* is halophilic and sensitive to salt content (Chien et al., 2007). It was found that maximum cell density and polymer production could be achieved at 20 g L^{-1} sodium chloride which was in agreement with the previous report on PHB production from *Vibrio* sp. (Wei et al., 2011). Other related *Vibrio* spp. such as *V. azureus* exhibited maximum PHA production at 15 g L^{-1} sodium chloride (Sasidharan et al., 2014) whereas *Vibrio* sp. MK4 showed increased polymer production from 15 - 30% sodium chloride (Arun et al., 2009). But, in case of certain halophiles such as *Halomonas* spp., high salt concentration was required for optimum growth and polymer accumulation (Cervantes-Uc et al., 2014; Strazzullo et al., 2008).

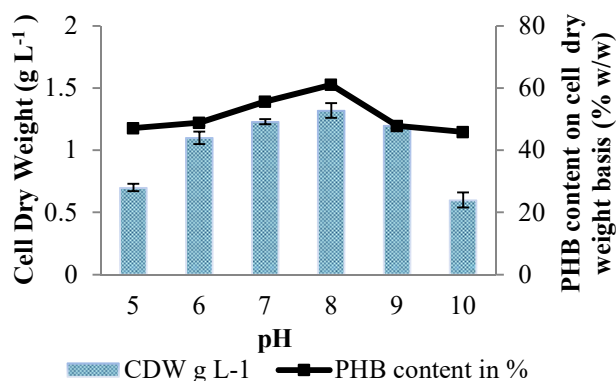


Fig. 3.2 Effect of pH on the growth and PHB production of *V. harveyi* MCCB 284 using glucose 20 g L^{-1} as carbon source. Data shown are mean standard deviations of triplicate

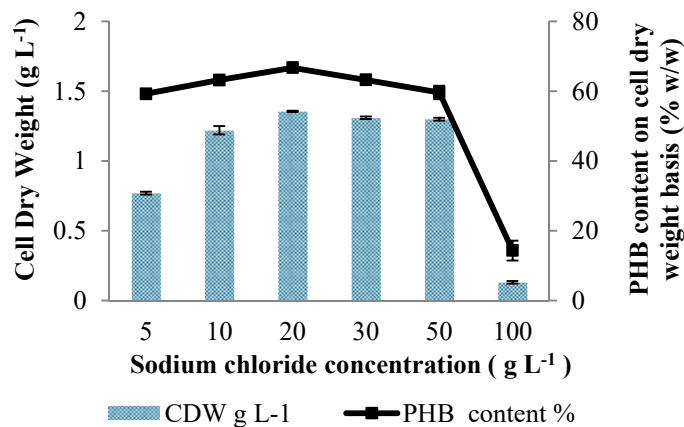


Fig. 3.3 Effect of sodium chloride concentration on the growth and PHB production of *V. harveyi* MCCB 284 using glucose 20 g L⁻¹ as carbon source. Data shown are mean standard deviations of triplicate

3.3.3.3 Effect of carbon sources

The ability of the isolate MCCB 284 to utilise different carbon sources (glucose, fructose, xylose, mannitol, glycerol, lactose, sodium acetate, sucrose and starch) for PHB production was investigated. Carbon sources were sterilized separately and added at the concentration of 20 g L⁻¹ in the production medium. Among the carbon sources evaluated, glycerol supported maximum biomass yield and PHB production followed by glucose and fructose. Glucose, being easily available for assimilation and metabolism by bacteria than other sugars was the most widely used carbon source for cell growth and polymer accumulation. CDW and PHB production in the presence of glycerol was 3 ± 0.27 g L⁻¹ and $68 \pm 3.76\%$ (w/w) respectively (Fig. 3.4). Lactose and sucrose were not suitable carbon sources for both biomass and PHB production, which might be due to the fact that both these sugars are disaccharides that are less suitable than

monosaccharides (such as glucose and fructose). This result coincides with the earlier report that disaccharides such as lactose and sucrose were less utilised for microbial growth and PHB production (Poomipuk et al., 2014). In addition, it was noticed that the isolate MCCB 284 was able to utilise pure form of pentose sugar, xylose for PHB production. Till date, only a few strains of bacteria have been known to metabolize pentose for the PHB production (Cesário et al., 2014). Though the isolate MCCB 284 utilised xylose for PHB production, low biomass yield (0.9 g L^{-1}) and subsequently low polymer accumulation was noticed. In a similar study to optimize the carbon sources for PHB production in *V. proteolyticus* DCM CAS2, fructose appeared to be the best carbon source and 55% PHB production based on CDW was reported (Melba and Ananthan, 2016).

Further, different glycerol concentrations (10, 20, 30, 40 and 50 g L^{-1}) were also examined and 20 g L^{-1} glycerol provided highest biomass yield and PHB production (Fig. 3.5). The present result complies with the previous reports of glycerol being the preferred sole source of carbon for PHB biosynthesis in Gram negative bacteria. Chien et al. (2007) reported PHB production of 41% (w/w) in *Vibrio* sp. utilising glycerol as carbon source. In *Halomonas* sp. SA8, PHB content and CDW could reach 43% (w/w) and 4.1 g L^{-1} , respectively, after 96 h of cultivation using glycerol (de Castro et al., 2014). PHB production in a marine isolate *Vibrio* sp. BM-1 showed CDW of 3.7 g L^{-1} and PHB content 15.7% (w/w) in presence of 10 g L^{-1} glycerol as carbon source (Wei et al., 2011). In another study, an isolate of *Z. denitrificans* ZD1 utilised 20 g L^{-1} glycerol for PHB synthesis and showed a CDW of 4.8 g L^{-1} and PHB content of 85% (w/w) after 96 h incubation (Ibrahim and Steinbüchel, 2010).

Therefore, glycerol, the major by-product of biodiesel industry could be utilised as an excellent carbon source for PHB production.

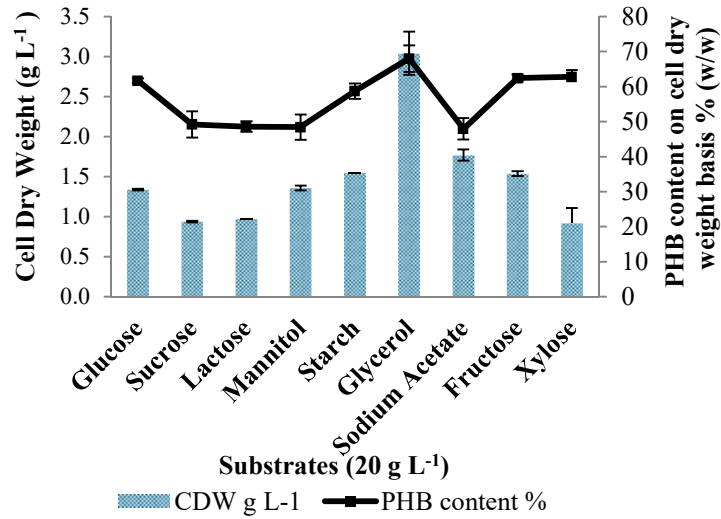


Fig. 3.4 Effect of different carbon sources on the growth and PHB production of *V. harveyi* MCCB 284 after 72 h incubation at 28 °C and 150 rpm. Data shown are mean standard deviations of triplicate

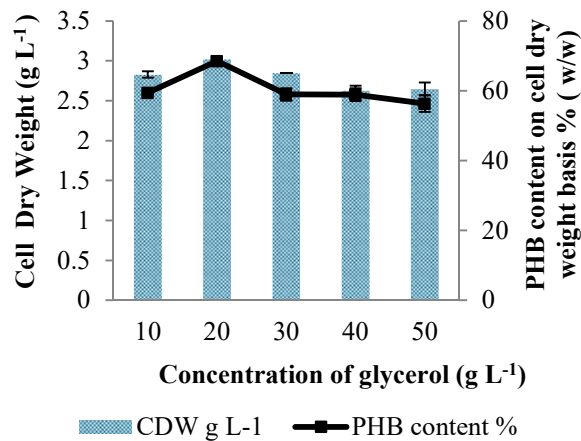


Fig. 3.5 Effect of different concentration of glycerol on the growth and PHB production of *V. harveyi* MCCB 284. Data shown are mean standard deviations of triplicate

3.3.3.4 Effect of incubation time

From the growth study, it was noticed that *V. harveyi* MCCB 284 reached the logarithmic phase in 3 h followed by the stationary phase in 9 h of cultivation and hence the carbon source was added at the 9th hour after inoculation to enhance PHB accumulation. To study the effect of incubation time on the growth and PHB production of MCCB 284, samples were taken every 6 h to determine both CDW and PHB content. The PHB accumulation commenced at the early phase of growth of 6 h ($34 \pm 2.3\%$ w/w), reached $60 \pm 2.19\%$ (w/w) with a CDW of $1.5 \pm 0.07 \text{ g L}^{-1}$ at 24 h, which later decreased to $42 \pm 3\%$ (w/w) at 36 h of cultivation. A maximum CDW of $3.5 \pm 0.02 \text{ g L}^{-1}$ was observed at 36 h which subsequently declined. After 48 h of incubation, a steady state in the PHB production with increasing accumulation was observed till 72 h. Maximum PHB content of $68 \pm 2.31\%$ (w/w) was attained at 72 h of cultivation with a CDW of $3 \pm 0.1 \text{ g L}^{-1}$ and PHB yield of $2.16 \pm 0.9 \text{ g L}^{-1}$ (Fig. 3.6). The effect of incubation time on PHB production varied among different bacterial genera and was found to be a critical control factor, as increase in time may result in utilisation of the produced polymer as carbon source by the bacteria itself. In a similar experiment carried out in a marine isolate *Halomonas campisalis* MCM B-1027, PHB production started from 3 h itself (26% w/w) which increased up to 67% (w/w) till 24 h and then decreased slightly to 53% (w/w) at 48 h (Kulkarni et al., 2010). The effect of incubation time on growth and PHB production in marine *B. megaterium* SRKP-3 strain showed maximum PHB production at 36 h incubation in dairy waste and sea water based medium (Pandian et al., 2010). Another marine isolate *Brevibacterium casei* MS104 showed

maximum polymer accumulation of 6.74 g L^{-1} after 96 h of incubation (Kiran et al., 2014).

During the time course study of growth and polymer production in MCCB 284, it was noted that the polymer accumulation commenced at an early phase of growth and the isolate was able to accumulate the biopolymer within 24 h. The results implied that PHB production in this isolate was associated with the cell growth. From the bacterial growth study, the generation time and specific growth rate of *V. harveyi* MCCB 284 was estimated to be 0.3 h and 2.31 h^{-1} respectively. Precisely, the shorter generation time and higher growth rate of this isolate would be beneficial for commercial production of PHB.

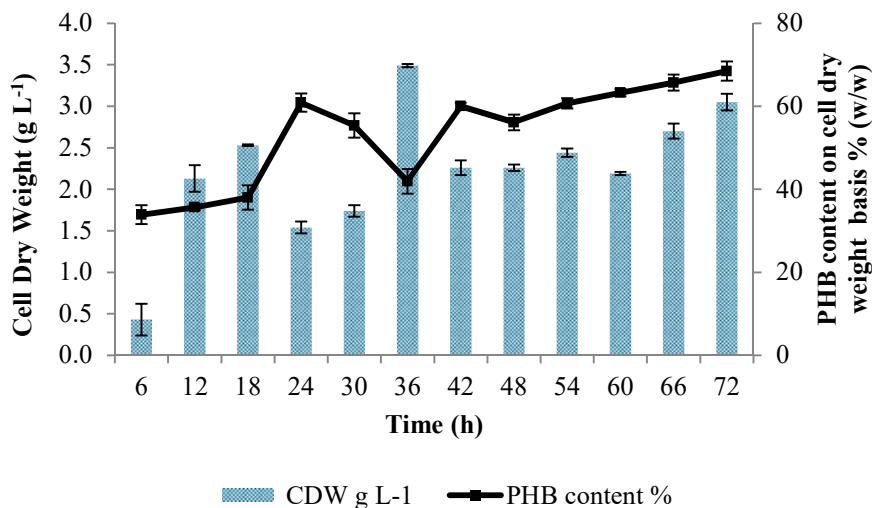


Fig. 3.6 Effect of incubation time on growth and PHB production of *V. harveyi* MCCB 284 with glycerol 20 g L^{-1} as carbon source. Data shown are mean standard deviations of triplicate

3.3.3.5 Effect of inoculum size

The effect of initial inoculum size (0.1, 0.5, 1, 2, 4, 6, 8 and 10% v/v) on PHB production was investigated under the optimized culture conditions. An inoculum size of 0.5% (v/v) showed the maximum CDW of $3.2 \pm 0.3 \text{ g L}^{-1}$ and PHB content of $72 \pm 1.57\%$ (w/w) (Fig. 3.7).

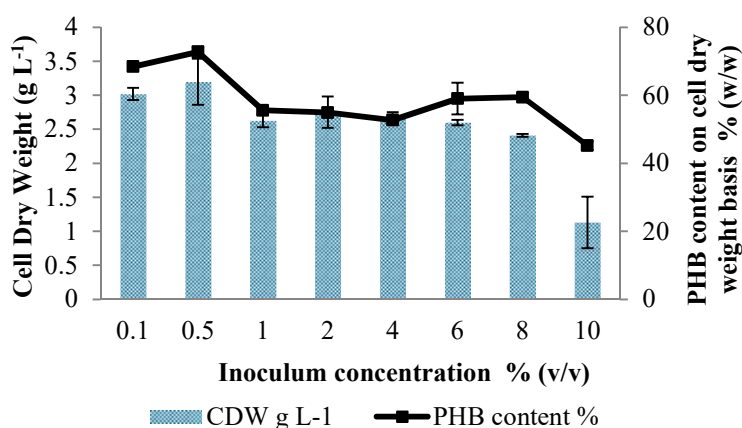


Fig. 3.7 Effect of initial inoculum size on the growth and PHB production of *V. harveyi* MCCB 284 after 72 h incubation at 28 °C and 150 rpm. Glycerol 20 g L⁻¹ was used as carbon source. Data shown are mean standard deviations of triplicate.

It was noticed that, lower initial inoculum size could enable a relatively good biomass yield and PHB production than higher inoculum size. As the inoculum size increased, the biomass yield and polymer production decreased. At high inoculum concentration of 10% (v/v), the biomass yield and PHB production was low which might be due to the utilisation of accumulated polymer at high cell counts (Yamane et al., 1996). A similar study in *V. azureus* BTKB33 showed an inoculum concentration of 2.5% (v/v) supported maximum PHB production

(0.37 g L⁻¹) and PHB content 22% (w/w) (Sasidharan et al., 2014). For *Bacillus* sp. CFR 256, 1% (v/v) initial inoculum favoured PHB production (Vijayendra et al., 2007), and for certain other *Bacillus* sp. NII 0838, 3% (v/v) inoculum concentration was desirable (Sindhu et al., 2011). The amount of PHB accumulated in *B. subtilis* AJ-3 and *E. coli* K-12 was found to increase upon increasing the inoculum concentration up to 8% (v/v) with PHB content 82 and 77% (w/w) respectively. Further increase in the inoculum size decreased PHB content and cell growth (Gomaa, 2014).

3.3.3.6 Effect of temperature

The effect of temperature on growth and PHB production of the isolate MCCB 284 was evaluated and the optimal temperature was found at 30 °C. CDW of 3.1 ± 0.13 g L⁻¹ and PHB content of $71 \pm 3.42\%$ (w/w) were achieved (Fig. 3.8). The isolate showed considerable growth and PHB production at 35 °C; however no growth occurred at 40 °C. In a related study to determine the effect of temperature for PHB production in *V. proteolyticus* DCM CAS2 showed the optimum temperature at 30 °C with PHB yield 5.57 g L⁻¹ (Melba and Ananthan, 2016). PHB production studies to optimize incubation temperature performed in *B. subtilis* MSBN17 isolated from marine sponge (Sathiyarayanan et al., 2013a), *Vibrio* sp. MK4 from marine environment (Arun et al., 2009) and *B. cereus* FA11 from soil sample also showed optimum temperature at 30 °C for maximum polymer production (Masood et al., 2011).

Considering all the above factors, the isolate *V. harveyi* MCCB 284 could be designated as a potential prospect for industrial production of

PHB. Based on the statistical analysis, factors such as the initial pH, carbon source, incubation time and inoculum size were identified to have significant impact on the growth and PHB production in *V. harveyi* MCCB 284.

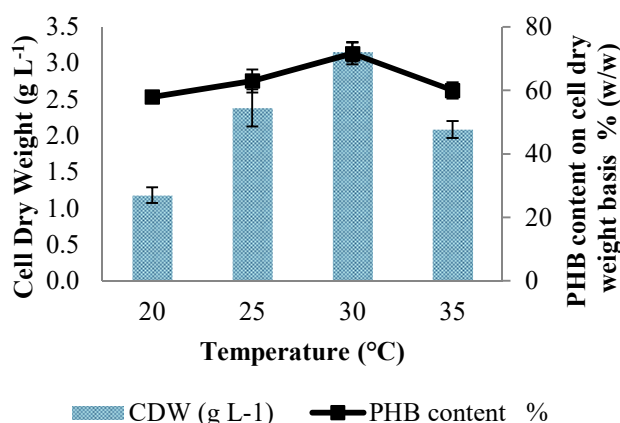


Fig. 3.8 Effect of incubation temperature on the growth and PHB production of *V. harveyi* MCCB 284. Glycerol 20 g L⁻¹ was used as carbon source. Data shown are mean standard deviations of triplicate

3.3.4 Polymer characterization

3.3.4.1 FTIR

The FTIR spectrum of extracted PHB revealed the presence of distinct peak at 1638 cm⁻¹ corresponding to C=O ester carbonyl group. Other absorption peaks at 1112 cm⁻¹, 1323 cm⁻¹ and 3444 cm⁻¹ represented C–O–C group, CH₃ group and OH group respectively (Fig. 3.9). The pattern of the spectrum obtained was similar to commercial PHB (Sigma, USA) with distinct peaks at 1727 cm⁻¹, 1286 cm⁻¹, 1381 cm⁻¹, 3440 cm⁻¹ corresponding to C=O, C-O-C, CH₃, OH groups respectively. The

polymer was mainly characterized by two intense absorption peaks at 1720 cm^{-1} and $1120\text{--}1280\text{ cm}^{-1}$ corresponding to C=O and C–O–C groups respectively. The observed peaks in the FTIR spectrum at 1638 cm^{-1} , 1112 cm^{-1} , 1323 cm^{-1} and 3444 cm^{-1} represented C=O ester, C–O–C, CH_3 and OH groups of the polymer respectively, in agreement with the previous reports (Hong et al., 1999 ; Silverstein et al., 2005).

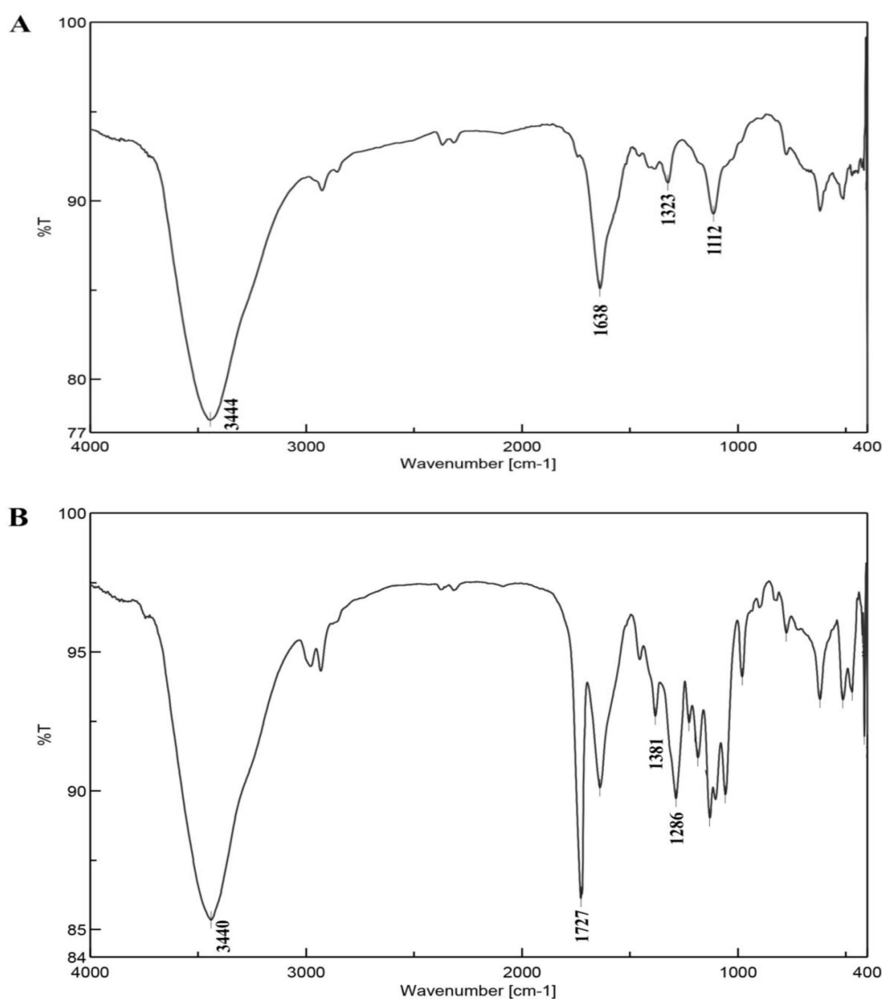


Fig. 3.9 Infrared spectra of (A) purified polymer from *V. harveyi* MCCB 284; (B) commercial PHB

3.3.4.2 DSC

The thermal properties of the extracted PHB were determined by DSC and TGA techniques. The melting temperature (T_m) of the extracted polymer was calculated to be 163 °C from the DSC endothermic peak (Fig. 3.10). The X_c of the polymer extracted was calculated to be 68%. The PHB synthesized by isolate MCCB 284 was found to be highly crystalline in nature. Highly crystalline polymers are stiff and brittle in nature resulting in very poor mechanical properties with low extension at break, but they have very low resistance to thermal degradation. The T_m of PHB obtained from isolate MCCB 284 was similar to that reported in *C. necator* (Radhika and Murugesan, 2012) but less than that of the commercial PHB (Sigma, USA). The degree of crystallinity of polymers was significantly influenced by the composition and monomer fractions of PHA. The incorporation of 3-HV or 4-HB could reduce the crystallinity of PHB and improves the mechanical properties of the homopolymer.

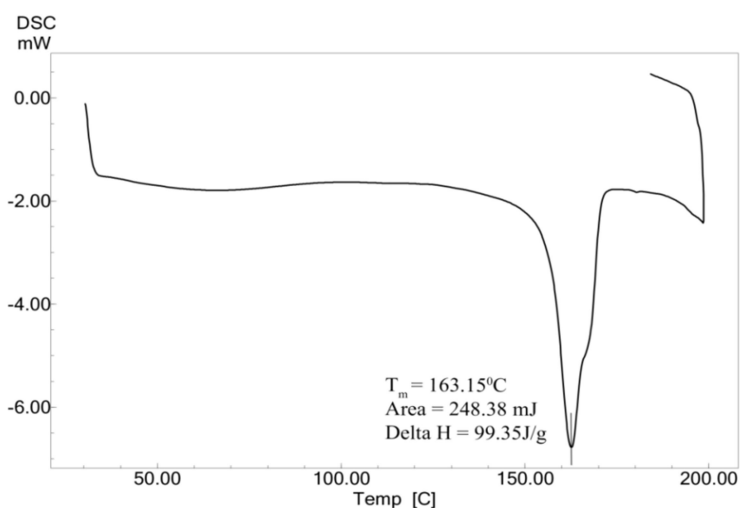


Fig. 3.10 Differential scanning calorimetry curve of polymer extracted from *V. harveyi* MCCB 284

Melting temperature and the enthalpy of melting are dependent on the thickness of the crystalline lamellae of PHB which varies with crystallization conditions. Therefore the melting temperature as detected in the DSC depends on crystallization conditions such as crystallization temperature, crystallization time and annealing treatment (Laycock et al., 2013).

3.3.4.3 TGA

From the TGA-DTG plot (Fig. 3.11), the initial thermal decomposition temperature of the extracted PHB was determined to be 182 °C with a mass loss of 5%. The maximum thermal decomposition was observed at 260 °C with a total mass loss of 86%. The temperature at which 50% of the polymer undergoes decomposition ($D_{1/2}$) was detected at 220 °C. The maximum thermal decomposition observed was at 260 °C and was associated with the ester cleavage of PHB by β -elimination reaction (Choi et al., 2003). The degradation of PHB can be divided into two stages according to the difference of temperature. When the processing temperature was between 160 ° and 180 °C, the random chain scission of molecular chains occurred and the thermal stability of PHB decreased significantly. Further on increasing the processing temperature to 180–200 °C, a drastic decrease in molecular weight of PHB was found due to the rapid random scission according to the β -elimination mechanism (Wang et al., 2016).

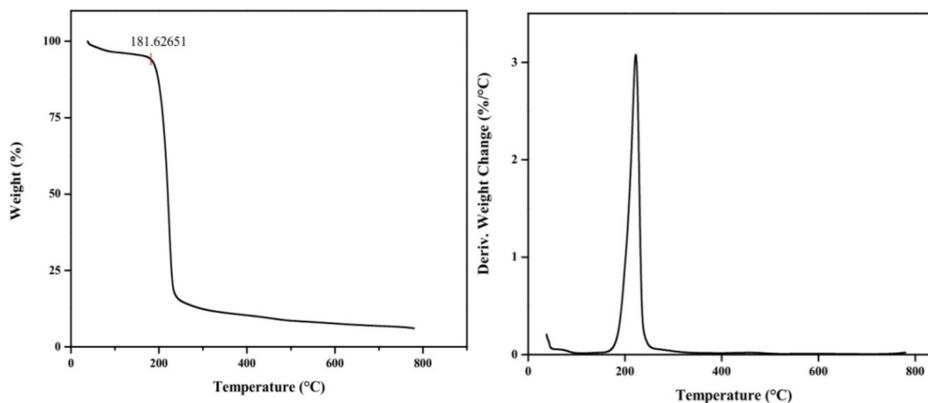


Fig. 3.11 Thermogravimetric (TGA - DTG) plot of PHB obtained from *V. harveyi* MCCB 284

3.3.4.4 NMR

The ^1H NMR spectrum of PHB exhibited the characteristic signals for three different groups namely; methyl ($-\text{CH}_3$), methylene ($-\text{CH}_2$), and methine ($-\text{CH}$). The obtained spectrum showed a doublet at 1.21 ppm corresponding to the methyl group coupled to one proton. The doublet of quadruplet at 2.56 ppm corresponded to the methylene group adjacent to an asymmetric carbon atom bearing a single atom. The multiplet at 5.22 ppm was characteristic of methine group (Fig. 3.12). The banding pattern of commercial PHB (Sigma, USA) was similar to the extracted polymer depicting the presence of strong signals at 1.21 ppm, 2.57 ppm and 5.23 ppm corresponding to methyl ($-\text{CH}_3$), methylene ($-\text{CH}_2$), and methine ($-\text{CH}$) groups respectively. The pattern of the spectrum of MCCB 284 correlates with the results obtained from other marine bacteria (Kiran et al., 2014; Sathiyarayanan et al., 2013; Shrivastav et al., 2010) indicating the polymer to be polyhydroxybutyrate.

However, expansion of the spectral region between 3.0 and 4.5 ppm revealed the presence of additional resonances corresponding to terminal glycerol groups. The expanded region with three resonances at 4.1 ppm, 3.7 ppm, and 4.2 ppm showed the terminal esterification of glycerol to PHB through the primary hydroxyls (C₁ or C₃ positions of glycerol). Resonance at 4.09 ppm showed glycerol end-capping of PHB through the secondary hydroxyl group. Because glycerol was composed of 2 primary and 1 secondary hydroxyl groups, the possibility exists that the glycerol termination of PHB polymers could also be the result of covalent bonding at the secondary hydroxyl group of glycerol. Glycerol acts as a terminal end-group during PHB synthesis resulting in a reduction of the molecular weight of the polymer. The obtained result was consistent with previous reports showing the presence of terminal glycerol groups in the NMR spectrum (Ashby et al., 2005; Tanadchangsaeng and Yu, 2012).

¹³C NMR spectrum of the MCCB 284 showed the chemical shift signals at 19.76 ppm, 40.79 ppm, 67.61 ppm, 169.14 ppm corresponding to the methyl (-CH₃), methylene (-CH₂), methine (-CH) and carbonyl (-C=O) groups respectively (Fig. 3.13). In commercial PHB, the characteristic peaks observed at 19.76 ppm, 40.8 ppm, 67.62 ppm and 169.14 ppm represented the methyl (-CH₃), methylene (-CH₂), methine (-CH) and carbonyl (-C=O) groups respectively. In addition, the previous studies have shown the presence of prominent peaks in ¹³C NMR spectrum at 19.76 ppm, 40.79 ppm, 67.61 ppm, 169.14 ppm representing methyl (CH₃), methylene (CH₂), methine (CH) and carbonyl (C=O) groups respectively of the PHB polymer (Doi et al., 1986; Sindhu et al., 2011).

The NMR analysis revealed that the polymer produced by *V. harveyi* MCCB 284 was homopolymer polyhydroxybutyrate.

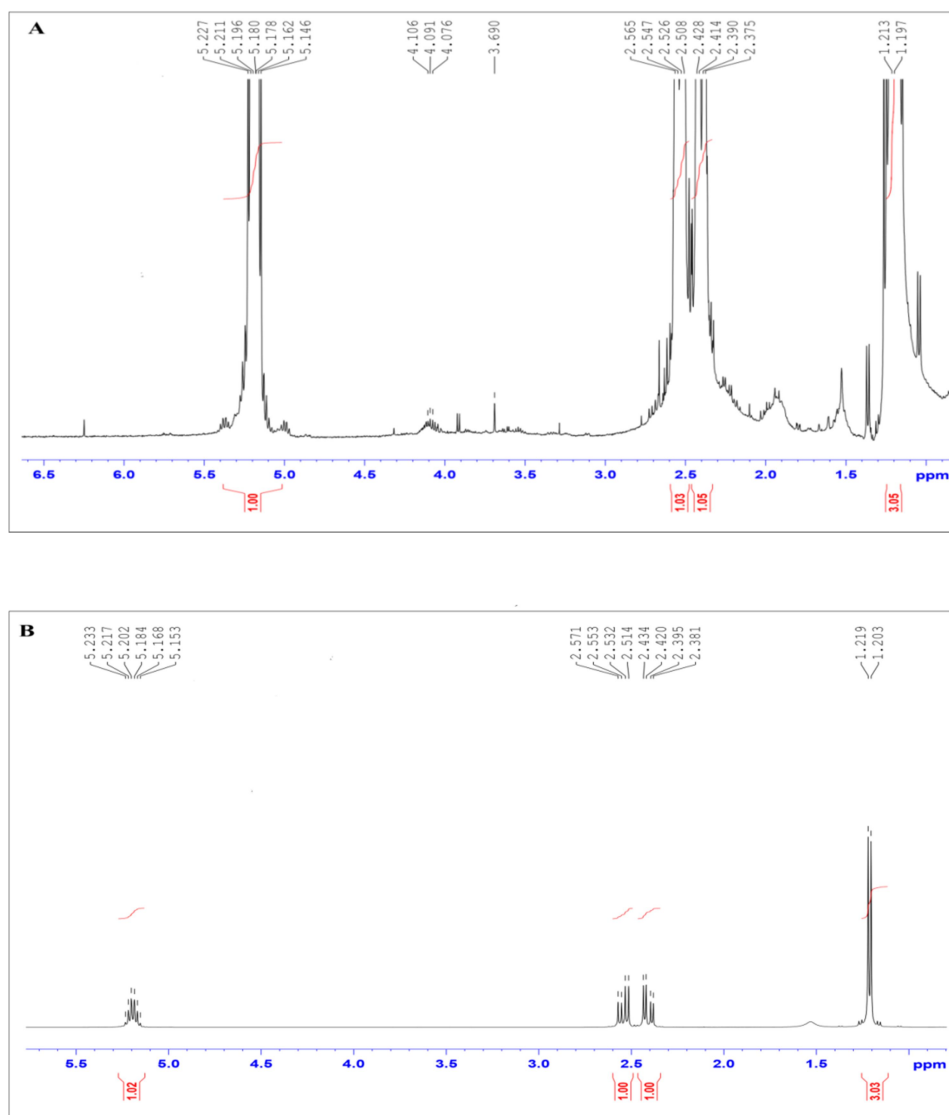


Fig. 3.12 ¹H Nuclear magnetic resonance spectra of (A) purified polymer from *V. harveyi* MCCB 284; (B) commercial PHB

3.3.4.5 GPC

The molecular mass of PHB produced from *V. harveyi* MCCB 284 was detected by GPC analysis. In the present study, relatively low molecular mass PHB was obtained with weight average molecular weight (Mw) 1.1- 153 kDa, number average molecular weight (Mn) 0.98-150 kDa and a polydispersity index (PDI) (Mw/Mn) of 1.04 with multimodal molecular weight distribution (Fig. 3.14). The average molecular weight of PHB produced from an extreme halophile *H. nitroreducens* also showed multimodal molecular weight distribution ranging from 136 to 704 kDa (Cervantes-Uc et al., 2014). The low molecular weight of the polymer was due to the glycerol end-capping of PHB as substantiated by the proton NMR study. Similar observations have been noticed from previous studies (Madden et al., 1999; Rodríguez-Contreras et al., 2015) which showed that the molecular weight of the PHB produced by *R. eutropha* NCIMB 40529 and *C. necator* DSM 545 from glycerol was considerably lower than the polymer obtained from glucose. GPC analysis of PHB isolated from *B. aryabhatai* PHB10 utilising glycerol as carbon source suggested that the polymer has a low number average molecular weight (Mn) of 74.87 kDa and a weight average molecular weight (Mw) of 199.74 kDa with high polydispersity index (PDI) 2.67 (Balakrishna Pillai et al., 2017). The weight average molecular mass of PHB produced by wild-type strain of *C. necator* ranges from 100 to 1000 kDa with a polydispersity (Mw/Mn) of around 2. The molecular mass of the polymer strongly depends on the composition of the substrate and culture conditions, including the method of PHB extraction which

causes severe damage to the granules and lead to loss of molecular mass of polymer (Radhika and Murugesan, 2012).

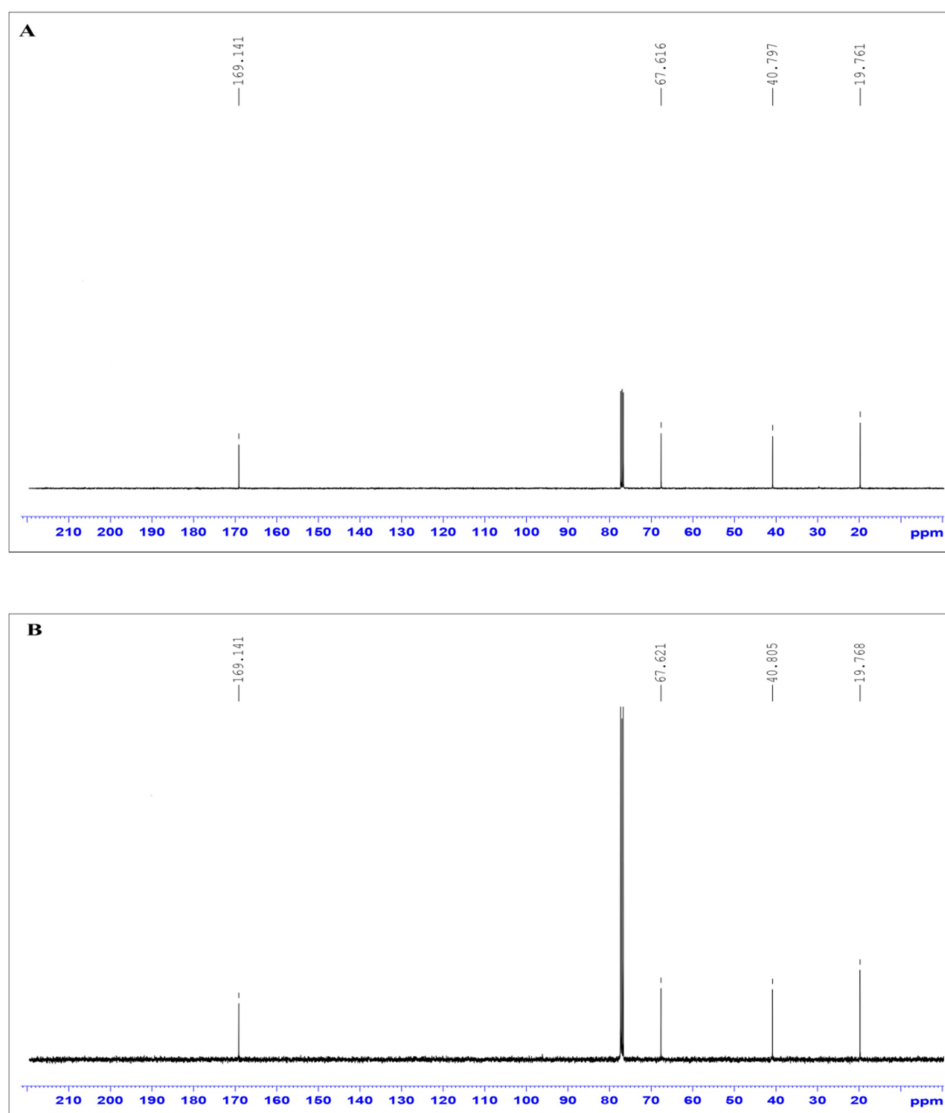


Fig. 3.13 ^{13}C Nuclear magnetic resonance spectra of (A) purified polymer from *V. harveyi* MCCB 284; (B) commercial PHB

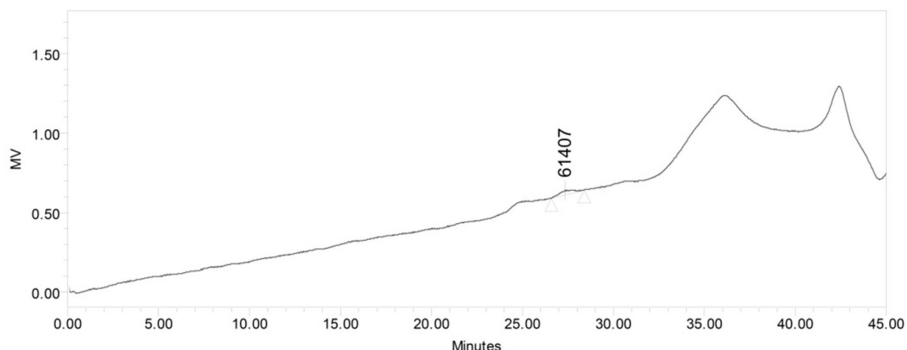


Fig. 3.14 Gel permeation chromatogram of purified polymer produced by *V. harveyi* MCCB 284

3.4 Conclusion

Vibrio harveyi MCCB 284 isolated from tunicate *A. nigra* collected from Vizhinjam Bay, Kerala was found to accumulate PHB up to 60% based on CDW in presence of glucose as carbon source. The optimization of process factors for PHB production showed maximum CDW of 3.2 g L⁻¹, PHB yield of 2.3 g L⁻¹ and polymer accumulation up to 72% based on CDW with glycerol after 72 h incubation at 30 °C, 150 rpm. This is the first report of a moderate halophilic isolate of *V. harveyi* that demonstrated high biomass yield and PHB production with glycerol as the sole carbon source. The polymer after extraction was purified and characterized using FTIR, NMR and DSC-TGA techniques to be identified as polyhydroxybutyrate. These results suggest that *V. harveyi* MCCB 284 is a good candidate for industrial production of PHB using glycerol as the substrate, as donor of genes for synthetic biology or its recombinant production.

..........

Chapter 4

BIOSYNTHESIS AND CHARACTERIZATION OF POLYHYDROXYALKANOATE FROM MARINE *BACILLUS CEREUS* MCCB 281 UTILISING GLYCEROL AS CARBON SOURCE

| | |
|-----------------|-----------------------------------|
| Contents | 4.1 <i>Introduction</i> |
| | 4.2 <i>Materials and methods</i> |
| | 4.3 <i>Results and discussion</i> |
| | 4.4 <i>Conclusion</i> |

4.1 Introduction

Polyhydroxyalkanoates (PHAs) are bio-based polymers synthesized by a wide variety of Gram positive and Gram negative bacteria as carbon storage inclusions under unfavourable growth conditions (Anderson and Dawes, 1990). The simplest and best characterized PHA is PHB, accumulated by several bacterial species such as *B. megaterium*, *C. necator*, *A. lata*, and recombinant *E. coli* (Anjum et al., 2016). PHAs are attractive base materials for wide range of medical, pharmaceutical and industrial applications due to their biodegradable, biocompatible, non-toxic and hydrophobic properties. As these polymers can be produced from renewable resources, PHAs are sustainable and carbon neutral. The unfavourable properties of PHB such as high crystallinity, stiffness and

brittleness can be overcome by incorporating different monomeric units such as 3-HV and 4-HB (Nakamura et al., 1992) which refine the material properties, thereby increasing their commercial potential. Most bacteria require the addition of precursors such as propionic acid or valeric acid for the synthesis of poly3-hydroxybutyrate-co-3-hydroxyvalerate (PHBV) co-polymers (Salgaonkar and Bragança, 2015; Van-Thuoc and Quillaguamán, 2013; Volova et al., 2014). The addition of precursors lead to modification in the PHA biosynthetic pathway resulting in incorporation of 3-HV monomers in the polymer chain, along with 3-HB units (Steinbüchel and Lütke-Eversloh, 2003). The incorporation of 3-HV monomers into PHB can improve its thermo-mechanical properties, and hence have more potential in biomedical and industrial applications than PHB homopolymers.

The cost of PHA production can be significantly reduced by utilisation of renewable and inexpensive carbon resources such as agricultural residues (Patel et al., 2016, 2015; Sindhu et al., 2013) and industrial wastes (Pandian et al., 2010) for microbial fermentation. Glycerol, a by-product of biodiesel industry has now become an attractive feedstock for PHA production using pure cultures as well as mixed microbial consortia (Dobroth et al., 2011; Kumar et al., 2015; Naranjo et al., 2013). In spite of the commercial use of glycerol in food and beverages, pharmaceuticals, cosmetics, personal care and other industries, it is expensive to refine crude glycerol to the purity needed for these applications (Tan et al., 2013). Therefore, the development of sustainable processes for utilisation of this by-product is all the more desirable to promote the growing biodiesel industry in a larger scale (Yang et al.,

2012). In addition, glycerol is regarded as a favourable substrate for PHA production, as carbon atoms in glycerol are in a highly reduced state compared to other carbohydrates, thereby stimulating intracellular polymer synthesis in bacteria (Hermann-Krauss et al., 2013). Hence, valorization of glycerol through PHA production will be a good strategy to recycle the industrial by-product to synthesize valuable bio-products.

Another important aspect of focus is the process optimization of fermentation to enhance PHA yield. Enhancement in process economics is feasible by design and implementation of efficient bioprocess strategies for improving the overall process, and thereby resulting in higher PHA productivity (Kaur, 2015). Design of experiment (DoE) is a powerful methodology used to evaluate important experimental variables in a bioprocess or to perform an optimization in order to avoid the experimental biases and reduces the required number of experiments (Mandenius and Brundin, 2008). The statistical DoE based approach using response surface methodology (RSM) provides more systematic data prediction and validation for different fermentation processes. RSM consists of a group of mathematical and statistical techniques that are based on the fit of empirical models to the experimental data obtained in relation to experimental design. It can be applied when a response or a set of responses of interest are governed by several variables. The main objective is to simultaneously optimize the levels of these variables to achieve maximum production (Bezerra et al., 2008). Statistical tools like Plackett-Burman (PB) design is a two-level screening design used to identify the most significant variables in an experiment when complete knowledge is usually unavailable. It allows the investigation of $n-1$

variables in at least n experiments. A minimum of $4n$ experiments is needed for estimating the effects for $4n-1$ factors (Plackett and Burman, 1946) which means that 4, 5, 6 or 7 variables require 8 experimental runs, 8, 9, 10 or 11 variables require 12 runs, and so on. In PB designs, each variable is represented at two levels, the higher level denoted as “+” and the lower as “-”.

This design is based on a first-order model:

$$Y = \beta_0 + \sum \beta_i X_i \dots\dots\dots(4.1)$$

where Y is the response, β_0 is the model intercept, β_i is the linear coefficient and X_i is the level of the independent variable. However, this model cannot be used to describe the interaction among the variables (Mukherjee and Rai, 2011; Warda et al., 2016). Central Composite Design (CCD) is the most popular statistical design employed to study the interactive effect of various factors for the optimization of PHA production using different microorganisms. CCD design requires 3 design points- factorial points representing all combinations of coded values $x = \pm 1$ which are in the corners of cube, axial points at a distance $\pm \alpha$ from the origin which are in the center of each face of the cube, and center points with all levels set to coded level 0, which are in the center of the cube. A CCD estimate the response calculated in the form of a second-degree polynomial equation:

$$Y = \beta_0 + \sum \beta_i X_i + \sum \beta_{ii} X_i^2 + \sum \beta_{ij} X_i X_j \dots\dots\dots(4.2)$$

where Y is the predicted response variable, β_0 is the interception, β_i are the linear coefficients, β_{ii} are the quadratic coefficients, β_{ij} are coefficients of the interaction and $X_i X_j$ are coded experimental levels of independent

variables (Bezerra et al., 2008; Varshosaz et al., 2010). The visualization of the predicted model equation in RSM can be obtained by the response surface plot (3D) or contour plot (2D) that show the relationship between the responses and the independent variables. Different media components such as nitrogen sources, carbon sources and physical factors such as pH, salinity, incubation time, temperature and agitation which play significant roles in PHA accumulation were optimized using CCD (Dhangdhariya et al., 2015; Sharma and Bajaj, 2015).

The present study focuses on the production and optimization of polyhydroxyalkanoate in *B. cereus* MCCB 281 utilising glycerol as the sole carbon source. The polymer production was optimized using response surface methodology and fermenter scale up was performed under optimized conditions. The extracted polymer was purified and characterized by Fourier Transform Infrared Spectroscopy (FTIR), Nuclear Magnetic Resonance Spectroscopy (NMR), Gas Chromatography- Mass Spectrometry (GC-MS), X-ray Diffraction (XRD) and Gel Permeation Chromatography (GPC) techniques.

4.2 Materials and methods

4.2.1 PHA production and quantification

For PHA production, the isolate *B. cereus* MCCB 281 was grown on ZoBell's marine agar slants for 16 h, 28 °C. Aliquot of 2 mL sterile production medium (composition: Peptone- 5 g L⁻¹, Yeast extract- 1 g L⁻¹) was added to the slant; cells dislodged using sterile inoculation loop and aseptically transferred to another tube. Cell density was measured using UV-visible spectrophotometer (Shimadzu, Japan) at 600 nm and the

absorbance adjusted to 1.0 prior to inoculation. Production medium was prepared in sea water and pH was adjusted to 7.5. Inoculum (1% v/v) was added to 100 mL production medium and incubated for 48 h at 28 °C, 200 rpm. Glucose was used as carbon source (final concentration 20 g L⁻¹) for PHA production. Cell growth was monitored every 12 h by measuring optical density at 600 nm.

Cell dry weight (CDW) and PHA content were measured as explained in sections 2.2.4 and 2.2.5 of Chapter 2.

4.2.2 Identification of *phaC* gene

The polyhydroxyalkanoate synthase (*phaC*) gene of the potent isolate MCCB 281 was amplified using gene specific primers (forward 5'-GGG AAA AGC AAT TAG AGC TAT ACC C-3' and reverse 5'-TCT ACC TTT TGT CCG CGA ATA AC-3'). PCR mixture (25 µL) contain 1 µL genomic DNA, 12.5 µL emerald mix (Takara, Japan), 1.25 µL each of forward and reverse primers and the remaining volume was made up with sterile milliq. PCR was performed with an initial denaturation at 95 °C for 3 min followed by 35 cycles of denaturation at 95 °C for 30 s, annealing at 60 °C for 40 s, extension at 72 °C for 1 min and final extension at 72 °C for 5 min. The amplified products were sequenced at SciGenom Labs, Cochin, Kerala. The partial forward and reverse sequences of the amplified products were aligned using software GeneTool and homology search was performed in NCBI database using Blast tool. The nucleotide sequence was deposited in GenBank and accession number obtained. Conserved protein domain search was performed in NCBI to find the conserved domain of the protein. Multiple sequence alignment of amino

acid sequence of *phaC* gene of *B. cereus* MCCB 281 with other related species obtained from NCBI database was also done using Bioedit software to identify the conserved amino acids present in the protein. Phylogenetic tree was constructed using the neighbor-joining method (Saitou and Nei, 1987) with bootstrap value of 1000 replicates (Felsenstein, 1985) in MEGA 6.0 software (Tamura et al., 2013).

4.2.3 Transmission Electron Microscopy (TEM)

Protocol as described in section 3.2.2 of Chapter 3.

4.2.4 Effect of initial pH, temperature and substrates on PHA production

PHA production of *B. cereus* MCCB 281 was carried out in the presence of different pH (6.0-9.0), temperature (25-40 °C) and carbon sources (glucose, glycerol, sucrose, xylose, lactose, fructose, sodium acetate) by one-factor-at-a-time approach keeping other parameters constant. Different carbon sources (final concentration 20 g L⁻¹) were prepared in sea water, sterilized separately and added to the production medium at the time of inoculation. To evaluate the effect of precursor on PHA production, different concentrations of propionic acid (0.1, 0.5, 1 and 2% v/v) was added to the production medium. Fermentation was carried out in 100 mL production medium with 1% (v/v) inoculum and incubated for 48 h at 200 rpm. CDW and PHA content were estimated. For all the experiments, optical density of the inoculum was adjusted to 1.0 at 600 nm corresponding to 10⁸ CFU mL⁻¹.

4.2.5 Statistical optimization of PHA production

4.2.5.1 Plackett-Burman design for screening of significant variables

Design of experiment (DoE) approach was used for optimization of process variables for PHA production using the software Design-Expert version 10.0.7 (Stat-Ease Inc., Minneapolis, USA). Plackett-Burman design was selected to identify the process variables which influence PHA production. A total of five variables were selected, which were salt concentration (10-30 g L⁻¹ sodium chloride), glycerol (2-4% v/v), inoculum size (4-8% v/v), yeast extract (1-3 g L⁻¹) and incubation time (24-48 h). Each variable was set at a higher (+) and lower (-) limit to identify which variables have the significant influence on PHA production (Table 4.1). These variables were evaluated in twelve experimental runs with CDW (g L⁻¹) and PHA yield (g L⁻¹) as the responses. CDW and PHA yield were determined using crotonic acid estimation. The experiments were carried out in triplicate in 250 mL Erlenmeyer flasks containing 100 mL production medium and inoculated with 1 OD₆₀₀ culture corresponding to 10⁸ CFU mL⁻¹ and incubated in orbital shaker at 250 rpm. The responses obtained were subjected to Analysis of Variance (ANOVA) and the significant (p<0.05) variables were selected for further optimization.

Table 4.1 Range of independent variables selected for Plackett-Burman design for PHA production

| Variables | Symbol | Units | Lower limit (-) | Higher limit (+) |
|--------------------|--------|-------------------|-----------------|------------------|
| Salt concentration | A | g L ⁻¹ | 10 | 30 |
| Glycerol | B | % v/v | 2 | 4 |
| Inoculum size | C | % v/v | 4 | 8 |
| Yeast extract | D | g L ⁻¹ | 1 | 3 |
| Incubation time | E | h | 24 | 48 |

4.2.5.2 Response Surface Methodology

Response Surface approach using Face-centered Central Composite Design (FCCD) was used to analyse the interactive effects of the significant variables that affect PHA production. A set of 30 experiments in triplicate was designed to study the influence of four selected variables, i.e. salt concentration, glycerol, inoculum size and incubation time on the responses CDW (g L^{-1}) and PHA yield (g L^{-1}). CDW and PHA yield were determined after each run. The experiments were carried out in 250 mL Erlenmeyer flasks containing 100 mL production medium and incubated in orbital shaker at 250 rpm. Each variable was examined at five different levels ($-\alpha$, -1, 0, +1, $+\alpha$) (Table 4.2), the responses were analysed using second order polynomial equation and the results were fitted into the equation by multiple regression analysis. Three-dimensional surface plots were used to analyse the interaction of process variables and to determine the optimum concentration of each variable favouring the responses. Statistical analysis of the model was done for evaluation of analysis of variance (ANOVA).

Table 4.2 Range of independent variables selected for the response surface central composite design for PHA production

| Variables | Symbol | Units | Levels of variables | | | | |
|--------------------|--------|-------------------|---------------------|-----|----|-----|-----------|
| | | | $-\alpha$ | -1 | 0 | +1 | $+\alpha$ |
| Salt concentration | A | g L^{-1} | 8 | 9 | 10 | 11 | 12 |
| Glycerol | B | % v/v | 3 | 3.5 | 4 | 4.5 | 5 |
| Inoculum size | C | % v/v | 7 | 7.5 | 8 | 8.5 | 9 |
| Incubation time | D | h | 20 | 22 | 24 | 26 | 28 |

4.2.5.3 Validation of the model

For validation of the model, experiments were conducted with the optimized values for each variable given by point prediction method to corroborate the predicted value and the observed value for polymer production. The experiment was carried out in triplicate and the results were expressed as mean \pm standard deviation. The obtained result was compared with the un-optimized culture conditions to determine the effectiveness of entire optimization process.

4.2.6 Fermenter level production

Batch fermentation was carried out in 5 L fermenter (B-Lite, Sartorius, Germany) with 3 L working volume. The production medium was added to the fermenter, pH was adjusted to 7.0 and medium was sterilized *in situ*. The pH and temperature were maintained at 7.0 and 30 °C respectively throughout the process. Agitation was kept at 250 rpm and aeration was set at 2.0 L air/min. All the factors were maintained at the optimum conditions obtained from the CCD design. The experiment was carried out in triplicate and results were expressed as mean \pm standard deviation. Cells were harvested after incubation for polymer extraction.

4.2.7 PHA extraction

Protocol as described in section 3.2.4 of Chapter 3.

4.2.8 Polymer characterization

4.2.8.1 FTIR

Purified polymer (2 mg) was ground with potassium bromide crystals to form a pellet. FTIR spectrum was recorded between 4000 and

400 cm⁻¹ using Nicolet Avatar 370 spectrometer (Thermo Scientific, USA). The spectrum obtained was compared with commercially available PHBV (12mol% 3-HV) (Sigma, USA).

4.2.8.2 XRD

X-ray diffraction analysis of PHA was carried out with D8 Advance diffractometer (Bruker, Germany) using Cu radiation (wavelength 1.5406 Å) in the range of $2\theta = 3-70^\circ$. The operating mode of the instrument was 40 kV and 40 mA. The pattern obtained was compared with commercially available PHBV (12mol% 3-HV) (Sigma, USA). The crystallinity of the polymer was calculated using the following equation (Chan et al., 2011)

$$\text{Crystallinity (\%)} = (F_c / (F_c + F_a)) * 100 \dots\dots\dots(4.3)$$

where F_c and F_a are the areas of crystalline (peak) and non-crystalline regions respectively.

4.2.8.3 GC-MS

The polymer (100 mg) was dissolved in 2 mL chloroform, mixed with 2 mL acidified methanol containing 3% (v/v) conc. H₂SO₄ and incubated at 100 °C for 120 min for methanolysis. The mixture was then cooled to room temperature, 1 mL distilled water was added, shaken vigorously for 10 min and centrifuged at 2000 g for 5 min (Braunegg et al., 1978). The organic layer with methyl esters was analysed by GC-MS using the Agilent 7890A GC/5975 MSD system equipped with a HP-5 column (Agilent, USA).

4.2.8.4 NMR

^1H and ^{13}C NMR of the extracted polymer and commercial PHBV (12mol% 3-HV) were analysed on Bruker Avance III spectrometer operated at 400 MHz at 25 °C. About 10 mg of sample was dissolved in deuterated chloroform and the spectra were recorded.

All the above analyses were carried out at the Sophisticated Test and Instrumentation Centre (STIC), Kerala.

4.2.8.5 GPC

Number-average molecular weight (M_n), weight-average molecular weight (M_w) and polydispersity index (PDI) of polymer were determined by GPC using Waters HPLC/GPC system with 600 Series Pump and Waters Styragel HR series HR5E/4E/2/0.5 column equipped with a 7725 Rheodyne injector and refractive index 2414 detector (Waters Corporation, USA). A quantity of 1 mg PHA was completely dissolved in 1 mL chloroform and filtered through 0.2 μm PVDF membranes. The injection volume was 20 μL . The mobile phase was chloroform at a flow rate of 1.0 mL min^{-1} . Polystyrene standards of molecular weight 1865000, 100000, 9130 were used for relative calibration. The analysis was performed at Sree Chitra Tirunal Institute for Medical Sciences and Technology, Trivandrum, Kerala.

4.3 Results and discussion

4.3.1 PHA production

PHA production of *B. cereus* MCCB 281 was investigated in presence of 20 g L^{-1} glucose as carbon source and the culture was incubated for 48 h at 28 °C, 200 rpm. A maximum CDW of $2.11 \pm 0.06 \text{g L}^{-1}$,

PHA yield of $1.3 \pm 0.08 \text{ g L}^{-1}$ and PHA content of $61.33 \pm 1.8\%$ (w/w) was observed after 48 h. In a related study, PHA production of a moderately halophilic isolate *V. harveyi* MCCB 284 showed PHA yield of 0.8 g L^{-1} with a CDW of 1.34 g L^{-1} in presence of glucose as carbon source after 72 h incubation (Mohandas et al., 2016). Similarly, PHA yield of 2.02 g L^{-1} and CDW of 2.77 g L^{-1} was observed in a halotolerant *Bacillus* sp. MG12 using glucose after 48 h incubation (Moorkoth and Nampoothiri, 2016).

4.3.2. Identification of phaC gene

The *phaC* synthase gene of MCCB 281 was amplified using gene specific primers and partial gene sequence of 751 bp (Fig. 4.1) was deposited in GenBank under the accession number KX463674. The partial sequence was translated using ExpASy tool and the open-reading frame (ORF) of *phaC* synthase was identified with the ORF Finder tool.

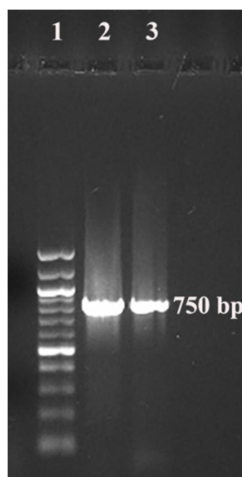


Fig. 4.1 PCR amplification of *phaC* synthase gene of *B. cereus* MCCB 281 using gene specific primers. Lane 1- 100 bp DNA ladder; Lane 2, 3- 750 bp amplified product

The deduced amino acid sequence showed 99% homology to *phaC* gene of *B. cereus* FC11 and *B. cereus* SPV using Blastp search in NCBI. Phylogenetic tree of the synthase gene was constructed using MEGA 6 software which showed closest match with *B. cereus* PHA synthase (AD187591) (Fig. 4.2).

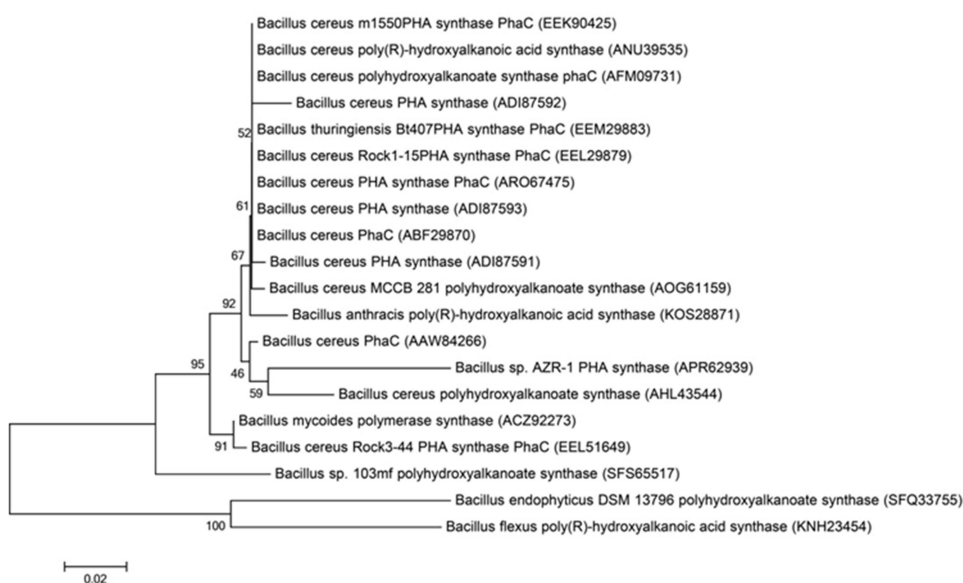


Fig. 4.2 Phylogenetic tree of *phaC* synthase gene of *B. cereus* MCCB 281 with its closely related species based on amino acid sequences from GenBank. Bootstrap values are denoted at the nodes.

The *phaC* gene of MCCB 281 encoded for class IV polyhydroxyalkanoate synthase which prefer Co-enzymeA thioesters of (R)-3-hydroxy fatty acids constituting 3 to 5 carbon atoms (short chain length hydroxyalkanoates). *Bacillus* spp. that synthesized PHAs possesses class IV synthase that comprise *phaC* and its *phaR* subunits. The *phaC* subunit of class IV synthase resembles class III synthases, but *phaR* was replaced by *phaE* subunit (Valappil et al., 2007). Multiple sequence alignment of the amino

acid sequence of *phaC* synthase of MCCB 281 marked the presence of amino acid Cys₁₂₃ present in putative lipase box region (G-X-C₁₂₃-X-G) which was highly conserved in all PHA synthases and was involved in the covalent catalysis (Fig. 4.3).

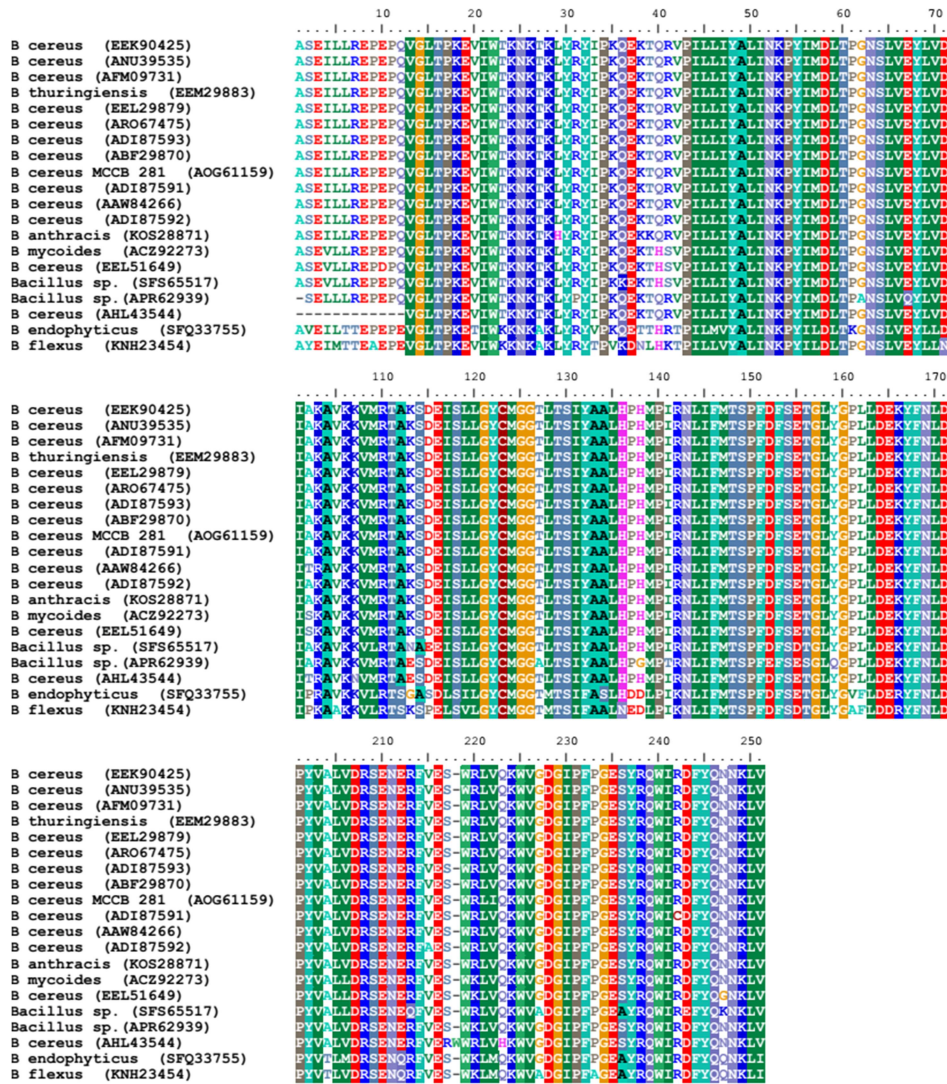


Fig. 4.3 Multiple sequence alignment of amino acid sequences of *phaC* gene of *B. cereus* MCCB 281 with other related species obtained from NCBI database

4.3.3 TEM

TEM analysis showed the presence of PHA granules in *B. cereus* MCCB 281 grown in ZoBell's marine broth containing 20 g L⁻¹ glucose for 48 h. The cells contained PHA granules that varied in size and number (Fig. 4.4).

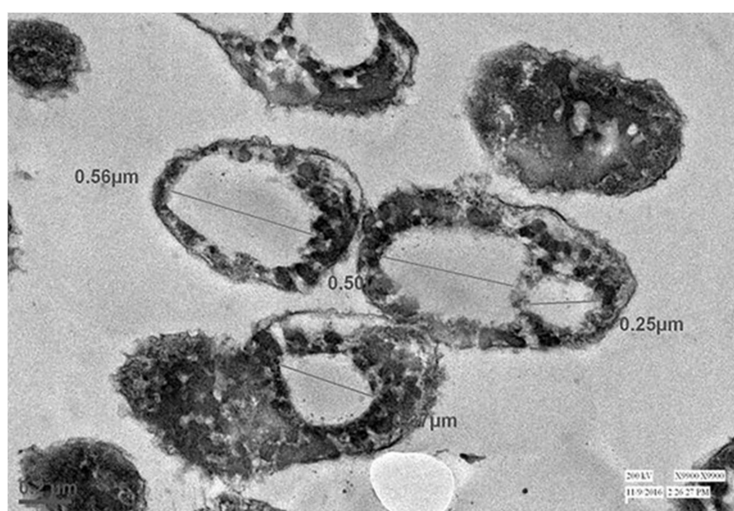


Fig. 4.4 TEM of *B. cereus* MCCB 281 showing the presence of PHA granules

4.3.4 Effect of initial pH, temperature and substrates on PHA production

The various factors such as initial pH, temperature, carbon sources and addition of precursor that influence PHA production in *B. cereus* MCCB 281 were sequentially optimized by 'one-factor-at-a-time' approach in shake flask conditions. The optimized value for each factor was used in subsequent stages of the optimization.

4.3.4.1 Effect of initial pH

To examine the effect of initial pH, the isolate MCCB 281 was inoculated into 100 mL production medium of varying pH 6.0-9.0 and incubated at 28 °C for 48 h. The pH was adjusted using 1 M NaOH or 1 M HCl prior to sterilization. A maximum CDW of $2.04 \pm 0.04 \text{ g L}^{-1}$ and PHA content of $60.41 \pm 2\%$ (w/w) were recorded at pH 7.0 (Fig. 4.5). The production declined at low pH compared to alkaline pH, where the production was stable.

4.3.4.2 Effect of temperature

The effect of different incubation temperatures on PHA synthesis showed highest percentage of PHA content $61.23 \pm 1.3\%$ (w/w) and CDW of $2.21 \pm 0.1 \text{ g L}^{-1}$ at the optimum temperature 30 °C. Also, the isolate showed considerable growth and PHA yield at 35 °C and 40 °C; however no growth was noticed at 45 °C (Fig. 4.6). These findings were in agreement with the previous report on PHA production from *B. cereus* FA11 (Masood et al., 2011).

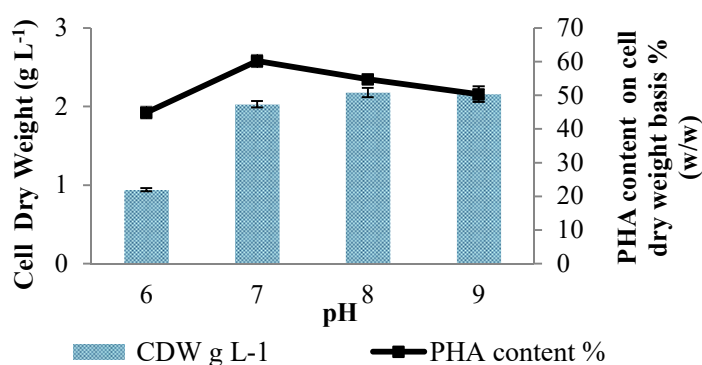


Fig. 4.5 Effect of pH on PHA production in *B. cereus* MCCB 281 using glucose 20 g L^{-1} as carbon source. Data shown are mean standard deviations of triplicate

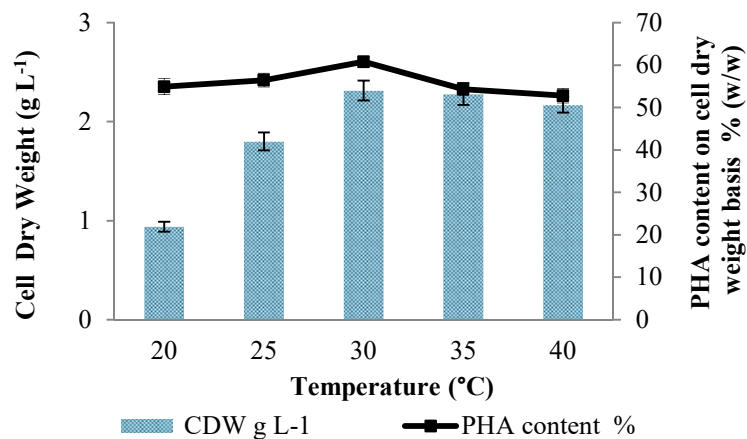


Fig. 4.6 Effect of temperature on PHA production in *B. cereus* MCCB 281 using glucose 20 g L⁻¹ as carbon source. Data shown are mean standard deviations of triplicate

4.3.4.3 Effect of carbon sources

The study of different carbon sources on PHA production showed maximum yield in the presence of glucose and glycerol as the sole carbon sources. However, CDW of 2.33 ± 0.11 g L⁻¹ and PHA content of $62.23 \pm 1.42\%$ (w/w) were obtained exclusively in the presence of 20 g L⁻¹ glycerol as the sole carbon source, even though good growth was favoured by sucrose, fructose and sodium acetate (Fig. 4.7) as well. It was notable that the isolate MCCB 281 could synthesize PHA co-polymer with 3-HV units in presence of glucose, glycerol, sucrose and fructose as the sole carbon sources. *Bacillus* spp. has the ability to utilise wide range of substrates such as volatile fatty acids, different ligno-cellulosic bio wastes as well as pure sugars such as glucose for efficient production of PHA homo- and co-polymers along with hydrogen which in turn improves the efficiency, sustainability and economics of the process (Patel et al., 2012, 2011; Porwal et al., 2008; Singh et al., 2013). This heterogeneity of PHAs

in the genus *Bacillus* was speculated to be due to PHA synthase which has relatively broad monomer specificity (Valappil et al., 2007).

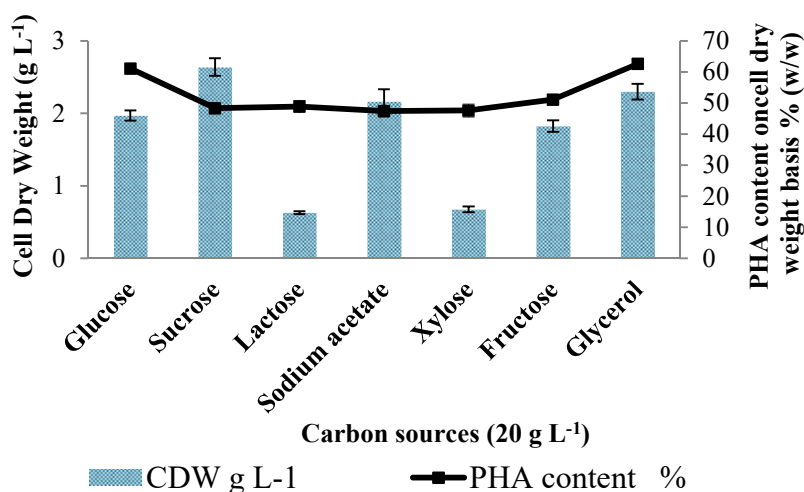


Fig. 4.7 Effect of carbon sources on PHA production in *B. cereus* MCCB 281. Data shown are mean standard deviations of triplicate

PHA yields are highly variable among the different *Bacillus* species which was largely due to either the type of strain or feed used in the process (Kumar et al., 2013). With *B. thuringiensis* EGU45, PHA production using 5% (v/v) glycerol demonstrated co-polymer accumulation with 3-HV content, and a CDW of 4.9 g L⁻¹ and PHA content of 72% after 48 h incubation (Kumar et al., 2015). Using *B. cereus* UW85, the production of tercopolymer of 3HB, 3HV and 6HHx was recorded with ϵ -caprolactone as sole carbon source in mineral salts medium without any glucose. The isolate produced a CDW of 0.41 g L⁻¹ and PHA content 8.9 % after 24 h incubation. However, addition of glucose along with ϵ -caprolactone suppressed co-polymer synthesis and PHB homopolymer was produced (Labuzek and Radecka, 2001). PHA co-polymer production was reported

in an endophytic bacterium *B. cereus* RCL 02 in presence of 4% (w/v) sugarcane molasses as sole carbon source with CDW of 9.4 g L⁻¹ and PHA content of 83 % (Das et al., 2019). PHA production using glycerol as carbon source in *B. megaterium* also showed 10–20% lower production cost compared with glucose. A CDW of 5.7 g L⁻¹ and PHA content of 60% was obtained in presence of 2% glycerol (Naranjo et al., 2013). PHA yield from the isolate MCCB 281 utilising glycerol was comparable with previous reports from other *Bacillus* sp. (Deepthi et al., 2011; Kumar et al., 2015; Moorkoth and Nampoothiri, 2016). Therefore, considering the ability of MCCB 281 to utilise less expensive carbon source glycerol for efficient co-polymer production, it was chosen specifically as the carbon source of choice for PHA optimization studies.

4.3.4.4 Effect of precursor

To examine the influence of precursor propionic acid (PA) on PHA production of MCCB 281, different concentrations of PA were added after 12 h incubation. Addition of propionate was effective in increasing the 3-HV content as previously reported (Du et al., 2001), and the addition of both 1% and 2% v/v PA resulted in increasing the 3-HV content up to 30mol% (Table 4.3). Even though, there was an increase in valerate content on addition of the precursor, PHA yield was considerably low on co-feeding with PA; probably due to the toxic effect of the volatile fatty acid on the growth of the isolate. Similar result was observed by Du et al. (2001) where as high PA to carbon ratio resulted in lower polymer productivity. Investigations on PHA production in the presence of precursor supplementation in *B. thuringiensis* EGU45 demonstrated PHA co-polymer production with 13mol% 3-HV content in high nitrogen containing medium

having 0.5% v/v propionic acid. However, in this case increase of PA concentration up to 2% v/v resulted in the lowering of 3-HV% (Kumar et al., 2015). Similarly, in *A. lata* MTCC 231, when PA concentration was increased from 10 to 50 mmol L⁻¹, CDW, PHA yield and 3-HV content increased in the beginning, attained maximum at 30 mmol L⁻¹ with 9.6 g L⁻¹ CDW, 5.6 g L⁻¹ PHA yield and 16.5mol% 3-HV content and thereafter started to decrease at 50 mmol L⁻¹ (Zafar et al., 2012).

Table 4.3 Effect of different concentrations of propionic acid on PHA production

| Propionic acid (% v/v) | CDW (g L ⁻¹) | PHA content (% w/w) | 3-HB (%) | 3-HV (%) |
|---------------------------|-----------------------------|------------------------|-------------|-------------|
| 0.1 | 2.22 ± 0.05 | 55.26 ± 1.8 | 88 | 12 |
| 0.5 | 2.08 ± 0.08 | 52.55 ± 1.3 | 80 | 20 |
| 1.0 | 1.56 ± 0.12 | 50.36 ± 2.5 | 70 | 30 |
| 2.0 | 0.93 ± 0.07 | 45.17 ± 1.2 | 70 | 30 |

Data shown as mean ± SD (n=3)

4.3.5 Statistical optimization of PHA production

4.3.5.1 Plackett-Burman design for screening of significant variables

Statistical optimization was performed to increase the polymer yield and to find out the significant variables and their interactions on PHA production. Table 4.4 shows the PB design and the responses obtained in the study. When the value of the coefficient of the tested variable was found to be positive, then the variable has a positive effect on the response, and the coefficient value was negative, the variable has a negative effect on the response. The p value less than 0.05 indicate that the model terms were significant. Table 4.5 represent p values for the

effect of variables on cell dry weight and PHA production. Evaluation of the results from PB design showed that salt concentration, glycerol, inoculum size and incubation time were significant for the responses in MCCB 281. Similar observation was noticed in PB-designed experiments performed in another isolate *B. cereus* PS10 where, inoculum size and incubation time showed significant influence on PHA production (Sharma and Bajaj, 2015). The variables salt concentration and incubation time had a negative coefficient on cell dry weight in *B. cereus* MCCB 281. In the case of PHA yield, glycerol and inoculum size had a positive co-efficient, while incubation time showed a negative co-efficient. The other variables were kept constant in further experiments.

Table 4.4 Results of the experimental Plackett - Burman design for PHA production from *B. cereus* MCCB 281

| Run No. | Experimental variables ^a | | | | | Response | |
|---------|-------------------------------------|--------------|--------------|---------------------------|----------|-----------------------------|-----------------------------------|
| | A (g L ⁻¹) | B (% v/v) | C (% v/v) | D (g L ⁻¹) | E (h) | CDW (g L ⁻¹) | PHA yield (g L ⁻¹) |
| 1 | 10 | 4 | 8 | 1 | 24 | 3.25 | 2.10 |
| 2 | 10 | 4 | 8 | 3 | 24 | 2.82 | 1.80 |
| 3 | 10 | 4 | 4 | 1 | 48 | 2.75 | 1.69 |
| 4 | 30 | 4 | 8 | 1 | 48 | 2.13 | 1.10 |
| 5 | 30 | 2 | 8 | 1 | 48 | 2.47 | 1.31 |
| 6 | 10 | 2 | 4 | 3 | 48 | 2.87 | 1.26 |
| 7 | 30 | 2 | 8 | 3 | 24 | 2.86 | 1.69 |
| 8 | 10 | 2 | 8 | 3 | 48 | 2.87 | 1.62 |
| 9 | 10 | 2 | 4 | 1 | 24 | 3.36 | 1.28 |
| 10 | 30 | 4 | 4 | 3 | 48 | 2.30 | 1.16 |
| 11 | 30 | 2 | 4 | 1 | 24 | 3.07 | 1.60 |
| 12 | 30 | 4 | 4 | 3 | 24 | 3.10 | 1.74 |

^aA: Salt concentration, B: Glycerol, C: Inoculum size, D: Yeast extract, E: Incubation time

Table 4.5 ANOVA for cell dry weight and PHA yield of selected factorial model under Plackett-Burman design

| Source | Cell dry weight (g L ⁻¹) | | | PHA yield (g L ⁻¹) | | |
|--------------------|--------------------------------------|---------|----------|--------------------------------|---------|--------|
| | SS | F-Value | Prob> F | SS | F-Value | Prob>F |
| Model | 3.34 | 56.73 | < 0.0001 | 0.94 | 95.86 | 0.0104 |
| Salt concentration | 1.14 | 96.47 | < 0.0001 | - | - | - |
| Glycerol | - | - | - | 0.14 | 128.64 | 0.0077 |
| Inoculum size | - | - | - | 0.15 | 133.84 | 0.0074 |
| Incubation time | 1.97 | 167.42 | < 0.0001 | 0.14 | 129.04 | 0.0077 |

SS - sum of squares

4.3.5.2 Response Surface Methodology

Central composite design (CCD) was used to investigate the significant interactions affecting PHA production based on the results obtained from PB design. CCD based optimization of four variables i.e. salt concentration, glycerol, inoculum size and incubation period was performed for PHA production (Table 4.6), while other factors were maintained at constant level. The statistical significance of the model was evaluated by the F-test for ANOVA to determine the goodness of fit. The results of ANOVA for cell dry weight (Table 4.7) and PHA yield (Table 4.8) showed that the model was significant ($p < 0.0001$).

The second order polynomial equation for cell dry weight in terms of coded factors is given below:

$$\begin{aligned}
 \text{CDW (g L}^{-1}\text{)} = & +3.22 - 0.0204 * A + 0.0046 * B + 0.0271 \\
 & * C - 0.0129 * D + 0.0068 * A^2 - 0.0295 \\
 & * B^2 + 0.0093 * C^2 + 0.0155 * D^2 + 0.0594 \\
 & * AB + 0.0144 * AC - 0.0444 * AD - 0.0469 \\
 & * BC - 0.0106 * BD - 0.1131 * CD \dots\dots\dots (4.4)
 \end{aligned}$$

where A = salt concentration (g L⁻¹); B = glycerol (v/v); C = inoculum size (v/v) and D = incubation time (h). The equation in terms of coded

factors can be used to make predictions about the response for given levels of each factor. The coded equation was useful for identifying the relative impact of the factors by comparing the factor coefficients.

Table 4.6 Results of central composite design for PHA production from *B. cereus* MCCB 281

| Run No. | Experimental variables ^a | | | | Response | |
|---------|-------------------------------------|-----------|-----------|-------|--------------------------|--------------------------------|
| | A (g L ⁻¹) | B (% v/v) | C (% v/v) | D (h) | CDW (g L ⁻¹) | PHA yield (g L ⁻¹) |
| 1 | 9 | 4.5 | 8.5 | 22 | 3.30 | 1.94 |
| 2 | 9 | 4.5 | 7.5 | 26 | 3.38 | 1.80 |
| 3 | 11 | 3.5 | 7.5 | 22 | 3.00 | 1.80 |
| 4 | 9 | 3.5 | 7.5 | 26 | 3.39 | 1.69 |
| 5 | 10 | 4.0 | 8.0 | 24 | 3.20 | 2.16 |
| 6 | 11 | 3.5 | 8.5 | 26 | 3.07 | 1.87 |
| 7 | 10 | 4.0 | 7.0 | 24 | 3.20 | 1.80 |
| 8 | 10 | 4.0 | 8.0 | 20 | 3.30 | 2.08 |
| 9 | 10 | 4.0 | 8.0 | 24 | 3.21 | 2.14 |
| 10 | 11 | 3.5 | 7.5 | 26 | 3.10 | 1.70 |
| 11 | 12 | 4.0 | 8.0 | 24 | 3.20 | 1.89 |
| 12 | 10 | 5.0 | 8.0 | 24 | 3.13 | 1.85 |
| 13 | 10 | 4.0 | 8.0 | 28 | 3.27 | 1.79 |
| 14 | 9 | 3.5 | 8.5 | 26 | 3.30 | 1.89 |
| 15 | 10 | 3.0 | 8.0 | 24 | 3.08 | 1.79 |
| 16 | 11 | 4.5 | 8.5 | 26 | 3.10 | 1.80 |
| 17 | 11 | 4.5 | 7.5 | 26 | 3.30 | 1.80 |
| 18 | 8 | 4.0 | 8.0 | 24 | 3.30 | 1.80 |
| 19 | 11 | 4.5 | 8.5 | 22 | 3.40 | 1.92 |
| 20 | 10 | 4.0 | 8.0 | 24 | 3.21 | 2.15 |
| 21 | 10 | 4.0 | 8.0 | 24 | 3.21 | 2.10 |
| 22 | 10 | 4.0 | 8.0 | 24 | 3.23 | 2.14 |
| 23 | 9 | 3.5 | 7.5 | 22 | 3.10 | 1.82 |
| 24 | 11 | 3.5 | 8.5 | 22 | 3.40 | 1.94 |
| 25 | 9 | 3.5 | 8.5 | 22 | 3.40 | 2.00 |
| 26 | 10 | 4.0 | 9.0 | 24 | 3.32 | 2.05 |
| 27 | 11 | 4.5 | 7.5 | 22 | 3.25 | 2.03 |
| 28 | 10 | 4.0 | 8.0 | 24 | 3.28 | 2.17 |
| 29 | 9 | 4.5 | 8.5 | 26 | 3.00 | 1.90 |
| 30 | 9 | 4.5 | 7.5 | 22 | 3.04 | 2.00 |

^aA: Salt concentration, B: Glycerol, C: Inoculum size, D: Incubation Time

In case of cell dry weight, the model F-value of 21.01 indicated that the model was significant. The "Lack of Fit F-value" of 1.56 implied that the Lack of Fit was not significant relative to the pure error. Non-significant lack of fit is good for the model to fit. The model was found to be highly reliable with coefficient of determination (R^2) value 0.9515 and 'adjusted R^2 ' value 0.9062. The predicted R^2 of 0.7713 was in reasonable agreement with the adjusted R^2 value. A very low value of coefficient of the variation (CV: 1.15%) demonstrated a very high degree of precision and reliability of the experimental data. The coefficient of variance (CV) was the ratio of standard error of estimate to the mean value of the response.

Table 4.7 ANOVA for response surface model of cell dry weight from *B. cereus* MCCB 281

| Source | SS | F-Value | Prob> F | |
|----------------------|--------|---------|----------|-----------------|
| Model | 0.4048 | 21.01 | < 0.0001 | significant |
| A-Salt concentration | 0.0100 | 7.27 | 0.0166 | |
| B-Glycerol | 0.0005 | 0.3664 | 0.5540 | |
| C-Inoculum size | 0.0176 | 12.79 | 0.0028 | |
| D-Incubation time | 0.0040 | 2.91 | 0.1087 | |
| AB | 0.0564 | 40.99 | < 0.0001 | |
| AC | 0.0033 | 2.40 | 0.1420 | |
| AD | 0.0315 | 22.90 | 0.0002 | |
| BC | 0.0352 | 25.55 | 0.0001 | |
| BD | 0.0018 | 1.31 | 0.2699 | |
| CD | 0.2048 | 148.79 | < 0.0001 | |
| A ² | 0.0013 | 0.9138 | 0.3543 | |
| B ² | 0.0238 | 17.32 | 0.0008 | |
| C ² | 0.0024 | 1.71 | 0.2103 | |
| D ² | 0.0066 | 4.80 | 0.0446 | |
| Residual | 0.0206 | | | |
| Lack of Fit | 0.0156 | 1.56 | 0.3245 | not significant |
| Pure Error | 0.0050 | | | |
| Cor Total | 0.4254 | | | |

SS- sum of squares; $R^2 = 0.9515$; Adjusted $R^2 = 0.9062$

Regression analysis of the response demonstrated that the linear model terms (A and C), quadratic model terms (B^2 and D^2) and the interactive model terms (AB, AD, BC and CD) were significant. The linear significant variables that influenced cell dry weight were salt concentration (A) and inoculum size (C). The three-dimensional surface plots are graphical representations of the regression equation that depicted interaction of the process variables and identified the optimum level of each variable for maximum PHA production. The response surface plots describing the interactive effect of different process variables are presented in Fig 4.8. Interactive effects of variables AB (salt concentration and glycerol) showed positive impact on cell dry weight. Also, effects of variables AD (salt concentration and incubation time), BC (glycerol and inoculum size) and CD (inoculum size and incubation time) showed negative interaction for the response.

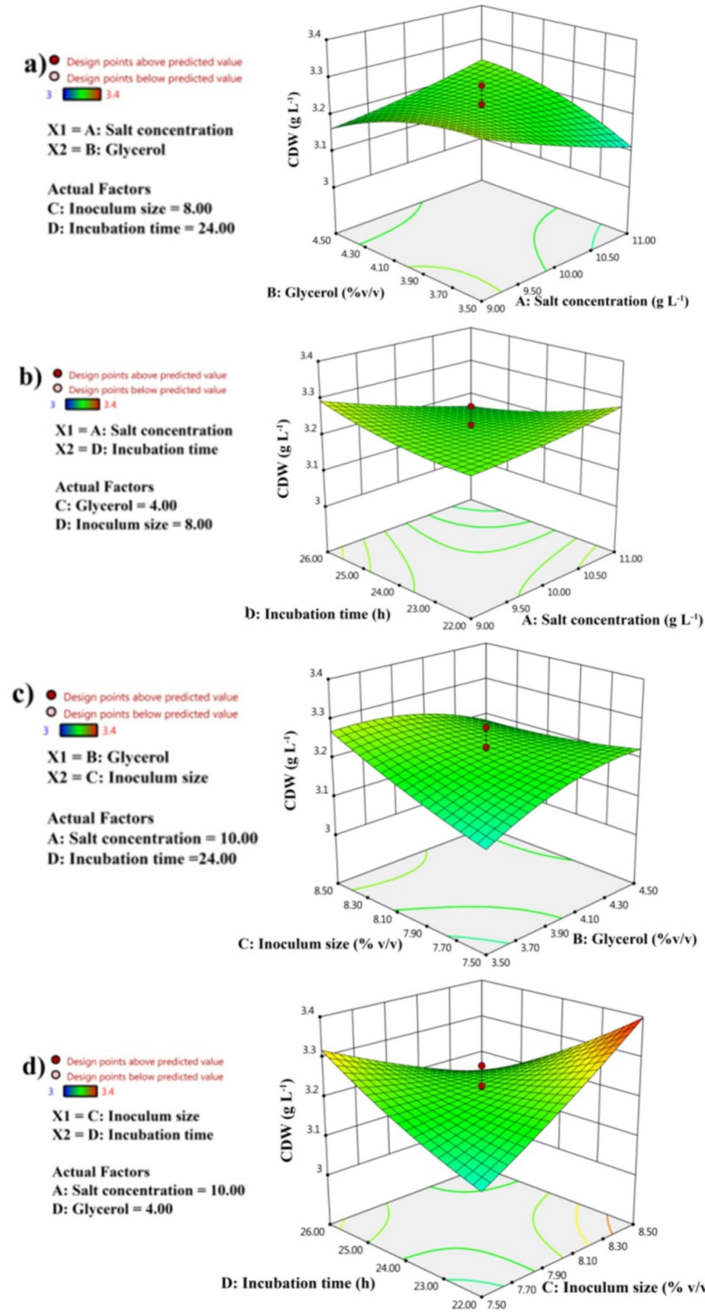


Fig. 4.8 Response surface 3D plots showing interactive effect of process variables for cell dry weight (a) salt concentration and glycerol (b) salt concentration and incubation time (c) glycerol and inoculum size (d) inoculum size and incubation time on PHA production from *B. cereus* MCCB 281

The second order polynomial equation for PHA yield in terms of coded factors is given below:

$$\begin{aligned} \text{PHA yield (g L}^{-1}\text{)} = & +2.14 + 0.0020 * A + 0.0250 * B + 0.0467 \\ & * C - 0.0658 * D - 0.0767 * A^2 - 0.0829 \\ & * B^2 - 0.0567 * C^2 - 0.0542 * D^2 + 0.0010 \\ & * AB - 0.0137 * AC - 0.0025 * AD - 0.0475 \\ & * BC - 0.0112 * BD + 0.0200 * CD \dots\dots\dots(4.5) \end{aligned}$$

where A = salt concentration (g L⁻¹); B = glycerol (v/v); C = inoculum size (v/v) and D = incubation time (h).

Table 4.8 ANOVA for response surface model of PHA yield from *B. cereus* MCCB 281

| Source | SS | F-Value | Prob> F | |
|-----------------------|--------|---------|----------|-----------------|
| Model | 0.5897 | 31.03 | < 0.0001 | significant |
| A- Salt concentration | 0.0018 | 1.18 | 0.2942 | |
| B-Glycerol | 0.0150 | 11.05 | 0.0046 | |
| C-Inoculum size | 0.0523 | 38.51 | < 0.0001 | |
| D-Incubation time | 0.1040 | 76.64 | < 0.0001 | |
| AB | 0.0052 | 3.38 | 0.0859 | |
| AC | 0.0030 | 2.23 | 0.1562 | |
| AD | 0.0001 | 0.0737 | 0.7898 | |
| BC | 0.0361 | 26.60 | < 0.0001 | |
| BD | 0.0020 | 1.49 | 0.2408 | |
| CD | 0.0064 | 4.72 | 0.0463 | |
| A ² | 0.1612 | 118.79 | < 0.0001 | |
| B ² | 0.1886 | 138.94 | < 0.0001 | |
| C ² | 0.0881 | 64.89 | < 0.0001 | |
| D ² | 0.0805 | 59.29 | < 0.0001 | |
| Residual | 0.0204 | | | |
| Lack of Fit | 0.0174 | 2.97 | 0.1206 | not significant |
| Pure Error | 0.0029 | | | |
| Cor Total | 0.6100 | | | |

SS- sum of squares; R² = 0.9666; Adjusted R² = 0.9355

For PHA yield, the model F-value of 31.03 indicated that the model was significant. The "Lack of Fit F-value" of 2.97 implied that the Lack of Fit was not significant relative to the pure error. Non-significant lack of fit is good for the model to fit. The model was found to be highly reliable with coefficient of determination (R^2) value of 0.9666 and 'adjusted R^2 ' value of 0.9355. The predicted R^2 of 0.8285 was in reasonable agreement with the adjusted R^2 value. A very low value of coefficient of the variation (CV: 1.91%) again demonstrated a very high degree of precision and reliability of the experimental data. It was observed that inoculum size (C) appeared to be the most significant variable for increasing PHA production, followed by glycerol (B) and salt concentration (A). Regression analysis of the response demonstrated that the linear model terms (B, C and D), quadratic model terms (A^2 , B^2 , C^2 and D^2) and the interactive model terms (BC and CD) were significant. The significant variables that influenced PHA yield were glycerol (B), inoculum size (C) and incubation time (D). Glycerol (B) and inoculum size (C) were found to be significant factors that positively correlated PHA production. The response surface plots describing the interactive effect of different process variables are presented in Fig 4.9. It was noticed that, the interactive effect of variables BC had negative effect on PHA production. As the inoculum size (C) increased, PHA yield also increased. The increase in concentration of glycerol (B) showed an increase in PHA yield up to a certain limit after which, higher concentrations slightly reduced PHA production (Fig 4.9a). A similar trend was observed in PHA production by *Pannonibacter phragmitetus* ERC8 isolate which showed reduced polymer production at higher glycerol concentrations (Ray et al., 2016). Moreover, glycerol concentration higher than 2% showed negative effect on PHA

production in *B. firmus* NII 0830 (Deepthi et al., 2011). The interactive effect of CD exhibited positive relationship on PHA yield (Fig. 4.9b). However, increase in incubation time (D) resulted in reduced PHA yield, whereas increase in inoculum size (C) simultaneously increased PHA yield. In an optimization study for PHA production using acid pre-treated rice straw in *B. firmus* NII 0830, high inoculum concentration (7.0 - 8.0% v/v) reported maximum PHA yield (Sindhu et al., 2013). Numerous studies were carried out employing central composite design for PHA optimization in different *Bacillus* spp. using agro-industrial residues (Geethu et al., 2019; Pandian et al., 2010; Sathiyarayanan et al., 2013; Sharma and Bajaj, 2015).

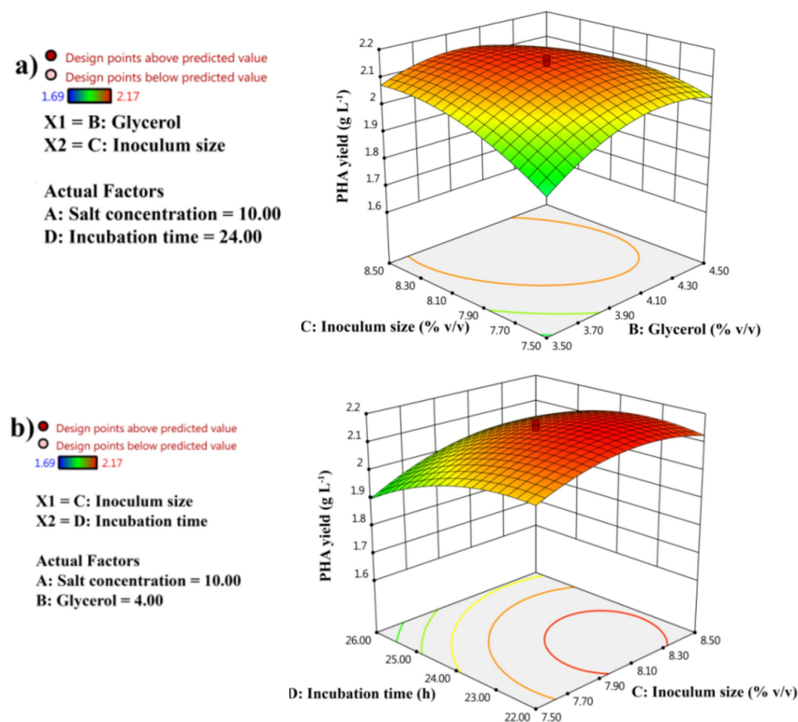


Fig. 4.9 Response surface 3D plots showing interactive effect of process variables for PHA yield (a) glycerol and inoculum size (b) inoculum size and incubation time on PHA production from *B. cereus* MCCB 281

4.3.5.3 Validation of the model

The optimized conditions for maximum PHA production in *B. cereus* MCCB 281 were 9.99 g L⁻¹ salt concentration, 4.06% (v/v) glycerol, 8.13% (v/v) inoculum size and 22.86 h incubation time at 30 °C. To validate the prediction of the model, experiments were conducted in the optimized conditions and CDW of 3.22 ± 0.06 g L⁻¹ with a PHA yield of 2.14 ± 0.08 g L⁻¹ was achieved. The predicted values for CDW and PHA yield were 3.31 g L⁻¹ and 2.18 g L⁻¹ respectively. Thus, there was a good agreement between the predicted and experimental results, thus validating the model. There was a 1.3 fold higher (38% increase) CDW yield and 1.4 (48 % increase) fold higher PHA yield than un-optimized conditions. CDW yield was increased from 2.33 g L⁻¹ to 3.22 g L⁻¹ and PHA yield was increased from 1.44 g L⁻¹ to 2.14 g L⁻¹. Therefore, a good increase in CDW and PHA yield was observed after process optimization using RSM approach. Also, maximum PHA yield was obtained within shorter incubation time. Similar result was reported in marine *B. megaterium* JK4h strain that showed maximum PHA production within 24 h incubation and 2.61 fold increment in PHA yield following media optimization using CCD (Dhangdhariya et al., 2015). Optimization of PHA production using CCD in *B. megaterium* SRKP-3 strain showed a maximum yield of 6.37 g L⁻¹ in shake flask using sea water and dairy waste as media components (Pandian et al., 2010). In a study in *C. necator* ATCC 17699 using basal mineral salt medium, it was found that PHA content increased from 1.03 g L⁻¹ to 7.48 g L⁻¹ after optimization using CCD (Aramvash et al., 2015).

4.3.6 Fermenter level studies

Batch fermentation for PHA production of MCCB 281 was performed under the optimized culture conditions. A volume of 240 mL of 16 h old culture was inoculated to the production medium (pH 7.0) containing 120 mL of glycerol as the sole source of carbon and incubated at 30 °C (Fig. 4.10).



Fig. 4.10 Scale up of PHA production in 5L fermenter in the optimized culture conditions

The maximum PHA yield of $2.53 \pm 0.07 \text{ g L}^{-1}$, CDW of $3.72 \pm 0.04 \text{ g L}^{-1}$ and PHA content of $68.27 \pm 1.2\%$ (w/w) was observed within 24 h fermentation. Higher biomass yield and PHA production was

observed in fermenter studies than shake flask conditions. The PHA yield obtained was comparable with other *Bacillus* spp. such as *B. cereus* SPV (Valappil et al., 2007a) and *Bacillus* sp. SV13 (Suwannasing et al., 2015).

4.3.7 Polymer characterization

4.3.7.1 FTIR

FTIR spectrum of purified PHA showed distinct bands at 1090, 1224 and 1724 cm^{-1} that represented asymmetric stretching of saturated ester linkage (C-O-C) group and carbonyl (-C=O) group respectively (Fig. 4.11). The bands at 1374 and 1451 cm^{-1} corresponded to the C-H bending of symmetric methyl (-CH₃) group. Other strong absorption bands at 2873, 2922, 2969 and 3434 cm^{-1} represented C-H stretching of symmetric methyl (-CH₃), asymmetric methylene (-CH₂), asymmetric methyl (-CH₃) group and hydroxyl (-OH) groups respectively (Sato et al., 2011). This pattern was similar to commercial PHBV (12mol% 3-HV) (Sigma, USA).

4.3.7.2 XRD

The physical nature of the purified polymer was deduced by X-ray diffraction (XRD). The characteristic peaks for PHA co-polymer were at $2\theta = 13.5^\circ$, 16.9° , 22.3° , 25.5° and 30.2° corresponding to (020), (110), (111), (121) and (002) reflections respectively (Fig. 4.12). The polymer showed strong crystalline peaks at $2\theta = 13.5^\circ$ and 16.9° that determine the crystallinity of the polymer (Škrbić and Divjaković, 1996). The higher intensities of these peaks indicate higher order of crystallinity of the PHA. The crystallinity of the polymer was calculated to be 42%. Highly

crystalline polymers are brittle and find a narrower range of applications. The incorporation of 3-HV monomers into the 3-HB polymer chain was found to reduce its crystallinity thereby enhancing its material properties as previously reported (Sankhla et al., 2010).

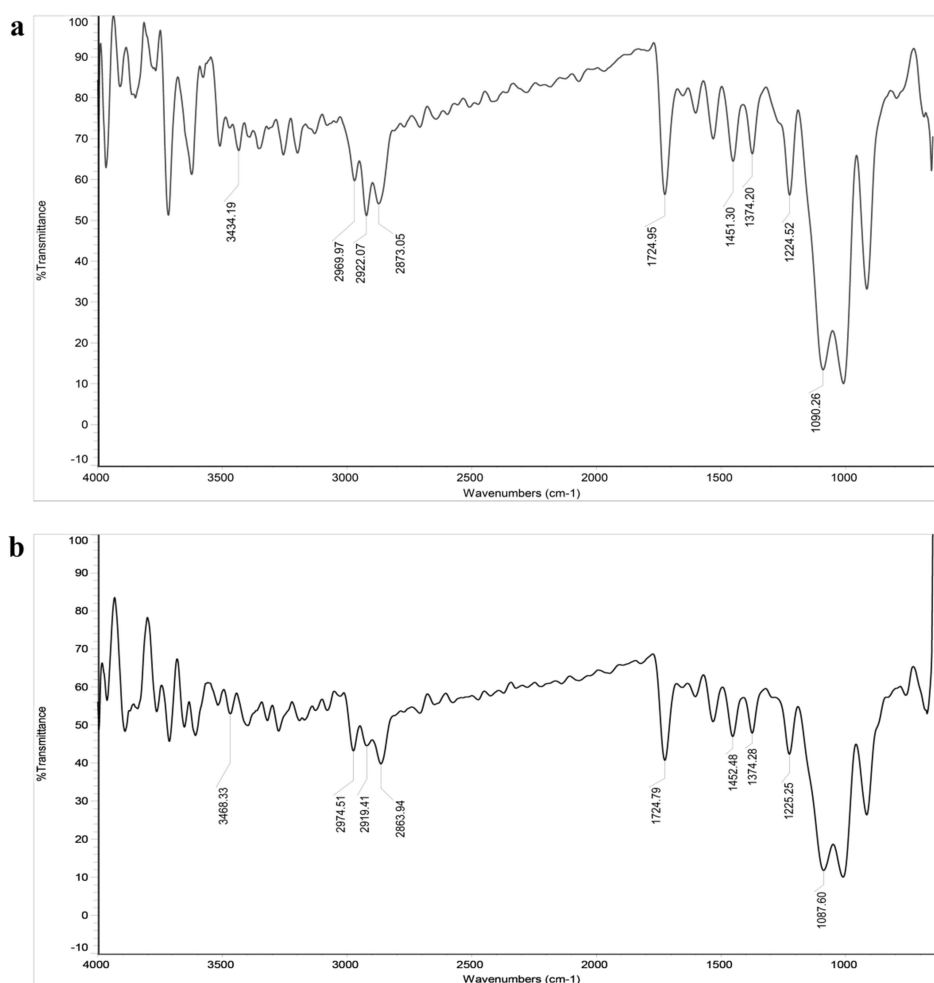


Fig. 4.11 FTIR spectra of (a) purified polymer from *B. cereus* MCCB 281; (b) commercial PHBV (12mol% 3-HV)

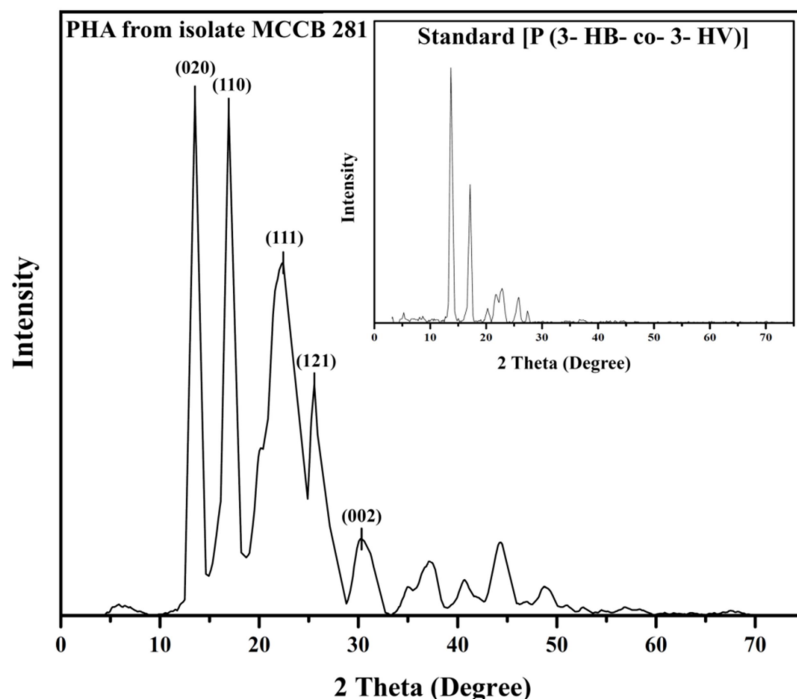


Fig. 4.12 X-ray diffraction pattern of PHA produced by MCCB 281 and commercial PHBV (12mol% 3-HV)

4.3.7.3 GC-MS

The structure of co-polymer was determined by GC-MS based on the peak areas of ions. In the mass spectrum of methyl 3-HB, the peak at 43 m/z represented the hydroxyl end of the molecule which occurred due to the cleavage of the bond between C₃ and C₄ (Fig. 4.13). The peak at 74 m/z represented the carbonyl end of the molecule which originated due to the cleavage of bond between C₃ and C₄ following McLafferty rearrangement. In the mass spectrum of methyl 3-HV, the peak at 59 m/z represented the hydroxyl end of the molecule which occurred due to the cleavage at bonds between C₃ and C₄. The peak at 74 m/z represented the carbonyl end of the

molecule due to McLafferty rearrangement. The peak at 103 m/z was caused by α -cleavage between C₃ and C₄ (Reddy et al., 2009). The result obtained confirmed the presence of methyl esters of HB and HV units.

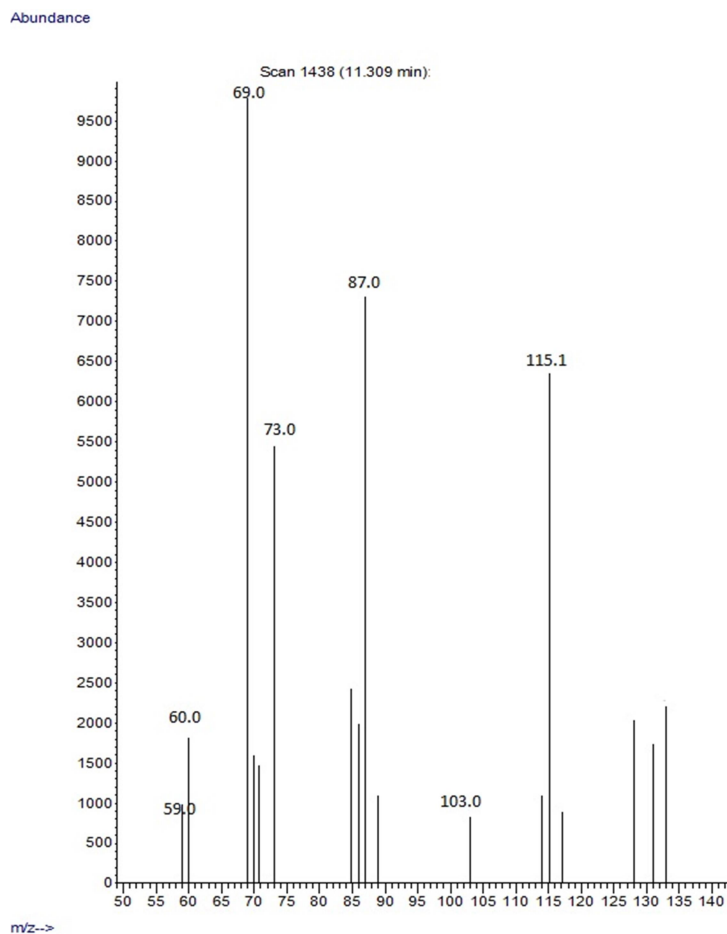


Fig. 4.13 GC-MS spectrum of purified PHA produced by MCCB 281

4.3.7.4 NMR

In the ¹H NMR spectrum, the characteristic peaks at 0.89 and 1.26 ppm were assigned to the resonance absorption of methyl (-CH₃) group from HB and HV units respectively. The peaks at 1.62, 2.44 and

2.57 ppm represented the methylene (-CH₂) group of HV and methylene (-CH₂) group of (HV and HB units) respectively. The signals at 5.25 and 5.29 ppm corresponded to methine (-CH) group of HB and HV units respectively (Fig. 4.14).

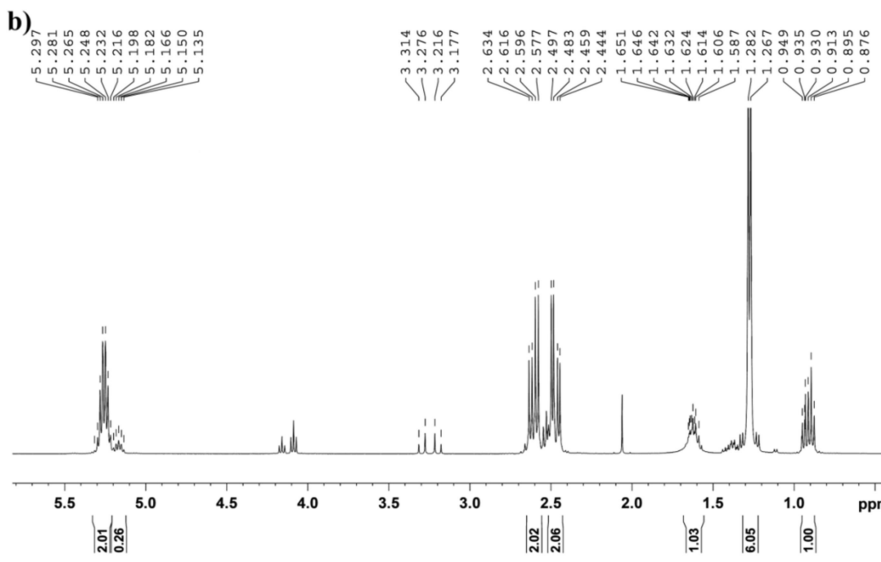
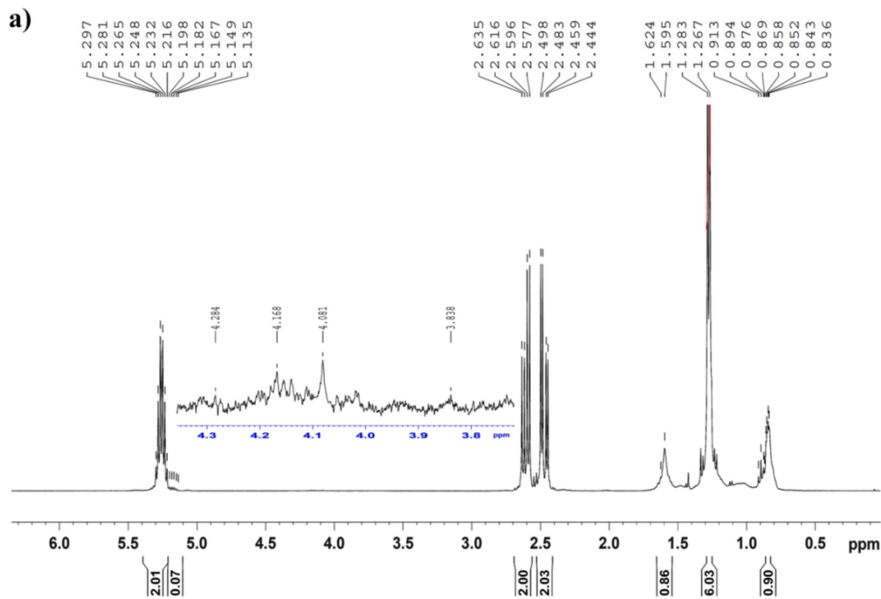
The signals obtained in the spectrum correlated with the previous results (Moorkoth and Nampoothiri, 2016; Reddy et al., 2009). Integration of the area under the peaks at 0.89 and 1.26 ppm in the spectrum confirmed that the polymer produced by isolate MCCB 281 was poly(3-hydroxybutyrate-co-3-hydroxyvalerate) (PHBV) with 13mol% 3-HV content using the following equation (Bloembergen et al., 1986).

$$\text{HV mol\%} = [\text{Area CH}_3 \text{ (HV)} / (\text{Area CH}_3 \text{ (HV)} + \text{Area CH}_3 \text{ (HB)})] * 100 \dots\dots\dots(4.6)$$

Expansion of the ¹H NMR spectral region between 3.0 and 4.5 ppm revealed the presence of additional resonances corresponding to terminal glycerol groups. The region with three resonances at 4.16, 3.80, and 4.28 ppm showed the terminal esterification of glycerol to PHA through the primary hydroxyls (the C₁ or C₃ positions of glycerol). The resonance at 4.08 ppm corresponded to glycerol end-capping of PHA through the secondary hydroxyl group. The glycerol thus acts as a chain transfer agent resulting in the termination of polymerization, which led to low molecular weight PHA (Ashby et al., 2005).

In the ¹³C NMR spectrum, the characteristic peaks at 9.3 and 19.7 ppm represents methyl (-CH₃) group of HV and HB units respectively. Peaks at 37.4 and 40.8 ppm represents methylene (-CH₂) group of HV and HB units and peak at 26.9 ppm corresponded to methylene (-CH₂)

group of HV unit of PHA co-polymer. Other specific peaks at 67.6 and 71.9 represents methine (-CH) group of HB and HV units respectively. The strong signal at 169.1ppm indicated carbonyl (-C=O) group of both HV and HB units (Doi et al., 1986).



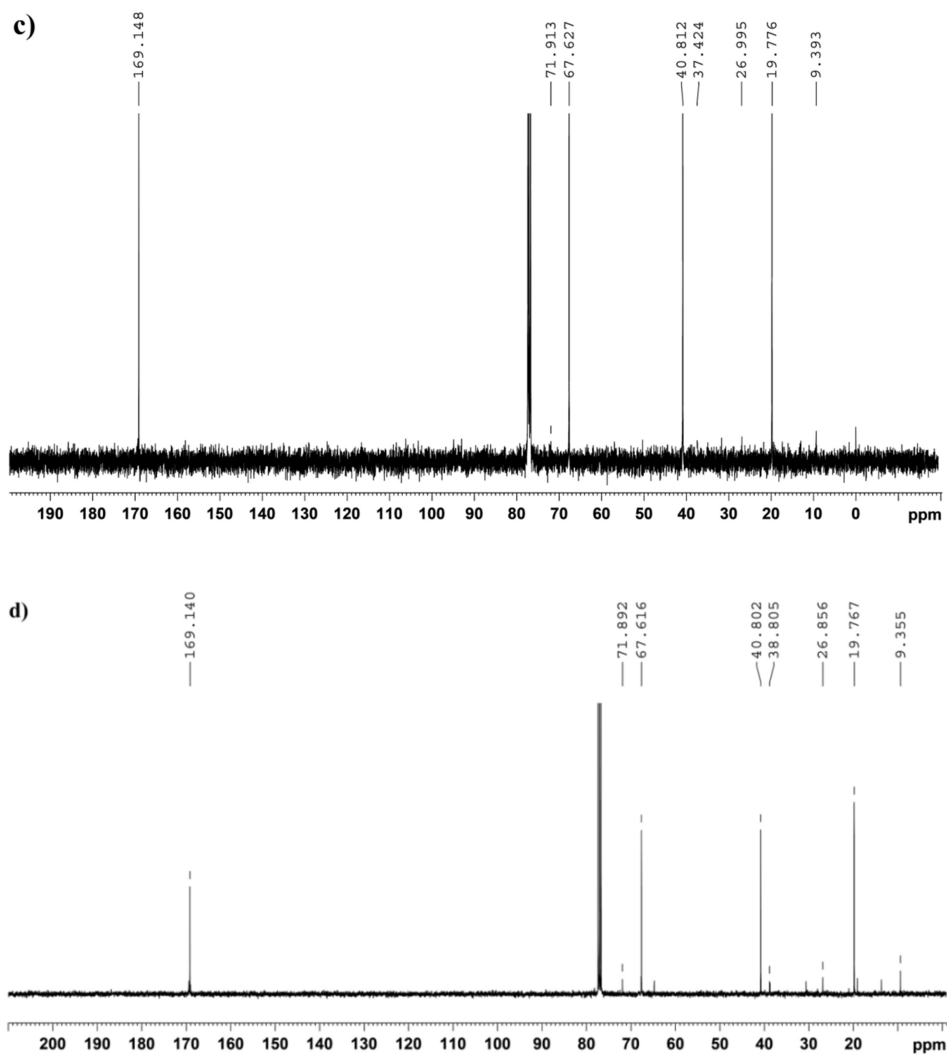


Fig. 4.14 ^{13}C NMR spectra of (a) purified polymer from MCCB 281; (b) commercial PHBV (12mol% 3-HV); ^{13}C NMR spectra of (c) purified polymer from MCCB 281; (d) commercial PHBV (12mol% 3-HV)

4.3.7.5 GPC

The molecular mass of PHA co-polymer produced from *B. cereus* MCCB 281 was detected by GPC analysis. The weight average molecular weight (M_w) was 2.56×10^5 Da and number average molecular weight (M_n) was 1.05×10^5 Da with a polydispersity index (PDI) (M_w/M_n) of 2.44 (Fig. 4.15). The molecular weight was low when compared to *B. thuringiensis* EGU45 utilising crude glycerol for PHA production (Kumar et al., 2015), but higher than that reported in other *Bacillus* sp. (Moorkoth and Nampoothiri, 2016; Phukon et al., 2012). The low molecular weight of the polymer was due to the glycerol end-capping of PHA as substantiated by the NMR studies.

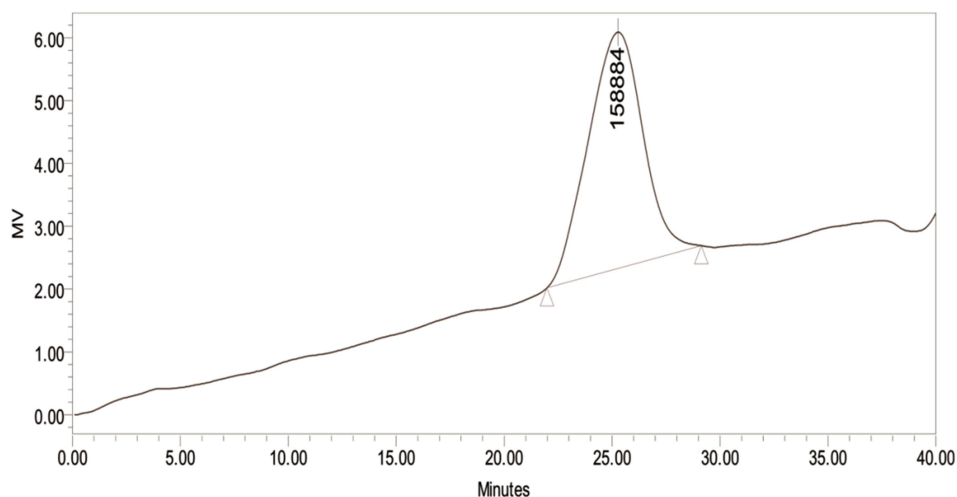


Fig. 4.15 Gel permeation chromatogram of purified polymer produced by *B. cereus* MCCB 281

4.4 Conclusion

This study demonstrated the synthesis of biopolymer PHA from a moderate halophile isolate *Bacillus cereus* MCCB 281 utilising glycerol as sole carbon source. PHA co-polymer with 13mol% 3-hydroxyvalerate content was produced in presence of glycerol without the addition of any precursors. The addition of propionic acid as precursor during fermentation increased valerate content up to 30mol%. The response surface methodology based optimization of cell dry weight and PHA production in *B. cereus* MCCB 281 resulted in 1.4 fold increase in polymer yield. The significant variables that influenced PHA production were glycerol, inoculum size and incubation period. The optimized process factors were further used for fermenter scale production in MCCB 281. Cell dry weight of 3.72 g L⁻¹ and PHA yield of 2.53 g L⁻¹ was achieved within 24 h incubation time in fermenter studies. These results suggest that *B. cereus* MCCB 281 is a good candidate for industrial production of PHA using glycerol as the substrate and further increase in polymer production could be achieved with fed-batch culture systems. Also, the incorporation of 3-HV units in the polymer was found to improve its material properties and thus, beneficial for use in biomedical applications.

.....✪.....

BIOCOMPATIBILITY OF POLYHYDROXYBUTYRATE-CO-HYDROXYVALERATE FROM *BACILLUS CEREUS* MCCB 281 FOR MEDICAL APPLICATIONS

| | |
|-----------------|-----------------------------------|
| Contents | 5.1 <i>Introduction</i> |
| | 5.2 <i>Materials and methods</i> |
| | 5.3 <i>Results and discussion</i> |
| | 5.4 <i>Conclusion</i> |

5.1 Introduction

Over the past few years, advanced developments in research have led to the emergence and commercialization of bio-based polymers for industrial and biomedical applications. Bio-based polymers are prospective materials for medical devices as they exhibit biocompatible, biodegradable and versatile physico-mechanical properties. These materials possess physical properties matching the surrounding tissue to provide cytocompatibility, cell adhesion, proliferation, stability and mechanical strength (Naveen et al., 2015). They also have great potential to be used as alternative to petroleum-based plastics. In this context, polyhydroxyalkanoates (PHAs) has been emerging as one of the attractive biopolymer material used for tissue engineering and drug delivery applications. PHAs show physical properties similar to petroleum-based polypropylene (Akaraonye et al., 2010) and can be completely degraded

by several microorganisms such as bacteria and fungi (Domínguez-Díaz et al., 2015). These biodegradable polymers have a higher rank among all the commercially relevant bio-based polymers which are used as substitutes for plastics, mainly in terms of sustainability and energy reserves (Butt et al., 2018). PHAs produced from Gram positive bacteria such as *Bacillus* sp, *Streptomyces* sp. and *Rhodococcus* sp. do not elicit any immune response as they lack the presence of pyrogenic endotoxin lipopolysaccharide (LPS) and therefore, better suited for biomedical applications. However, the commercial PHA producers are mainly Gram negative bacteria such as *C. necator* and recombinant *E. coli* which contain LPS endotoxin that need to be removed for their application in medical devices. The endotoxin content that may be present in a medical device is regulated by the Food and Drug Administration (FDA) and the value can reach a maximum concentration of 20 EU per medical device (Furrer et al., 2007).

Although, homopolymer PHB exhibits undesirable properties like high crystallinity, rigidity and low elongation to break which causes difficulties in material processibility, co-polymers of PHB with 3-HV units, yields poly(3-hydroxybutyrate-co-3-hydroxyvalerate), (PHBV) which facilitate the improvement of physico-chemical and mechanical properties of the biopolymer (Steinbuechel et al., 1993). The incorporation of 3-HV units (C₂H₅ group) in the C3 position of PHB results in the formation of PHBV co-polymer and the concentration of valerate in the co-polymer can be manipulated by addition of different carbon sources such as propionate, valerate and acetate in the medium (Wang et al., 2013). As a result, PHBV tend to possess greater potential over PHB in biomedical

applications including tissue engineering, medical devices, drug delivery carriers, surgery and wound dressing materials (Zinn et al., 2001). The increase in the amount of 3-HV in the PHB polymer leads to a more amorphous structure that is more convenient for drug release, as drugs can diffuse easily through polymeric amorphous region. Due to its superior characteristics, PHBV has become more attractive for integrate biomedical applications, especially related to drug delivery (Tebaldi et al., 2019). Presently, PHAs are used as scaffolds for tissue engineering of skin, cardiovascular tissue, heart valve tissue, nerve conduit tissue, cartilage and bone tissues; medical devices such as orthopedic pins, surgical sutures and meshes, stents, slings, articular cartilage repair devices, tendon repair devices, adhesion barriers, nerve repair devices, cardiovascular patches and wound dressings (Syromotina et al., 2016).

Polymeric nanoformulations are highly beneficial for pharmacological uses due to their low toxicity, high stability providing longer circulation in blood stream and smaller size (≤ 200 nm) which enable increased cellular permeability for passive targeting of solid tumor site with enhanced permeation and retention (EPR) effect (Nair et al., 2012). PHA nanoparticles and microspheres are used for the delivery of several therapeutic agents such as anticancer drugs, hormones, antibiotics, steroids etc. PHA nanoparticles encapsulated with antibiotic gentamycin exhibited sustained release of the drug at a constant rate against infections of *S. haemolyticus* and *S. aureus* for 6 weeks potentially reducing complication in hip surgery (Rossi et al., 2004). PHA composite microspheres encapsulated with gentamycin showed controlled release of the drug which facilitated the possibility of these microspheres to be

applied as alternative drug controlled release systems for bone repair (Li and Chang, 2005). The ability to encapsulate highly toxic and poorly water-soluble chemotherapeutics is another important feature of using PHA in drug delivery (Masood et al., 2013). PHB based microspheres loaded with water insoluble antitumor drug paclitaxel showed prolonged and effective suppression of growth of breast cancer MCF7 tumor cells due to sustained release of drug from PHB microspheres (Bonartsev et al., 2012). In another study, PHA nanoparticles loaded with paclitaxel exhibited a low *in vitro* rate of release, intracellular uptake and a high cytotoxicity in ovarian cancer cell line and in primary cultures of human ovarian cancer cells (Vilos et al., 2013). The *in vivo* studies of PHA nanoparticles conjugated with specific ligands such as folic acid, and loaded with anticancer drug doxorubicin for targeted drug delivery showed good antitumor activity and better therapeutic efficacy in inhibiting tumor growth (Zhang et al., 2010). PHA microparticles loaded with doxorubicin was also proven to be effective against HeLa tumor cells (Murueva et al., 2013)

Investigations have shown that PHAs provide good biocompatibility and support for the growth of various mammalian cell types such as chondrocytes (Zheng et al., 2005), fibroblasts, osteocytes (Han et al., 2017), keratinocytes (Xie et al., 2013) and stem cells (Wang et al., 2010). PHAs also display low immunogenicity and non-toxicity to tissue and blood enabling its use as blood-contact graft materials for medical applications (Liu et al., 2010). PHO/PHB blend films were prepared with tailored desirable properties to be used as biodegradable stent in coronary stent development. Biocompatibility assay performed in presence of these

blends did not show any cytotoxic effect on human microvascular endothelial cells (HMEC-1). The surface, mechanical and thermal properties of these blends favoured their application as medical device for stent development (Basnett et al., 2013). Collagen grafted PHBV film was used to increase the loading of BSA capped silver (Ag/BSA) nanoparticles to promote the growth of bone cells and inhibit bacterial growth (Bakare et al., 2014). Surface functionalized PHA films coated with recombinant cell binding motifs has been found effective for neural stem cells proliferation and cell adhesion and could be used for neural tissue engineering applications (Xie et al., 2013). Surface modification of PHA films with acrylate monomers was performed to efficiently functionalize and tailor their surface properties for inducing antibacterial properties against *S. aureus* and *E. coli* (Manecka et al., 2014; Poupart et al., 2015). In addition, several *in vivo* studies have also demonstrated low level of inflammatory response in presence of PHAs, favouring cell growth, cell adhesion and wound healing properties (Han et al., 2017; Misra et al., 2010; Shishatskaya et al., 2016) .

PHAs have several advantages over other bio-based polymers such as PLA and poly (lactide-co-glycolide) (PLGA) in medical applications. The degradation products of PHA extracted in buffer solutions at 37 °C are significantly less bioactive and acidic when compared to glycolic acids and lactic acids leading to higher biocompatibility (Francis et al., 2016). Moreover, the degradation of PHBV is slower than PLA polymers, hence it can be used in implants requiring low biodegradation rate such as bone repair and regeneration (Han et al., 2017). PHA degradation occurs by surface erosion, rather than bulk degradation of PLA or PLGA,

leading to controlled degradation, highly desirable for tissue engineering applications (Rai et al., 2017).

The present study focuses on the synthesis, characterization and *in vitro* biocompatibility of PHBV nanoparticles synthesized using oil-in-water method. Also PHBV thin films were made by solvent-casting technique and its characterization to study the surface morphology, thermal and mechanical properties was performed. *In vitro* biocompatibility of polymer films and nanoparticles was determined using L929 mouse fibroblast cells. Furthermore, blood compatibility of PHBV films was also investigated.

5.2 Materials and methods

Poly-3-hydroxybutyrate-co-3-hydroxyvalerate (PHBV, M_w 256 kDa, 13mol% 3-HV) synthesized by *Bacillus cereus* MCCB 281 was used for the synthesis of nanoparticles and thin films. Polyhydroxybutyrate (PHB, M_w 600 kDa, Sigma, USA) was used as the standard material for thin film synthesis, characterization and biocompatibility studies. The culture conditions for maximum polymer production in MCCB 281 were optimized using response surface methodology and the co-polymer was extracted using sodium hypochlorite-chloroform dispersion method as described in chapter 4. The main reasons for selecting the co-polymer produced from isolate MCCB 281 for the application studies were (a) the absence of endotoxin LPS in gram positive isolate MCCB 281 that permits its direct use for biomedical application; (b) PHBV co-polymer produced in presence of glycerol as sole carbon source has improved physical, thermal, mechanical and surface properties than PHB homopolymer obtained from isolate MCCB 284.

L929 cell line (obtained from NCCS, Pune, India) used for biocompatibility studies of the polymer films and nanoparticles was grown in minimum essential medium (MEM) containing Earl's salt, L- glutamine, non-essential amino acids supplemented with 10% fetal bovine serum (FBS), 100 U mL⁻¹ penicillin, and 100 µg mL⁻¹ streptomycin (HiMedia, India). The medium was replaced once in every 2 days and the fibroblasts were incubated at 37 °C. When the cells reached confluence, they were trypsinised (0.25% trypsin and 0.001% EDTA) and passaged in the growth medium for further studies.

5.2.1 Nanoparticle synthesis and characterization

PHBV nanoparticles were synthesized by oil-in-water emulsion method. In brief, 10 mg polymer was dissolved in 2 mL dichloromethane at 70 °C. Polyvinyl alcohol (PVA, mol. wt 9000-10000, Sigma, USA) solution (4 mL of 3% w/v) was added to the polymer solution and sonicated for 10 min at 40% amplitude for 5 s ON and 9 s OFF kept in ice. The emulsion was diluted with PVA solution (50 mL, 0.1% w/v) and kept for solvent evaporation overnight in a magnetic stirrer (Eke et al., 2014). Nanoparticles were separated by centrifugation at 15000 g for 35 min at room temperature and lyophilized. Characterization of nanoparticles was done by Dynamic Light Scattering (DLS) using Nano partica SZ-100 (Horiba Scientific, Japan) and microscopic techniques. For DLS analysis, 0.2 mg of nanoparticles was dispersed in 1 mL milliQ and sonicated for 20-30 s before the analysis. In case of TEM, the dispersed nanoparticle was first sonicated and then spread on TEM carbon grids and dried under vacuum before analysis. For scanning electron microscopy (SEM), the

lyophilized nanoparticles were powdered properly to prevent their agglomeration and coated on carbon grids and viewed under the microscope.

5.2.2 *In vitro* biocompatibility assay

The MTT assay was used to evaluate cytotoxicity of the PHBV nanoparticles, where yellow coloured salt of MTT [3-(4, 5-Dimethylthiazol-2-yl)-2, 5-diphenyl tetrazolium bromide] was reduced to purple coloured formazan by mitochondrial dehydrogenases. Since reduction of MTT can only occur in metabolically active cells, the level of activity is a measure of viability of the cells. For the MTT assay, L929 mouse fibroblast cells were trypsinised, counted using a haemocytometer and seeded in 96 well tissue culture plate (CellStar Grenier Bio-One, USA) with a cell density of 1×10^3 cells per well and incubated for 24 h. Five different concentrations of the PHBV nanoparticles (0.1, 0.3, 0.5, 0.7, and 1 mg mL^{-1}) were dispersed in the culture medium, $100 \mu\text{L}$ of each concentration was added to the wells and incubated for 24 h. Cells devoid of nanoparticles served as negative control. After incubation, $100 \mu\text{L}$ MTT reagent (5 mg mL^{-1}) was added to each well and incubated for 4 h at 37°C to form formazan crystals. Subsequently, $100 \mu\text{L}$ dimethyl sulfoxide was added and incubated at 37°C for 30 min to dissolve the formazan crystals. The optical density was measured at 570 nm using microplate reader (TECAN Infinite M 200, Austria). The percentage cell survival rate was calculated as difference between the absorbance of the tests and that of the control $\times 100$. Data were expressed as mean \pm standard deviation.

5.2.3 Film synthesis and characterization

Films of PHBV and PHB were prepared using the solvent casting method. For this, 200 mg of the polymer was thoroughly dissolved in 10 mL chloroform at 70 °C. The polymer solution was then poured into glass petri dishes (6 cm diameter). The solvent was allowed to evaporate at room temperature and the resultant film was kept at 60 °C for one week. For all the experiments, pristine PHBV and PHB films were used. The thickness of the film was measured using a screw gauge at six random positions on the film and the mean thickness was calculated.

Surface morphology of the films was visualised using scanning electron microscopy (SEM, JEOL Model JSM - 6390LA, USA) operated at a voltage of 5 kV. The films were sputter coated with a thin layer of gold prior to observation. Contact angle measurements were carried out to evaluate the surface wettability of the films. The measurements of contact angles of liquid droplets on the film surfaces were carried by the sessile drop method in a chamber with a goniometer (SEO Phoenix, Korea). Approximately 2 µL each of distilled water and diiodomethane was gently dropped onto the surface of the films for measurement. Surface free energy and polarity was calculated using the software Surfaceware 7. The values were reported as the average of at least five measurements.

Surface topography and roughness of PHBV and PHB films were analysed by atomic force microscope AFM A-100 (APE Research, Italy) in contact mode under ambient conditions. The AFM tip of approximately 8 nm diameter and cantilever of length $450 \pm 5 \mu\text{m}$ and a resonance frequency of 13 kHz was used for the sampling area of $5 \mu\text{m} \times 5 \mu\text{m}$. The

scan rate and length was 2500 nm s⁻¹ and 2 μm respectively. The average roughness (R_a) and root mean square roughness (R_{rms}) was calculated using Gwyddion software. These analyses were performed at the International and Inter University Centre for Nanoscience and Nanotechnology, Mahatma Gandhi University, Kerala.

The melting temperature, glass transition temperature and crystallinity of the films were determined by differential scanning calorimeter (DSC) measurements using DSC 60 plus (Shimadzu, Japan), calibrated with an indium standard. Sample (3-4 mg) was sealed in an aluminium pan and heated from -10 °C to 200 °C at 10 °C min⁻¹ in nitrogen atmosphere at a flow rate of 100 mL min⁻¹ and isothermally maintained at 200 °C for 4 min, followed by cooling cycle from 200 °C to -10 °C. The second heating was operated from -10 °C to 200 °C at a rate of 10 °C min⁻¹. The crystallization temperature (T_c), melting temperature (T_m), and melting enthalpy (ΔH_m) were determined from the cooling and second heating curve. T_m and ΔH_m were taken as the peak temperature and area of the melting endotherm, respectively. The crystallinity (X_c) was calculated by the following equation:

$$X_c(\%) = (\Delta H / \Delta H_{PHB}^0) * 100 \dots\dots\dots(5.1)$$

where ΔH_m (J/g) is the melting enthalpy of the polymer film, (ΔH⁰) is the melting enthalpy of 100% crystalline PHB (146 J/g) (Barham et al., 1984).

Thermal stability of the films was studied by thermogravimetric analysis (TGA) using Diamond TG/DTA (Perkin Elmer, USA.). Films were heated from 30 °C to 500 °C at 10 °C min⁻¹ in nitrogen atmosphere

at a flow rate of 100 mL min⁻¹. The onset thermal degradation temperature and complete degradation temperature were measured.

Mechanical properties of the films were evaluated using an Autograph AG -1 universal testing machine (Shimadzu, Japan) according to ASTM D882 standard method (Allen R, et al., 1993). The tensile strength and elongation at break was obtained from the stress-strain curves. Film strips were placed in film-extension grips with the gauge length 40 mm and stretched until breaking at an extension speed of 5 mm min⁻¹. Measurements were taken in five replicates at 25 °C.

5.2.4 Cell proliferation

Prior to cell culture assays, polymer films were sterilized in 75% (v/v) ethanol solution overnight and thoroughly rinsed with sterile phosphate buffered saline (PBS) three times. For cell proliferation assay, 25 µL of L929 fibroblast cells (1*10⁴ cells/well) were seeded on sterile circular polymer film discs (diameter 14mm) placed in 24 well plate, incubated at 37 °C for 1 h for cell attachment and fresh medium was added to each well afterwards. Cells were incubated for 48 h and cell counting was done after treating the cells with 0.25% (w/v) trypsin-EDTA for 1 min. Cell viability was conducted using trypan blue dye exclusion technique and the cells were counted using an inverted microscope (Hu et al., 2004). Cells grown on tissue culture polystyrene plate (Greiner, Austria) were considered as control. The morphology of the L929 cells adhered to the film surface was observed by SEM. For this, the films were washed three times with PBS, immersed in PBS containing 2.5% (v/v) glutaraldehyde (pH = 7.4) and kept for fixation at 4 °C overnight. The

samples were post-fixed for 1-2 h in 2% (v/v) osmium tetroxide in the same buffer. Then samples were dehydrated in a series of ethanol (30, 40, 50, 60, 70, 80 and 100% v/v) for 15 min and were freeze dried. The films were sputter-coated with platinum and observed at 10 kV under SEM.

5.2.5 Cell staining

Polymer films were placed in 24 well plate and fibroblast cells (1×10^3 cells/well) were seeded onto the film surface and incubated for 48 h at 37 °C. Samples were washed with PBS, stained with Hoechst 33258 dye (Sigma, USA) for 10 min at dark to stain live cell nucleus, followed by washing three times with PBS to remove excess dye and observed under inverted fluorescence microscope (Jain et al., 2013).

5.2.6 Haemocompatibility studies

Haemocompatibility of the polymer films was examined by conducting haemolysis assay, platelet adhesion and blood coagulation tests. For haemolysis assay, fresh human blood was collected and mixed with 3.8% (v/v) trisodium citrate (9: 1) to obtain anticoagulated blood. Diluted anticoagulated blood solution was prepared by mixing 4 mL whole blood with 5 mL PBS. Aliquot of 200 μ L of diluted blood was added to each tube with the polymer films and incubated for 2 h at 37 °C. The sample was centrifuged at 900 g for 10 min at room temperature and the absorbance of the resultant supernatant was measured at 545 nm in UV-Visible spectrophotometer and the haemolysis ratio was calculated. Distilled water and PBS was used as positive and negative control respectively (Wang et al., 2016).

$$\% \text{ haemolysis} = [(A_{\text{sample}} - A_{\text{negative control}}) / (A_{\text{positive control}} - A_{\text{negative control}})] \times 100 \dots (5.2)$$

For platelet adhesion experiments, whole human blood mixed with 3.8% (v/v) trisodium citrate anticoagulant (9:1) was centrifuged at 250 g for 15 min at 25 °C to obtain platelet-rich plasma (PRP). PRP (1 mL) pre-warmed at 37 °C was added to the films, and then incubated at 37 °C for 2 h with shaking (Lee et al., 2000). The morphology of the platelets adhered to the film surface was observed by SEM.

Blood coagulation studies were performed using platelet-poor plasma (PPP) collected after centrifugation of fresh human whole blood at 2500 g for 10 min. Film samples were incubated at 37 °C for 30 min, and then analysed for prothrombin time (PT) and activated partial thromboplastin time (aPTT) using standard procedure (Amarnath et al., 2006).

5.2.7 Statistical analysis

All experiments were performed in triplicate and the values reported in terms of means \pm standard deviation (SD).

5.3 Results and discussion

5.3.1 Nanoparticle synthesis and characterization

There are several methods employed for the preparation of polymer microparticles and nanoparticles however; in the case of PHA-based particles, the emulsion solvent-evaporation method has been mainly used (Michalak et al., 2017). Using this method, the particle sizes in the nano to micrometer range can be achieved. In this method, PHBV polymer dissolved in dichloromethane was mixed with PVA emulsifier and stirred overnight for solvent evaporation, thereby resulting in the synthesis of

PHBV nanoparticles. To determine the average particle size and distribution, lyophilized PHBV nanoparticles were first suspended in milliQ and subjected to sonication for 20-30 s before analysis. The average mean particle size of the nanoparticles determined by dynamic light scattering was found to be 179 ± 12.1 nm (Fig. 5.1). In order to facilitate intravenous administration of polymeric nanoparticles for drug delivery, the diameter of the nanoparticles should be ≤ 200 nm. This size range of nanoparticles are known to facilitate prolonged circulation with reduced mononuclear phagocyte system clearance and accumulation in spleen or other organs (Pramual et al., 2016). Particle size of the synthesized PHBV nanoparticles was found to be in this range to satisfy the intravenous administration of the nanoparticles encapsulated with suitable drugs for drug delivery applications. The surface charge in terms of zeta potential of PHBV nanoparticles was -60.9 mV (Fig. 5.2). A negative zeta potential value was due to the presence of carboxylic end groups from PHBV polymers (Pramual et al., 2016). In addition, micro and nanoparticles with negative zeta potential are more advantageous as drug delivery systems because it prolong the circulation of the particulate in the bloodstream, minimizes non-specific binding with cell surfaces and decrease their uptake by the mononuclear phagocyte system (MPS) (Vilos et al., 2012).

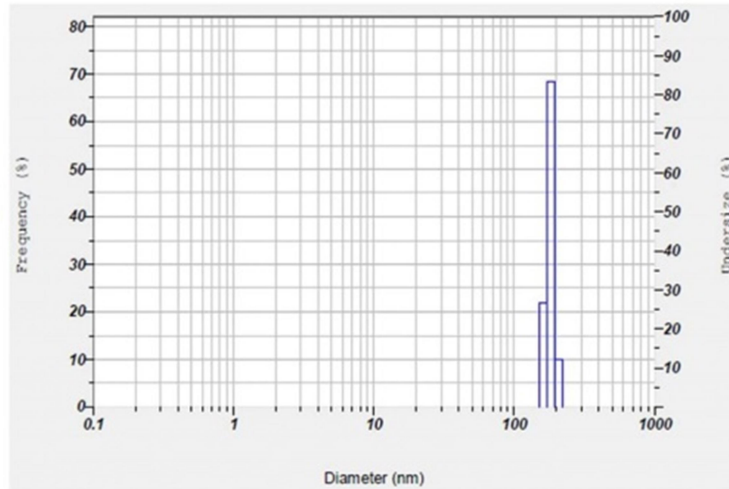


Fig. 5.1 Particle size micrograph of PHBV nanoparticles produced using oil-in-water-emulsion technique

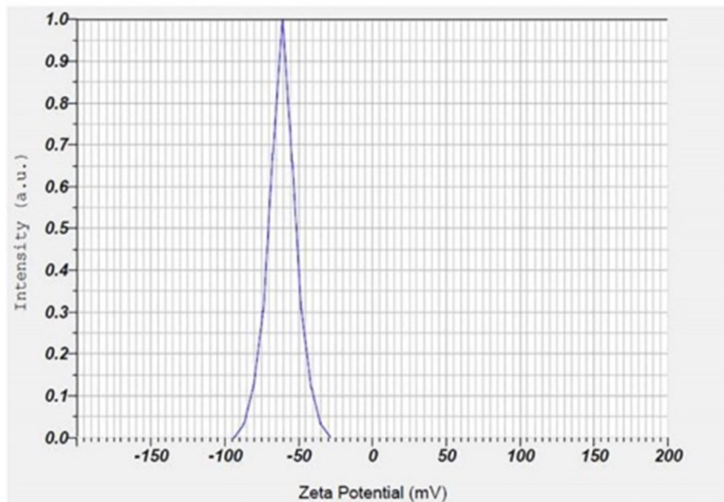


Fig. 5.2 Zeta potential micrograph of PHBV nanoparticles produced using oil-in-water-emulsion technique

Size of synthesized PHBV nanoparticles was also confirmed by TEM imaging (Fig. 5.3). The surface morphology was determined using SEM that showed spherical morphology of nanoparticles with clumping

of particles (Fig. 5.4). The synthesized PHBV nanoparticles showed a smaller size and good zeta potential which indicated high stability in suspension as justified from previous studies (Masood et al., 2013; Moorkoth and Nampoothiri, 2016; Vilos et al., 2013). Thus, PHBV nanoparticles could be used as carriers for drug delivery applications especially in chemotherapy.

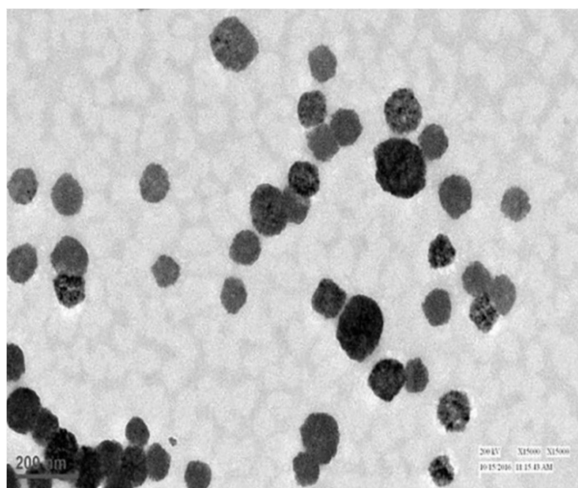


Fig. 5.3 Transmission electron micrograph of PHBV nanoparticles

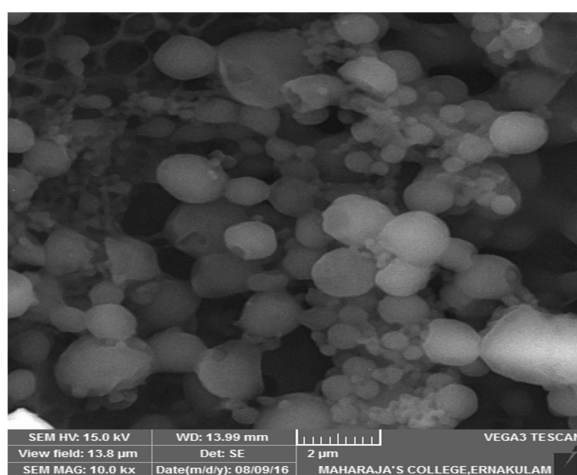


Fig. 5.4 Scanning electron micrograph of PHBV nanoparticles

5.3.2 Biocompatibility of nanoparticles

Biocompatibility of PHBV nanoparticles evaluated by MTT assay in L929 fibroblast cell line demonstrated absence of cytotoxicity after incubation with nanoparticles up to a concentration of 1 mg mL^{-1} (Fig. 5.5). In a similar study, PHBV microparticles of concentration up to 10 mg mL^{-1} did not show any cytotoxic effect on Hep-G2 cells (Vilos et al., 2012). The previous studies have also exhibited similar results showing biocompatibility of PHBV nanoparticles for effective controlled and targeted drug delivery applications (Eke et al., 2014; Masood et al., 2013). In addition, the degradation product of PHA, 3-HB was one of the ketone body present in human blood and tissue which rapidly diffuses through peripheral tissues and readily penetrates membranes to enter cells where it served as oxidative fuel and lipogenic precursor. Moreover, 3-HB supports high levels of cell growth in L929 cells, not by stimulating the cell cycle, but by suppressing cell death, particularly at high cell density. This enables polymers containing 3-HB monomer to support enhanced levels of growth in cell culture (Cheng et al., 2006).

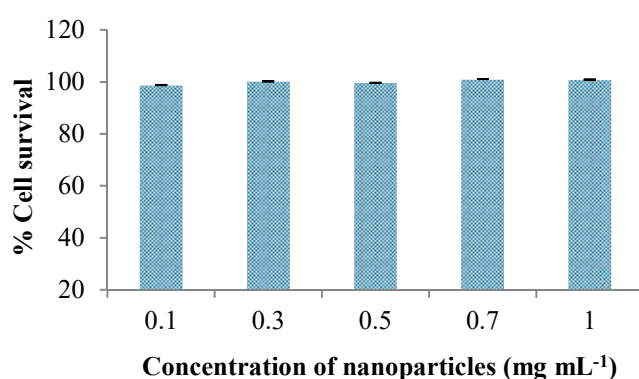


Fig. 5.5 Cytotoxicity results of MTT assay with PHBV nanoparticles using L929 mouse fibroblast cells. Data shown as mean \pm SD (n=6)

5.3.3 Film synthesis and characterization

PHBV and PHB films each of $40 \pm 0.2 \mu\text{m}$ thicknesses were synthesized using solvent casting technique (Fig. 5.6). Surface morphology of PHBV film showed relatively smooth surface with interconnected porous structures (Fig. 5.7) which may be attributed due to the crystallization process during the evaporation of chloroform (Gao et al., 2006) whereas, PHB film showed rough surface with less pores similar as reported earlier (Xie et al., 2013).

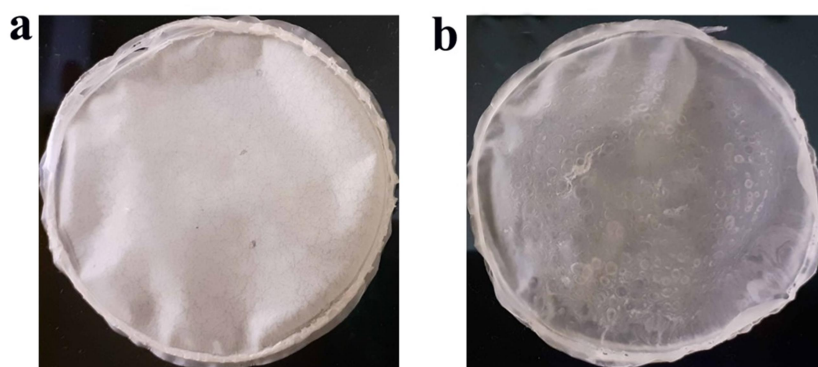


Fig. 5.6 Film synthesis using solvent casting method (a) PHBV (b) PHB

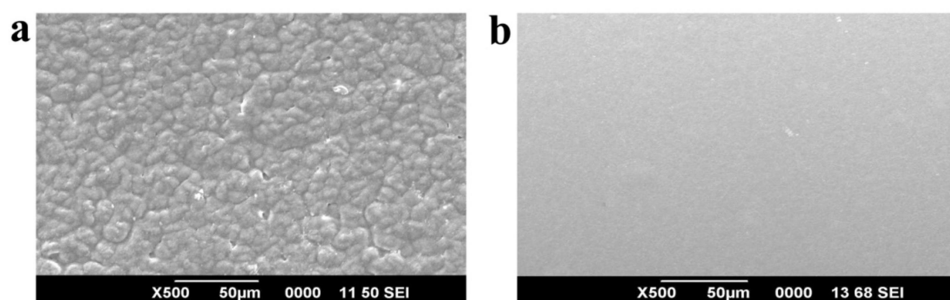


Fig. 5.7 Scanning electron micrograph of (a) PHBV (b) PHB film obtained by solvent casting technique

Surface hydrophilicity and morphology have been reported as the two main factors that determine interactions between the cells and biomaterial. Moderate hydrophilicity benefits for cells to adhere and spread due to higher protein absorption and conformational change occurred on hydrophilic film (Han et al., 2017). The static contact angle measurements of PHBV and PHB films were performed with water and diiodomethane as solvents to determine surface hydrophilicity. The contact angles and total surface free energy of PHBV and PHB films are summarized in Table 5.1. Water contact angle smaller than 65° was considered as hydrophilic and larger than 65° as hydrophobic one (Vogler, 1998). PHBV and PHB films showed a water contact angle of 67.2° and 71.3° respectively indicating that these films had hydrophobic surface (Fig. 5.8). But the PHBV surface behaved less hydrophobic than PHB film as indicated by contact angle measurement. In addition, the lower surface free energy of the PHB film also confirmed high level of hydrophobicity. As surface energy of a material decreases, its hydrophobicity generally increases. Similar results were observed for PHBV films produced from other halophilic bacteria (Han et al., 2015; Zhao et al., 2015).

Table 5.1 Static contact angle and surface free energy measurements of PHBV and PHB films

| Samples | Water contact angle θ ($^\circ$) | Diiodomethane contact angle θ ($^\circ$) | Surface free energy mJ m^{-2} |
|---------|---|---|--|
| PHB | 71.3 ± 0.9 | 57.0 ± 1.5 | 38.40 ± 1.6 |
| PHBV | 67.2 ± 0.6 | 54.2 ± 1.3 | 41.48 ± 1.8 |

Data shown as mean \pm SD (n=5)

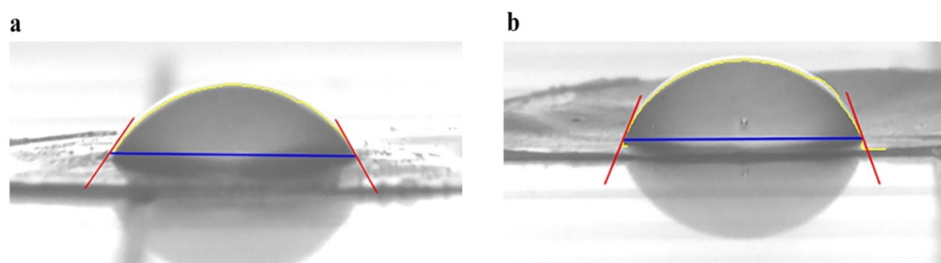


Fig. 5.8 Water contact angle images of (a) PHBV (b) PHB films

Surface topography and roughness were other important criteria that affected the interaction between biomaterial and its surrounding biological environment. Surface morphology and roughness of PHBV and PHB films was examined by AFM in contact mode under ambient conditions (Table 5.2). The results demonstrated that both the polymer films showed surface roughness in nano meter scale. The surface of PHBV was relatively smooth with an average roughness (R_a) of 43.66 nm, whereas PHB surface was rough with R_a of 67.93 nm (Fig. 5.9). Surface roughness was known to increase the potential surface area for cell attachment and biomaterial–cell interactions (Itälä et al., 2002). Further, the nano scale roughness of films plays vital role for cell mobility, cell proliferation and differentiation, and hence beneficial for their biomedical applications (Xu et al., 2014).

Table 5.2 Surface roughness of PHBV and PHB films

| Samples | Rough surface | | Smooth surface | |
|---------|---------------------|-----------------------|---------------------|-----------------------|
| | R _a (nm) | R _{rms} (nm) | R _a (nm) | R _{rms} (nm) |
| PHB | 67.93 | 87.03 | 43.63 | 56.78 |
| PHBV | 43.66 | 59.27 | 33.71 | 44.07 |

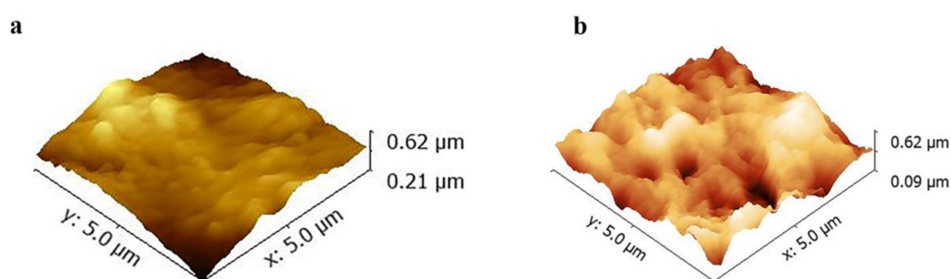


Fig. 5.9 Atomic force micrograph of rough surface of (a) PHBV (b) PHB films

DSC thermogram of PHBV film showed a glass transition temperature (T_g) of $-5.3\text{ }^{\circ}\text{C}$, crystallization temperature (T_c) at $51\text{ }^{\circ}\text{C}$ (Table 5.3) and a melting peak at $146.4\text{ }^{\circ}\text{C}$ and $158.5\text{ }^{\circ}\text{C}$. The presence of two overlapping melting peaks could be related to the occurrence of melting-re-crystallisation – re-melting process during subsequent heating of PHBV. In addition, it was noticed that the melting temperatures were lower than the melting temperature $172\text{ }^{\circ}\text{C}$ of PHB. This indicates that the incorporation of 3-HV unit into polymer chain decreases the melting point, which potentially resulted in improvement in the impact strength and flexibility of the polymer (Alsafadi and Al-Mashaqbeh, 2017). The crystallinity of the polymer was also reduced due to the addition of 3-HV

monomer units facilitating desirable thermo-mechanical properties to PHBV co-polymer. The crystallinity (X_c) of PHBV and PHB was found to 36% and 77% respectively.

TGA was used to evaluate the thermal stability and decomposition of the polymeric biomaterials. TGA curve depicts the thermal degradation temperature (temperature at which 5% weight loss T_d) and the complete degradation temperature (temperature at which 95% weight loss). The onset thermal degradation temperature of PHBV and PHB was 263 °C and 252 °C respectively and the complete degradation temperatures of PHBV and PHB were 300 °C and 275 °C respectively (Fig. 5.10). The TGA results also confirmed that incorporation of 3-HV content improved the thermal stability of PHBV films. The degradation of PHA at 180–200 °C was found due to the rapid random scission according to the β -elimination mechanism and at temperature above 250 °C, the polymer was completely volatilized to form dimeric and trimeric oligomers together with crotonic acid (Verhoogt et al., 1996).

Table 5.3 Thermal properties of PHBV and PHB films

| Samples | T_g (°C) | T_c (°C) | T_m (°C) | T_d (°C) |
|---------|------------|------------|------------|------------|
| PHB | 3.6 | 91 | 172 | 252 |
| PHBV | -5.3 | 51 | 158 | 263 |

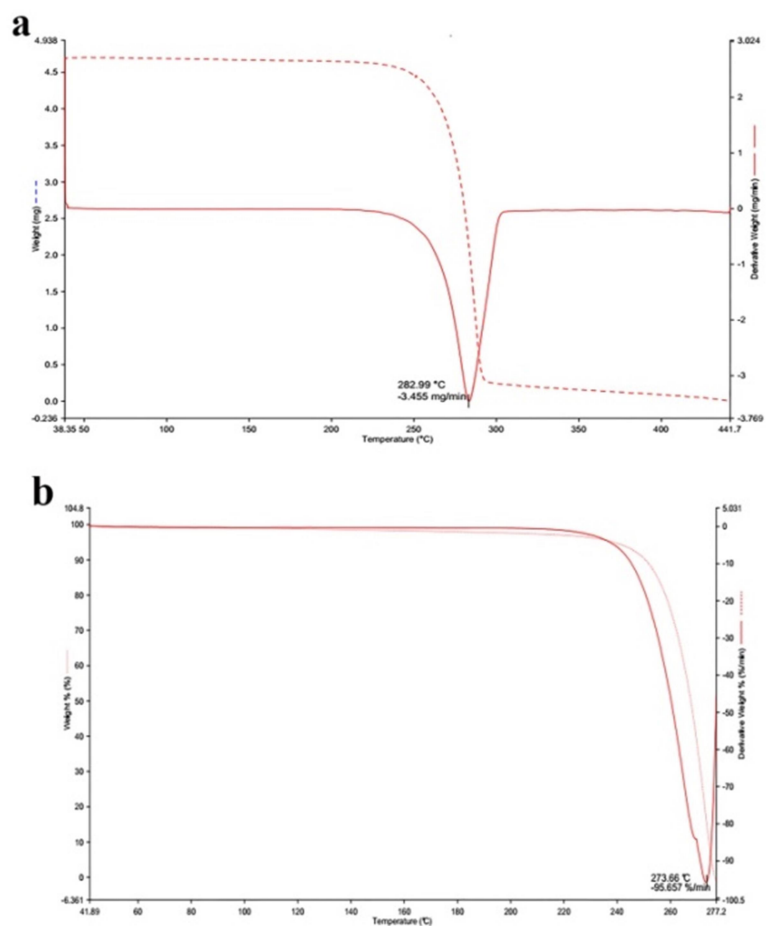


Fig. 5.10 TGA thermograms of (a) PHBV and (b) PHB films

Mechanical properties of the polymer films were summarized in Table 5.4. It was noticed that, the presence of 3-HV unit has resulted in improving the mechanical properties of the polymer as previously reported (Khanna and Srivastava, 2005). The PHBV co-polymer has improved tensile strength and absorbs more strain than pure PHB film. The percentage elongation at break for PHBV films improved to 3.8% on incorporation of 3-HV monomers.

Table 5.4 Mechanical properties of PHBV and PHB films

| Samples | Max. stress (MPa) | Max. strain (%) |
|---------|-------------------|-----------------|
| PHB | 20.9 ± 2.5 | 2.66 ± 0.9 |
| PHBV | 16.5 ± 2.6 | 3.84 ± 0.5 |

Data shown as mean ± SD (n=5)

5.3.4 Cell attachment and proliferation

Cell attachment and proliferation studies showed that L929 cells adhered on both PHBV and PHB films. The presence of elongated spindle shaped morphology of L929 fibroblast cells indicated that the cells were growing well on both the film surfaces. The increased hydrophobicity of the polymers may decrease the cell viability early at 24 h incubation as previously reported (Ou et al., 2011). However, good growth was observed after 48 h incubation for both the tested films and analysis of cell viability was performed. Also, cell growth was homogeneous throughout the surface of the film without any apparent toxic effect when compared with the control (i.e., without film sample). The viability of cells cultured on the tissue culture plate was taken as control (100% cell viability) to obtain the relative viability of the cells. The viability of the cells on the polymer film surfaces was reported as percentage with respect to the control (Fig. 5.11). The highest percent of viable fibroblasts of 80% was observed for PHBV films, whereas PHB films showed 59% viability after 48 h incubation when compared with control (100%).

Similar study was carried out using PHA composite films to study the growth of human keratinocytes (HaCaT) and the films showed increased growth of cells progressively with time, also better cell

attachment and proliferation on composite films (Rai et al., 2017). It was noticed that, with the presence of 3-HV content, the films of PHBV appeared to have a smooth surface that favoured fibroblasts attachment and growth as previously pointed out (Han et al., 2017; Wang et al., 2003). SEM images of fibroblasts attached on the polymer film surfaces of both PHBV and PHB also showed good attachment and spindle shaped morphology of L929 cells (Fig. 5.12). The greater cell viability exhibited by L929 fibroblasts on PHBV film when compared to PHB might be due to the increased surface hydrophilicity and smooth nature that favours the attachment and growth of fibroblasts on PHBV film surface. Thus, it was reasonable to notice that the PHBV films behaved better than PHB in terms of fibroblasts cells due to their slightly hydrophilic and smooth surface.

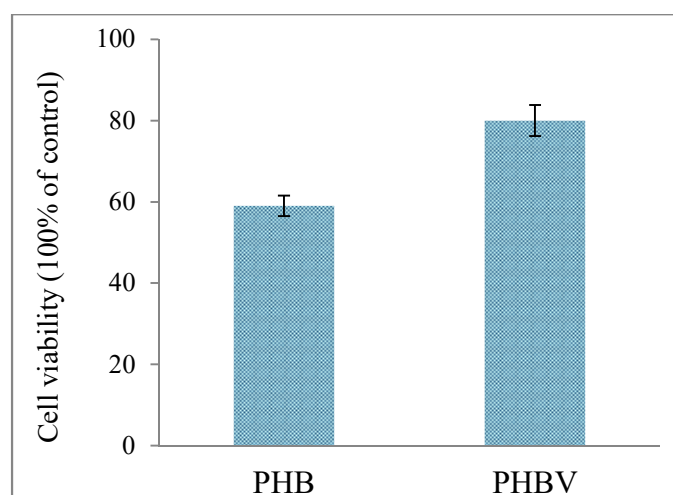


Fig. 5.11 Cell viability of L929 cells grown on PHB and PHBV films after 48 h incubation at 37 ° C. Cells grown on tissue culture plate (without film) were used as 100 % control. Data shown as mean \pm SD (n=4)

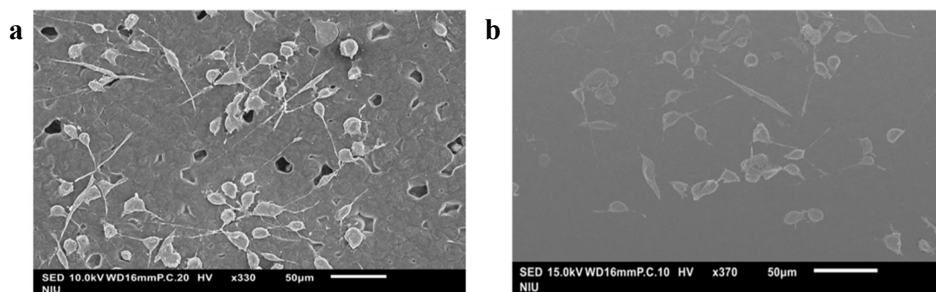


Fig. 5.12 Scanning electron micrograph of morphology of L929 cells adhered to (a) PHBV (b) PHB film surface after 48 h incubation at 37 °C.

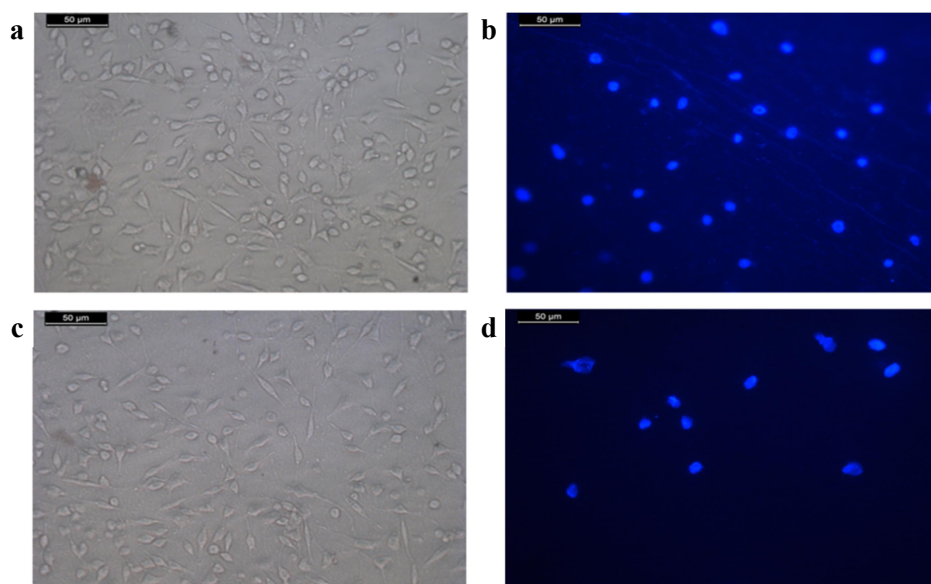


Fig. 5.13 Microscopic images of L929 cells on (a) PHBV and (c) PHB films after 48 h incubation. Fluorescent microscopic images of L929 cells after staining with Hoechst 33258 dye on (b) PHBV and (d) PHB films after 48 h incubation

Cell staining employing fluorescence microscopy also revealed good adhesion of cells on the surface of PHBV film (Fig. 5.13). The blue colour indicated the presence of live nuclei inside the cells. The number

of live nuclei increased with incubation time indicating cell growth and proliferation on the surface of the films. Thus, the PHBV co-polymer produced by marine *B. cereus* MCCB 281 was better than PHB in terms of fibroblast cell attachment and growth.

5.3.5 Haemocompatibility studies

Haemolysis assay and platelet adhesion were used to evaluate the haemocompatibility of PHBV and PHB films. The degree of haemolysis was an indicator of the extent of destruction to red blood cells when exposed to biomaterials. High-performance biomaterials desired for long-term blood contact purposes must possess excellent haemocompatibility. According to ASTM F756-00 (2000) standard (*ASTM F756-00, Standard Practice for Assessment of Hemolytic Properties of Materials*), biomaterials were grouped as non-haemolytic (0-2%), slightly haemolytic (2-5%) or hemolytic (>5%) based on hemolysis percentage. Haemolysis assay (Fig. 5.14) demonstrated that PHBV film was non-haemolytic (0.7%) whereas PHB film was slightly haemolytic (2.5%). Therefore, it was suggested that the PHBV films have no harmful effect on red blood cells and could be made suitable for wound healing applications. This result was similar to the previous report that, PHBV does not promote haemolysis and could be used as blood contact biomaterial (Zhao et al., 2015).

Platelet adhesion and activation was the most crucial parameter in determining the blood compatibility of biomaterials. Platelet activation was characterized by a drastic shape change, which promotes platelet–platelet contact, aggregation and spreading. Platelet activation causes

changes in their morphology, forms pseudopodia and spread on the biomaterial surface. Low platelet adhesion and activation denotes good haemocompatibility, while a higher degree of platelet adhesion could result in thrombus formation (Shen et al., 2010). In case of both the tested films, less number of platelets was attached on the film surface with no pseudopodia formation and change in platelet morphology after incubation with PRP for 2 h at 37 °C as evident from SEM analysis (Fig. 5.15) denoting blood compatibility. Similar phenomenon was reported by (Zhao et al., 2015) in which few inactivated platelets were attached on the surface of PHBV film produced from *H. amylolyticum*. However, for PHB film, the more hydrophobicity with the higher crystallization would be the reason to have low platelet adhesion.

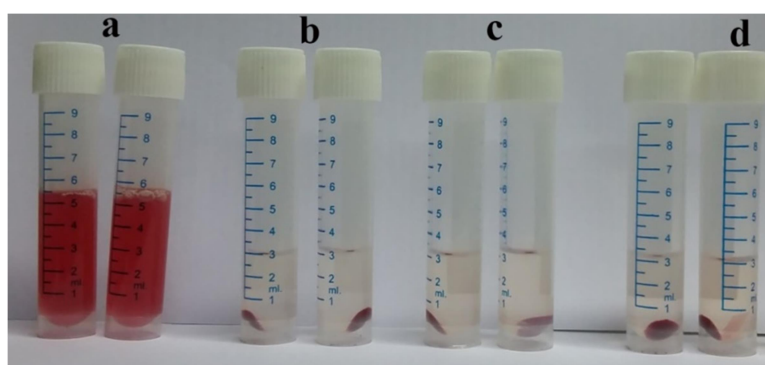


Fig. 5.14 Haemolysis assay of polymer films (a) positive control (b) negative control (c) PHBV film (d) PHB film

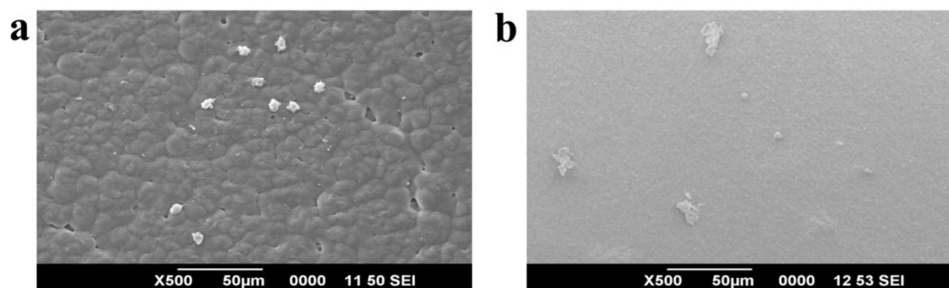


Fig. 5.15 Scanning electron micrograph of morphology of platelets adhered to (a) PHBV (b) PHB film surface after incubation with PRP for 2 h at 37 °C

Blood coagulation assays were performed to assess any change in plasma coagulation properties upon incubation with biomaterials which might in turn lead to thrombosis (Shen et al., 2010). In this study, prothrombin time (PT) and activated partial thromboplastin time (aPTT) was determined to measure abnormalities in the extrinsic and intrinsic coagulation pathways. aPTT was a simple and highly reliable measurement of the ability of blood to coagulate through the intrinsic coagulation mechanism and to study the effect of the biomaterial on the process. PT was a measure of the integrity of the extrinsic and final common pathways of the coagulation cascade. The results showed that the values obtained for PT and aPTT were within the normal range of 12–15 s and 25–35 s respectively (Table 5.5). No significant difference was observed in PT and aPTT values between the PHB and PHBV films, suggesting good blood compatibility of the polymer films. Hence, PHBV and PHB films did not affect the normal blood extrinsic and intrinsic coagulation pathways. From the above results, it was concluded that PHBV polymer

film showed better bio- and haemocompatibility than PHB film, and hence could be used for medical applications involving blood and tissues.

Table 5.5 Blood coagulation analysis of PHBV and PHB films

| Samples | PT (s) | aPTT (s) |
|---------|------------|------------|
| PHB | 14.3 ± 0.3 | 31 ± 1.3 |
| PHBV | 14.5 ± 0.2 | 29.2 ± 1.2 |

Data shown as mean ± SD (n=3)

5.4 Conclusion

This study evaluated the biocompatibility of the PHBV co-polymer produced by marine *Bacillus cereus* MCCB 281 using L929 mouse fibroblast cells. PHBV nanoparticles with particle size 179 nm were synthesized using oil-in-water emulsion method and biocompatibility studies performed showed no cytotoxicity for L929 mouse fibroblast cell line. The results opens up the potential of PHBV co-polymer synthesized from *B. cereus* MCCB 281 for controlled and targeted drug delivery. Solvent-cast film of PHBV was synthesized and characterized to study the surface morphology, roughness, thermal and mechanical properties. Thermo-mechanical properties of the co-polymer were improved with the incorporation of 3-HV units, thereby enhancing the material processibility than PHB. The surface characterization of PHBV demonstrated a smooth surface with interconnected pores and nano scale roughness which is more desirable for the attachment and growth of fibroblast cells. Biocompatibility study also showed good cell viability and attachment of L929 mouse fibroblasts to PHBV films after 48 h incubation. PHBV film also displayed low platelet adhesion and haemolysis revealing good

haemocompatibility. The results from the study demonstrated the ability of PHBV co-polymer as a potential candidate in various biomedical applications.

.....

Biodegradable polymers are recently an emerging area of research and development due to their remarkable properties to substitute synthetic plastics in various fields such as packaging, agriculture, aquaculture and biomedical uses. PHAs are natural polyesters produced by bacteria as energy reserve inclusion bodies in presence of nutrient limitations of nitrogen, phosphorous and in excess of carbon. PHAs are biodegradable and biocompatible polymers that have use in tissue engineering, drug delivery and other biomedical applications. PHAs are used as scaffolds in tissue engineering of bone and skin, as medical devices such as sutures, patches and orthopaedic pins, as nano/microspheres for controlled and targeted delivery of therapeutic drugs and other molecules. The main reason that hampers the commercialization of PHAs is the high production cost compared to other polymers. The isolation of novel bacterial strains that can efficiently utilize cheap carbon substrates and optimization of PHA production would be crucial for the economic feasibility of PHA industry.

Marine environment is a rich source of unique biodiversity for the exploration of novel microorganisms and bioactive products. Microorganisms thriving in these environments have adapted to diverse

conditions of nutrient availability that enables their capacity to produce varieties of PHAs. Marine environment provides adequate scope for the isolation of novel bacteria that can produce different types of PHAs, utilize various renewable and cheap carbon sources and accumulate high polymer content. In this context, a study was designed to isolate, screen and identify PHA producing bacteria from various marine environments, to optimize PHA production using statistical tools for enhanced cell growth and polymer accumulation, and to synthesize PHA nanoparticles and thin films for different biomedical applications.

Salient findings of the present study are:

- A total of 175 marine bacterial isolates were obtained from different marine environments which included 25 isolates from tunicate samples collected from the Vizhinjam bay, Kerala and 150 isolates from water sample collected on-board during cruise 321 along the south-west coast of India.
- The medium used for bacterial growth, sub-culturing and screening studies was ZoBell's marine agar.
- In the primary screening assay using Nile red dye and glucose (20 g L⁻¹) as carbon source, 33 isolates showed orange fluorescence indicating PHA production. Secondary screening using Nile red staining also confirmed the presence of orange fluorescent PHA granules in the cells.
- In PHA production study using shake flask, seven isolates showed more than 50% polymer production based on cell dry weight in

presence of glucose (20 g L⁻¹) as carbon source after 72 h incubation. The constituents of production medium were peptone and yeast extract prepared in sea water. The seven isolates were identified using biochemical characteristics and 16S rRNA gene sequencing. The isolates were submitted to National Centre for Aquatic Animal Health microbial culture collection and Centre for Marine Living Resources and Ecology, Ministry of Earth Sciences.

- The isolates were identified as *Alteromonas macleodii* MCCB 278 (KR921917), *Bacillus cereus* MCCB 279 (KR921918), *Bacillus cereus* MCCB 281 (KR921920), *Halomonas meridiana* MCCB 282 (KR921921), *Vibrio rotiferianus* MCCB 283 (KR921928), *Vibrio harveyi* MCCB 284 (KR921929) and *Vibrio jascicida* MCCB 285 (KR921930).
- Among seven selected bacteria, isolates MCCB 284 (*V. harveyi*) isolated from tunicates and MCCB 281 (*B. cereus*) isolated from water samples showed the maximum PHA accumulation and were selected for further PHA production studies.
- Bacterial growth curve of the selected isolates showed log phase at 3 h and stationary phase at the end of 9 h for *V. harveyi* MCCB 284 and, log phase at 4 h and stationary phase at the end of 16 h for *B. cereus* MCCB 281. The generation time and specific growth rate of MCCB 284 was estimated to be 0.3 h and 2.31 h⁻¹ respectively. This isolate showed a short generation time indicating faster growth. The generation time and specific growth rate of MCCB 281 was found to be 0.6 h and 1.15 h⁻¹ respectively.

- Transmission electron microscopy was done to visualize the presence of PHA granules inside the cells of isolates MCCB 281 and 284.
- PHB production in *V. harveyi* MCCB 284 in presence of glucose (20 g L⁻¹) showed a cell dry weight of 1.34 ± 0.1 g L⁻¹, PHA yield of 0.8 ± 0.19 g L⁻¹ and PHA content of 60 ± 0.63% based on cell dry weight.
- Optimization of PHB production in MCCB 284 was done by ‘one-factor-at-a-time’ approach in shake flask conditions. The optimum conditions for maximum PHB production was initial pH 8.0, NaCl concentration 20 g L⁻¹, glycerol (20 g L⁻¹) as carbon source, incubation time 72 h, initial inoculum size 0.5% (v/v) and incubation temperature 30 °C. A maximum cell dry weight of 3.2 ± 0.3 g L⁻¹, PHB yield of 2.3 ± 0.9 g L⁻¹ and PHB content of 72 ± 1.57% based on cell dry weight was obtained after 72 h incubation at 150 rpm. Based on the statistical analysis using one-way ANOVA followed by the Tukey-Kramer multiple comparisons test, factors such as the initial pH, carbon source, incubation time and inoculum size were identified to have significant impact on the growth and PHB production in *V. harveyi* MCCB 284.
- The polymer was extracted using chloroform-hypochlorite dispersion method and the purified PHB was characterized by FTIR, NMR, DSC, TGA and GPC techniques.

- In FTIR, the characteristic peaks at 1638 cm^{-1} , 1112 cm^{-1} , 1323 cm^{-1} and 3444 cm^{-1} represented C=O ester, C–O–C, CH₃ and OH groups of the polymer respectively. In proton NMR, the presence of signals at 1.21, 2.56 and 5.22 ppm corresponded to the methyl, methylene and methine groups respectively. In carbon NMR, chemical signals at 19.76, 40.79, 67.61 and 169.14 ppm corresponded to the methyl, methylene, methine and carbonyl groups of the polymer respectively. From the NMR analysis, it was concluded that the extracted polymer was PHB homopolymer.
- The melting temperature of PHB was found to be 163 °C and the decomposition temperature was 260 °C. GPC analysis of PHB showed a multimodal molecular weight distribution with weight average molecular weight (Mw) 1.1- 153 kDa, number average molecular weight (Mn) 0.98-150 kDa and a polydispersity index (PDI) (Mw/Mn) of 1.04.
- PHA production in *B. cereus* MCCB 281 investigated in presence of glucose (20 g L^{-1}) as carbon source showed a cell dry weight of $2.11 \pm 0.06\text{ g L}^{-1}$, PHA yield of $1.3 \pm 0.08\text{ g L}^{-1}$ and PHA content of $61.33 \pm 1.8\%$ based on cell dry weight after 48 h incubation.
- Partial *phaC* synthase gene of MCCB 281 was amplified using gene specific primers and 751 bp gene sequence obtained was deposited in GenBank under the accession number KX463674. The *phaC* gene encoded for class IV polyhydroxyalkanoate synthase that comprises of *phaC* and *phaR* subunits.

- Optimization of PHA production in MCCB 281 was carried out by ‘one-factor-at-a-time’ approach in shake flask conditions. The optimum conditions were initial pH 7.0, incubation temperature 30 °C and glycerol (20 g L⁻¹) as carbon source.
- Plackett-Burman design of experiments showed that salt concentration, glycerol, inoculum size and incubation time were significant variables that influenced cell dry weight and PHA production in MCCB 281. The variables salt concentration and incubation time had a negative coefficient on cell dry weight. Glycerol and inoculum size had a positive coefficient on PHA yield, while incubation time showed a negative coefficient.
- Central composite design was used to investigate the significant interactions affecting PHA production. The results showed that salt concentration and inoculum size showed significant influence on cell dry weight whereas, glycerol, inoculum size and incubation time showed significant influence on PHA yield. The interactive effects of salt concentration and glycerol, salt concentration and incubation time, glycerol and inoculum size and inoculum size and incubation time were significant for the response cell dry weight. The interactive effects of glycerol and inoculum size, inoculum size and incubation time were significant for PHA production.
- There was a good agreement between the predicted and experimental results, thus validating the model. The predicted values for cell dry weight and PHA yield were 3.31 g L⁻¹ and 2.18 g L⁻¹ respectively. There was a 1.3 fold higher (38% increase) cell dry weight yield

and 1.4 (48% increase) fold higher PHA yield than un-optimized conditions. Cell dry weight yield was increased from 2.33 g L⁻¹ (un-optimized) to 3.22 g L⁻¹ and PHA yield was increased from 1.44 g L⁻¹ (un-optimized) to 2.14 g L⁻¹. Therefore, a good increase in cell dry weight and PHA yield was observed after process optimization using central composite design.

- The maximum PHA yield of 2.53 ± 0.07 g L⁻¹, CDW of 3.72 ± 0.04 g L⁻¹ and PHA content of $68.27 \pm 1.2\%$ (w/w) was achieved within 24 h in 3L batch fermenter studies.
- The ability of isolates MCCB 281 and 284 to utilize cheap and easily available glycerol as sole carbon source for PHA accumulation could reduce the PHA production cost to a great extent.
- The isolate MCCB 281 was able to produce PHA co-polymers in the presence of glucose and glycerol as sole carbon sources without the addition of any precursor substances.
- The polymer was extracted using chloroform-hypochlorite dispersion method and the purified PHA was characterized by FTIR, XRD, NMR, GC-MS and GPC techniques.
- FTIR spectrum of purified PHA showed distinct bands at 1090, 1224 and 1724 cm⁻¹ that represented asymmetric stretching of saturated ester linkage (C-O-C) and carbonyl (-C=O) groups of PHA respectively. In XRD pattern, PHA showed strong crystalline peaks at $2\theta = 13.5^\circ$ and 16.9° that determined the crystallinity of the polymer and the crystallinity was calculated to be 42%. From

the proton and carbon NMR spectra, the purified polymer from MCCB 281 was identified as a PHA co-polymer with 13mol% hydroxyvalerate and 87mol% hydroxybutyrate and, was designated as PHBV.

- From the GPC analysis, the weight average molecular weight (M_w) was 2.56×10^5 Da and number average molecular weight (M_n) was 1.05×10^5 Da with a polydispersity index (PDI) (M_w/M_n) of 2.44.
- The molecular weight of the PHAs produced by isolates MCCB 281 and 284 in presence of glycerol as carbon source was low when compared with glucose (common sugar used for PHA production) due to the end-capping of glycerol. Glycerol acts as a chain transfer agent resulting in the termination of PHA polymerization, which led to low molecular weight PHA as substantiated by proton NMR spectrum.
- PHBV produced by isolate MCCB 281 lack the presence of endotoxin lipopolysaccharide, as the polymer was produced by a Gram positive bacterium and hence the purified PHA could be directly used for biomedical applications. In addition, the PHBV produced was a co-polymer of 3-HB and 3-HV units. Presence of 3-HV units improved the thermal and mechanical properties of the polymer which in turn enhances its material processability and biomedical potential. Due to these favourable features, the PHBV produced by isolate MCCB 281 was selected for the application studies involving the synthesis of nanoparticles and thin films. For the thin film synthesis and characterization, PHB purchased from Sigma was used as the standard material.

- PHBV nanoparticles were synthesized using oil-in-water method using PVA as emulsifier. The average particle size of the nanoparticles determined by dynamic light scattering was found to be 179 ± 12.1 nm. The surface charge in terms of zeta potential of PHBV nanoparticles was -60.9 mV. PHBV nanoparticles showed a smaller size and good zeta potential which indicated high stability in suspension. Thus, PHBV nanoparticles could be used as carriers for drug delivery applications.
- Biocompatibility of PHBV nanoparticles evaluated by MTT assay in L929 fibroblast cell line demonstrated absence of cytotoxicity up to a concentration of 1 mg mL^{-1} .
- PHBV and PHB films each of 40 ± 0.2 μm thicknesses were synthesized using solvent casting technique. Surface morphology evaluated by SEM and AFM showed smooth surface for PHBV and relatively rough surface for PHB films. PHBV film was less hydrophobic than PHB film as justified from the water contact angle and surface free energy values.
- Thermal and mechanical properties of PHBV film was improved in comparison with PHB due to the incorporation of 3- HV units. Crystallinity of PHBV film was 36% and that of PHB was 77% calculated from the DSC analysis. The decrease in crystallinity was due to the presence of 3-HV units in the co-polymer.
- Cell attachment and proliferation assay performed using L929 fibroblast cells showed better cell growth and attachment on PHBV film surface due to smooth and slightly hydrophilic nature of PHBV

than PHB film surface. PHBV film could be used as a suitable matrix for attachment, growth and proliferation of cells in *in vitro* cell culture studies.

- Haemocompatibility studies such as haemolysis assay, platelet attachment and coagulation studies also showed better results for PHBV than PHB film. Thus, PHBV films could be made suitable as blood contact biomaterial and for wound healing applications.

Scope for future research

- Large scale production of PHA using fed-batch systems to increase cell growth and polymer productivity.
- PHBV nanoparticles loaded with suitable anticancer drugs or antibiotics could be developed for controlled and targeted drug delivery.
- *In vitro* and *in vivo* experiments of PHBV nanoparticles and films need to be performed to demonstrate the biocompatibility of the polymer and to study the inflammatory responses in the host.
- Transformation of the PHBV nanoparticles and films in to “medical grade base material” nomenclature “PHBVMG nanoparticles and films” for a wide variety of applications in human and veterinary medicine, and getting the required approval from the Medical and Veterinary Councils of India.

.....✂.....

References

- Aeschelmann, F., Carus, M., 2015. Biobased Building Blocks and Polymers in the World: Capacities, Production, and Applications–Status Quo and Trends Towards 2020. *Ind. Biotechnol.* 11, 154–159. doi:10.1089/ind.2015.28999.fae
- Ahn, W.S., Park, S.J., Lee, S.Y., 2000. Production of Poly(3-hydroxybutyrate) by fed-batch culture of recombinant *Escherichia coli* with a highly concentrated whey solution. *Appl. Environ. Microbiol.* 66, 3624–7. doi:10.1128/aem.66.8.3624-3627.2000
- Akaraonye, E., Keshavarz, T., Roy, I., 2010. Production of polyhydroxyalkanoates: the future green materials of choice. *J. Chem. Technol. Biotechnol.* 85, 732–743. doi:10.1002/jctb.2392
- Allen R, Baldini N, Donofrio P, Gutman E, Keefe E, Kramer J, Leinweber C, M.V.P. (Ed.), 1993. ASTM, D882 91: Standard test methods for tensile properties of thin plastic sheeting, Annual Book of ASTM Standards. ASTM International Publishers.
- Alsafadi, D., Al-Mashaqbeh, O., 2017. A one-stage cultivation process for the production of poly-3-(hydroxybutyrate-co-hydroxyvalerate) from olive mill wastewater by *Haloferax mediterranei*. *N. Biotechnol.* 34, 47–53. doi:10.1016/j.nbt.2016.05.003
- Amarnath, L.P., Srinivas, A., Ramamurthi, A., 2006. In vitro hemocompatibility testing of UV-modified hyaluronan hydrogels. *Biomaterials* 27, 1416–1424. doi:10.1016/j.biomaterials.2005.08.008
- Anderson, A.J., Dawes, E.A., 1990. Occurrence, metabolism, metabolic role, and industrial uses of bacterial polyhydroxyalkanoates. *Microbiol. Rev.* 54, 450–72.

- Anjum, A., Zuber, M., Zia, K.M., Noreen, A., Anjum, M.N., Tabasum, S., 2016. Microbial production of polyhydroxyalkanoates (PHAs) and its copolymers: A review of recent advancements. *Int. J. Biol. Macromol.* 89, 161–174. doi:10.1016/j.ijbiomac.2016.04.069
- Anupam, K., Dutta, S., Bhattacharjee, C., Datta, S., 2011. Adsorptive removal of chromium (VI) from aqueous solution over powdered activated carbon: Optimisation through response surface methodology. *Chem. Eng. J.* 173, 135–143. doi:10.1016/j.cej.2011.07.049
- Aramvash, A., Akbari Shahabi, Z., Dashti Aghjeh, S., Ghafari, M.D., 2015. Statistical physical and nutrient optimization of bioplastic polyhydroxybutyrate production by *Cupriavidus necator*. *Int. J. Environ. Sci. Technol.* 12, 2307–2316. doi:10.1007/s13762-015-0768-3
- Arun, A., Arthi, R., Shanmugabalaji, V., Eyini, M., 2009. Microbial production of poly-beta-hydroxybutyrate by marine microbes isolated from various marine environments. *Bioresour. Technol.* 100, 2320–2323. doi:10.1016/j.biortech.2008.08.037
- Ashby, R.D., Solaiman, D.K.Y., Foglia, T.A., 2005. Synthesis of Short-/Medium-Chain-Length Poly(hydroxyalkanoate) Blends by Mixed Culture Fermentation of Glycerol †. *Biomacromolecules* 6, 2106–2112. doi:10.1021/bm058005h
- ASTM F756-00, Standard Practice for Assessment of Hemolytic Properties of Materials, n.d. ASTM International, West Conshohocken, PA. doi:10.1520/F0756-17
- Atlić, A., Koller, M., Scherzer, D., Kutschera, C., Grillo-Fernandes, E., Horvat, P., Chiellini, E., Braunegg, G., 2011. Continuous production of poly([R]-3-hydroxybutyrate) by *Cupriavidus necator* in a multistage bioreactor cascade. *Appl. Microbiol. Biotechnol.* 91, 295–304. doi:10.1007/s00253-011-3260-0

- Bakare, R.A., Bhan, C., Raghavan, D., 2014. Synthesis and Characterization of Collagen Grafted Poly(hydroxybutyrate–valerate) (PHBV) Scaffold for Loading of Bovine Serum Albumin Capped Silver (Ag/BSA) Nanoparticles in the Potential Use of Tissue Engineering Application. *Biomacromolecules* 15, 423–435. doi:10.1021/bm401686v
- Balakrishna Pillai, A., Jaya Kumar, A., Thulasi, K., Kumarapillai, H., 2017. Evaluation of short-chain-length polyhydroxyalkanoate accumulation in *Bacillus aryabhatai*. *Brazilian J. Microbiol.* 48, 451–460. doi:10.1016/j.bjm.2017.01.005
- Balebona, M.C., Moriñigo, M.A., Faris, A., Krovacek, K., Månsson, I., Bordas, M.A., Borrego, J.J., 1995. Influence of salinity and pH on the adhesion of pathogenic *Vibrio strains* to *Sparus aurata* skin mucus. *Aquaculture* 132, 113–120. doi:10.1016/0044-8486(94)00376-Y
- Barham, P.J., Keller, A., Otun, E.L., Holmes, P.A., 1984. Crystallization and morphology of a bacterial thermoplastic: poly-3-hydroxybutyrate. *J. Mater. Sci.* 19, 2781–2794. doi:10.1007/BF01026954
- Basnett, P., Ching, K.Y., Stolz, M., Knowles, J.C., Boccaccini, a. R., Smith, C., Locke, I., Keshavarz, T., Roy, I., 2013. Novel Poly (3-hydroxyoctanoate)/ Poly (3-hydroxybutyrate) blends for Medical Applications. *React. Funct. Polym.* 73, 1340 - 1348. doi:10.1016/j.reactfunctpolym.2013.03.019
- Baumann, P., Baumann, L., Mandel, M., 1971. Taxonomy of marine bacteria: the genus *Beneckeia*. *J. Bacteriol.* 107, 268–94.
- Berger, E., Ramsay, B.A., Ramsay, J.A., Chavarie, C., Braunegg, G., 1989. PHB recovery by hypochlorite digestion of non-PHB biomass. *Biotechnol. Tech.* 3, 227–232. doi:10.1007/BF01876053
- Bezerra, M.A., Santelli, R.E., Oliveira, E.P., Villar, L.S., Escalera, L.A., 2008. Response surface methodology (RSM) as a tool for optimization in analytical chemistry. *Talanta* 76, 965–977. doi:10.1016/j.talanta.2008. 05.019

- Biswas, K., Paul, D., Sinha, S.N., 2016. Marine Bacteria: A Potential Tool for Antibacterial Activity. *J. Appl. Environ. Microbiol.* 4, 25–29. doi:10.12691/jaem-4-1-3
- Bloembergen, S., Holden, D.A., Hamer, G.K., Bluhm, T.L., Marchessault, R.H., 1986. Studies of composition and crystallinity of bacterial poly(β -hydroxybutyrate-co- β -hydroxyvalerate). *Macromolecules* 19, 2865–2871. doi:10.1021/ma00165a034
- Bonartsev, A.P., Yakovlev, S.G., Filatova, E. V., Soboleva, G.M., Makhina, T.K., Bonartseva, G.A., Shaitan, K. V., Popov, V.O., Kirpichnikov, M.P., 2012. Sustained release of the antitumor drug paclitaxel from poly(3-hydroxybutyrate)-based microspheres. *Biochem. Suppl. Ser. B Biomed. Chem.* 6, 42–47. doi:10.1134/S1990750812010027
- Boyandin, A., Kalacheva, G.S., Medvedeva, S., Rodicheva, E. and Volova, T.G., 2008. Luminous bacteria as producers of polyhydroxyalkanoates. *Macromol. Symp.* 269, 17–22. doi:10.1002/masy.200850904
- Braunegg, G., Lefebvre, G., Renner, G., Zeiser, A., Haage, G., Loidl-Lanthaler, K., 1995. Kinetics as a tool for polyhydroxyalkanoate production optimization. *Can. J. Microbiol.* 41, 239–248. doi:10.1139/ m95-192
- Braunegg, G., Sonnleitner, B., Lafferty, R.M., 1978. A rapid gas chromatographic method for the determination of poly- β -hydroxybutyric acid in microbial biomass. *Eur. J. Appl. Microbiol. Biotechnol.* 6, 29–37. doi:10.1007/BF00500854
- Bugnicourt, E., Cinelli, P., Lazzeri, a, Alvarez, V., 2014. Polyhydroxyalkanoate (PHA): Review of synthesis, characteristics, processing and potential applications in packaging expresspolymlett. 8, 791–808. doi:10.3144/expresspolymlett. 2014.82
- Burdon, K.L., 1946. Fatty Material in Bacteria and Fungi Revealed by Staining Dried, Fixed Slide Preparations. *J. Bacteriol.* 52, 665–78.

- Butt, F.I., Muhammad, N., Hamid, A., Moniruzzaman, M., Sharif, F., 2018. Recent progress in the utilization of biosynthesized polyhydroxyalkanoates for biomedical applications - Review. *Int. J. Biol. Macromol* 120 (Pt.A), 1294-1305. doi:10.1016/j.ijbiomac.2018.09.002
- Cai, S., Cai, L., Zhao, D., Liu, G., Han, J., Zhou, J., Xiang, H., 2015. A Novel DNA-Binding Protein, PhaR, Plays a Central Role in the Regulation of Polyhydroxyalkanoate Accumulation and Granule Formation in the Haloarchaeon *Haloferax mediterranei*. *Appl. Environ. Microbiol.* 81, 373–385. doi:10.1128/AEM.02878-14
- Cambon-Bonavita, M.-A., Ragueneas, G., Jean, J., Vincent, P., Guezennec, J., 2002. A novel polymer produced by a bacterium isolated from a deep-sea hydrothermal vent polychaete annelid. *J. Appl. Microbiol.* 93, 310–315. doi:10.1046/j.1365-2672.2002.01689.x
- Cervantes-Uc, J.M., Catzin, J., Vargas, I., Herrera-Kao, W., Moguel, F., Ramirez, E., Rincón-Arriaga, S., Lizama-Uc, G., 2014. Biosynthesis and characterization of polyhydroxyalkanoates produced by an extreme halophilic bacterium, *Halomonas nitroreducens*, isolated from hypersaline ponds. *J. Appl. Microbiol.* 117, 1056 - 1065. doi:10.1111/jam.12605
- Cesário, M.T., Raposo, R.S., de Almeida, M.C.M.D., van Keulen, F., Ferreira, B.S., da Fonseca, M.M.R., 2014. Enhanced bioproduction of poly-3-hydroxybutyrate from wheat straw lignocellulosic hydrolysates. *N. Biotechnol.* 31, 104–113. doi:10.1016/j.nbt.2013.10.004
- Chan, R.T.H., Marçal, H., Russell, R.A., Holden, P.J., Foster, L.J.R., 2011. Application of Polyethylene Glycol to Promote Cellular Biocompatibility of Polyhydroxybutyrate Films. *Int. J. Polym. Sci.* 2011, 1–9. doi:10.1155/2011/473045
- Chanprateep, S., 2010. Current trends in biodegradable polyhydroxyalkanoates. *J. Biosci. Bioeng.* 110, 621–632. doi:10.1016/j.jbiosc.2010.07.014

- Chen, G., 2010. Plastics Completely Synthesized by Bacteria : Polyhydroxyalkanoates, in: Chen, G.G.-Q. (Ed.), Plastics from Bacteria: Natural Functions and Applications, Microbiology Monographs. Springer-Verlag, Berlin Heidelberg, pp. 17–37. doi:10.1007/978-3-642-03287_5_2
- Chen, K., Neimark, H., Rumore, P., Steinman, C.R., 1989. Broad range DNA probes for detecting and amplifying eubacterial nucleic acids. FEMS Microbiol. Lett. 57, 19–24. doi:10.1111/j.1574-6968.1989.tb03213.x
- Chen, Y., Chen, J., Yu, C., Du, G., Lun, S., 1999. Recovery of poly-3-hydroxybutyrate from *Alcaligenes eutrophus* by surfactant–chelate aqueous system. Process Biochem. 34, 153–157. doi:10.1016/S0032-9592(98)00082-X
- Cheng, H.-R., Jiang, N., 2006. Extremely rapid extraction of DNA from bacteria and yeasts. Biotechnol. Lett. 28, 55–9. doi:10.1007/s10529-005-4688-z
- Cheng, S., Chen, G., Leski, M., Zou, B., Wang, Y., Wu, Q., 2006. The effect of d,l-β-hydroxybutyric acid on cell death and proliferation in L929 cells. Biomaterials 27, 3758–3765. doi:10.1016/j.biomaterials.2006.02.046
- Chien, C., Chen, C., Choi, M., Kung, S., Wei, Y., 2007. Production of poly-beta-hydroxybutyrate (PHB) by *Vibrio* spp. isolated from marine environment. J. Biotechnol. 132, 259–63. doi:10.1016/j.jbiotec.2007.03.002
- Choi, J. il, Lee, S.Y., 1999. Efficient and economical recovery of poly(3-hydroxybutyrate) from recombinant *Escherichia coli* by simple digestion with chemicals. Biotechnol. Bioeng. 62, 546–553. doi:10.1002/(SICI)1097-0290(19990305)62:5<546::AID-BIT6>3.0.CO;2-0
- Choi, J., Lee, S.Y., 1999. Factors affecting the economics of polyhydroxyalkanoate production by bacterial fermentation. Appl. Microbiol. Biotechnol. 51, 13–21. doi:10.1007/s002530051357

- Choi, J.Y., Lee, J.K., You, Y., Park, W.H., 2003. Epoxidized polybutadiene as a thermal stabilizer for poly (3-hydroxybutyrate). II. Thermal stabilization of poly(3-hydroxybutyrate) by epoxidized polybutadiene. *Fibers Polym* 4, 195–198. doi: 10.1007/BF02908278.
- Christensen, A., Martin, G.D.A., 2017. Identification and bioactive potential of marine microorganisms from selected Florida coastal areas. *MicrobiologyOpen* 6, e00448. doi:10.1002/mbo3.448
- Das, R., Pal, A., Paul, A.K., 2019. Bioconversion of sugarcane molasses to poly(3-hydroxybutyrate-co-3- hydroxyvalerate) by endophytic *Bacillus cereus* RCL 02. *J. Appl. Biol. Biotechnol.* 7, 20–24. doi:10.7324/JABB.2019.70204
- de Castro, J.S., 2014. Bioconversion of Commercial and Waste Glycerol into Value-Added Polyhydroxyalkanoates by Bacterial Strains. *J. Microb. Biochem. Technol.* 06, 337 - 345. doi:10.4172/1948-5948.1000165
- De Schryver, P., Sinha, A.K., Kunwar, P.S., Baruah, K., Verstraete, W., Boon, N., De Boeck, G., Bossier, P., 2010. Poly-3-hydroxybutyrate (PHB) increases growth performance and intestinal bacterial range-weighted richness in juvenile European sea bass, *Dicentrarchus labrax*. *Appl. Microbiol. Biotechnol.* 86, 1535–1541. doi:10.1007/s00253-009-2414-9
- de Smet, M.J., Eggink, G., Witholt, B., Kingma, J., Wynberg, H., 1983. Characterization of intracellular inclusions formed by *Pseudomonas oleovorans* during growth on octane. *J. Bacteriol.* 154, 870–8.
- Deepthi, S.K., Binod, P., Sindhu, R., Pandey, A., 2011. Media engineering for production of poly- β -hydroxybutyrate by *Bacillus firmus* NII 0830. *J. Sci. Ind. Res.* 70, 968–975.

- Defoirdt, T., Halet, D., Vervaeren, H., Boon, N., Van de Wiele, T., Sorgeloos, P., Bossier, P., Verstraete, W., 2007. The bacterial storage compound poly-beta-hydroxybutyrate protects *Artemia franciscana* from pathogenic *Vibrio campbellii*. *Environ. Microbiol.* 9, 445–52. doi:10.1111/j.1462-2920.2006.01161.x.
- Dhangdhariya, J.H., Dubey, S., Trivedi, H.B., Pancha, I., Bhatt, J.K., Dave, B.P., Mishra, S., 2015. Polyhydroxyalkanoate from marine *Bacillus megaterium* using CSMCRI's Dry Sea Mix as a novel growth medium. *Int. J. Biol. Macromol.* 76, 254–61. doi:10.1016/j.ijbiomac.2015.02.009
- Dinesh, K.G., 2016. A Review on Biodegradation of Polymers. *Biotechnol. An Indian J.* 12.
- Divyashree, M.S., Shamala, T.R., Rastogi, N.K., 2009. Isolation of polyhydroxyalkanoate from hydrolyzed cells of *Bacillus flexus* using aqueous two-phase system containing polyethylene glycol and phosphate. *Biotechnol. Bioprocess Eng.* 14, 482–489. doi:10.1007/s12257-008-0119-z
- Dobroth, Z.T., Hu, S., Coats, E.R., McDonald, A.G., 2011. Polyhydroxybutyrate synthesis on biodiesel wastewater using mixed microbial consortia. *Bioresour. Technol.* 102, 3352–9. doi:10.1016/j.biortech.2010.11.053
- Doi, Y., Kunioka, M., Nakamura, Y., Soga, K., 1986. Nuclear magnetic resonance studies on poly(β -hydroxybutyrate) and a copolyester of β -hydroxybutyrate and β -hydroxyvalerate isolated from *Alcaligenes eutrophus* H16. *Macromolecules* 19, 2860–2864. doi:10.1021/ma00165a033
- Domínguez-Díaz, M., Meneses-Acosta, A., Romo-Uribe, A., Peña, C., Segura, D., Espin, G., 2015. Thermo-mechanical properties, microstructure and biocompatibility in poly- β -hydroxybutyrates (PHB) produced by OP and OPN strains of *Azotobacter vinelandii*. *Eur. Polym. J.* 63, 101–112. doi:10.1016/j.eurpolymj.2014.12.002

- Doyle, C., Tanner, E.T., Bonfield, W., 1991. *In vitro* and *in vivo* evaluation of polyhydroxybutyrate and of polyhydroxybutyrate reinforced with hydroxyapatite. *Biomaterials* 12, 841–847. doi:10.1016/0142-9612(91)90072-I
- Drancourt, M., Bollet, C., Carlioz, A., Martelin, R., Gayral, J.P., Raoult, D., 2000. 16S ribosomal DNA sequence analysis of a large collection of environmental and clinical unidentifiable bacterial isolates. *J. Clin. Microbiol.* 38, 3623–30.
- Du, G.C., Chen, J., Yu, J., Lun, S., 2001. Feeding strategy of propionic acid for production of poly(3-hydroxybutyrate-co-3-hydroxyvalerate) with *Ralstonia eutropha*. *Biochem. Eng. J.* 8, 103–110. doi:10.1016/S1369-703X(01)00091-2
- Eke, G., Kuzmina, A.M., Goreva, A. V., Shishatskaya, E.I., Hasirci, N., Hasirci, V., 2014. In vitro and transdermal penetration of PHBV micro/nanoparticles. *J. Mater. Sci. Mater. Med.* 25, 1471–1481. doi:10.1007/s10856-014-5169-5
- Felsenstein, J., 1985. Confidence Limits on Phylogenies: An Approach Using the Bootstrap. *Evolution* (N. Y). 39, 783. doi:10.2307/2408678
- Fiorese, M.L., Freitas, F., Pais, J., Ramos, A.M., de Aragao, G.M.F., Reis, M.A.M., 2009. Recovery of polyhydroxybutyrate (PHB) from *Cupriavidus necator* biomass by solvent extraction with 1,2-propylene carbonate. *Eng. Life Sci.* 9, 454–461. doi:10.1002/elsc.200900034
- Francis, L., Meng, D., Locke, I.C., Knowles, J.C., Mordan, N., Salih, V., Boccaccini, A.R., Roy, I., 2016. Novel poly(3-hydroxybutyrate) composite films containing bioactive glass nanoparticles for wound healing applications. *Polym. Int.* 65, 661–674. doi:10.1002/pi.5108

- Furrer, P., Panke, S., Zinn, M., 2007. Efficient recovery of low endotoxin medium-chain-length poly([R]-3-hydroxyalkanoate) from bacterial biomass. *J. Microbiol. Methods* 69, 206–213. doi:10.1016/j.mimet.2007.01.002
- Gahlawat, G., Srivastava, A.K., 2012. Estimation of Fundamental Kinetic Parameters of Polyhydroxybutyrate Fermentation Process of *Azohydromonas australica* Using Statistical Approach of Media Optimization. *Appl. Biochem. Biotechnol.* 168, 1051–1064. doi:10.1007/s12010-012-9840-3
- Gahlawat, G., Srivastava, A.K., 2013. Development of a mathematical model for the growth associated Polyhydroxybutyrate fermentation by *Azohydromonas australica* and its use for the design of fed-batch cultivation strategies. *Bioresour. Technol.* 137, 98–105. doi:10.1016/j.biortech.2013.03.023
- Galán, B., Dinjaski, N., Maestro, B., de Eugenio, L.I., Escapa, I.F., Sanz, J.M., García, J.L., Prieto, M.A., 2011. Nucleoid-associated PhaF phasin drives intracellular location and segregation of polyhydroxyalkanoate granules in *Pseudomonas putida* KT2442. *Mol. Microbiol.* 79, 402–418. doi:10.1111/j.1365-2958.2010.07450.x
- Gao, Y., Kong, L., Zhang, L., Gong, Y., Chen, G., Zhao, N., Zhang, X., 2006. Improvement of mechanical properties of poly(dl-lactide) films by blending of poly(3-hydroxybutyrate-co-3-hydroxyhexanoate). *Eur. Polym. J.* 42, 764–775. doi:10.1016/j.eurpolymj.2005.09.028
- Geethu, M., Vrundha, R., Raja, S., Raghu Chandrashekar, H., Divyashree, M.S., 2019. Improvement of the Production and Characterisation of Polyhydroxyalkanoate by *Bacillus endophyticus* Using Inexpensive Carbon Feedstock. *J. Polym. Environ.* 27, 917 - 928. doi:10.1007/s10924-019-01397-z

- Ghatnekar, M.S., Pai, J.S., Ganesh, M., 2002. Production and recovery of poly-3-hydroxybutyrate from *Methylobacterium* sp V49. J. Chem. Technol. Biotechnol. 77, 444–448. doi:10.1002/jctb.570.
- Gomaa, E.Z., 2014. Production of polyhydroxyalkanoates (PHAs) by *Bacillus subtilis* and *Escherichia coli* grown on cane molasses fortified with ethanol. Brazilian Arch. Biol. Technol. 57, 145–154. doi:10.1590/S1516-89132014000100020
- Gouda, M.K., Swellam, A.E., Omar, S.H., 2001. Production of PHB by a *Bacillus megaterium* strain using sugarcane molasses and corn steep liquor as sole carbon and nitrogen sources. Microbiol. Res. 156, 201–207. doi:10.1078/0944-5013-00104
- Grage, K., Jahns, A.C., Parlane, N., Palanisamy, R., Rasiah, I.A., Atwood, J.A., Rehm, B.H.A., 2009. Bacterial Polyhydroxyalkanoate Granules: Biogenesis, Structure, and Potential Use as Nano-/Micro-Beads in Biotechnological and Biomedical Applications. Biomacromolecules 10, 660–669. doi:10.1021/bm801394s
- Grothe, E., Moo-Young, M., Chisti, Y., 1999. Fermentation optimization for the production of poly(bhydroxybutyric acid) microbial thermoplastic. Enzyme Microb Technol 25, 132–141. doi: 10.1016/ S0141-0229(99) 00023-X
- Gumel, A.M., Annuar, M.S.M. and Chisti, Y., 2013. Recent advances in the production, recovery and applications of polyhydroxyalkanoates. J. Polym. Environ. 21, 580–60. doi:10.1007/s10924-012-0527-1
- Gürsel, I., Hasirci, V., 1995. Properties and drug release behaviour of poly(3-hydroxybutyric acid) and various poly(3-hydroxybutyrate-hydroxyvalerate) copolymer microcapsules. J. Microencapsul. 12, 185–193. doi:10.3109/02652049509015289

- Hahn, S.K., Chang, Y.K., Kim, B.S., Chang, H.N., 1994. Optimization of microbial poly(3-hydroxybutyrate) recovery using dispersions of sodium hypochlorite solution and chloroform. *Biotechnol. Bioeng.* 44, 256–261. doi:10.1002/bit.260440215
- Halet, D., Defoirdt, T., Van Damme, P., Vervaeren, H., Forrez, I., Van de Wiele, T., Boon, N., Sorgeloos, P., Bossier, P., Verstraete, W., 2007. Poly- β -hydroxybutyrate-accumulating bacteria protect gnotobiotic *Artemia franciscana* from pathogenic *Vibrio campbellii*. *FEMS Microbiol. Ecol.* 60, 363–9. doi:10.1111/j.1574-6941.2007.00305.x
- Han, J., Wu, L.P., Hou, J., Zhao, D., Xiang, H., 2015. Biosynthesis, characterization, and hemostasis potential of tailor-made poly(3-hydroxybutyrate-co-3-hydroxyvalerate) produced by *Haloferax mediterranei*. *Biomacromolecules* 16, 578–588. doi:10.1021/bm5016267
- Han, J., Wu, L.P., Liu, X. Bin, Hou, J., Zhao, L.L., Chen, J.Y., Zhao, D.H., Xiang, H., 2017. Biodegradation and biocompatibility of haloarchaea-produced poly(3-hydroxybutyrate-co-3-hydroxyvalerate) copolymers. *Biomaterials* 139, 172–186. doi:10.1016/j.biomaterials.2017.06.006
- Hejazi, P., Vasheghani-Farahani, E., Yamini, Y., 2003. Supercritical Fluid Disruption of *Ralstonia eutropha* for Poly(β -hydroxybutyrate) Recovery. *Biotechnol. Prog.* 19, 1519–1523. doi:10.1021/bp034010q
- Hermann-Krauss, C., Koller, M., Muhr, A., Fasl, H., Stelzer, F., Braunegg, G., 2013. Archaeal Production of Polyhydroxyalkanoate (PHA) Co- and Terpolyesters from Biodiesel Industry-Derived By-Products. *Archaea* 2013, 1–10. doi:10.1155/2013/129268
- Higuchi-Takeuchi, M., Morisaki, K., Numata, K., 2016. A Screening Method for the Isolation of Polyhydroxyalkanoate-Producing Purple Non-sulfur Photosynthetic Bacteria from Natural Seawater. *Front. Microbiol.* 7, 1509. doi:10.3389/fmicb.2016.01509

- Hong, K., Sun, S., Tian, W., Chen, G.Q., Huang, W., 1999. A rapid method for detecting bacterial polyhydroxyalkanoates in intact cells by Fourier transform infrared spectroscopy. *Appl Microbiol Biotechnol* 51, 523–526. doi: 10.1007/s002530051427
- Hoskisson, P.A., Hobbs, G., 2005. Continuous culture - Making a comeback? *Microbiology*, 151, 3153-3159. doi:10.1099/mic.0.27924-0
- Hu, S.G., Jou, C.H., Yang, M.C., 2004. Biocompatibility and antibacterial activity of chitosan and collagen immobilized poly(3-hydroxybutyric acid-co-3-hydroxyvaleric acid). *Carbohydr. Polym.* 58, 173–179. doi:10.1016/j.carbpol.2004.06.039
- Huang, T.-Y., Duan, K.-J., Huang, S.-Y., Chen, C.W., 2006. Production of polyhydroxyalkanoates from inexpensive extruded rice bran and starch by *Haloferax mediterranei*. *J. Ind. Microbiol. Biotechnol.* 33, 701–706. doi:10.1007/s10295-006-0098-z
- Ibrahim, M.H. a, Steinbüchel, A., 2010. *Zobellella denitrificans* strain MW1, a newly isolated bacterium suitable for poly(3-hydroxybutyrate) production from glycerol. *J. Appl. Microbiol.* 108, 214–25. doi:10.1111/j.1365-2672.2009.04413.x
- Ibrahim, M.H.A., Steinbüchel, A., 2009. Poly(3-hydroxybutyrate) production from glycerol by *Zobellella denitrificans* MW1 via high-cell-density fed-batch fermentation and simplified solvent extraction. *Appl. Environ. Microbiol.* 75, 6222–6231. doi:10.1128/AEM.01162-09
- Imhoff, J.F., Labes, A. and Wiese, J., 2011. Bio-mining the microbial treasures of the ocean: new natural products. *Biotechnol. Adv.* 29, 468–482. doi: 10.1016/j.biotechadv.2011.03.001
- Itälä, A., Ylänen, H.O., Yrjans, J., Heino, T., Hentunen, T., Hupa, M., Aro, H.T., 2002. Characterization of microrough bioactive glass surface: Surface reactions and osteoblast responses in vitro. *J. Biomed. Mater. Res.* 62, 404–411. doi:10.1002/jbm.10273

- Jacquel, N., Lo, C.-W., Wei, Y.-H., Wu, H.-S., Wang, S.S., 2008. Isolation and purification of bacterial poly(3-hydroxyalkanoates). *Biochem. Eng. J.* 39, 15–27. doi:10.1016/j.bej.2007.11.029
- Jain, R., Kosta, S., Tiwari, A., 2010. Polyhydroxyalkanoates : A way to sustainable development of bioplastics. *Chronicles Young Sci.* 1, 10–15. doi:10.4103/4444-4443.76448
- Jain, S., Sharma, A., Basu, B., 2013. *In vitro* cytocompatibility assessment of amorphous carbon structures using neuroblastoma and Schwann cells. *J. Biomed. Mater. Res. - Part B Appl. Biomater.* 101, 520–531. doi:10.1002/jbm.b.32852.
- Johnston, B., Radecka, I., Hill, D., Chiellini, E., Ilieva, V., Sikorska, W., Musioł, M., Zięba, M., Marek, A., Keddie, D., Mendrek, B., Darbar, S., Adamus, G., Kowalczyk, M., 2018. The Microbial Production of Polyhydroxyalkanoates from Waste Polystyrene Fragments Attained Using Oxidative Degradation. *Polymers.* 10, 957. doi:10.3390/polym10090957
- Kahar, P., Tsuge, T., Taguchi, K., Doi, Y., 2004. High yield production of polyhydroxyalkanoates from soybean oil by *Ralstonia eutropha* and its recombinant strain. *Polym. Degrad. Stab.* 83, 79–86. doi:10.1016/S0141-3910(03)00227-1
- Kalil, S.J., Maugeri, F., Rodrigues, M.I., 2000. Response surface analysis and simulation as a tool for bioprocess design and optimization. *Process Biochem.* 35, 539–550. doi:10.1016/S0032-9592(99)00101-6
- Kapritchkoff, F.M., Viotti, A.P., Alli, R.C.P., Zuccolo, M., Pradella, J.G.C., Maiorano, A.E., Miranda, E.A., Bonomi, A., 2006. Enzymatic recovery and purification of polyhydroxybutyrate produced by *Ralstonia eutropha*. *J. Biotechnol.* 122, 453–462. doi:10.1016/j.jbiotec.2005.09.009

- Kassab, A.C., Xu, K., Denkbaş, E.B., Dou, Y., Zhao, S., Pişkin, E., 1997. Rifampicin carrying polyhydroxybutyrate microspheres as a potential chemoembolization agent. *J. Biomater. Sci. Polym. Ed.* 8, 947–61. doi: 10.1163/156856297X00119
- Kaur, G., 2015. Strategies for Large-scale Production of Polyhydroxyalkanoates. *Chem. Biochem. Eng. Q.* 29, 157–172. doi:10.15255/CABEQ.2014.2255
- Kawata, Y., Aiba, S., 2010. Poly(3-hydroxybutyrate) Production by Isolated *Halomonas* sp. KM-1 Using Waste Glycerol. *Biosci. Biotechnol. Biochem.* 74, 175–177. doi:10.1271/bbb.90459
- Ke, Y., Liu, C., Zhang, X., Xiao, M., Wu, G., 2017. Surface Modification of Polyhydroxyalkanoates toward Enhancing Cell Compatibility and Antibacterial Activity. *Macromol. Mater. Eng.* 302, 1700258. doi:10.1002/mame.201700258
- Kenar, H., Kose, G.T., Hasirci, V., 2010. Design of a 3D aligned myocardial tissue construct from biodegradable polyesters. *J. Mater. Sci. Mater. Med.* 21, 989–997. doi:10.1007/s10856-009-3917-8
- Khanna, S., Srivastava, A.K., 2005. Recent advances in microbial polyhydroxyalkanoates. *Process Biochem.* 40, 607–619. doi:10.1016/j.procbio.2004.01.053
- Kiran, G., Lipton, A., Priyadarshini, S., Anitha, K., Suárez, L., Arasu, M., Choi, K., Selvin, J., Al-Dhabi, N., 2014. Antiadhesive activity of poly-hydroxy butyrate biopolymer from a marine *Brevibacterium casei* MS 104 against shrimp pathogenic vibrios *Microb. Cell Fact.* 13, 114. doi:10.1186/s12934-014-0114-3
- Kılıçay, E., Demirbilek, M., Türk, M., Güven, E., Hazer, B., Denkbas, E.B., 2011. Preparation and characterization of poly(3-hydroxybutyrate-co-3-hydroxyhexanoate) (PHBHHX) based nanoparticles for targeted cancer therapy. *Eur. J. Pharm. Sci.* doi:10.1016/j.ejps.2011.08.013

- Koller, M., 2015. Recycling of Waste Streams of the Biotechnological Poly(hydroxyalkanoate) Production by *Haloferax mediterranei* on Whey. *Int. J. Polym. Sci.* 2015, 1–8. doi:10.1155/2015/370164
- Koller, M., Braunegg, G., 2015. Potential and Prospects of Continuous Polyhydroxyalkanoate (PHA) Production *Bioengineering* 2, 94–121. doi:10.3390/bioengineering2020094
- Koller, M., Hesse, P., Salerno, A., Reiterer, A., Braunegg, G., 2011. A viable antibiotic strategy against microbial contamination in biotechnological production of polyhydroxyalkanoates from surplus whey. *Biomass and Bioenergy* 35, 748–753. doi:10.1016/j.biombioe.2010.10.008
- Köse, G.T., Korkusuz, F., Özkul, A., Soysal, Y., Özdemir, T., Yildiz, C., Hasirci, V., 2005. Tissue engineered cartilage on collagen and PHBV matrices. *Biomaterials* 26, 5187–5197. doi:10.1016/j.biomaterials.2005.01.037
- Kourmentza, C., Plácido, J., Venetsaneas, N., Burniol-Figols, A., Varrone, C., Gavala, H.N., Reis, M.A.M., 2017. Recent Advances and Challenges towards Sustainable Polyhydroxyalkanoate (PHA) Production. *Bioengineering* 4, 55. doi:10.3390/bioengineering4020055
- Kulkarni, S.O., Kanekar, P.P., Nilegaonkar, S.S., Sarnaik, S.S., Jog, J.P., 2010. Production and characterization of a biodegradable poly (hydroxybutyrate-co-hydroxyvalerate) (PHB-co-PHV) copolymer by moderately haloalkalitolerant *Halomonas campisalis* MCM B-1027 isolated from Lonar Lake, India. *Bioresour. Technol.* 101, 9765–9771. doi:10.1016/j.biortech.2010.07.089
- Kumar, P., Patel, S.K.S., Lee, J.-K., Kalia, V.C., 2013. Extending the limits of *Bacillus* for novel biotechnological applications. *Biotechnol. Adv.* 31, 1543–1561. doi:10.1016/j.biotechadv.2013.08.007

- Kumar, P., Ray, S., Patel, S.K.S., Lee, J.-K., Kalia, V.C., 2015. Bioconversion of crude glycerol to polyhydroxyalkanoate by *Bacillus thuringiensis* under non-limiting nitrogen conditions. *Int. J. Biol. Macromol.* 78, 9–16. doi:10.1016/j.ijbiomac.2015.03.046
- Kunasundari, B., Sudesh, K., 2011. Isolation and recovery of microbial polyhydroxyalkanoates. *Express Polym. Lett.* 5, 620–634. doi:10.3144/expresspolymlett.2011.60
- Labuzek, S. an., Radecka, I., 2001. Biosynthesis of PHB tercopolymer by *Bacillus cereus* UW85. *J. Appl. Microbiol.* 90, 353–357. doi:10.1046/j.1365-2672.2001.01253.x
- Laycock, B., Halley, P., Pratt, S., Werker, A., Lant, P., 2013. The chemomechanical properties of microbial polyhydroxyalkanoates. *Prog. Polym. Sci.* 38, 536–583. doi:10.1016/j.progpolymsci.2012.06.003
- Law, J.H., Slepecky, R.A., 1961. Assay of poly-beta-hydroxybutyric acid. *J. Bacteriol* 82, 33–36.
- Lee, J.H., Ju, Y.M., Kim, D.M., 2000. Platelet adhesion onto segmented polyurethane film surfaces modified by addition and crosslinking of PEO-containing block copolymers. *Biomaterials* 21, 683–691. doi:10.1016/S0142-9612(99)00197-0
- Lemoigne, M., 1926. Products of dehydration and of polymerization of β -hydroxybutyric acid. *Bull Soc Chem Biol* 8, 770–782.
- Li, H., Chang, J., 2005. Preparation, characterization and in vitro release of gentamicin from PHBV/wollastonite composite microspheres. *J. Control. Release* 107, 463–473. doi:10.1016/j.jconrel.2005.05.019
- Li, X.-T., Zhang, Y., Chen, G.-Q., 2008. Nanofibrous polyhydroxyalkanoate matrices as cell growth supporting materials. *Biomaterials* 29, 3720–3728. doi:10.1016/j.biomaterials.2008.06.004

- Li, Z., Loh, X.J., 2017. Recent advances of using polyhydroxyalkanoate-based nanovehicles as therapeutic delivery carriers. Wiley Interdiscip. Rev. Nanomedicine Nanobiotechnology 9, e1429. doi:10.1002/wnan.1429
- Liu, H., Pancholi, M., Stubbs, J., Raghavan, D., 2010. Influence of hydroxyvalerate composition of polyhydroxy butyrate valerate (PHBV) copolymer on bone cell viability and *in vitro* degradation. J. Appl. Polym. Sci. 116, 3225 - 3231. doi:10.1002/app.31915
- Lu, X.-Y., Ciraolo, E., Stefania, R., Chen, G.-Q., Zhang, Y., Hirsch, E., 2011. Sustained release of PI3K inhibitor from PHA nanoparticles and *in vitro* growth inhibition of cancer cell lines. Appl. Microbiol. Biotechnol. 89, 1423–1433. doi:10.1007/s00253-011-3101-1
- Madden, L.A., Anderson, A.J., Shah, D.T., Asrar, J., 1999. Chain termination in polyhydroxyalkanoate synthesis: involvement of exogenous hydroxy-compounds as chain transfer agents. Int. J. Biol. Macromol. 25, 43–53. doi:10.1016/S0141-8130(99)00014-8
- Madison, L.L., Huisman, G.W., 1999. Metabolic engineering of poly(3-hydroxyalkanoates): from DNA to plastic. Microbiol. Mol. Biol. Rev. 63, 21–53.
- Malm, T., Bowald, S., Bylock, A., Busch, C., Saldeen, T., 1994. Enlargement of the Right Ventricular Outflow Tract and the Pulmonary Artery with a New Biodegradable Patch in Transannular Position. Eur. Surg. Res. 26, 298–308. doi:10.1159/000129349
- Mandenius, C.-F., Brundin, A., 2008. Bioprocess optimization using design-of-experiments methodology. Biotechnol. Prog. 24, 1191–1203. doi:10.1002/btpr.67

- Manecka, G.M., Labrash, J., Rouxel, O., Dubot, P., Lalevée, J., Andaloussi, S.A., Renard, E., Langlois, V., Versace, D.L., 2014. Green Photoinduced Modification of Natural Poly(3-hydroxybutyrate-co-3-hydroxyvalerate) Surface for Antibacterial Applications. *ACS Sustain. Chem. Eng.* 2, 996–1006. doi:10.1021/sc400564r
- Masood, F., Chen, P., Yasin, T., Hasan, F., Ahmad, B., Hameed, A., 2013. Synthesis of poly-(3-hydroxybutyrate-co-12 mol % 3-hydroxyvalerate) by *Bacillus cereus* FB11: its characterization and application as a drug carrier. *J. Mater. Sci. Mater. Med.* 24, 1927–1937. doi:10.1007/s10856-013-4946-x
- Masood, F., Hasan, F., Ahmed, S., Hameed, A., 2011. Biosynthesis and characterization of poly(3-hydroxybutyrate-co-3-hydroxyvalerate) from *Bacillus cereus* FA11 isolated from TNT-contaminated soil. *Ann. Microbiol.* 62, 1377–1384. doi:10.1007/s13213-011-0386-3
- Mata, J.A., Martínez-Cánovas, J., Quesada, E., Béjar, V., 2002. A detailed phenotypic characterisation of the type strains of *Halomonas* species. *Syst. Appl. Microbiol.* 25, 360–75. doi:10.1078/0723-2020-00122
- Melba, D.C.C., Ananthan, G., 2016. Production and optimization of poly(3-hydroxybutyrate) biopolymer by ascidian associated bacterium *Vibrio proteolyticus* DCM CAS2. *Int. J. Sci. Invent. Today* 5, 13–21.
- Michalak, M., Kurcok, P., Hakkarainen, M., 2017. Polyhydroxyalkanoate-based drug delivery systems. *Polym. Int.* 66, 617–622. doi:10.1002/pi.5282
- Misra, S.K., Ansari, T.I., Valappil, S.P., Mohn, D., Philip, S.E., Stark, W.J., Roy, I., Knowles, J.C., Salih, V., Boccaccini, A.R., 2010. Poly(3-hydroxybutyrate) multifunctional composite scaffolds for tissue engineering applications. *Biomaterials* 31, 2806–2815. doi:10.1016/j.biomaterials.2009.12.045

- Mohandas, S.P., Balan, L., Lekshmi, N., Cubelio, S.S., Philip, R., Bright Singh, I.S., 2016. Production and characterization of polyhydroxybutyrate from *Vibrio harveyi* MCCB 284 utilizing glycerol as carbon source. J. Appl. Microbiol. 122, 698 - 707. doi:10.1111/jam.13359
- Mohapatra, S., Maity, S., Dash, H.R., Das, S., Pattnaik, S., Rath, C.C., Samantaray, D., 2017. Bacillus and biopolymer: Prospects and challenges. Biochem. Biophys. Reports 12, 206–213. doi:10.1016/j.bbrep.2017.10.001
- Moorkoth, D., Nampoothiri, K.M., 2016. Production and characterization of poly(3-hydroxy butyrate-co-3 hydroxyvalerate) (PHBV) by a novel halotolerant mangrove isolate. Bioresour. Technol. 201, 253–260. doi:10.1016/j.biortech.2015.11.046
- Mosahebi, A., Fuller, P., Wiberg, M., Terenghi, G., 2002. Effect of Allogeneic Schwann Cell Transplantation on Peripheral Nerve Regeneration. Exp. Neurol. 173, 213–223. doi:10.1006/exnr.2001.7846
- Mozumder, M.S.I., De Wever, H., Volcke, E.I.P., Garcia-Gonzalez, L., 2014. A robust fed-batch feeding strategy independent of the carbon source for optimal polyhydroxybutyrate production. Process Biochem. 49, 365–373. doi:10.1016/j.procbio.2013.12.004
- Mukherjee, A.K., Rai, S.K., 2011. A statistical approach for the enhanced production of alkaline protease showing fibrinolytic activity from a newly isolated Gram-negative *Bacillus* sp. strain AS-S20-I. N. Biotechnol. 28, 182–189. doi:10.1016/j.nbt.2010.11.003
- Murueva, A. V., Shishatskaya, E.I., Kuzmina, A.M., Volova, T.G., Sinskey, A.J., 2013. Microparticles prepared from biodegradable polyhydroxyalcanoates as matrix for encapsulation of cytostatic drug. J. Mater. Sci. Mater. Med. 24, 1905–1915. doi:10.1007/s10856-013-4941-2

- Myers, Raymond H., Montgomery, Douglas C., Anderson-Cook, C.M., 2009. Response Surface Methodology: Process and Product Optimization Using Designed Experiments, Third. ed. John Wiley & Sons Inc., New York.
- Nair, K.L., Thulasidasan, A.K.T., Deepa, G., Anto, R.J., Kumar, G.S.V., 2012. Purely aqueous PLGA nanoparticulate formulations of curcumin exhibit enhanced anticancer activity with dependence on the combination of the carrier. *Int. J. Pharm.* 425, 44–52. doi:10.1016/j.ijpharm.2012.01.003
- Nakamura, S., Doi, Y., Scandola, M., 1992. Microbial synthesis and characterization of poly(3-hydroxybutyrate-co-4-hydroxybutyrate). *Macromolecules* 25, 4237–4241. doi:10.1021/ma00043a001
- Naranjo, J.M., Posada, J.A., Higuera, J.C., Cardona, C.A., 2013. Valorization of glycerol through the production of biopolymers: The PHB case using *Bacillus megaterium*. *Bioresour. Technol.* 133, 38–44. doi:10.1016/j.biortech.2013.01.129
- Narayanan, A., Ramana, K.V., 2012. Polyhydroxybutyrate production in *Bacillus mycoides* DFC1 using response surface optimization for physico-chemical process parameters. *3 Biotech* 2, 287–296. doi:10.1007/s13205-012-0054-8
- Naveen, S.V., Tan, I.K.P., Goh, Y.S., Balaji Raghavendran, H.R., Murali, M.R., Kamarul, T., 2015. Unmodified medium chain length polyhydroxyalkanoate (uMCL-PHA) as a thin film for tissue engineering application - Characterization and in vitro biocompatibility. *Mater. Lett.* 141, 55–58. doi:10.1016/j.matlet.2014.10.144
- Nhan, D.T., Wille, M., De Schryver, P., Defoirdt, T., Bossier, P., Sorgeloos, P., 2010. The effect of poly 3-hydroxybutyrate on larviculture of the giant freshwater prawn *Macrobrachium rosenbergii*. *Aquaculture* 302, 76–81. doi:10.1016/j.aquaculture.2010.02.011

- Noda, I., Lindsey, S.B., Caraway, D., 2010. Nodax™ Class PHA Copolymers: Their Properties and Applications. pp. 237–255. doi:10.1007/978-3-642-03287-5_10
- Numata, K., Doi, Y., 2012. Biosynthesis of polyhydroxyalkanoates by a novel facultatively anaerobic *Vibrio* sp. under marine conditions. Mar. Biotechnol. (NY). 14, 323–331. doi:10.1007/s10126-011-9416-1
- Ostle, A.G., Holt, J.G., 1982. Nile blue A as a fluorescent stain for Fluorescent Stain for Poly-3- Hydroxybutyrate. Appl. Environ. Microbiol. 44, 238–41.
- Ou, W., Qiu, H., Chen, Z., Xu, K., 2011. Biodegradable block poly(ester-urethane)s based on poly(3-hydroxybutyrate-co-4-hydroxybutyrate) copolymers. Biomaterials 32, 3178–3188. doi:10.1016/j.biomaterials.2011.01.031
- Page, W.J., Cornish, A., 1993. Growth of *Azotobacter vinelandii* UWD in fish peptone medium and simplified extraction of poly-3-hydroxybutyrate. Appl. Environ. Microbiol. 59, 4236–4244.
- Pan, P., Inoue, Y., 2009. Polymorphism and isomorphism in biodegradable polyesters. Prog. Polym. Sci. 34, 605–640. doi:10.1016/j.progpolymsci.2009.01.003
- Pandian, S.R., Deepak, V., Kalishwaralal, K., Rameshkumar, N., Jeyaraj, M., Gurunathan, S., 2010. Optimization and fed-batch production of PHB utilizing dairy waste and sea water as nutrient sources by *Bacillus megaterium* SRKP-3. Bioresour. Technol. 101, 705–11. doi:10.1016/j.biortech.2009.08.040
- Pantazaki, A.A., Papaneophytou, C.P., Pritsa, A.G., Liakopoulou-Kyriakides, M., Kyriakidis, D. A., 2009. Production of polyhydroxyalkanoates from whey by *Thermus thermophilus* HB8. Process Biochem. 44, 847–853. doi:10.1016/j.procbio.2009.04.002

- Patel, S.K., Kumar, P., Singh, M., Lee, J. K., Kalia, V.C., 2015. Integrative approach to produce hydrogen and polyhydroxybutyrate from biowaste using defined bacterial cultures. *Bioresour. Technol.* 176, 136–141. doi:10.1016/j.biortech.2014.11.029
- Patel, S.K.S., Lee, J.-K., Kalia, V.C., 2016. Integrative Approach for Producing Hydrogen and Polyhydroxyalkanoate from Mixed Wastes of Biological Origin. *Indian J. Microbiol.* 56, 293–300. doi:10.1007/s12088-016-0595-3
- Patel, S.K.S., Singh, M., Kalia, V.C., 2011. Hydrogen and Polyhydroxybutyrate Producing Abilities of *Bacillus* spp. From Glucose in Two Stage System. *Indian J. Microbiol.* 51, 418–423. doi:10.1007/s12088-011-0236-9
- Patel, S.K.S., Singh, M., Kumar, P., Purohit, H.J., Kalia, V.C., 2012. Exploitation of defined bacterial cultures for production of hydrogen and polyhydroxybutyrate from pea-shells. *Biomass and Bioenergy* 36, 218–225. doi:10.1016/j.biombioe.2011.10.027
- Penloglou, G., Chatzidoukas, C., Kiparissides, C., 2012. Microbial production of polyhydroxybutyrate with tailor-made properties: An integrated modelling approach and experimental validation. *Biotechnol. Adv.* 30, 329–337. doi:10.1016/j.biotechadv.2011.06.021
- Pereira, J.R., Araújo, D., Marques, A.C., Neves, L.A., Grandfils, C., Sevrin, C., Alves, V.D., Fortunato, E., Reis, M.A.M., Freitas, F., 2019. Demonstration of the adhesive properties of the medium-chain-length polyhydroxyalkanoate produced by *Pseudomonas chlororaphis* subsp. *aurantiaca* from glycerol. *Int. J. Biol. Macromol.* 122, 1144–1151. doi:10.1016/j.ijbiomac.2018.09.064

- Pfeiffer, D., Wahl, A., Jendrossek, D., 2011. Identification of a multifunctional protein, PhaM, that determines number, surface to volume ratio, subcellular localization and distribution to daughter cells of poly(3-hydroxybutyrate), PHB, granules in *Ralstonia eutropha* H16. *Mol. Microbiol.* 82, 936–951. doi:10.1111/j.1365-2958.2011.07869.x
- Philip, S., Keshavarz, T., Roy, I., 2007. Polyhydroxyalkanoates: biodegradable polymers with a range of applications. *J. Chem. Technol. Biotechnol.* 82, 233–247. doi:10.1002/jctb.1667
- Phukon, P., Saikia, J.P., Konwar, B.K., 2012. Bio-plastic (P-3HB-co-3HV) from *Bacillus circulans* (MTCC 8167) and its biodegradation. *Colloids Surfaces B Biointerfaces* 92, 30–34. doi:10.1016/j.colsurfb.2011.11.011
- Plackett, R.L., Burman, J.P., 1946. The Design of Optimum Multifactorial Experiments. *Biometrika* 33, 305–325. doi:10.1093/biomet/33.4.305
- Poli, A., Di Donato, P., Abbamondi, G.R., Nicolaus, B., Donato, P. Di, 2011. Synthesis, production, and biotechnological applications of exopolysaccharides and polyhydroxyalkanoates by archaea. *Archaea* 2011, 693253. doi:10.1155/2011/693253
- Poomipuk, N., Reungsang, A., Plangklang, P., 2014. Poly- β -hydroxyalkanoates production from cassava starch hydrolysate by *Cupriavidus* sp. KKU38. *Int. J. Biol. Macromol.* 65C, 51–64. doi:10.1016/j.ijbiomac.2014.01.002
- Porwal, S., Kumar, T., Lal, S., Rani, A., Kumar, S., Cheema, S., Purohit, H.J., Sharma, R., Singh Patel, S.K., Kalia, V.C., 2008. Hydrogen and polyhydroxybutyrate producing abilities of microbes from diverse habitats by dark fermentative process. *Bioresour. Technol.* 99, 5444–5451. doi:10.1016/j.biortech.2007.11.011

- Pötter, M., Steinbüchel, A., 2005. Poly(3-hydroxybutyrate) Granule-Associated Proteins: Impacts on Poly(3-hydroxybutyrate) Synthesis and Degradation †. *Biomacromolecules* 6, 552–560. doi:10.1021/bm049401n
- Poupart, R., Haider, A., Babinot, J., Kang, I.-K., Malval, J.-P., Lalevée, J., Andalloussi, S.A., Langlois, V., Versace, D.L., 2015. Photoactivable Surface of Natural Poly(3-hydroxybutyrate-co-3-hydroxyvalerate) for Antiadhesion Applications. *ACS Biomater. Sci. Eng.* 1, 525–538. doi:10.1021/acsbiomaterials.5b00002
- Pramual, S., Assavanig, A., Bergkvist, M., Batt, C.A., Sunintaboon, P., Lirdprapamongkol, K., Svasti, J., Niamsiri, N., 2016. Development and characterization of bio-derived polyhydroxyalkanoate nanoparticles as a delivery system for hydrophobic photodynamic therapy agents. *J. Mater. Sci. Mater. Med.* 27, 40. doi:10.1007/s10856-015-5655-4
- Qu, X.H., Wu, Q., Liang, J., Zou, B., Chen, G.Q., 2006. Effect of 3-hydroxyhexanoate content in poly(3-hydroxybutyrate-co-3-hydroxyhexanoate) on in vitro growth and differentiation of smooth muscle cells. *Biomaterials* 27, 2944–2950. doi:10.1016/j.biomaterials.2006.01.013
- Quillaguamán, J., Guzmán, H., Van-Thuoc, D., Hatti-Kaul, R., 2010. Synthesis and production of polyhydroxyalkanoates by halophiles: current potential and future prospects. *Appl. Microbiol. Biotechnol.* 85, 1687–1696. doi:10.1007/s00253-009-2397-6
- Radhika, D., Murugesan, A.G., 2012. Bioproduction, statistical optimization and characterization of microbial plastic (poly 3-hydroxy butyrate) employing various hydrolysates of water hyacinth (*Eichhornia crassipes*) as sole carbon source. *Bioresour. Technol.* 121, 83–92. doi:10.1016/j.biortech.2012.06.107

- Rai, R., Roether, J.A., Knowles, J.C., Mordan, N., Salih, V., Locke, I.C., Gordge, M.P., McCormick, A., Mohn, D., Stark, W.J., Keshavarz, T., Boccaccini, A.R., Roy, I., 2017. Highly elastomeric poly(3-hydroxyoctanoate) based natural polymer composite for enhanced keratinocyte regeneration. *Int. J. Polym. Mater. Polym. Biomater.* 66, 326–335. doi:10.1080/00914037.2016.1217530
- Ramadas, N. V, Soccol, C.R., Pandey, A., 2010. A statistical approach for optimization of polyhydroxybutyrate production by *Bacillus sphaericus* NCIM 5149 under submerged fermentation using central composite design. *Appl. Biochem. Microbiol.* 162, 996–1007. doi:10.1007/s12010-009-8807-5
- Ramsay, B.A., Saracovan, I., Ramsay, J.A., Marchessault, R.H., 1991. Continuous production of long-side-chain poly-3-hydroxyalkanoates by *Pseudomonas oleovorans*. *Appl. Environ. Microbiol.* 57, 625–629.
- Ramsay, J.A., Berger, E., Ramsay, B.A., Chavarie, C., 1990. Recovery of Poly-3-hydroxyalkanoic acid granules by a surfactant-Hypochlorite method. *Biotechnol. Tech.* 4, 221–226. doi: 10.1007/BF00158833
- Ramsay, J.A., Berger, E., Voyer, R., Chavarie, C., Ramsay, B.A., 1994. Extraction of poly-3-hydroxybutyrate using chlorinated solvents. *Biotechnol. Tech.* 8, 589–594. doi:10.1007/BF00152152
- Ray, S., Kalia, V.C., 2017. Biomedical Applications of Polyhydroxyalkanoates. *Indian J. Microbiol.* 57, 261–269. doi:10.1007/s12088-017-0651-7
- Ray, S., Prajapati, V., Patel, K., Trivedi, U., 2016. Optimization and characterization of PHA from isolate *Pannonibacter phragmitetus* ERC8 using glycerol waste. *Int. J. Biol. Macromol.* 86, 741–9. doi:10.1016/j.ijbiomac.2016.02.002

- Reddy, S.V., Thirumala, M., Mahmood, S.K., 2009. A novel *Bacillus* sp. accumulating poly (3-hydroxybutyrate-co-3-hydroxyvalerate) from a single carbon substrate. *J. Ind. Microbiol. Biotechnol.* 36, 837–843. doi:10.1007/s10295-009-0561-8
- Rehm, B.H.A., 2003. Polyester synthases: natural catalysts for plastics. *Biochem. J.* 376, 15–33. doi:10.1042/BJ20031254
- Ritopalomares, M., 2004. Practical application of aqueous two-phase partition to process development for the recovery of biological products. *J. Chromatogr. B* 807, 3–11. doi:10.1016/j.jchromb.2004.01.008
- Rivera-Terceros, P., Tito-Claros, E., Torrico, S., Carballo, S., Van-Thuoc, D., Quillaguamán, J., 2015. Production of poly(3-hydroxybutyrate) by *Halomonas boliviensis* in an air-lift reactor. *J. Biol. Res.* 22, 8. doi:10.1186/s40709-015-0031-6
- Rodríguez-Contreras, A., Koller, M., Miranda-de Sousa Dias, M., Calafell-Monfort, M., Braunegg, G., Marqués-Calvo, M.S., 2015. Influence of glycerol on poly(3-hydroxybutyrate) production by *Cupriavidus necator* and *Burkholderia sacchari*. *Biochem. Eng. J.* 94, 50–57. doi:10.1016/j.bej.2014.11.007
- Rossi, S., Azghani, A.O., Omri, A., 2004. Antimicrobial efficacy of a new antibiotic-loaded poly(hydroxybutyric-co-hydroxyvaleric acid) controlled release system. *J. Antimicrob. Chemother.* 54, 1013–1018. doi:10.1093/jac/dkh477
- Saitou, N., Nei, M., 1987. The neighbor-joining method: a new method for reconstructing phylogenetic trees. *Mol. Biol. Evol.* 4, 406–25.
- Salgaonkar, B.B., Bragança, J.M., 2015. Biosynthesis of poly(3-hydroxybutyrate-co-3-hydroxyvalerate) by *Halogeometricum borinquense* strain E3. *Int. J. Biol. Macromol.* 78, 339–346. doi:10.1016/j.ijbiomac.2015.04.016

- Salgaonkar, B.B., Mani, K., Braganca, J.M., 2013. Characterization of polyhydroxyalkanoates accumulated by a moderately halophilic salt pan isolate *Bacillus megaterium* strain H16. *J. Appl. Microbiol.* 114, 1347–1356. doi:10.1111/jam.12135
- Sankhla, I.S., Bhati, R., Singh, A.K., Mallick, N., 2010. Poly(3-hydroxybutyrate-co-3-hydroxyvalerate) co-polymer production from a local isolate, *Brevibacillus invocatus* MTCC 9039. *Bioresour. Technol.* 101, 1947–1953. doi:10.1016/j.biortech.2009.10.006
- Sasidharan, R.S., Bhat, S.G., Chandrasekaran, M., 2014. Biocompatible polyhydroxybutyrate (PHB) production by marine *Vibrio azureus* BTKB33 under submerged fermentation. *Ann. Microbiol.* 65, 455 - 465. doi:10.1007/s13213-014-0878-z
- Sathiyarayanan, G., Kiran, G.S., Selvin, J., Saibaba, G., 2013. Optimization of polyhydroxybutyrate production by marine *Bacillus megaterium* MSBN04 under solid state culture. *Int. J. Biol. Macromol.* 60, 253–61. doi:10.1016/j.ijbiomac.2013.05.031
- Sathiyarayanan, G., Saibaba, G., Seghal Kiran, G., Selvin, J., 2013a. A statistical approach for optimization of polyhydroxybutyrate production by marine *Bacillus subtilis* MSBN17. *Int. J. Biol. Macromol.* 59, 170–177. doi:10.1016/j.ijbiomac.2013.04.040
- Sato, H., Ando, Y., Mitomo, H., Ozaki, Y., 2011. Infrared Spectroscopy and X-ray Diffraction Studies of Thermal Behavior and Lamella Structures of Poly(3-hydroxybutyrate- co -3-hydroxyvalerate) (P(HB-co -HV)) with PHB-Type Crystal Structure and PHV-Type Crystal Structure. *Macromolecules* 44, 2829–2837. doi:10.1021/ma102723n
- Shamala, T.R., Chandrashekar, A., Vijayendra, S.V.N., Kshama, L., 2003. Identification of polyhydroxyalkanoate (PHA)-producing *Bacillus* spp. using the polymerase chain reaction (PCR). *J. Appl. Microbiol.* 94, 369–374. doi:10.1046/j.1365-2672.2003.01838.x

- Sharma, P., Bajaj, B.K., 2015. Production and characterization of poly-3-hydroxybutyrate from *Bacillus cereus* PS 10. *Int. J. Biol. Macromol.* 81, 241–248. doi:10.1016/j.ijbiomac.2015.08.008
- Shen, F., Zhang, E., Wei, Z., 2010. In vitro blood compatibility of poly (hydroxybutyrate-co-hydroxyhexanoate) and the influence of surface modification by alkali treatment. *Mater. Sci. Eng. C* 30, 369–375. doi:10.1016/j.msec.2009.12.003
- Sheu, D.S., Wang, Y.T., Lee, C.Y., 2000. Rapid detection of polyhydroxyalkanoate-accumulating bacteria isolated from the environment by colony PCR. *Microbiology* 146 2019–25. doi: 10.1099/00221287-146-8-2019
- Shishatskaya, E.I., Nikolaeva, E.D., Vinogradova, O.N., Volova, T.G., 2016. Experimental wound dressings of degradable PHA for skin defect repair. *J. Mater. Sci. Mater. Med.* 27, 165. doi:10.1007/s10856-016-5776-4
- Shishatskaya, E.I., Volova, T.G., Puzyr, A.P., Mogilnaya, O.A., Efremov, S.N., 2004. Tissue response to the implantation of biodegradable polyhydroxyalkanoate sutures. *J. Mater. Sci. Mater. Med.* 15, 719–728. doi:10.1023/B:JMSM.0000030215.49991.0d
- Shrivastav, A., Mishra, S.K., Shethia, B., Pancha, I., Jain, D., Mishra, S., 2010. Isolation of promising bacterial strains from soil and marine environment for polyhydroxyalkanoates (PHAs) production utilizing *Jatropha* biodiesel byproduct. *Int. J. Biol. Macromol.* 47, 283–7. doi:10.1016/j.ijbiomac.2010.04.007
- Shum-Tim, D., Stock, U., Hrkach, J., Shinoka, T., Lien, J., Moses, M.A., Stamp, A., Taylor, G., Moran, A.M., Landis, W., Langer, R., Vacanti, J.P., Mayer, J.E., 1999. Tissue engineering of autologous aorta using a new biodegradable polymer. *Ann. Thorac. Surg.* 68, 2298–2304. doi:10.1016/S0003-4975(99)01055-3

- Silverstein, R.M., Webster, F.X., Kiemle, D.J., 2005. Spectrometric Identification of Organic Compounds, 7th edn. New Jersey, USA: John Wiley & Sons Inc.
- Sindhu, R., Ammu, B., Binod, P., Deepthi, S.K., Ramachandran, K.B., Soccol, C.R., Pandey, A., 2011. Production and characterization of poly-3-hydroxybutyrate from crude glycerol by *Bacillus sphaericus* NII 0838 and improving its thermal properties by blending with other polymers. *Brazilian Arch. Biol. Technol.* 54, 783–794. doi:10.1590/S1516-89132011000400019
- Sindhu, R., Silviya, N., Binod, P., Pandey, A., 2013. Pentose-rich hydrolysate from acid pretreated rice straw as a carbon source for the production of poly-3-hydroxybutyrate. *Biochem. Eng. J.* 78, 67–72. doi:10.1016/j.bej.2012.12.015
- Singh, M., Kumar, P., Patel, S.K.S., Kalia, V.C., 2013. Production of Polyhydroxyalkanoate Co-polymer by *Bacillus thuringiensis*. *Indian J. Microbiol.* 53, 77–83. doi:10.1007/s12088-012-0294-7
- Škrbić, Z., Divjaković, V., 1996. Temperature influence on changes of parameters of the unit cell of biopolymer PHB. *Polymer.* 37, 505–507. doi:10.1016/0032-3861(96)82922-3
- Sodian, R., Hoerstrup, S.P., Sperling, J.S., Daebritz, S., Martin, D.P., Moran, A.M., Kim, B.S., Schoen, F.J., Vacanti, J.P., Mayer, J.E., 2000. Early In Vivo Experience With Tissue-Engineered Trileaflet Heart Valves. *Circulation* 102, III-22-III-29. doi:10.1161/01.CIR.102.suppl_3.III-22
- Soliev, A.B., Hosokawa, K., Enomoto, K., 2011. Bioactive Pigments from Marine Bacteria: Applications and Physiological Roles. Evidence-Based Complement. *Altern. Med.* 2011, 1–17. doi:10.1155/2011/670349

- Spiekermann, P., Rehm, B.H., Kalscheuer, R., Baumeister, D., Steinbüchel, A., 1999. A sensitive, viable-colony staining method using Nile red for direct screening of bacteria that accumulate polyhydroxyalkanoic acids and other lipid storage compounds. *Arch. Microbiol.* 171, 73–80. doi: 10.1007/s002030050681
- Steinbüchel, A., 1995. Diversity of bacterial polyhydroxyalkanoic acids. *FEMS Microbiol. Lett.* 128, 219–228. doi:10.1016/0378-1097(95)00125-O
- Steinbüchel, A., Lütke-Eversloh, T., 2003. Metabolic engineering and pathway construction for biotechnological production of relevant polyhydroxyalkanoates in microorganisms. *Biochem. Eng. J.* 16, 81–96. doi:10.1016/S1369-703X(03)00036-6
- Steinbüchel, A., Debzi, E.-M., Marchessault, R.H., Timm, A., 1993. Synthesis and production of poly(3-hydroxyvaleric acid) homopolyester by *Chromobacterium violaceum*. *Appl. Microbiol. Biotechnol.* 39, 443–449. doi:10.1007/BF00205030
- Strazzullo, G., Gambacorta, A., Vella, F.M., Immirzi, B., Romano, I., Calandrelli, V., Nicolaus, B., Lama, L., 2008. Chemical-physical characterization of polyhydroxyalkanoates recovered by means of a simplified method from cultures of *Halomonas campaniensis*. *World J. Microbiol. Biotechnol.* 24, 1513–1519. doi:10.1007/s11274-007-9637-7
- Su, Z., Li, P., Wu, B., Ma, H., Wang, Y., Liu, G., Zeng, H., Li, Z., Wei, X., 2014. PHBVHHx scaffolds loaded with umbilical cord-derived mesenchymal stem cells or hepatocyte-like cells differentiated from these cells for liver tissue engineering. *Mater. Sci. Eng. C* 45, 374–382. doi:10.1016/j.msec.2014.09.022
- Subin, R.S., Varghese, S.M. and Bhat, S.G., 2013. Isolation and characterization of polyhydroxyalkanoates accumulating *Vibrio* sp. strain BTTC26 from marine sediments and its production kinetics. *J. Sci. Ind. Res.* 72, 228–235

- Sudesh, K., Abe, H., Doi, Y., 2000. Synthesis, structure and properties of polyhydroxyalkanoates: biological polyesters. *Prog. Polym. Sci.* 25, 1503–1555. doi:10.1016/S0079-6700(00)00035-6
- Suguna, P., Binuramesh, C., Abirami, P., Saranya, V., Poornima, K., Rajeswari, V., Shenbagarathai, R., 2014. Immunostimulation by poly- β hydroxybutyrate-hydroxyvalerate (PHB-HV) from *Bacillus thuringiensis* in *Oreochromis mossambicus*. *Fish Shellfish Immunol.* 36, 90–7. doi:10.1016/j.fsi.2013.10.012
- Sun, W., Cao, J.G., Teng, K., Meighen, E. A., 1994. Biosynthesis of poly-3-hydroxybutyrate in the luminescent bacterium, *Vibrio harveyi*, and regulation by the lux autoinducer, N-(3- hydroxybutanoyl)homoserine lactone. *J. Biol. Chem.* 269, 20785–20790.
- Suwannasing, W., Imai, T., Kaewkannetra, P., 2015. Cost-effective defined medium for the production of polyhydroxyalkanoates using agricultural raw materials. *Bioresour. Technol.* 194, 67–74. doi:10.1016/j.biortech.2015.06.087
- Syromotina, D.S., Surmenev, R.A., Surmeneva, M.A., Boyandin, A.N., Epple, M., Ulbricht, M., Oehr, C., Volova, T.G., 2016. Oxygen and ammonia plasma treatment of poly(3-hydroxybutyrate) films for controlled surface zeta potential and improved cell compatibility. *Mater. Lett.* 163, 277–280. doi:10.1016/j.matlet. 2015.10.080.
- Tamer, I.M., Moo-Young, M., Chisti, Y., 1998. Disruption of *Alcaligenes latus* for Recovery of Poly(β -hydroxybutyric acid): Comparison of High-Pressure Homogenization, Bead Milling, and Chemically Induced Lysis. *Ind. Eng. Chem. Res.* 37, 1807–1814. doi:10.1021/ ie9707432
- Tamura, K., Stecher, G., Peterson, D., Filipowski, A., Kumar, S., 2013. MEGA6: Molecular Evolutionary Genetics Analysis Version 6.0. *Mol. Biol. Evol.* 30, 2725–2729. doi:10.1093/molbev/mst197

- Tan, D., Xue, Y.-S., Aibaidula, G., Chen, G.-Q., 2011. Unsterile and continuous production of polyhydroxybutyrate by *Halomonas* TD01. *Bioresour. Technol.* 102, 8130–8136. doi:10.1016/j.biortech.2011.05.068
- Tan, G.-Y., Chen, C.-L., Li, L., Ge, L., Wang, L., Razaad, I., Li, Y., Zhao, L., Mo, Y., Wang, J.-Y., 2014. Start a Research on Biopolymer Polyhydroxyalkanoate (PHA): A Review. *Polymers.* 6, 706–754. doi:10.3390/polym6030706
- Tan, H.W., Abdul Aziz, A.R., Aroua, M.K., 2013. Glycerol production and its applications as a raw material: A review. *Renew. Sustain. Energy Rev.* 27, 118–127. doi:10.1016/j.rser.2013.06.035
- Tanadchangsang, N., Yu, J., 2012. Microbial synthesis of polyhydroxybutyrate from glycerol: Gluconeogenesis, molecular weight and material properties of biopolyester. *Biotechnol. Bioeng.* 109, 2808–2818. doi:10.1002/bit.24546
- Tebaldi, M.L., Maia, A.L.C., Poletto, F., de Andrade, F.V., Soares, D.C.F., 2019. Poly(-3-hydroxybutyrate-co-3-hydroxyvalerate) (PHBV): Current advances in synthesis methodologies, antitumor applications and biocompatibility. *J. Drug Deliv. Sci. Technol.* 51, 115–126. doi:10.1016/j.jddst.2019.02.007
- Thai, T.Q., Wille, M., Garcia-Gonzalez, L., Sorgeloos, P., Bossier, P., De Schryver, P., 2014. Poly- β -hydroxybutyrate content and dose of the bacterial carrier for *Artemia* enrichment determine the performance of giant freshwater prawn larvae. *Appl. Microbiol. Biotechnol.* 98, 5205 - 5215. doi:10.1007/s00253-014-5536-7
- Thompson, F.L., Iida, T., Swings, J., 2004. Biodiversity of Vibrios. *Microbiol. Mol. Biol. Rev.* 68, 403–431. doi:10.1128/MMBR.68.3.403-431.2004

- Tokiwa, Y., Calabia, B.P., Ugwu, C.U. and Aiba, S., 2009. Biodegradability of plastics. *Int. J. Mol. Sci.* 10, 3722–3742. doi: 10.3390/ijms10093722
- Tringe, S.G., Hugenholtz, P., 2008. A renaissance for the pioneering 16S rRNA gene. *Curr. Opin. Microbiol.* 11, 442–446. doi:10.1016/j.mib.2008.09.011
- Tripathi, A.D., Srivastava, S.K., Singh, R.P., 2013. Statistical optimization of physical process variables for bio-plastic (PHB) production by *Alcaligenes* sp. *Biomass and Bioenergy* 55, 243–250. doi:10.1016/j.biombioe.2013.02.017
- Valappil, S.P., Boccaccini, A.R., Bucke, C., Roy, I., 2007. Polyhydroxyalkanoates in Gram-positive bacteria: insights from the genera *Bacillus* and *Streptomyces*. *Antonie Van Leeuwenhoek* 91, 1–17. doi:10.1007/s10482-006-9095-5
- Valappil, S.P., Misra, S.K., Boccaccini, A.R., Keshavarz, T., Bucke, C., Roy, I., 2007a. Large-scale production and efficient recovery of PHB with desirable material properties, from the newly characterised *Bacillus cereus* SPV. *J. Biotechnol.* 132, 251–8. doi:10.1016/j.jbiotec.2007.03.013
- Valentino, F., Morgan-Sagastume, F., Fraraccio, S., Corsi, G., Zanaroli, G., Werker, A. and Majone, M., 2015. Sludge minimization in municipal wastewater treatment by polyhydroxyalkanoate (PHA) production. *Environ. Sci. Pollut. Res. Int.* 22, 7281–7294. doi: 10.1007/s11356-014-3268-y
- Van Hung, N., De Schryver, P., Tam, T.T., Garcia-Gonzalez, L., Bossier, P., Nevejan, N., 2015. Application of poly- β -hydroxybutyrate (PHB) in mussel larviculture. *Aquaculture* 446, 318–324. doi:10.1016/j.aquaculture.2015.04.036

- Van-Thuoc, D., Quillaguamán, J., Mamo, G., Mattiasson, B., 2008. Utilization of agricultural residues for poly(3-hydroxybutyrate) production by *Halomonas boliviensis* LC1. *J. Appl. Microbiol.* 104, 420–8. doi:10.1111/j.1365-2672.2007.03553.x
- Van-Thuoc, D., Quillaguamán, J., 2013. Improving culture conditions for poly(3-hydroxybutyrate-co-3-hydroxyvalerate) production by *Bacillus* sp. ND153, a bacterium isolated from a mangrove forest in Vietnam. *Ann. Microbiol.* 64, 991 - 997 doi:10.1007/s13213-013-0736-4
- Varshosaz, J., Ghaffari, S., Khoshayand, M.R., Atyabi, F., Azarmi, S., Kobarfard, F., 2010. Development and optimization of solid lipid nanoparticles of amikacin by central composite design. *J. Liposome Res.* 20, 97–104. doi:10.3109/08982100903103904
- Verhoogt, H., Ramsay, B.A., Favis, B.D., Ramsay, J.A., 1996. The influence of thermal history on the properties of poly(3-hydroxybutyrate-co-12%-3-hydroxyvalerate). *J. Appl. Polym. Sci.* 61, 87–96. doi:10.1002/(SICI)1097-4628(19960705)61:1<87::AID-APP10>3.0.CO;2-X
- Vijayendra, S.V.N., Rastogi, N.K., Shamala, T.R., Anil Kumar, P.K., Kshama, L., Joshi, G.J., 2007. Optimization of polyhydroxybutyrate production by *Bacillus* sp. CFR 256 with corn steep liquor as a nitrogen source. *Indian J. Microbiol.* 47, 170–175. doi:10.1007/s12088-007-0033-7
- Vilos, C., Morales, F.A., Solar, P.A., Herrera, N.S., Gonzalez-Nilo, F.D., Aguayo, D.A., Mendoza, H.L., Comer, J., Bravo, M.L., Gonzalez, P.A., Kato, S., Cuello, M.A., Alonso, C., Bravo, E.J., Bustamante, E.I., Owen, G.I., Velasquez, L.A., 2013. Paclitaxel-PHBV nanoparticles and their toxicity to endometrial and primary ovarian cancer cells. *Biomaterials* 34, 4098–4108. doi:10.1016/j.biomaterials. 2013.02.034

- Vilos, C.A., Constandil, L., Herrera, N., Solar, P., Escobar-Fica, J., Velásquez, L.A., 2012. Ceftriaxone-loaded PHBV microparticles: A potential formulation for a long-acting antibiotic to treat animal infections. *Electron. J. Biotechnol.* 15. doi:10.2225/vol15-issue4-fulltext-2
- Vogler, E.A., 1998. Structure and reactivity of water at biomaterial surfaces. *Adv. Colloid Interface Sci.* 74, 69–117. doi:10.1016/S0001-8686(97)00040-7
- Volova, T., Kiselev, E., Vinogradova, O., Nikolaeva, E., Chistyakov, A., Sukovaty, A., Shishatskaya, E., 2014. A glucose-utilizing strain, *Cupriavidus euthrophus* B-10646: Growth kinetics, characterization and synthesis of multicomponent PHAs. *PLoS One* 9, e87551. doi:10.1371/journal.pone.0087551
- Wang, C., Zheng, Y., Sun, Y., Fan, J., Qin, Q., Zhao, Z., 2016. A novel biodegradable polyurethane based on poly(3-hydroxybutyrate-co-3-hydroxyvalerate) and poly(ethylene glycol) as promising biomaterials with the improvement of mechanical properties and hemocompatibility. *Polym. Chem.* 7, 6120–6132. doi:10.1039/C6PY01131D
- Wang, L., Wang, Z.H., Shen, C.Y., You, M.L., Xiao, J.F., Chen, G.Q., 2010. Differentiation of human bone marrow mesenchymal stem cells grown in terpolyesters of 3-hydroxyalkanoates scaffolds into nerve cells. *Biomaterials* 31, 1691–1698. doi:10.1016/j.biomaterials.2009.11.053
- Wang, S., Chen, W., Xiang, H., Yang, J., Zhou, Z., Zhu, M., 2016. Modification and Potential Application of Short-Chain-Length Polyhydroxyalkanoate (SCL-PHA). *Polymers*. 8, 273. doi:10.3390/polym8080273
- Wang, Y.-W., Wu, Q., Chen, G.-Q., 2003. Reduced mouse fibroblast cell growth by increased hydrophilicity of microbial polyhydroxyalkanoates via hyaluronan coating. *Biomaterials* 24, 4621–4629. doi:10.1016/S0142-9612(03)00356-9

- Wang, Y., Chen, R., Cai, J.Y., Liu, Z., Zheng, Y., Wang, H., Li, Q., He, N., 2013. Biosynthesis and Thermal Properties of PHBV Produced from Levulinic Acid by *Ralstonia eutropha*. PLoS One 8, e60318. doi:10.1371/journal.pone.0060318
- Wang, Y., Wang, X., Wei, K., Zhao, N., Zhang, S., Chen, J., 2007. Fabrication, characterization and long-term in vitro release of hydrophilic drug using PHBV/HA composite microspheres. Mater. Lett. 61, 1071–1076. doi:10.1016/j.matlet.2006.06.062
- Warda, E.A., Abeer, A.A.E.A., Eman, R.H., Mahmoud, A.S., Ahmed, I.E.-D., 2016. Applications of Plackett–Burman and Central Composite Design for the Optimization of Novel *Brevundimonas diminuta* KT277492 Chitinase Production, Investigation of its Antifungal Activity. Brazilian Arch. Biol. Technol. 59, e16160245 doi:10.1590/1678-4324-2016160245
- Wecker, P., Moppert, X., Simon-Colin, C., Costa, B., Berteaux-Lecellier, V., 2015. Discovery of a mcl-PHA with unexpected biotechnical properties: the marine environment of French Polynesia as a source for PHA-producing bacteria. AMB Express 5, 74 - 83. doi:10.1186/s13568-015-0163-y
- Wei, Y.H., Chen, W., Wu, H., Janarthanan, O., 2011. Biodegradable and biocompatible biomaterial, polyhydroxybutyrate, produced by an indigenous *Vibrio* sp. BM-1 isolated from marine environment. Mar. Drugs 9, 615–24. doi:10.3390/md9040615
- Woo, P.C.Y., Lau, S.K.P., Teng, J.L.L., Tse, H., Yuen, K.-Y., 2008. Then and now: use of 16S rDNA gene sequencing for bacterial identification and discovery of novel bacteria in clinical microbiology laboratories. Clin. Microbiol. Infect. 14, 908–934. doi:10.1111/j.1469-0691.2008.02070.x

- Xie, H., Li, J., Li, L., Dong, Y., Chen, G.-Q., Chen, K.C., 2013. Enhanced proliferation and differentiation of neural stem cells grown on PHA films coated with recombinant fusion proteins. *Acta Biomater.* 9, 7845–54. doi:10.1016/j.actbio.2013.04.038
- Xu, L.-C., Bauer, J.W., Siedlecki, C.A., 2014. Proteins, platelets, and blood coagulation at biomaterial interfaces. *Colloids Surfaces B Biointerfaces* 124, 49–68. doi:10.1016/j.colsurfb.2014.09.040
- Xu, X.-Y., Li, X.-T., Peng, S.-W., Xiao, J.-F., Liu, C., Fang, G., Chen, K.C., Chen, G.-Q., 2010. The behaviour of neural stem cells on polyhydroxyalkanoate nanofiber scaffolds. *Biomaterials* 31, 3967–3975. doi:10.1016/j.biomaterials.2010.01.132
- Yamane, T., Fukunaga, M., Lee, Y.W., 1996. Increased PHB productivity by high-cell-density fed-batch culture of *Alcaligenes latus*, a growth-associated PHB producer. *Biotechnol. Bioeng.* 50, 197–202. doi:10.1002/(SICI)1097-0290(19960420)50:2<197::AID-BIT8>3.0.CO;2-H
- Yang, F., Hanna, M.A., Sun, R., 2012. Value-added uses for crude glycerol-- a byproduct of biodiesel production. *Biotechnol. Biofuels* 5, 13. doi:10.1186/1754-6834-5-13
- Yang, Y.-H., Brigham, C., Willis, L., Rha, C., Sinskey, A., 2011. Improved detergent-based recovery of polyhydroxyalkanoates (PHAs). *Biotechnol. Lett.* 33, 937–42. doi:10.1007/s10529-010-0513-4
- Yellore, V., Desai, A., 1998. Production of poly-3-hydroxybutyrate from lactose and whey by *Methylobacterium* sp. ZP24. *Lett. Appl. Microbiol.* 26, 391–394. doi:10.1046/j.1472-765X.1998.00362.x
- Yu, J., Chen, L.X.L., 2006. Cost-Effective Recovery and Purification of Polyhydroxyalkanoates by Selective Dissolution of Cell Mass. *Biotechnol. Prog.* 22, 547–553. doi:10.1021/bp050362g

- Zafar, M., Kumar, S., Kumar, S., Dhiman, A.K., 2012. Artificial intelligence based modeling and optimization of poly(3-hydroxybutyrate-co-3-hydroxyvalerate) production process by using *Azohydromonas lata* MTCC 2311 from cane molasses supplemented with volatile fatty acids: A genetic algorithm paradigm. *Bioresour. Technol.* 104, 631–641. doi:10.1016/j.biortech.2011.10.024
- Zengler, K., Toledo, G., Rappe, M., Elkins, J., Mathur, E.J., Short, J.M., Keller, M., 2002. Nonlinear partial differential equations and applications: Cultivating the uncultured. *Proc. Natl. Acad. Sci.* 99, 15681–15686. doi:10.1073/pnas.252630999
- Zhang, C., Zhao, L., Dong, Y., Zhang, X., Lin, J., Chen, Z., 2010. Folate-mediated poly(3-hydroxybutyrate-co-3-hydroxyoctanoate) nanoparticles for targeting drug delivery. *Eur. J. Pharm. Biopharm.* 76, 10–16. doi:10.1016/j.ejpb.2010.05.005
- Zhao, Y., Rao, Z., Xue, Y., Gong, P., Ji, Y., Ma, Y., 2015. Biosynthesis, property comparison, and hemocompatibility of bacterial and haloarchaeal poly(3-hydroxybutyrate-co-3-hydroxyvalerate). *Sci. Bull.* 60, 1901–1910. doi:10.1007/s11434-015-0923-8
- Zheng, Z., Bei, F.F., Tian, H.L., Chen, G.Q., 2005. Effects of crystallization of polyhydroxyalkanoate blend on surface physicochemical properties and interactions with rabbit articular cartilage chondrocytes. *Biomaterials* 26, 3537–3548. doi:10.1016/j.biomaterials.2004.09.041
- Zhu, C., Nomura, C.T., Perrotta, J.A., Stipanovic, A.J., Nakas, J.P., 2009. Production and characterization of poly-3-hydroxybutyrate from biodiesel-glycerol by *Burkholderia cepacia* ATCC 17759. *Biotechnol. Prog.* 26, 424–30. doi:10.1002/btpr.355

References

- Zinn, M., Witholt, B., Egli, T., 2001. Occurrence, synthesis and medical application of bacterial polyhydroxyalkanoate. *Adv. Drug Deliv. Rev.* 53, 5–21. doi:10.1016/S0169-409X(01)00218-6
- ZoBell, C.E., 1941. Studies on marine bacteria. I. The cultural requirements of heterotrophic aerobes. *J. Mar. Res.* 4, 42–75.

.....✂.....

Appendix

GenBank Submission

1. Mohandas, S.P., Balan, L., Philip, R. and Bright Singh, I. S. Genbank Accession No: KR921915. *Halobacillus faecis* MCCB 286. 16S ribosomal RNA gene, partial sequence.
2. Mohandas, S. P., Balan, L., Jayanath, G., Philip, R. and Bright Singh, I. S. Genbank Accession No: KR921916. *Erythrobacter citreus* MCCB 277. 16S ribosomal RNA gene, partial sequence.
3. Mohandas, S. P., Balan, L., Jayanath, G., Philip, R. and Bright Singh, I. S. Genbank Accession No: KR921917. *Alteromonas macleodii* MCCB 278. 16S ribosomal RNA gene, partial sequence.
4. Mohandas, S. P., Balan, L., Jayanath, G., Philip, R. and Bright Singh, I. S. Genbank Accession No: KR921918. *Bacillus cereus* MCCB 279. 16S ribosomal RNA gene, partial sequence.
5. Mohandas, S. P., Balan, L., Jayanath, G., Philip, R. and Bright Singh, I. S. Genbank Accession No: KR921919. *Gordonia bronchialis* MCCB 280. 16S ribosomal RNA gene, partial sequence.
6. Mohandas, S. P., Balan, L., Jayanath, G., Philip, R. and Bright Singh, I. S. Genbank Accession No: KR921920. *Bacillus cereus* MCCB 281. 16S ribosomal RNA gene, partial sequence.
7. Mohandas, S. P., Balan, L., Jayanath, G., Philip, R. and Bright Singh, I. S. Genbank Accession No: KR9219121. *Halomonas meridiana* MCCB 282. 16S ribosomal RNA gene, partial sequence.
8. Balan, L., Mohandas, S. P., Priyaja, P., Philip, R. and Bright Singh, I. S. Genbank Accession No: KR921922. *Donghicola eburneus* MCCB 271. 16S ribosomal RNA gene, partial sequence.

9. Balan, L., Mohandas, S. P., Priyaja, P., Philip, R. and Bright Singh, I. S. Genbank Accession No: KR921923. *Ruegeria mobilis* MCCB 272. 16S ribosomal RNA gene, partial sequence.
10. Balan, L., Mohandas, S. P., Priyaja, P., Philip, R. and Bright Singh, I. S. Genbank Accession No: KR921924. *Marinobacter hydrocarbonoclasticus* MCCB 273. 16S ribosomal RNA gene, partial sequence.
11. Balan, L., Mohandas, S. P., Priyaja, P., Philip, R. and Bright Singh, I. S. Genbank Accession No: KR921925. *Labrenzia aggregata* MCCB 274. 16S ribosomal RNA gene, partial sequence.
12. Balan, L., Mohandas, S. P., Priyaja, P., Philip, R. and Bright Singh, I. S. Genbank Accession No: KR921926. *Labrenzia aggregata* MCCB 275. 16S ribosomal RNA gene, partial sequence.
13. Balan, L., Mohandas, S. P., Priyaja, P., Philip, R. and Bright Singh, I. S. Genbank Accession No: KR921927. *Brevibacterium casei* MCCB 276. 16S ribosomal RNA gene, partial sequence.
14. Mohandas, S. P., Balan, L., Lekshmi, N., Philip, R. and Bright Singh, I. S. Genbank Accession No: KR921928. *Vibrio rotiferianus* MCCB 283. 16S ribosomal RNA gene, partial sequence.
15. Mohandas, S. P., Balan, L., Lekshmi, N., Philip, R. and Bright Singh, I. S. Genbank Accession No: KR921929. *Vibrio harveyi* MCCB 284. 16S ribosomal RNA gene, partial sequence.
16. Mohandas, S. P., Balan, L., Lekshmi, N., Philip, R. and Bright Singh, I. S. Genbank Accession No: KR921930. *Vibrio jascicida* MCCB 285. 16S ribosomal RNA gene, partial sequence.
17. Balan, L., Mohandas, S. P., Jayanath, G., Philip, R. and Bright Singh, I. S. Genbank Accession No: KR921931. *Vibrio alginolyticus* MCCB 287. 16S ribosomal RNA gene, partial sequence.

18. Balan, L., Mohandas, S. P., Jayanath, G., Philip, R. and Bright Singh, I. S. Genbank Accession No: KR921932. *Vibrio alginolyticus* MCCB 288. 16S ribosomal RNA gene, partial sequence.
19. Balan, L., Mohandas, S. P., Jayanath, G., Philip, R. and Bright Singh, I. S. Genbank Accession No: KR921933. *Vibrio alginolyticus* MCCB 289. 16S ribosomal RNA gene, partial sequence.
20. Balan, L., Mohandas, S. P., Jayanath, G., Philip, R. and Bright Singh, I. S. Genbank Accession No: KR921934. *Vibrio alginolyticus* MCCB 290. 16S ribosomal RNA gene, partial sequence.
21. Balan, L., Mohandas, S. P., Priyaja, P., Philip, R. and Bright Singh, I. S. Genbank Accession No: KU521386. *Kocuria* sp. MCCB 337. 16S ribosomal RNA gene, partial sequence.
22. Balan, L., Mohandas, S. P., Priyaja, P., Philip, R. and Bright Singh, I. S. Genbank Accession No: KU521387. *Brevibacterium casei* MCCB 338. 16S ribosomal RNA gene, partial sequence.
23. Balan, L., Mohandas, S. P., Priyaja, P., Philip, R. and Bright Singh, I. S. Genbank Accession No: KU521388. *Alteromonas* sp. MCCB 339. 16S ribosomal RNA gene, partial sequence.
24. Balan, L., Mohandas, S. P., Priyaja, P., Philip, R. and Bright Singh, I. S. Genbank Accession No: KU521389. *Halomonas* sp. MCCB340. 16S ribosomal RNA gene, partial sequence.
25. Balan, L., Mohandas, S. P., Priyaja, P., Philip, R. and Bright Singh, I. S. Genbank Accession No: KU521390. *Aeromicrobium* sp. MCCB 341. 16S ribosomal RNA gene, partial sequence.
26. Balan, L., Mohandas, S. P., Priyaja, P., Philip, R. and Bright Singh, I. S. Genbank Accession No: KU521391. *Alteromonas* sp. MCCB 342. 16S ribosomal RNA gene, partial sequence.

27. Mohandas, S. P., Balan, L., Jayanath, G., Philip, R. and Bright Singh, I. S. Genbank Accession No: KU521392. *Vibrio harveyi* MCCB 343. 16S ribosomal RNA gene, partial sequence.
28. Mohandas, S. P., Balan, L., Jayanath, G., Philip, R. and Bright Singh, I. S. Genbank Accession No: KX463674. *Bacillus cereus* MCCB 281 polyhydroxyalkanoate synthase (phaC) gene, partial cds.

.....✂.....

List of Publications

- [1] **Sowmya P. Mohandas**, Linu Balan, Lekshmi. N, Sherine Sonia Cubelio, Rosamma Philip, I. S. Bright Singh. 2017. Production and characterization of polyhydroxybutyrate from *Vibrio harveyi* MCCB 284 utilizing glycerol as carbon source. Journal of Applied Microbiology, doi: 10.1111/jam.13359.
- [2] **Sowmya P. Mohandas**, Linu Balan, Jayanath. G, Anoop B. S, Rosamma Philip, Sherine Sonia Cubelio, I. S. Bright Singh. 2018. Biosynthesis and characterization of polyhydroxyalkanoate from marine *Bacillus cereus* MCCB 281 utilizing glycerol as carbon source. International Journal of Biological Macromolecules, doi:10.1016/j.ijbiomac.2018.07.044.
- [3] G. Jayanath, **Sowmya P. Mohandas**, Bhavya Kachiprath, Solly Solomon, T. P. Sajeevan, I. S. Bright Singh, Rosamma Philip. 2018. A novel solvent tolerant esterase of GDSGG motif subfamily from solar saltern through metagenomic approach: Recombinant expression and characterization. International Journal of Biological Macromolecules, doi: 10.1016/j.ijbiomac.2018.06.057.

Papers presented in Conferences

- [1] Sowmya P. Mohandas, Linu Balan, Lekshmi N, Sherine Sonia Cubelio, Rosamma Philip and I. S. Bright Singh, “Production and characterization of polyhydroxybutyrate from bioluminescent *Vibrio harveyi* MCCB284 isolated from *Phallusia nigra*” presented in an International conference on New Horizons in Biotechnology (NHBT 2015) jointly organized by The Biotech Research Society of India and CSIR-NIIST, Trivandrum, 2015.

- [2] Sowmya P. Mohandas, Linu Balan, Anoop Bhaskaran, Rosamma Philip and I. S. Bright Singh, “ Production and characterization of PHA from *Bacillus cereus* MCCB 281 and its biomedical application- A preliminary study” presented in an International conference on Nanomedicine and Tissue engineering (ICNT) organized by International and Inter University Centre for Nanoscience and Nanotechnology, Mahatma Gandhi University, Kottayam, 2016.
- [3] Linu Balan, Sowmya P Mohandas, Rosamma Philip and I. S. Bright Singh, “Screening and Isolation of Polyhydroxyalkanoate Producing Bacteria from Goa Coast” in an International Symposium Marine Ecosystems- Challenges and Opportunities (MECOS2) organized by Marine Biological Association of India, Kochi, 2014.

.....❧.....

Reprint of Papers Published

ORIGINAL ARTICLE

Production and characterization of polyhydroxybutyrate from *Vibrio harveyi* MCCB 284 utilizing glycerol as carbon source

S.P. Mohandas¹, L. Balan¹ , N. Lekshmi¹, S.S. Cubelio², R. Philip³ and I.S. Bright Singh¹

¹ National Centre for Aquatic Animal Health, Cochin University of Science and Technology, Kochi, Kerala, India

² Centre for Marine Living Resources and Ecology, Kakkannad, Kochi, Kerala, India

³ Department of Marine Biology, Microbiology and Biochemistry, Cochin University of Science and Technology, Kochi, Kerala, India

Keywords

characterization of PHB, glycerol, marine bacteria, polyhydroxybutyrate, *Vibrio harveyi*.

Correspondence

Isaac Sarojini Bright Singh, UGC BSR Faculty, National Centre for Aquatic Animal Health, Cochin University of Science and Technology, Kochi 682016, India.

E-mail: isbsingh@gmail.com

2016/1015: received 11 May 2016, revised 7 October 2016 and accepted 8 November 2016

doi:10.1111/jam.13359

Abstract

Aims: Production and characterization of polyhydroxybutyrate (PHB) from moderately halophilic bacterium *Vibrio harveyi* MCCB 284 isolated from tunicate *Phallusia nigra*.

Methods and Results: Twenty-five bacterial isolates were obtained from tunicate samples and three among them exhibited an orange fluorescence in Nile red staining indicating the presence of PHB. One of the isolates, MCCB 284, which showed rapid growth and good polymer yield, was identified as *V. harveyi*. The optimum conditions of the isolate for the PHB production were pH 8.0, sodium chloride concentration 20 g l⁻¹, inoculum size 0.5% (v/v), glycerol 20 g l⁻¹ and 72 h of incubation at 30°C. Cell dry weight (CDW) of 3.2 g l⁻¹, PHB content of 2.3 g l⁻¹ and final PHB yield of 1.2 g l⁻¹ were achieved. The extracted PHB was characterized by FTIR, NMR and DSC-TGA techniques.

Conclusions: An isolate of *V. harveyi* that could effectively utilize glycerol for growth and PHB accumulation was obtained from tunicate *P. nigra*. PHB produced was up to 72% based on CDW.

Significance and Impact of the Study: This is the first report of an isolate of *V. harveyi* which utilizes glycerol as the sole carbon source for PHB production with high biomass yield. This isolate could be of use as candidate species for commercial PHB production using glycerol as the feed stock or as source of genes for recombinant PHB production or for synthetic biology.

Introduction

Environmental impact of petroleum-based plastics has promoted research towards the development of biodegradable plastics as potential substitute for synthetic ones. Recent innovations in science and technology have created major advancements in the arena of 'biodegradable plastics' all over the world. Polyhydroxyalkanoates (PHAs) are a class of natural polyesters produced by micro-organisms during nutrient limiting conditions (Anderson and Dawes 1990). PHAs are synthesized by a wide variety of Gram-positive and Gram-negative bacteria including members of the family Halobacteriaceae and

Archaea and by several other marine bacteria (Grage *et al.* 2009). PHAs are classified into three types based on the number of carbon atoms in their monomer units as short-chain length with 3–5 carbon atoms, medium-chain length with 6–14 carbon atoms and long-chain length with more than 14 carbon atoms (Anderson and Dawes 1990).

Polyhydroxybutyrate (PHB) is a semi-crystalline, isotactic, thermoplastic polymer having properties similar to petroleum-derived polypropylene. PHB is a biodegradable and biocompatible polymer that undergoes complete degradation under aerobic and anaerobic conditions (Tokawa *et al.* 2009). PHB and its copolymers are known

to be extensively used for various applications in the field of medicine, tissue engineering, drug delivery, packaging and aquaculture (Gumel *et al.* 2013). The major drawback that hampers the large-scale production of PHB is the high cost of carbon source that accounts for 70–80% of the total expenses (Choi and Lee 1997). In this context, by-products from agriculture and industry have turned out to be the promising sources of carbon which could cut down the cost of PHB production (Suwannasing *et al.* 2015; Valentino *et al.* 2015). The nature of micro-organisms, inherited metabolic pathways, media constituents and bioprocess strategies are the significant factors that govern PHB production (Grothe *et al.* 1999). The use of glycerol, an industrial waste, has been proven an attractive feed material for the cost-effective production of PHA (Kumar *et al.* 2015). In addition, glycerol from the growing biodiesel industry can be efficaciously utilized by different bacteria to produce value-added products.

Marine environment, a largely unexplored source of microbial diversity, remains quite neglected towards developing industrial processes in equivalence to the terrestrial counter parts. Marine bacteria have the unique potential to produce biopolymers with relatively new properties (Imhoff *et al.* 2011). Numerous studies reported that marine bacteria such as *Vibrio* sp., *Bacillus* sp. and *Halomonas* sp. could accumulate PHB nearly to 50% of their cell dry weight (CDW) (Chien *et al.* 2007; Shrivastav *et al.* 2010; Wei *et al.* 2011; Sathiyarayanan *et al.* 2013). Several *Vibrio* sp. such as *Vibrio harveyi* (Sun *et al.* 1994), *V. natrigens* (Chien *et al.* 2007), *V. fischeri* (Boyandin *et al.* 2008) and *V. azureus* (Subin *et al.* 2013) have also been identified for PHB production. The advantages of using marine bacteria for industrial scale PHB synthesis include the possible reduction in the contamination caused by terrestrial/aerial bacteria that lack salt resistance and the option to use filtered seawater as culture medium (Numata and Doi 2012). The objectives of this study is to delineate the production, optimization and characterization of PHB produced by *V. harveyi* MCCB 284 isolated from Vizhinjam Bay, Trivandrum, Kerala, which utilizes glycerol as the sole carbon source.

Materials and methods

Media preparation

The medium used in the study was ZoBell's marine agar 2216 E (HiMedia, Mumbai, Maharashtra, India), for bacterial isolation and maintenance. PHB production medium was ZoBell's marine broth (peptone, 5 g l⁻¹ and yeast extract, 1 g l⁻¹ in sea water) and pH adjusted

to 7.8 using 1 mol l⁻¹ NaOH. Different carbon sources such as glucose, fructose, mannitol, xylose, glycerol, lactose, sodium acetate, sucrose and starch were prepared in sea water, autoclaved separately and added into the production medium. All chemicals used in this study were of analytical grade.

Isolation and screening of PHB producing bacteria

Tunicate samples were collected from Vizhinjam Bay, Trivandrum, Kerala (8°22'N, 76°59'E), by SCUBA diving, washed with sterile sea water and stored in ice for further analysis. Body of the tunicate was cut into small pieces and homogenized, and the resultant homogenate was serially diluted with sterile sea water, spread on ZoBell's marine agar plates and incubated at 28°C for 7 days. PHB-producing bacteria were isolated on ZoBell's marine agar medium with 20 g l⁻¹ glucose and 0.5 µg ml⁻¹ Nile Red dye (Spiekermann *et al.* 1999) and incubated at 28°C for 48 h. Nile red staining of the bacterial isolates was performed to confirm PHB production (Osle and Holt 1982), and the cells were observed under fluorescence microscope (Olympus, Tokyo, Japan).

16S rRNA gene sequencing and phylogenetic analysis

The positive isolate was identified based on the biochemical tests and 16S rRNA gene sequence analysis. Genomic DNA of the isolated pure culture was extracted according to Cheng and Jiang (2006), and 16S rRNA gene was amplified by PCR using universal primers 27F (5'-GAGTTTGATCCTGGCTCA-3') and 1492R (5'-ACGGCTACCTTGTACGACTT-3'). PCR was performed as follows: an initial denaturation at 94°C for 3 min, 29 cycles of denaturation at 94°C for 30 s, annealing at 58°C for 40 s, extension at 72°C for 1 min and final extension at 72°C for 5 min. The amplified product was sequenced at SciGenom Labs (Cochin, Kerala). The partial sequence was analysed in NCBI database using BLAST algorithm, and sequence alignment was performed using the software GeneTool Lite 1.0. Phylogenetic tree was constructed with MEGA 6.0 (Tamura *et al.* 2013) using neighbour-joining method (Saitou and Nei 1987) with bootstrapping for 1000 replicates to assess the stability of tree topology (Felsenstein 1985). The nucleotide sequence was deposited in GenBank database under accession number KR921929.

PHB production

For PHB production, inoculum was prepared by growing the culture on ZoBell's marine agar slants for 24 h at 28°C. Cells were suspended in ZoBell's marine broth and

absorbance measured in UV-Visible spectrophotometer (Shimadzu UV-1601, Kyoto, Japan) at a wavelength of 600 nm and then adjusted to 1.0 with a cell density of 2×10^8 CFU per ml. A two-stage cultivation strategy was adopted to increase PHB accumulation. The inoculum (0.1% v/v) was introduced to 200-ml production medium and incubated at 28°C for 24 h at 150 rev min⁻¹ in an orbital shaker. After 24 h, glucose was added to the culture medium (final concentration 20 g l⁻¹) for the enhanced PHB accumulation and was further incubated for 48 h before cell harvesting. Cell growth was monitored every 24 h by measuring optical density at 600-nm spectrophotometrically. For determination of CDW, 10-ml culture was centrifuged at 8000 g for 10 min at 28°C and cell pellet was rinsed twice with distilled water to remove salt and media components. The cell pellet was then transferred to preweighed tube and lyophilized.

Polymer recovery

A quantity of 1-g lyophilized cell pellet was treated with 50-ml chloroform and 50-ml hypochlorite solution (4% available chlorine) for 1 h at 30°C, and the mixture was centrifuged at 8000 g for 10 min. The lower chloroform phase was collected, and the dissolved PHB was precipitated by the addition of 10 volumes of ice cold methanol. The precipitated PHB was filtered and dried (Hahn *et al.* 1995). To the extracted polymer, 10 ml concentrated sulphuric acid was added and incubated at 100°C in a boiling water bath for 15 min. The absorbance of crotonic acid was measured at 235 nm using UV-Visible spectrophotometer (Shimadzu UV-1601) and the PHB yield was estimated (Law and Slepecky 1961).

Optimization for PHB production

Various parameters that influenced the PHB production of the selected isolate were analysed by 'one-factor-at-a-time' approach under shake flask culture conditions. For all experiments, the bacterial isolate was inoculated at a cell density corresponding to 2×10^8 CFU per ml in 25-ml production medium. PHB production under the varying conditions of initial pH (5.0–10.0), sodium chloride concentration (5–100 g l⁻¹), carbon sources (glucose, fructose, sucrose, xylose, lactose, mannitol, glycerol, sodium acetate and starch), concentration of carbon source (10–50 g l⁻¹), incubation period (6–72 h), initial inoculum size (0.1–10% v/v) and temperature (20–40°C) were investigated. The CDW and PHB content were estimated after 72 h as described earlier. The experiment was carried out in triplicate.

Transmission electron microscopy

Harvested cells containing PHB were washed with 0.1 mol l⁻¹ sodium cacodylate buffer (pH 7.0), postfixed with 2% (w/v) osmium tetroxide for 2 h at 8°C. It was again washed with the buffer and dehydrated with a graded series of acetone and embedded in epoxy resin. The embedded specimen was cut into ultrathin sections and stained with uranyl acetate and lead citrate. TEM observations were performed using a TECNAI 200 TEM (FEI; Electron Optics Hillsboro, OR, USA) at All India Institute of Medical Sciences (AIIMS), Delhi.

Polymer characterization

The polymer was ground with KBr crystals to form pellet and dried. The sample was subjected to FTIR analysis using Nicolet FT-IR Spectrometer (Thermo Scientific, Madison, WI, USA). The spectrum was recorded between 4000 and 400 cm⁻¹ with a resolution of 4 cm⁻¹ and was compared with commercially available PHB (Sigma).

Differential scanning calorimetry (DSC) was employed to record the thermal transitions of the extracted polymer. The polymer sample was heated from 25 to 200°C at a rate of 10°C min⁻¹ under nitrogen atmosphere (100 ml min⁻¹) using DSC 60 Plus (Shimadzu). The melting point (T_m) was determined from DSC endothermal peak.

Thermogravimetric analysis (TGA) was performed to determine the thermal stability and composition of polymer using TGA Q50 (TA Instruments, New Castle, DE, USA). Approximately 5–8 mg of the sample was heated from 30 to 800°C at a rate of 10°C min⁻¹ under nitrogen atmosphere (100 ml min⁻¹).

¹H and ¹³C nuclear magnetic resonance spectroscopy (NMR) of the extracted polymer and standard PHB were analysed on Bruker Avance III spectrometer operated at 400 MHz. The sample was dissolved in deuterated chloroform and the spectra were recorded. Tetramethylsilane was used as the internal standard. The analysis was carried out at the Sophisticated Test and Instrumentation Centre (STIC), CUSAT, Kerala.

Statistical analysis

Statistical analysis of the experimental data was carried out using one-way ANOVA followed by the Tukey-Kramer multiple comparisons test using the software GraphPad InStat ver. 3.0.

Results

Isolation, identification and phylogenetic analysis

Altogether, 25 bacterial isolates were obtained from the tunicate samples, out of which, three exhibited orange

fluorescence under UV light when grown on ZoBell's medium containing Nile red dye indicating PHB production. An isolate, MCCB 284, showing rapid growth and comparatively higher PHB accumulation was segregated and identified based on the biochemical tests and 16S rRNA gene sequence. The partial 16S rRNA gene sequence of the isolate was compared with sequences available in NCBI database using BLAST algorithm, and the isolate showed 100% similarity to *V. harveyi*. The phylogenetic analysis using MEGA 6.0 software also showed the closest match with *V. harveyi* strain FJXPH0612 (Fig. 1). *Vibrio harveyi* is a Gram-negative, motile, rod-shaped bioluminescent bacterium that can tolerate high levels of NaCl (10% w/v). The organism is deposited in the Microbial Culture Collection Bacteria (MCCB) of National Centre for Aquatic Animal Health.

PHB production and optimization

PHB production was carried out in 200-ml production medium (pH 7.8) with 0.1% (v/v) inoculum and incubated at 28°C for 72 h at 150 rev min⁻¹ in an orbital shaker. The isolate MCCB 284 produced a CDW of 1.34 g l⁻¹ with a PHB content of 60% (w/w). The various process parameters such as pH, NaCl concentration, carbon sources, incubation time, initial inoculum size, and incubation temperature were sequentially optimized

by 'one-factor-at-a-time' approach under shake flask conditions. The optimized value for each parameter was used in subsequent stages of the optimization.

Effect of initial pH

To examine the effect of initial pH, the isolate MCCB 284 was inoculated into 25-ml production medium of varying pH 5.0–10.0 and incubated at 28°C for 72 h. The pH was adjusted using 1 mol l⁻¹ NaOH or 1 mol l⁻¹ HCl prior to sterilization. Although the growth of the culture was favoured at lower and higher pH values, a maximum PHB production of 61% based on CDW was observed at the pH 8.0 (data not shown).

Effect of sodium chloride concentration

The isolate MCCB 284 was inoculated into the production medium with different salt concentrations ranging from 5 to 100 g l⁻¹. The optimum salt concentration for the PHB production was 20 g l⁻¹ with a biomass yield and PHB content of 1.3 g l⁻¹ and 66% (w/w), respectively, at the end of 72 h (data not shown). *Vibrio harveyi* MCCB 284 showed meagre growth and PHB production of 22% (w/w) at 100 g l⁻¹ NaCl concentration.

Effect of carbon sources

The ability of the isolate MCCB 284 to utilize different carbon sources (glucose, fructose, xylose, mannitol,

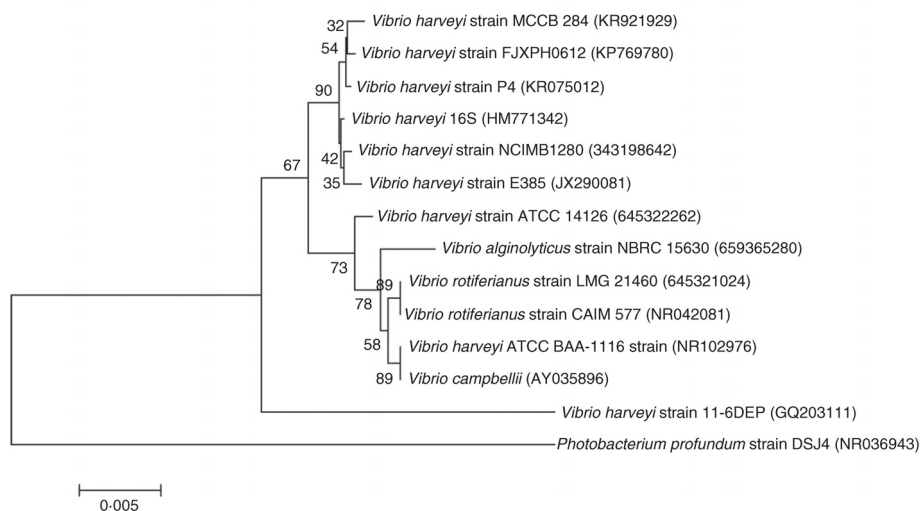


Figure 1 Phylogenetic analysis of *Vibrio harveyi* MCCB 284 with its closely related species based on 16S rRNA sequences. The tree was constructed with MEGA 6.0 software using Neighbour-joining method. *Photobacterium profundum* is the out-group. Bootstrap values indicated at nodes.

glycerol, lactose, sodium acetate, sucrose and starch) for PHB production was investigated. Carbon sources were added at the concentration of 20 g l^{-1} in the production medium. Among the carbon sources evaluated, glycerol supported maximum biomass yield and PHB production followed by glucose and fructose. Also, the isolate was able to utilize pentose sugar xylose for PHB production. The biomass yield and PHB production in the presence of glycerol was 3 g l^{-1} and 68% (w/w), respectively (Fig. 2a). Further, different glycerol concentrations (10, 20, 30, 40 and 50 g l^{-1}) were also examined and 20 g l^{-1} glycerol provided highest biomass yield and PHB production.

Effect of incubation time

From the growth study, it was noticed that *V. harveyi* MCCB 284 reached the logarithmic phase in 3 h followed by the stationary phase in 9 h of cultivation, and hence, the carbon source was added at the 9th hour after inoculation to enhance PHB accumulation. To study the

effect of incubation time on the growth and PHB production of MCCB 284, samples were taken every 6 h and both CDW and PHB content were determined. The PHB accumulation commenced at the early phase of growth of 6 h (34% w/w) and reached 60% (w/w) with a biomass yield of 1.5 g l^{-1} at 24 h, which later decreased to 42% (w/w) at 36 h of cultivation. A maximum cell density of 3.5 g l^{-1} was observed at 72 h which subsequently declined. After 48 h of incubation, a steady state in the PHB production with increasing accumulation was observed till 72 h (Fig. 2b). Maximum PHB content of 68% (w/w) was attained at 72 h of cultivation with a biomass yield of 3 g l^{-1} . The results implied that PHB production in this isolate was associated with the cell growth. The generation time and specific growth rate of *V. harveyi* MCCB 284 was estimated to be 0.3 h and 2.31 h^{-1} , respectively. Precisely, the shorter generation time and higher growth rate of this isolate would be beneficial for commercial production of PHB.

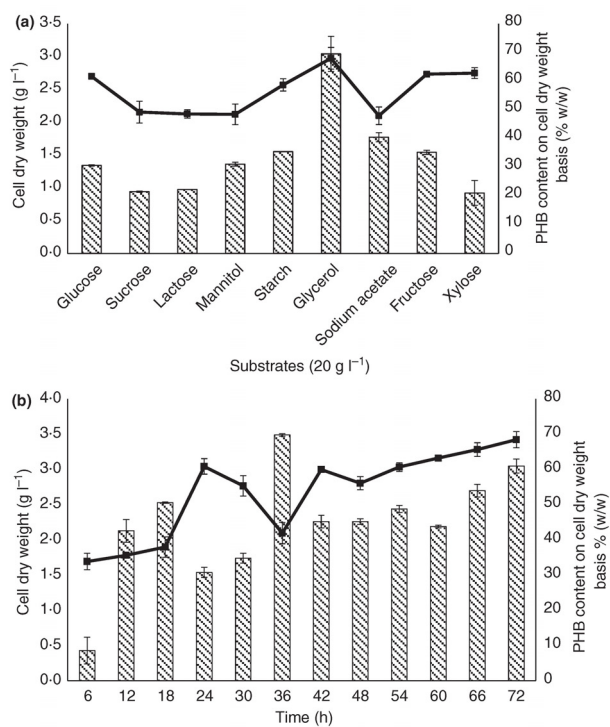


Figure 2 (a) Effect of different carbon sources on the growth and polyhydroxybutyrate (PHB) production of *Vibrio harveyi* MCCB 284 after 72-h incubation at 28°C and 150 rev min^{-1} . Data shown are mean \pm standard deviations of triplicate. (b) Effect of incubation time on growth and PHB production of *V. harveyi* MCCB 284. Glycerol 20 g l^{-1} was used as carbon source. Data shown are mean \pm standard deviations of triplicate. Cell dry weight (▨) and PHB content (—■).

Effect of inoculum size

The effect of initial inoculum size (0.1, 0.5, 1, 2, 4, 6, 8 and 10% v/v) on PHB production was investigated under the optimized culture conditions. An inoculum size of 0.5% (v/v) showed the maximum biomass yield of 3.2 g l^{-1} and PHB content of 72% (w/w). It was noticed that lower initial inoculum size could enable a relatively good biomass yield and PHB production than higher inoculum size (Fig. 3a).

Effect of temperature

The effect of temperature on growth and PHB production of the isolate MCCB 284 was evaluated and the optimal temperature was 30°C . Biomass yield of 3.1 g l^{-1} and PHB content of 71% (w/w) were achieved. The isolate showed considerable growth and PHB production at 35°C ; however, no growth occurred at 40°C (Fig. 3b).

Considering all the above factors, the isolate *V. harveyi* MCCB 284 could be designated as a potential prospect for industrial production of PHB. Based on the statistical analysis, various process parameters such as the pH,

carbon source, incubation time and inoculum size were identified to have significant impact on the growth and PHB production.

Transmission electron microscopy

TEM analysis showed the presence of granules in *V. harveyi* MCCB 284 grown in ZoBell's marine broth containing 20 g l^{-1} glucose for 48 h. The cells contain PHB granules that vary in size and number (Fig. 4).

Polymer characterization

The FTIR spectrum revealed the presence of distinct peak at 1638.23 cm^{-1} corresponding to C=O ester carbonyl group (Fig. 5). Other absorption bands at 1112.3 , 1323.89 and 3444.24 cm^{-1} represented C–O–C group, CH_3 group and OH group, respectively. The pattern of the spectrum obtained was similar to the PHB standard (Sigma).

The melting point (T_m) of the extracted polymer was calculated to be 163°C from the DSC endothermal peak (Fig. 6). From the TGA plot (Fig. 7), the initial thermal

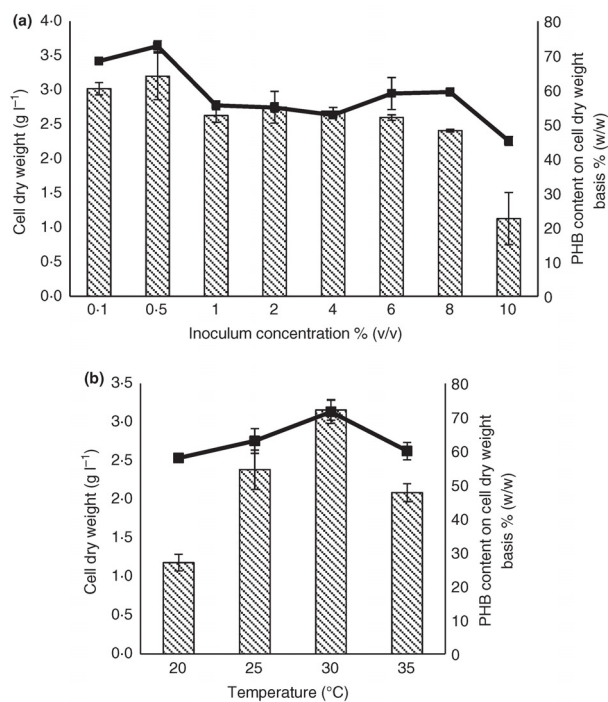


Figure 3 (a) Effect of initial inoculum size on the growth and polyhydroxybutyrate (PHB) production of *Vibrio harveyi* MCCB 284 after 72-h incubation at 28°C and 150 rev min^{-1} . Glycerol 20 g l^{-1} was used as carbon source. Data shown are mean \pm standard deviations of triplicate. (b) Effect of incubation temperature on the growth and PHB production of *V. harveyi* MCCB 284. Glycerol 20 g l^{-1} was used as carbon source. Data shown are mean \pm standard deviations of triplicate. Cell dry weight (▨) and PHB content (—■—).

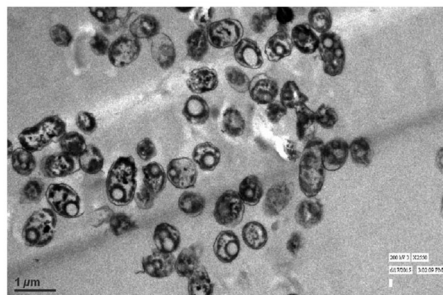


Figure 4 Transmission electron micrograph of polyhydroxybutyrate (PHB) accumulating *Vibrio harveyi* MCCB 284. PHB granules are seen distributed in cytoplasm of the cell after 48-h growth.

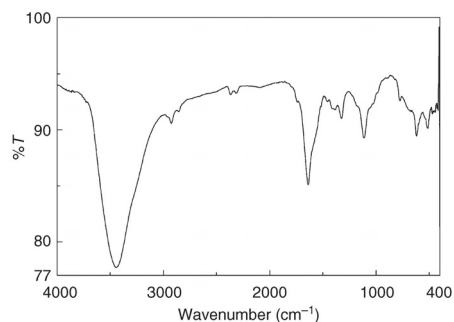


Figure 5 Infrared spectrum of the polymer extracted from *Vibrio harveyi* MCCB 284.

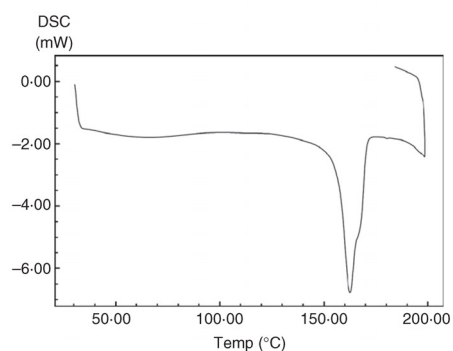


Figure 6 Differential scanning calorimetry curve of polymer extracted from *Vibrio harveyi* MCCB 284.

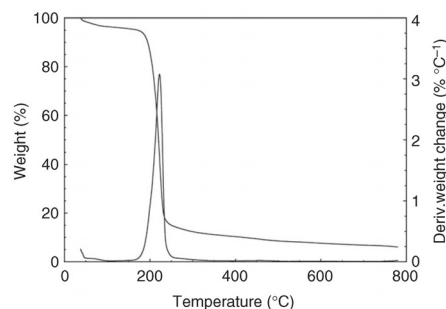


Figure 7 Thermogravimetric analysis of PHB homopolymer obtained from *Vibrio harveyi* MCCB 284.

decomposition of the extracted PHB was determined to be 182°C and the maximum thermal decomposition observed was at 260°C. The temperature at which 50% of the polymer undergoing decomposition ($D_{1/2}$) was detected at 220°C.

The ^1H NMR spectrum of PHB (Fig. 8a) exhibited the characteristic signals for three different groups namely methyl ($-\text{CH}_3$), methylene ($-\text{CH}_2$) and methine ($-\text{CH}$) at 1.21, 2.56 and 5.22 ppm, respectively. ^{13}C NMR spectrum (Fig. 8b) of the polymer showed the chemical shift signals at 19.76, 40.79, 67.61, 169.14 ppm corresponding to the methyl ($-\text{CH}_3$), methylene ($-\text{CH}_2$), methine ($-\text{CH}$) and carbonyl ($-\text{C}=\text{O}$) groups, respectively.

Discussion

Marine habitat constitutes an untapped source of novel microbes, their compounds and metabolic pathways which are largely exploited for biotechnological applications. Marine environment has rich biodiversity for isolation of novel PHA producing bacteria with the desired properties and diverse compositions. In this study, a moderately halophilic bacterium isolated from tunicate *Phallusia nigra* was detected to accumulate PHB during the time of its growth. The isolate was identified as *V. harveyi* MCCB 284 and showed 100% similarity to *V. harveyi* strain. The biochemical characteristics of the culture exhibited the ability to hydrolyse xylan, starch, pectin, gelatin and Tween 80. PHB synthesis and luminescence in this bacterium is highly dependent on cell density (Sun *et al.* 1994). The isolate MCCB 284 showed 60% (w/w) PHB accumulation in the presence of 20 g l^{-1} glucose as carbon source.

In the process of optimization for enhanced PHB production in MCCB 284, the effect of physical parameters such as pH, temperature and sodium chloride concentration was investigated. The isolate MCCB 284 grew well

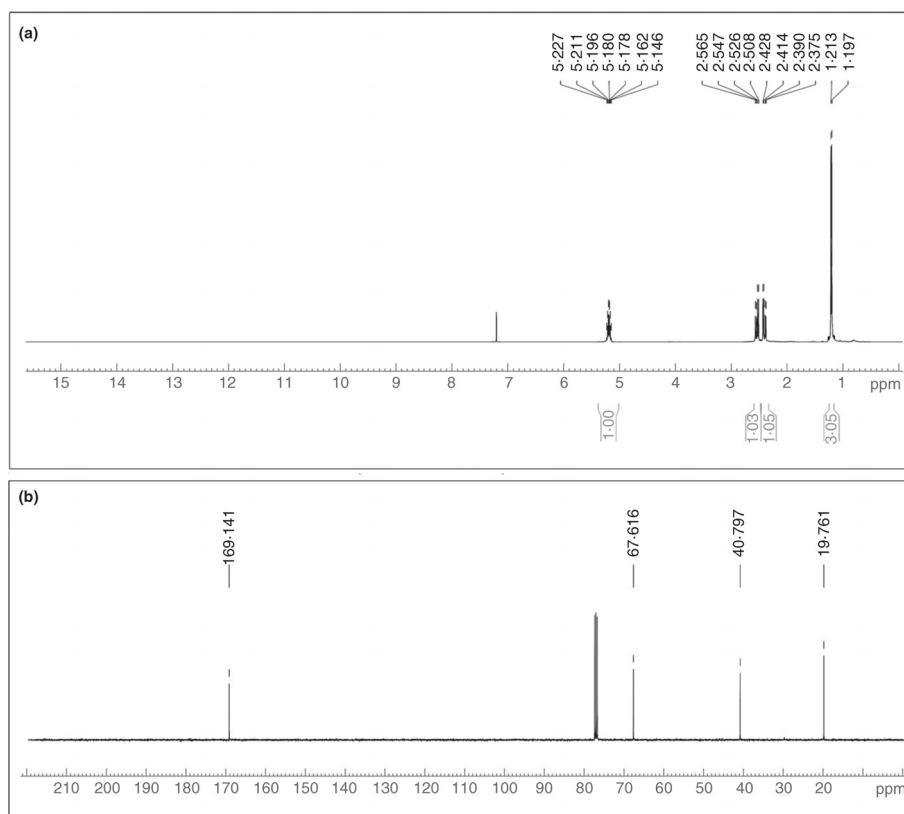


Figure 8 Nuclear magnetic resonance spectra of PHB produced by *Vibrio harveyi* MCCB 284. (a) ^1H NMR spectrum and (b) ^{13}C NMR spectrum.

throughout the pH ranges, 6.0–9.0, but the optimum pH for biomass and polymer production was 8.0. The isolate MCCB 284 showed maximum biomass yield and PHB accumulation at 30°C. The concentration of sodium chloride in the culture medium has crucial impact on PHB production, as *Vibrio* is halophilic and sensitive to salt content (Chien *et al.* 2007). It was found that maximum cell density and polymer production could be achieved at 20 g l⁻¹ NaCl. This finding was in agreement with the earlier report on PHB production from *Vibrio* sp. (Wei *et al.* 2011). Other related *Vibrio* sp. like *V. azureus* exhibited maximum PHA production at 15 g l⁻¹ NaCl (Sasidharan *et al.* 2015). The potential of the isolate MCCB 284 to utilize different carbon sources for the PHB production was examined and glycerol supported

the maximum biomass production (3 g l⁻¹) and PHB yield (68%) based on CDW. The present result complies with the previous reports of glycerol being the preferred sole source of carbon for PHB biosynthesis in Gram-negative bacteria. Chien *et al.* (2007) reported PHB production of 41% (w/w) in *Vibrio* sp utilizing glycerol as carbon source. In *Halomonas* sp. SA8, PHB content and CDW could reach 43% (w/w) and 4.1 g l⁻¹, respectively, after 96 h of cultivation using glycerol (De Castro *et al.* 2014). In another study, an isolate of *Zobellella denitrificans* ZD1 utilized 20 g l⁻¹ glycerol for PHB synthesis and showed a CDW of 4.8 g l⁻¹ and PHB content of 85% (w/w) after 96-h incubation (Ibrahim and Steinbüchel 2010). Glycerol, the major by-product of biodiesel industry could be utilized as an excellent carbon source for

PHB production. Till date, only a few strains of bacteria have been known to metabolize pentose for the PHB production (Cesário *et al.* 2014). Although the isolate MCCB 284 utilized xylose for PHB production, a poor biomass yield (0.9 g l^{-1}) and subsequently low polymer accumulation were noticed. In a similar study to optimize the carbon sources for PHB production in *Vibrio proteolyticus* DCM CAS2, fructose appeared to be the best carbon source and 55% PHB production based on CDW was reported (Melba and Ananthan 2016).

During the time course of growth and polymer production, it was noted that the polymer accumulation commenced at an early phase of growth and the isolate MCCB 284 was able to accumulate the biopolymer within 24 h. The influence of initial inoculum size on PHB production demonstrated that the maximum biomass yield and production were achieved at a low inoculum size (0.5% v/v). As the inoculum size increased, the biomass yield and polymer production decreased. At 10% (v/v), the biomass yield and PHB production were low which might be due to the utilization of accumulated polymer at high cell counts (Yamane *et al.* 1996).

The extracted polymer was purified and characterized by FTIR, NMR, DSC and TGA techniques. The observed peaks in the FTIR spectrum at 1638.23, 1112.3, 1323.89 and 3444.24 cm^{-1} represented C=O ester, C–O–C, CH₃ and OH groups of the polymer, respectively, in agreement with the previous reports (Hong *et al.* 1999; Silverstein *et al.* 2005). In addition, the prominent peaks in ¹³C NMR spectrum at 19.76, 40.79, 67.61, 169.14 ppm represented methyl (CH₃), methylene (CH₂), methine (CH) and carbonyl (C=O) groups, respectively, of the polymer (Doi *et al.* 1986). The maximum thermal decomposition observed was at 260°C and is associated with the ester cleavage of PHB by β-elimination reaction (Choi *et al.* 2003). All these results revealed that the polymer produced by *V. harveyi* MCCB 284 is PHB homopolymer.

This is the first report of a moderate halophilic isolate of *V. harveyi* that demonstrated high biomass yield and PHB production with glycerol as the sole carbon source. The results suggest that *V. harveyi* MCCB 284 is a good candidate for industrial production of PHB using glycerol as the substrate, as donor of genes for synthetic biology or its recombinant production.

Acknowledgements

The authors are grateful to the Centre for Marine Living Resources and Ecology, Ministry of Earth Sciences, Government of India, for the research grant (MoES/CMLRE 10-MLR-TD/09/2012) with which the work was carried out.

Conflict of Interest

No conflict of interest declared.

References

- Anderson, A.J. and Dawes, E.A. (1990) Occurrence, metabolism, metabolic role, and industrial uses of bacterial polyhydroxyalkanoates. *Microbiol Rev* **54**, 450–472.
- Boyardin, A., Kalacheva, G.S., Medvedeva, S., Rodicheva, E. and Volova, T.G. (2008) Luminous bacteria as producers of polyhydroxyalkanoates. *Macromol Symp* **269**, 17–22.
- Cesário, M.T., Raposo, R.S., de Almeida, M.C.M.D., van Keulen, F., Ferreira, B.S. and da Fonseca, M.M.R. (2014) Enhanced bioproduction of poly-3-hydroxybutyrate from wheat straw lignocellulosic hydrolysates. *N Biotechnol* **31**, 104–113.
- Cheng, H.R. and Jiang, N. (2006) Extremely rapid extraction of DNA from bacteria and yeasts. *Biotechnol Lett* **28**, 55–59.
- Chien, C.C., Chen, C.C., Choi, M.H., Kung, S.S. and Wei, Y.H. (2007) Production of poly-beta-hydroxybutyrate (PHB) by *Vibrio* spp. isolated from marine environment. *J Biotech* **132**, 259–263.
- Choi, J.I. and Lee, S.Y. (1997) Process analysis and economic evaluation for Poly(3-hydroxybutyrate) production by fermentation. *Biotechnol Bioprocess Eng* **17**, 335–342.
- Choi, J.Y., Lee, J.K., You, Y. and Park, W.H. (2003) Epoxidized polybutadiene as a thermal stabilizer for poly(3-hydroxybutyrate). II. Thermal stabilization of poly(3-hydroxybutyrate) by epoxidized polybutadiene. *Fibers Polym* **4**, 195–198.
- De Castro, J.S., Nguyen, L.D. and Seppala, J. (2014) Bioconversion of commercial and waste glycerol into value-added polyhydroxyalkanoates by bacterial strains. *J Microb Biochem Technol* **6**, 337–345.
- Doi, Y., Kunioka, M., Nakamura, Y. and Soga, K. (1986) Nuclear magnetic resonance studies on poly(β-hydroxybutyrate) and a copolyester of β-hydroxybutyrate and β-hydroxyvalerate isolated from *Alcaligenes eutrophus* H16. *Macromolecules* **19**, 2860–2864.
- Felsenstein, J. (1985) Confidence limits on phylogenies: an approach using the bootstrap. *Evolution* **39**, 783.
- Grage, K., Jahns, A.C., Parlani, N., Palanisamy, R., Rasiyah, I.A., Atwood, J.A. and Rehm, B.H.A. (2009) Bacterial polyhydroxyalkanoate granules: biogenesis, structure, and potential use as nano-/micro-beads in biotechnological and biomedical applications. *Biomacromolecules* **10**, 660–669.
- Grothe, E., Moo-Young, M. and Chisti, Y. (1999) Fermentation optimization for the production of poly(β-hydroxybutyric acid) microbial thermoplastic. *Enzyme Microb Technol* **25**, 132–141.

- Gumel, A.M., Annuar, M.S.M. and Chisti, Y. (2013) Recent advances in the production, recovery and applications of polyhydroxyalkanoates. *J Polym Environ* **21**, 580–605.
- Hahn, S.K., Chang, Y.K. and Lee, S.Y. (1995) Recovery and characterization of poly (3-hydroxybutyric acid) synthesized in *Alcaligenes eutrophus* and recombinant *Escherichia coli*. *Appl Environ Microbiol* **61**, 34–39.
- Hong, K., Sun, S., Tian, W., Chen, G.Q. and Huang, W. (1999) A rapid method for detecting bacterial polyhydroxyalkanoates in intact cells by Fourier transform infrared spectroscopy. *Appl Microbiol Biotechnol* **51**, 523–526.
- Ibrahim, M.H.A. and Steinbüchel, A. (2010) *Zobellella denitrificans* strain MW1, a newly isolated bacterium suitable for poly(3-hydroxybutyrate) production from glycerol. *J Appl Microbiol* **108**, 214–225.
- Imhoff, J.F., Labes, A. and Wiese, J. (2011) Bio-mining the microbial treasures of the ocean: new natural products. *Biotechnol Adv* **29**, 468–482.
- Kumar, P., Ray, S., Patel, S.K.S., Lee, J.K. and Kalia, V.C. (2015) Bioconversion of crude glycerol to polyhydroxyalkanoate by *Bacillus thuringiensis* under non-limiting nitrogen conditions. *Int J Biol Macromol* **78**, 9–16.
- Law, J.H. and Slepecky, R.A. (1961) Assay of poly-beta-hydroxybutyric acid. *J Bacteriol* **82**, 33–36.
- Melba, D.C.C. and Ananthan, G. (2016) Production and optimization of poly (3-hydroxybutyrate) biopolymer by ascidian associated bacterium *Vibrio proteolyticus* DCM CAS2. *Int J Sci Invt Today* **5**, 13–21.
- Numata, K. and Doi, Y. (2012) Biosynthesis of polyhydroxyalkanoates by a novel facultatively anaerobic *Vibrio* sp. under marine conditions. *Mar Biotechnol (NY)* **14**, 323–331.
- Ostle, A.G. and Holt, J.G. (1982) Nile blue A as a fluorescent stain for fluorescent stain for poly-3- hydroxybutyrate. *Appl Environ Microbiol* **44**, 238–241.
- Saitou, N. and Nei, M. (1987) The neighbor-joining method: as new method for reconstructing phylogenetic trees. *Mol Biol Evol* **4**, 406–425.
- Sasidharan, R.S., Bhat, S.G. and Chandrasekaran, M. (2015) Biocompatible polyhydroxybutyrate (PHB) production by marine *Vibrio azureus* BTKB33 under submerged fermentation. *Ann Microbiol* **65**, 455–465.
- Sathiyarayanan, G., Kiran, G.S., Selvin, J. and Saibaba, G. (2013) Optimization of polyhydroxybutyrate production by marine *Bacillus megaterium* MSBN04 under solid state culture. *Int J Biol Macromol* **60**, 253–261.
- Shrivastav, A., Mishra, S.K., Shethia, B., Pancha, I., Jain, D. and Mishra, S. (2010) Isolation of promising bacterial strains from soil and marine environment for polyhydroxyalkanoates (PHAs) production utilizing *Jatropha* biodiesel byproduct. *Int J Biol Macromol* **47**, 283–287.
- Silverstein, R.M., Webster, F.X. and Kiemle, D.J. (2005) *Spectrometric Identification of Organic Compounds*, 7th edn. New Jersey, USA: John Wiley & Sons Inc.
- Spiekermann, P., Rehm, B.H., Kalscheuer, R., Baumeister, D. and Steinbüchel, A. (1999) A sensitive, viable-colony staining method using Nile red for direct screening of bacteria that accumulate polyhydroxyalkanoic acids and other lipid storage compounds. *Arch Microbiol* **171**, 73–80.
- Subin, R.S., Varghese, S.M. and Bhat, S.G. (2013) Isolation and characterization of polyhydroxyalkanoates accumulating *Vibrio* sp. strain BTTC26 from marine sediments and its production kinetics. *J Sci Ind Res* **72**, 228–235.
- Sun, W., Cao, J.G., Teng, K. and Meighen, E.A. (1994) Biosynthesis of poly-3-hydroxybutyrate in the luminescent bacterium, *Vibrio harveyi*, and regulation by the lux autoinducer, N-(3- hydroxybutanoyl) homoserine lactone. *J Biol Chem* **269**, 20785–20790.
- Suwannasing, W., Imai, T. and Kaewkannetra, P. (2015) Cost-effective defined medium for the production of polyhydroxyalkanoates using agricultural raw materials. *Bioresour Technol* **194**, 67–74.
- Tamura, K., Stecher, G., Peterson, D., Filipski, A. and Kumar, S. (2013) MEGA6: molecular evolutionary genetics analysis version 6.0. *Mol Biol Evol* **30**, 2725–2729.
- Tokiwa, Y., Calabia, B.P., Ugwu, C.U. and Aiba, S. (2009) Biodegradability of plastics. *Int J Mol Sci* **10**, 3722–3742.
- Valentino, F., Morgan-Sagastume, F., Fraraccio, S., Corsi, G., Zanolli, G., Werker, A. and Majone, M. (2015) Sludge minimization in municipal wastewater treatment by polyhydroxyalkanoate (PHA) production. *Environ Sci Pollut Res Int* **22**, 7281–7294.
- Wei, Y.H., Chen, W.C., Wu, H.S. and Janarthanan, O.M. (2011) Biodegradable and biocompatible biomaterial, polyhydroxybutyrate, produced by an indigenous *Vibrio* sp. BM-1 isolated from marine environment. *Mar Drugs* **9**, 615–624.
- Yamane, T., Fukunaga, M. and Lee, Y.W. (1996) Increased PHB productivity by high-cell-density fed-batch culture of *Alcaligenes latus*, a growth-associated PHB producer. *Biotechnol Bioeng* **50**, 197–202.



Contents lists available at ScienceDirect

International Journal of Biological Macromolecules

journal homepage: <http://www.elsevier.com/locate/ijbiomac>

Biosynthesis and characterization of polyhydroxyalkanoate from marine *Bacillus cereus* MCCB 281 utilizing glycerol as carbon source

Sowmya P. Mohandas^a, Linu Balan^a, Jayanath G.^b, Anoop B.S.^a, Rosamma Philip^b, Sherine Sonia Cubelio^c, I.S. Bright Singh^{a,*}

^a National Centre for Aquatic Animal Health, Cochin University of Science and Technology, Fine Arts Avenue, Kochi, Kerala, India

^b Dept. of Marine Biology, Microbiology and Biochemistry, Cochin University of Science and Technology, Fine Arts Avenue, Kochi, Kerala, India

^c Centre for Marine Living Resources and Ecology, Kakkanad, Kochi, Kerala, India

ARTICLE INFO

Article history:

Received 9 April 2018

Received in revised form 11 July 2018

Accepted 11 July 2018

Available online 17 July 2018

Keywords:

Polyhydroxyalkanoates

Glycerol

Bacillus

Marine

Optimization

ABSTRACT

Polyhydroxyalkanoates (PHAs) are aliphatic polyesters produced by bacteria from renewable resources which serve as a substitute of synthetic plastics. In the present study isolation, screening, identification of PHA producing bacteria from marine water samples and optimization of process variables for increased PHA production were accomplished. The potent isolate identified as *Bacillus cereus* MCCB 281 synthesized PHA co-polymer with 13 mol % 3-hydroxyvalerate in presence of glycerol. Process parameters optimized using central composite design for enhanced PHA production showed 1.5 fold higher PHA yield. Cell dry weight of $3.72 \pm 0.04 \text{ g L}^{-1}$, PHA yield $2.54 \pm 0.07 \text{ g L}^{-1}$ and PHA content of $68.27 \pm 1.2\%$ (w/w) was achieved in fermenter at the optimized conditions. Purified polymer was characterized by Fourier-transform infrared spectroscopy, Nuclear magnetic resonance spectroscopy, Gas chromatography–Mass spectrometry, X-ray powder diffraction techniques and molecular weight of PHA was found to be $2.56 \times 10^5 \text{ Da}$. PHA nanoparticles with average particle size 179 nm were synthesized for medical applications and biocompatibility analysis was performed with L929 mouse fibroblast cell line. This is the first report of a moderately halophilic *B. cereus*, which utilizes glycerol as the sole carbon source for PHA co-polymer production.

© 2018 Elsevier B.V. All rights reserved.

1. Introduction

Polyhydroxyalkanoates (PHAs) are bio-based polymers synthesized by a wide variety of Gram positive and Gram negative bacteria as carbon storage inclusions under unfavorable growth conditions [1]. Over 150 different types of hydroxyalkanoic acid (HA) monomers have been identified as constituents of PHA synthesized by various microorganisms [2]. The simplest and best characterized PHA, polyhydroxybutyrate (PHB) is a homopolymer of 3-hydroxybutyrate (3-HB) units accumulated by several bacterial species such as *Bacillus megaterium*, *Cupriavidis necator*, *Alcaligenes latus*, and recombinant *Escherichia coli* [3]. The unfavorable properties of PHB such as high crystallinity, stiffness and brittleness can be overcome by incorporating different monomeric units such as 3-hydroxyvalerate (3-HV) and 4-hydroxybutyrate (4-HB) [4] which refine the material properties, thereby increasing their commercial potential. Most bacteria require the addition of precursors such as propionic acid or valeric acid for the synthesis of poly(3-hydroxybutyrate-co-3-hydroxyvalerate) [P (3-HB-co-3-HV)] co-

polymers. PHAs are thermoplastic polyesters that exhibit properties similar to petroleum-derived polypropylene [5]. As these polymers can be produced from renewable resources, PHAs are sustainable and carbon neutral. Owing to their biodegradable, biocompatible, non-toxic and hydrophobic properties, PHAs are attractive base materials for wide range of medical, pharmaceutical and industrial applications.

The main obstacle for the growth of PHA based industries is the high cost of carbon source required for PHA production accounting 70 to 80% of total raw material cost [6]. The cost of PHA production can be significantly reduced by utilization of renewable and inexpensive carbon resources such as agricultural residues [7–9] and industrial wastes [10] for microbial fermentation. Glycerol, a by-product of biodiesel industry has now become an attractive feedstock for PHA production using pure cultures as well as mixed microbial consortia [11–13]. In spite of the commercial use of glycerol in food and beverages, pharmaceuticals, cosmetics, personal care and other industries, it is expensive to refine crude glycerol to the purity needed for these applications [14]. Therefore, the development of sustainable processes for utilization of this by-product is all the more desirable to promote the growing biodiesel industry in a larger scale [15]. In addition, glycerol is regarded as a favorable substrate for PHA production, as carbon atoms in glycerol are in a highly reduced state compared to other carbohydrates, thereby stimulating

* Corresponding author at: UGC BSR Faculty, National Centre for Aquatic Animal Health, Cochin University of Science and Technology, Kochi 682016, India.
E-mail address: isbsingh@gmail.com (I.S. Bright Singh).

intracellular polymer synthesis in bacteria [16]. Hence, valorization of glycerol through PHA production will be a good strategy to recycle the industrial by-product to synthesize valuable bio-products.

Another important aspect of focus in this study is the process optimization of fermentation to enhance PHA yield. The statistical design of experiment (DoE) based approach using response surface methodology (RSM) provides more systematic data prediction and validation for numerous fermentation processes. Central Composite Design (CCD) is the most popular statistical design employed to study the interactive effect of various parameters for the optimization of PHA production using different microorganisms. Different media components such as nitrogen sources, carbon sources and physical factors such as pH, temperature and agitation which play significant roles in PHA accumulation were optimized using CCD [17, 18].

Marine environment, a rich source of microbial diversity remains quite neglected towards several developing industrial processes in equivalence to the terrestrial counter parts [19]. Marine bacteria are a potential source of polymer production as they synthesize different types of PHAs due to wide variations in nutrient availability that exists in the marine environment [20]. Additionally, marine bacteria can utilize sterilized sea water as culture medium instead of mineral medium, which can reduce the cost of PHA production [21]. Marine bacteria such as *Vibrio* sp., *Bacillus* sp. and *Halomonas* sp. have been identified as potent PHA producers using various carbon sources [19, 22, 23]. The present study focuses on the production and optimization of polyhydroxyalkanoate in *B. cereus* MCCB 281 utilizing glycerol as the sole carbon source. The purified polymer has been characterized by Fourier-transform infrared spectroscopy (FTIR), Nuclear magnetic resonance spectroscopy (NMR), Gas chromatography–Mass spectrometry (GC–MS), X-ray powder diffraction (XRD) and Gel permeation chromatography (GPC) techniques. PHA nanoparticles were synthesized using purified polymer and biocompatibility was investigated for medical applications.

2. Materials and methods

2.1. Isolation and screening of PHA producing bacteria

Water samples were collected onboard FORV Sagar Sampada (Cruise No.321) from 16 stations along the south west coast of India (Latitudes: 7°05'03"N to 9°58'26"N and Longitudes: 76°00'39"E to 75°35'21"E) (Supplementary Table 1) and serially diluted in sterile sea water, spread on ZoBell's marine agar 2216 E plates (HiMedia, India) and incubated at 28 °C for 7 days. Morphologically distinct colonies were sub-cultured on ZoBell's marine agar plates supplemented with 2% (w/v) glucose and 0.5 µg mL⁻¹ Nile red dye. The plates were incubated at 28 °C for 48 h to determine PHA accumulation [24]. The bacterial isolates were also stained with Nile red dye and examined under fluorescence microscope (Olympus, Japan) to detect the presence of PHA granules inside the cells [25]. Glycerol stocks of all the selected isolates were stored at –80 °C.

2.2. 16S rRNA gene sequencing and phylogenetic tree

The potent PHA producing isolate was identified based on biochemical characteristics and 16S rRNA gene sequencing. The biochemical characteristics studied included Gram staining, spore staining, catalase test, oxidase test, nitrate reduction test, hydrolysis of starch, gelatin, xylan and acid production from various sugars. The isolation of genomic DNA was done according to Cheng and Jiang [26] and the partial 16S rRNA gene was amplified by PCR using universal primers 27 F 5'-GAG TTT GAT CCT GGC TCA-3' and 1492R (5'-ACG GCT ACC TTG TTA CGA CTT-3'). PCR was performed with an initial denaturation at 94 °C for 3 min followed by 29 cycles of denaturation at 94 °C for 30 s, annealing at 58 °C for 40 s, extension at 72 °C for 1 min and final extension at 72 °C for 5 min.

The polyhydroxyalkanoate synthase (*phaC*) gene of the potent isolate was also amplified using gene specific primers (forward 5'-GGG AAA AGC AAT TAG AGC TAT ACC C-3' and reverse 5'-TCT ACC TTT TGT CCG CGA ATA AC-3'). PCR was performed with an initial denaturation at 95 °C for 3 min followed by 35 cycles of denaturation at 95 °C for 30 s, annealing at 60 °C for 40 s, extension at 72 °C for 1 min and final extension at 72 °C for 5 min. The amplified products were sequenced at SciGenom Labs, Cochin, Kerala. The partial forward and reverse sequences of the amplified products were aligned using software GeneTool and homology search was performed in NCBI database using Blast tool. The nucleotide sequences were deposited in GenBank and accession numbers were obtained. Phylogenetic tree was constructed using the neighbor-joining method [27] with bootstrap value of 1000 replicates [28] in MEGA 6.0 software [29].

2.3. PHA production and quantification

For PHA production, inoculum was prepared by growing the isolates in ZoBell's marine agar slants for 16 h, 28 °C. Aliquot of 2 mL sterile production medium was added to the slant; cells dislodged using sterile inoculation loop and aseptically transferred to another tube. Cell density was measured using UV-visible spectrophotometer (Shimadzu, Japan) at 600 nm and the absorbance adjusted to 1.0 prior to inoculation. Production medium (composition: Peptone- 5 g L⁻¹, Yeast extract- 1 g L⁻¹) was prepared in sea water and pH was adjusted to 7.5. Inoculum (1% v/v) was added to 100 mL production medium and incubated for 48 h at 28 °C, 200 rpm. Cell growth was monitored every 12 h by measuring optical density at 600 nm.

To determine the cell dry weight (CDW) and PHA content, 10 mL culture was centrifuged at 10000g for 10 min, cell pellet was rinsed twice with distilled water and transferred to pre-weighed tube and lyophilized. To the lyophilized cell biomass, 1 mL concentrated sulphuric acid was added and incubated for 15 min at 100 °C in a boiling water bath. The polymer was converted into crotonic acid which turned into brown colour after the addition of sulphuric acid. The absorbance of crotonic acid was measured at 235 nm using UV-visible spectrophotometer and the PHA content was estimated based on CDW with crotonic acid as standard [30].

2.4. Transmission electron microscopy (TEM)

Harvested cells were washed with 0.1 M sodium cacodylate buffer (pH 7.0), treated with 2.5% glutaraldehyde overnight at 4 °C and post fixed with 2% osmium tetroxide for 2–4 h at 4 °C. It was again washed with the buffer, dehydrated with a graded series of acetone and embedded in epoxy resin. The embedded specimen was cut into ultrathin sections and stained with uranyl acetate and lead citrate. TEM observations were performed using a TECNAI 200 TEM (FEI; Electron Optics, USA) at All India Institute of Medical Sciences (AIIMS), New Delhi.

2.5. Effect of initial pH, temperature and substrates on PHA production

PHA production of the potent isolate was carried out in the presence of different pH (6.0–9.0), temperature (25–40 °C) and carbon sources (glucose, glycerol, sucrose, xylose, lactose, fructose, sodium acetate) by one-variable-at-a-time approach keeping other parameters constant. Different carbon sources (final concentration 2%) were prepared in sea water, sterilized separately and added to the production medium at the time of inoculation. To evaluate the effect of precursor on PHA production, different concentrations of propionic acid (0.1, 0.5, 1 and 2% v/v) were added to the production medium. Fermentation was carried out in 100 mL production medium with 1% (v/v) inoculum and incubated for 48 h at 200 rpm. CDW and PHA content were estimated. For all the experiments, optical density of the inoculum was adjusted to 1.0 at 600 nm corresponding to 10⁸ CFU mL⁻¹.

2.6. Statistical optimization of PHA production using response surface methodology

Design of experiment (DoE) approach was used for optimization of process variables for PHA production using the software Design-Expert version 10.0.7 (Stat-Ease Inc., Minneapolis, USA). Plackett-Burman design was selected to identify the process variables which influence PHA production. A total of five variables were selected, which were sodium chloride (10–30 g L⁻¹), glycerol (2–4% v/v), inoculum size (4–8% v/v), yeast extract (1–3 g L⁻¹), and incubation time (24–48 h). These variables were evaluated in twelve experimental runs with CDW (g L⁻¹) and PHA yield (g L⁻¹) as the responses. The experiments were carried out in triplicate. The interactive effects of the significant variables that affect PHA production were analyzed using response surface central composite design. A set of 30 experiments in triplicate was designed to study the influence of four selected variables, i.e. sodium chloride, glycerol, inoculum size and incubation time on the responses CDW (g L⁻¹) and PHA yield (g L⁻¹). Each variable was examined at five different levels ($-\alpha$, -1 , 0 , $+1$, $+\alpha$) as shown in Table 1. The responses were analyzed using second order polynomial equation and the results were fitted into the equation by multiple regression analysis. Three-dimensional surface plots were used to analyze the interaction of different process variables. Statistical analysis of the model was done for evaluation of analysis of variance (ANOVA). For validation of the model, experiments were conducted with the optimized values for each variable given by point prediction method to corroborate the predicted value and the observed value for polymer production.

2.7. Fermenter level production

Batch fermentation was carried out in 5 L fermenter (B-Lite, Sartorius, Germany) with 3 L working volume. The production medium was added to the fermenter, pH was adjusted to 7.0 and medium was sterilized in situ. The pH and temperature were maintained at 7.0 and 30 °C respectively throughout the process. Agitation was kept at 250 rpm and aeration was set at 2.0 L air/min. All the process parameters were maintained at the optimum conditions obtained from the CCD design. Samples were withdrawn every 3 h to determine CDW and PHA yield.

2.8. PHA extraction

For the polymer extraction, equal volume of chloroform and sodium hypochlorite solution (4% available chlorine) was added to the lyophilized cell pellet, incubated for 1 h at 30 °C, 200 rpm and the mixture was centrifuged at 8000g for 10 min. The lower chloroform phase was collected and PHA was precipitated by addition of 10 volumes of 70% (v/v) ice cold methanol. The precipitated PHA was filtered and dried at 70 °C overnight [31].

2.9. PHA characterization

2.9.1. FTIR

Purified polymer (2 mg) was ground with potassium bromide crystals to form a pellet. FTIR spectrum was recorded between 4000 and

400 cm⁻¹ using Nicolet Avatar 370 spectrometer (Thermo Scientific, USA). The spectrum obtained was compared with commercially available [P (3-HB-co-3-HV)] (12 mol% 3-HV) (Sigma, USA).

2.9.2. XRD

X-ray diffraction analysis of PHA was carried out with D8 Advance diffractometer (Bruker, Germany) using Cu radiation (wavelength 1.5406 Å) in the range of $2\theta = 3$ –70°. The operating mode of the instrument was 40 kV and 40 mA.

2.9.3. GC-MS

The polymer (100 mg) was dissolved in 2 mL chloroform, mixed with 2 mL acidified methanol containing 3% (v/v) conc. H₂SO₄ and incubated at 100 °C for 120 min for methanolysis. The mixture was then cooled to room temperature, 1 mL distilled water was added, shaken vigorously for 10 min and centrifuged at 2000g for 5 min [32]. The organic layer with methyl esters was analyzed by GC-MS using the Agilent 7890A GC/5975 MSD system equipped with a HP-5 column (Agilent, USA).

2.9.4. NMR

¹H and ¹³C NMR of the extracted polymer and commercial [P (3-HB-co-3-HV)] (12 mol% 3-HV) were analyzed on Bruker Avance III spectrometer operated at 400 MHz at 25 °C. About 10 mg of sample was dissolved in deuterated chloroform and the spectra were recorded.

All the above analysis was carried out at the Sophisticated Test and Instrumentation Centre (STIC), Kerala.

2.9.5. GPC

Number-average molecular weight (M_n), weight-average molecular weight (M_w) and poly dispersion index (PDI) of polymer were determined by GPC using Waters HPLC/GPC system with 600 Series Pump and Waters Styragel HR series HR5E/4E/2/0.5 column equipped with a 7725 Rheodyne injector and refractive index 2414 detector (Waters Corporation, USA). A quantity of 1 mg PHA was completely dissolved in 1 mL chloroform and filtered through 0.2 µm PVDF membranes. The injection volume was 20 µL. The mobile phase was chloroform at a flow rate of 1.0 mL min⁻¹. Polystyrene standards of molecular weight 1,865,000, 100,000, 9130 were used for relative calibration. The analysis was performed at Sree Chitra Tirunal Institute for Medical Sciences and Technology, Trivandrum, Kerala.

2.10. Nanoparticle synthesis and characterization

PHA nanoparticles were synthesized by oil-in-water emulsion method. In brief, 10 mg polymer was dissolved in 2 mL dichloromethane at 70 °C. Polyvinyl alcohol (PVA, mol. wt 9000–10,000, Sigma, USA) solution (4 mL of 3% w/v) was added to the above and sonicated for 10 min at 40% amplitude for 5 s ON and 9 s OFF kept in ice. The emulsion was diluted with PVA solution (50 mL, 0.1% w/v) and kept for solvent evaporation overnight in a magnetic stirrer [33]. Nanoparticles were separated by centrifugation at 15000g for 35 min at room temperature and lyophilized. Characterization of nanoparticles was done by Dynamic Light Scattering using Nano partica SZ-100 (Horiba Scientific, Japan) and TEM.

2.11. In vitro biocompatibility studies

L929 mouse fibroblast cell line obtained from National Centre for Cell Science, Pune was maintained in Minimum Essential Medium (MEM) supplemented with 10% fetal bovine serum, 2 mM L-glutamine, 100 U mL⁻¹ penicillin and 100 µg mL⁻¹ streptomycin (HiMedia, India). The cells were incubated at 37 °C in an atmosphere of 5% CO₂. The MTT assay was used to evaluate cytotoxicity of the PHA nanoparticles, where yellow coloured salt of MTT [3-(4, 5-Dimethylthiazol-2-yl)-2,5-diphenyl tetrazolium bromide] was

Table 1
Range of independent variables selected for the response surface central composite design for PHA production.

| Variables | Symbol | Units | Levels of variables | | | | |
|-----------------|--------|-------------------|---------------------|------|-----|------|-----------|
| | | | $-\alpha$ | -1 | 0 | $+1$ | $+\alpha$ |
| Sodium chloride | A | g L ⁻¹ | 8 | 9 | 10 | 11 | 12 |
| Glycerol | B | % v/v | 3 | 3.5 | 4 | 4.5 | 5 |
| Inoculum size | C | % v/v | 7 | 7.5 | 8 | 8.5 | 9 |
| Incubation time | D | h | 20 | 22 | 24 | 26 | 28 |

Table 2
16S rRNA gene identification of different bacterial isolates and their PHA production based on cell dry weight.

| Sl. no | Name of isolates | % similarity from NCBI database | PHA content based on CDW (% w/w) | GenBank accession number |
|--------|---------------------------------------|---------------------------------|----------------------------------|--------------------------|
| 1 | <i>Bacillus cereus</i> MCCB 281 | 99 | 60.33 ± 1.2 | KR921920 |
| 2 | <i>Erythrobacter citreus</i> MCCB 277 | 99 | 58.13 ± 1.4 | KR921916 |
| 3 | <i>Halomonas meridiana</i> MCCB 282 | 99 | 57.23 ± 2.5 | KR921921 |
| 4 | <i>Gordonia bronchialis</i> MCCB 280 | 99 | 56.45 ± 2.1 | KR921919 |
| 5 | <i>Bacillus cereus</i> MCCB 279 | 100 | 55.35 ± 1.6 | KR921918 |
| 6 | <i>Alteromonas macleodii</i> MLCB 2/8 | 99 | 54.28 ± 1.5 | KR921917 |

reduced to purple coloured formazan by mitochondrial dehydrogenases. For the MTT assay, cells were trypsinized, counted using a hemocytometer and seeded in 96 well tissue culture plate (CellStar Grenier Bio-One, USA) with a cell density of 1×10^3 cells/well and incubated for 24 h. Five different concentrations of the nanoparticles (0.1, 0.3, 0.5, 0.7, and 1 mg mL⁻¹) were prepared in the culture medium, 100 µL of each concentration was added to the wells and incubated for 24 h. Cells devoid of nanoparticles served as negative control. After incubation, 100 µL MTT solution (5 mg mL⁻¹) was added to each well and incubated for 4 h at 37 °C to form formazan crystals. Subsequently, 100 µL dimethyl sulfoxide was added and incubated at 37 °C for 30 min to dissolve the formazan crystals. The optical density was measured at 570 nm using microplate reader (TECAN Infinite M 200, Austria). Cytotoxicity tests were performed in triplicate. The percentage cell survival rate was calculated as difference between the absorbance of the tests and that of the control $\times 100$. Data were expressed as mean \pm standard deviation.

3. Results and discussion

3.1. Isolation, identification and phylogenetic analysis

A total of 30 marine bacterial isolates were obtained from various stations along the south west coast of India with PHA accumulation in the presence of glucose. These isolates showed orange fluorescence when exposed to UV light after 48 h incubation in ZoBell's marine agar with Nile red dye, and glucose as the carbon source. The isolate that showed highest PHA accumulation based on cell dry weight was

identified as *Bacillus cereus*, based on biochemical characteristics and 16S rRNA gene sequencing and coded as MCCB 281. The isolate was characterized as Gram positive, rod shaped, spore forming bacterium capable of hydrolyzing starch, gelatin and xylan. MCCB 281 was positive for catalase, oxidase, nitrate reduction tests and showed acid production from glucose, sucrose, fructose, maltose, trehalose and glycerol. Growth was observed over a wide range of pH (5–9), temperature (10–40 °C) and sodium chloride (0.5–10% w/v). PHA produced by *Bacillus* sp. are better sources for various biomedical applications, as Gram positive bacteria lack pyrogenic lipopolysaccharide (LPS) endotoxin which can cause immunogenic responses [34, 35]. The results of 16S rRNA gene identification of bacterial isolates, PHA production based on CDW along with their GenBank accession numbers are provided in Table 2.

The *phaC* synthase gene of MCCB 281 was amplified using gene specific primers and partial gene sequence of 751 bp was deposited in GenBank under the accession number KX463674. The deduced amino acid sequence showed 99% homology to *phaC* gene of *B. cereus* FC11 and *B. cereus* SPV using Blastp search in NCBI. The partial sequence was translated using ExPASy tool and the open-reading frame (ORF) of *phaC* synthase was identified with the ORF Finder tool. Phylogenetic tree of the synthase gene was constructed using MEGA 6 software which showed closest match with *B. cereus* PHA synthase (AD187591) (Fig. 1). The *phaC* gene of MCCB 281 encoded for class IV polyhydroxyalkanoate synthase which prefer Co-enzymeA thioesters of (R)-3-hydroxy fatty acids constituting 3 to 5 carbon atoms (short chain length hydroxyalkanoates). *Bacillus* spp. that synthesized PHAs possess class IV synthase that comprise *phaC* and its *phaR* subunits. The *phaC* subunit of class IV synthase resembles class III synthases, but

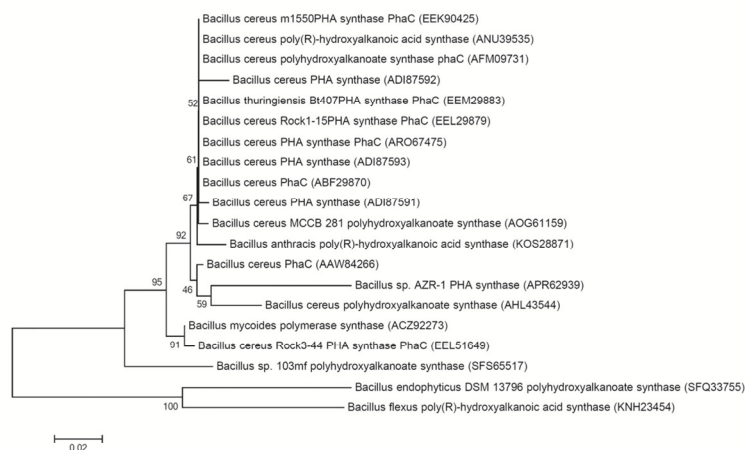


Fig. 1. Phylogenetic tree of *phaC* synthase gene of *B. cereus* MCCB 281 with its closely related species based on amino acid sequences from GenBank. Bootstrap values are denoted at the nodes.

phaR is replaced by phaE subunit [34]. The amino acid Cys₁₂₃ of phaC synthase of MCCB 281 marked the putative lipase box region (G-X-C₁₂₃-X-G) which was highly conserved in all PHA synthases and was involved in the covalent catalysis.

3.2. PHA production

PHA production of *B. cereus* MCCB 281 was investigated in presence of 2% w/v glucose as carbon source and the culture was incubated for 48 h at 28 °C, 200 rpm. Samples were withdrawn every 6 h to determine CDW and PHA yield. The PHA accumulation commenced at the early phase of growth of 6 h (18% w/w), reached 58% (w/w) with a CDW of $2 \pm 0.07 \text{ g L}^{-1}$ and PHA yield of $1.16 \pm 0.06 \text{ g L}^{-1}$ at 24 h. Thereafter, a steady state in PHA production was observed till 48 h (data not shown). The generation time (t_g) and specific growth rate (μ) of MCCB 281 was found to be 0.6 h and 1.15 h^{-1} respectively. In our previous study, PHA production of a moderately halophilic isolate *Vibrio harveyi* MCCB 284 showed PHA yield of 0.8 g L^{-1} with a CDW of 1.34 g L^{-1} in presence of glucose as carbon source [19]. Similarly, PHA yield of 2.02 g L^{-1} and CDW of 2.77 g L^{-1} was observed in a halotolerant *Bacillus* sp. MG12 using glucose after 48 h incubation [22].

3.3. TEM

TEM analysis showed the presence of PHA granules in *B. cereus* MCCB 281 grown in ZoBell's marine broth containing 2% w/v glucose for 48 h (Fig. 2). The cells contained PHA granules that varied in size and number.

3.4. Effect of initial pH, temperature and substrates on PHA production

The effect of initial pH, temperature and substrates on PHA production of moderate halophile *B. cereus* MCCB 281 was investigated using one-variable-at-a-time approach in shake flask. The maximum CDW of $2.04 \pm 0.04 \text{ g L}^{-1}$ and PHA content of $60.41 \pm 2\%$ (w/w) were recorded at pH 7.0 (Fig. 3a). The production declined at low pH compared to alkaline pH, where the production was stable. The effect of different incubation temperatures on PHA synthesis showed highest percentage of PHA content $61.23 \pm 1.3\%$ (w/w) and CDW of $2.21 \pm 0.1 \text{ g L}^{-1}$ at the optimum temperature 30 °C. Also, the isolate showed considerable growth and PHA yield at 35 °C and 40 °C; however no growth was noticed at 45 °C (Fig. 3b). These findings were in agreement with the previous report on PHA production from *B. cereus* FA11 [36].

The study of different carbon sources on PHA production showed maximum yield in the presence of glucose and glycerol as the sole carbon sources. However, CDW of $2.33 \pm 0.11 \text{ g L}^{-1}$ and PHA content of $62.23 \pm 1.42\%$ (w/w) were obtained exclusively in the presence of 2%

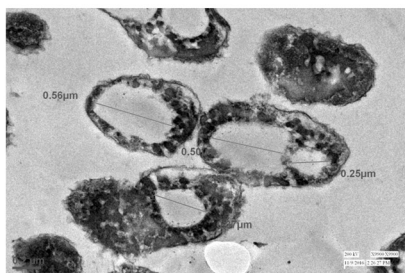


Fig. 2. Transmission electron micrograph of PHA granules inside the cells of *B. cereus* MCCB 281.

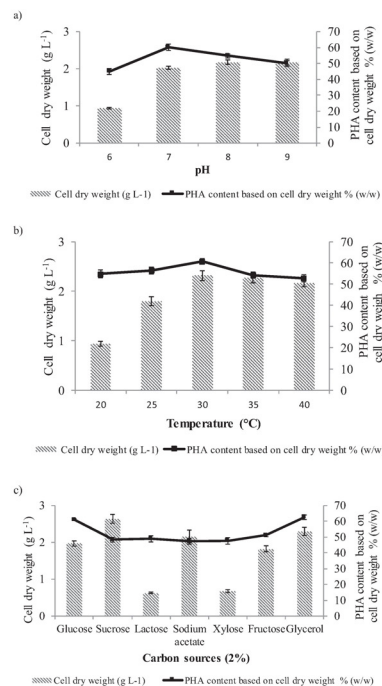


Fig. 3. Effect of (a) pH (b) temperature and (c) carbon sources on PHA production in *B. cereus* MCCB 281.

glycerol as the sole carbon source, even though good growth was favored by sucrose, fructose and sodium acetate (Fig. 3c) as well. It was notable that the isolate (MCCB 281) could synthesize PHA co-polymer with 3-HV units in presence of glucose, glycerol, sucrose and fructose as the sole carbon sources. *Bacillus* spp. has the ability to utilize different ligno-cellulosic bio wastes as well as pure sugars such as glucose for efficient production of PHA homo- and co-polymers along with hydrogen which in turn improves the efficiency, sustainability and economics of the process [37–40]. This heterogeneity of PHAs in the genus *Bacillus* was speculated to be due to PHA synthase which has relatively broad monomer specificity [34]. With *B. thuringiensis* EGU45, PHA production using different hydrolyzed bio wastes supplemented with glycerol demonstrated co-polymer accumulation with enhanced 3-HV content [41]. PHA production using glycerol as carbon source in *B. megaterium* also showed 10–20% lower production cost compared with glucose [12]. PHA yield from the isolate MCCB 281 utilizing glycerol was

Table 3
Effect of different concentrations of propionic acid on PHA production.

| Propionic acid (% v/v) | CDW (g L ⁻¹) | PHA content (% w/w) | 3-HB (%) | 3-HV (%) |
|------------------------|--------------------------|---------------------|----------|----------|
| 0.1 | 2.22 ± 0.05 | 55.26 ± 1.8 | 88 | 12 |
| 0.5 | 2.08 ± 0.08 | 52.55 ± 1.3 | 80 | 20 |
| 1.0 | 1.56 ± 0.12 | 50.36 ± 2.5 | 70 | 30 |
| 2.0 | 0.93 ± 0.07 | 45.17 ± 1.2 | 70 | 30 |

Data shown as mean ± SD (n = 3).

Table 4
Results of the experimental Plackett and Burman design for PHA production from *B. cereus* MCCB 281.

| Run no. | Experimental variables ^a | | | | | Response | |
|---------|-------------------------------------|-----------|-----------|------------------------|-------|--------------------------|--------------------------------|
| | A (g L ⁻¹) | B (% v/v) | C (% v/v) | D (g L ⁻¹) | E (h) | CDW (g L ⁻¹) | PHA yield (g L ⁻¹) |
| 1 | 10 | 4 | 8 | 1 | 24 | 3.25 | 2.10 |
| 2 | 10 | 4 | 8 | 3 | 24 | 2.82 | 1.80 |
| 3 | 10 | 4 | 4 | 1 | 48 | 2.75 | 1.69 |
| 4 | 30 | 4 | 8 | 1 | 48 | 2.13 | 1.10 |
| 5 | 30 | 2 | 8 | 1 | 48 | 2.47 | 1.31 |
| 6 | 10 | 2 | 4 | 3 | 48 | 2.87 | 1.26 |
| 7 | 30 | 2 | 8 | 3 | 24 | 2.86 | 1.69 |
| 8 | 10 | 2 | 8 | 3 | 48 | 2.87 | 1.62 |
| 9 | 10 | 2 | 4 | 1 | 24 | 3.36 | 1.28 |
| 10 | 30 | 4 | 4 | 3 | 48 | 2.30 | 1.16 |
| 11 | 30 | 2 | 4 | 1 | 24 | 3.07 | 1.60 |
| 12 | 30 | 4 | 4 | 3 | 24 | 3.10 | 1.74 |

^a A: Sodium chloride, B: Glycerol, C: Inoculum size, D: Yeast extract, E: Incubation Time.

comparable with previous reports from other *Bacillus* sp. [13, 22]. Therefore, considering the ability of MCCB 281 to utilize less expensive carbon source glycerol for efficient co-polymer production, it was chosen specifically as the carbon source of choice for PHA optimization studies. It has to be pointed out that, there are reports of a few *Bacillus* sp. having the capability to utilize crude glycerol for PHA production [13, 42].

To examine the influence of precursor propionic acid (PA) on PHA production of MCCB 281, different concentrations of PA were added after 12 h incubation. Addition of propionate was effective in increasing the 3-HV content, and addition of both 1% and 2% v/v PA resulted in 30 mol% 3-HV content increases (Table 3). Even though, there was an increase in valerate content on addition of the precursor, PHA yield was considerably low on co-feeding with propionic acid; probably due to the toxic effect of the volatile fatty acid on the organism. Similar result

Table 5
Results of central composite design for PHA production from *B. cereus* MCCB 281.

| Run no. | Experimental variables ^a | | | | Response | |
|---------|-------------------------------------|-----------|-----------|-------|--------------------------|--------------------------------|
| | A (g L ⁻¹) | B (% v/v) | C (% v/v) | D (h) | CDW (g L ⁻¹) | PHA yield (g L ⁻¹) |
| 1 | 9 | 4.5 | 8.5 | 22 | 3.30 | 1.94 |
| 2 | 9 | 4.5 | 7.5 | 26 | 3.38 | 1.80 |
| 3 | 11 | 3.5 | 7.5 | 22 | 3.00 | 1.80 |
| 4 | 9 | 3.5 | 7.5 | 26 | 3.39 | 1.69 |
| 5 | 10 | 4.0 | 8.0 | 24 | 3.20 | 2.16 |
| 6 | 11 | 3.5 | 8.5 | 26 | 3.07 | 1.87 |
| 7 | 10 | 4.0 | 7.0 | 24 | 3.20 | 1.80 |
| 8 | 10 | 4.0 | 8.0 | 20 | 3.30 | 2.08 |
| 9 | 10 | 4.0 | 8.0 | 24 | 3.21 | 2.14 |
| 10 | 11 | 3.5 | 7.5 | 26 | 3.10 | 1.70 |
| 11 | 12 | 4.0 | 8.0 | 24 | 3.20 | 1.89 |
| 12 | 10 | 5.0 | 8.0 | 24 | 3.13 | 1.85 |
| 13 | 10 | 4.0 | 8.0 | 28 | 3.27 | 1.79 |
| 14 | 9 | 3.5 | 8.5 | 26 | 3.30 | 1.89 |
| 15 | 10 | 3.0 | 8.0 | 24 | 3.08 | 1.79 |
| 16 | 11 | 4.5 | 8.5 | 26 | 3.10 | 1.80 |
| 17 | 11 | 4.5 | 7.5 | 26 | 3.30 | 1.80 |
| 18 | 8 | 4.0 | 8.0 | 24 | 3.30 | 1.80 |
| 19 | 11 | 4.5 | 8.5 | 22 | 3.40 | 1.92 |
| 20 | 10 | 4.0 | 8.0 | 24 | 3.21 | 2.15 |
| 21 | 10 | 4.0 | 8.0 | 24 | 3.21 | 2.10 |
| 22 | 10 | 4.0 | 8.0 | 24 | 3.23 | 2.14 |
| 23 | 9 | 3.5 | 7.5 | 22 | 3.10 | 1.82 |
| 24 | 11 | 3.5 | 8.5 | 22 | 3.40 | 1.94 |
| 25 | 9 | 3.5 | 8.5 | 22 | 3.40 | 2.00 |
| 26 | 10 | 4.0 | 9.0 | 24 | 3.32 | 2.05 |
| 27 | 11 | 4.5 | 7.5 | 22 | 3.25 | 2.03 |
| 28 | 10 | 4.0 | 8.0 | 24 | 3.28 | 2.17 |
| 29 | 9 | 4.5 | 8.5 | 26 | 3.00 | 1.90 |
| 30 | 9 | 4.5 | 7.5 | 22 | 3.04 | 2.00 |

^a A: Sodium chloride, B: Glycerol, C: Inoculum size, D: Incubation Time.

Table 6
ANOVA for response surface model of cell dry weight from *B. cereus* MCCB 281.

| Source | SS | df | MS | F-Value | Prob > F | |
|----------------------|--------|----|--------|---------|----------|-----------------|
| Model | 0.4048 | 14 | 0.0289 | 21.01 | <0.0001 | Significant |
| A-Salt concentration | 0.0100 | 1 | 0.0100 | 7.27 | 0.0166 | |
| B-Glycerol | 0.0005 | 1 | 0.0005 | 0.3664 | 0.5540 | |
| C-Inoculum size | 0.0176 | 1 | 0.0176 | 12.79 | 0.0028 | |
| D-Incubation time | 0.0040 | 1 | 0.0040 | 2.91 | 0.1087 | |
| AB | 0.0564 | 1 | 0.0564 | 40.99 | <0.0001 | |
| AC | 0.0033 | 1 | 0.0033 | 2.40 | 0.1420 | |
| AD | 0.0315 | 1 | 0.0315 | 22.90 | 0.0002 | |
| BC | 0.0352 | 1 | 0.0352 | 25.55 | 0.0001 | |
| BD | 0.0018 | 1 | 0.0018 | 1.31 | 0.2699 | |
| CD | 0.2048 | 1 | 0.2048 | 148.79 | <0.0001 | |
| A ² | 0.0013 | 1 | 0.0013 | 0.9138 | 0.3543 | |
| B ² | 0.0238 | 1 | 0.0238 | 17.32 | 0.0008 | |
| C ² | 0.0024 | 1 | 0.0024 | 1.71 | 0.2103 | |
| D ² | 0.0066 | 1 | 0.0066 | 4.80 | 0.0446 | |
| Residual | 0.0206 | 15 | 0.0014 | | | |
| Lack of fit | 0.0156 | 10 | 0.0016 | 1.56 | 0.3245 | Not significant |
| Pure error | 0.0050 | 5 | 0.0010 | | | |
| Cor total | 0.4254 | 29 | | | | |

SS- sum of squares; df- degrees of freedom; MS- mean square; R² = 0.9515; Adjusted R² = 0.9062.

was observed by Du et al. [43] where a high propionic acid to carbon ratio resulted in lower polymer productivity. Investigations on PHA production in the presence of precursor supplementation in *B. thuringiensis* EGU45 demonstrated PHA co-polymer production with 13 mol% 3-HV content in high nitrogen containing medium having 0.5% v/v propionic acid. However, in this case increase of PA concentration up to 2% v/v resulted in the lowering of 3-HV% [13].

3.5. Statistical optimization of PHA production using response surface methodology

Statistical optimization was performed to increase the polymer yield and to find out the interaction between independent variables on PHA production. Evaluation of the results from Plackett Burman design (Table 4), showed that sodium chloride, glycerol, inoculum size and incubation time were significant for the responses. Central composite design (CCD) was used to investigate the significant interactions affecting PHA production based on the above results. CCD based optimization of four variables i.e. sodium chloride, glycerol, inoculum size and incubation period was performed for PHA production (Table 5), while other

Table 7
ANOVA for response surface model of PHA yield from *B. cereus* MCCB 281.

| Source | SS | df | MS | F-Value | Prob > F | |
|----------------------|--------|----|--------|---------|----------|-----------------|
| Model | 0.5897 | 14 | 0.0421 | 31.03 | <0.0001 | Significant |
| A-Salt concentration | 0.0018 | 1 | 0.0018 | 1.18 | 0.2942 | |
| B-Glycerol | 0.0150 | 1 | 0.0150 | 11.05 | 0.0046 | |
| C-Inoculum size | 0.0523 | 1 | 0.0523 | 38.51 | <0.0001 | |
| D-Incubation time | 0.1040 | 1 | 0.1040 | 76.64 | <0.0001 | |
| AB | 0.0052 | 1 | 0.0052 | 3.38 | 0.0859 | |
| AC | 0.0030 | 1 | 0.0030 | 2.23 | 0.1562 | |
| AD | 0.0001 | 1 | 0.0001 | 0.0737 | 0.7898 | |
| BC | 0.0361 | 1 | 0.0361 | 26.60 | <0.0001 | |
| BD | 0.0020 | 1 | 0.0020 | 1.49 | 0.2408 | |
| CD | 0.0064 | 1 | 0.0064 | 4.72 | 0.0463 | |
| A ² | 0.1612 | 1 | 0.1612 | 118.79 | <0.0001 | |
| B ² | 0.1886 | 1 | 0.1886 | 138.94 | <0.0001 | |
| C ² | 0.0881 | 1 | 0.0881 | 64.89 | <0.0001 | |
| D ² | 0.0805 | 1 | 0.0805 | 59.29 | <0.0001 | |
| Residual | 0.0204 | 15 | 0.0014 | | | |
| Lack of fit | 0.0174 | 10 | 0.0017 | 2.97 | 0.1206 | Not significant |
| Pure error | 0.0029 | 5 | 0.0006 | | | |
| Cor total | 0.6100 | 29 | | | | |

SS- sum of squares; df- degrees of freedom; MS- mean square; R² = 0.9666; Adjusted R² = 0.9355.

parameters were maintained at constant level. The statistical significance of the model was evaluated by the F-test for ANOVA to determine the goodness of fit. The results of ANOVA for cell dry weight (Table 6) and PHA yield (Table 7) showed that the model was significant ($p < 0.0001$).

The second order polynomial equation for cell dry weight in terms of coded factors is given below:

$$\begin{aligned} \text{CDW (g L}^{-1}\text{)} = & +3.22 - 0.0204 * A + 0.0046 * B + 0.0271 \\ & * C - 0.0129 * D + 0.0068 * A^2 - 0.0295 * B^2 \\ & + 0.0093 * C^2 + 0.0155 * D^2 + 0.0594 * AB \\ & + 0.0144 * AC - 0.0444 * AD - 0.0469 \\ & * BC - 0.0106 * BD - 0.1131 * CD \end{aligned} \quad (1)$$

where A = sodium chloride (w/v); B = glycerol (v/v); C = inoculum size (v/v) and D = incubation time (h). The equation in terms of coded factors can be used to make predictions about the response for given levels of each factor. The coded equation is useful for identifying the relative impact of the factors by comparing the factor coefficients.

In case of cell dry weight, the model F-value of 21.01 indicated that the model was significant. The "Lack of Fit F-value" of 1.56 implied that the Lack of Fit was not significant relative to the pure error. Non-significant lack of fit is good for the model to fit. The model was found to be highly reliable with coefficient of determination (R^2) value 0.9515 and adjusted R^2 value 0.9062. The predicted R^2 of 0.7713 is in reasonable agreement with the adjusted R^2 value. A very low value of coefficient of the variation (CV: 1.15%) demonstrated a very high degree of precision and reliability of the experimental data. The coefficient of variance (CV) is the ratio of standard error of estimate to the mean value of the response.

Regression analysis of the response demonstrated that the linear model terms (A and C), quadratic model terms (B^2 and D^2) and the interactive model terms (AB, AD, BC and CD) were significant. The linear significant variables that influenced cell dry weight were sodium

chloride (A) and inoculum size (C). The three-dimensional surface plots are graphical representations of the regression equation that depicted interaction of the process variables and identified the optimum level of each variable for maximum PHA production. The response surface plots describing the interactive effect of different process variables are presented in Fig. 4. Interactive effects of variables AB (sodium chloride and glycerol) showed positive impact on cell dry weight. Also, effects of variables AD (sodium chloride and incubation time), BC (glycerol and inoculum size) and CD (inoculum size and incubation time) showed negative interaction for the response.

The second order polynomial equation for PHA yield in terms of coded factors is given below:

$$\begin{aligned} \text{PHA yield (g L}^{-1}\text{)} = & +2.14 + 0.0020 * A + 0.0250 * B + 0.0467 \\ & * C - 0.0658 * D - 0.0767 * A^2 - 0.0829 \\ & * B^2 - 0.0567 * C^2 - 0.0542 * D^2 + 0.0010 \\ & * AB - 0.0137 * AC - 0.0025 * AD - 0.0475 \\ & * BC - 0.0112 * BD + 0.0200 * CD \end{aligned} \quad (2)$$

where A = sodium chloride (w/v); B = glycerol (v/v); C = inoculum size (v/v) and D = incubation time (h).

For PHA yield, the model F-value of 31.03 indicated that the model was significant. The "Lack of Fit F-value" of 2.97 implied that the Lack of Fit was not significant relative to the pure error. Non-significant lack of fit is good for the model to fit. The model was found to be highly reliable with coefficient of determination (R^2) value of 0.9666 and adjusted R^2 value of 0.9355. The predicted R^2 of 0.8285 is in reasonable agreement with the adjusted R^2 value. A very low value of coefficient of the variation (CV: 1.91%) again demonstrated a very high degree of precision and reliability of the experimental data. It was observed that inoculum size (C) appeared to be the most significant variable for increasing PHA production, followed by glycerol (B) and sodium chloride (A). Regression analysis of the response demonstrated that the linear model terms (B, C and D), quadratic model terms (A^2 , B^2 , C^2 and D^2)

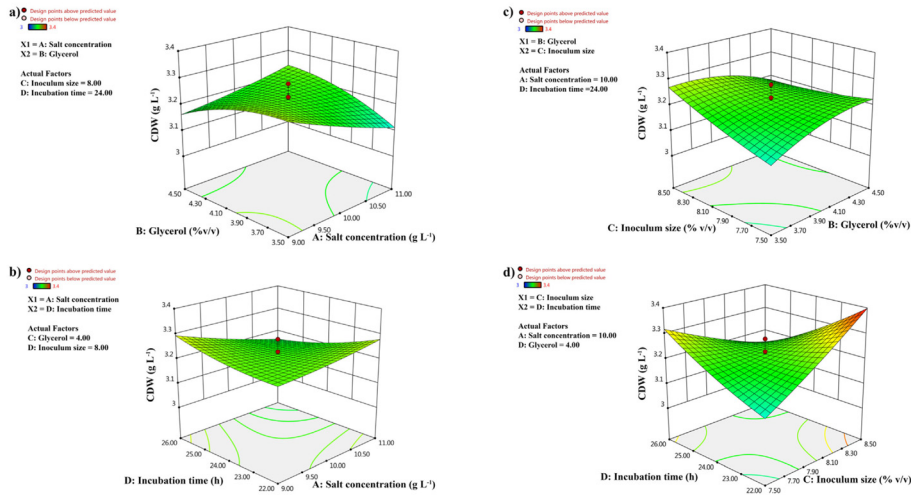


Fig. 4. Response surface 3D plots showing interactive effect of process variables for cell dry weight (a) sodium chloride and glycerol (b) sodium chloride and incubation time (c) glycerol and inoculum size (d) inoculum size and incubation time on PHA production from *B. cereus* MCB 281.

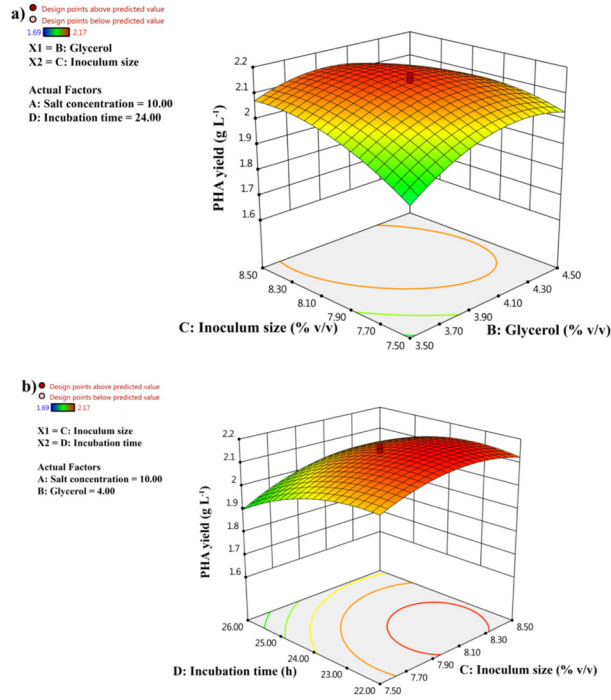


Fig. 5. Response surface 3D plots showing interactive effect of process variables for PHA yield (a) glycerol and inoculum size (b) inoculum size and incubation time on PHA production from *B. cereus* MCCB 281.

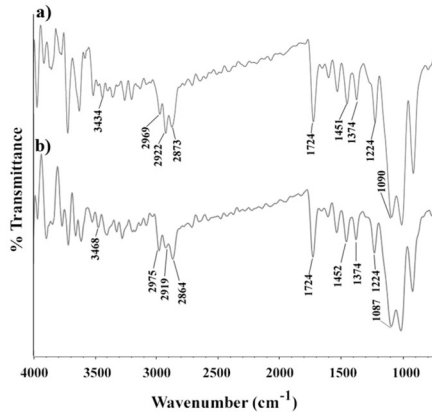


Fig. 6. FTIR spectrum of (a) purified PHA from *B. cereus* MCCB 281 (b) standard [P(3-HB-co-3-HV)] (12 mol% 3-HV).

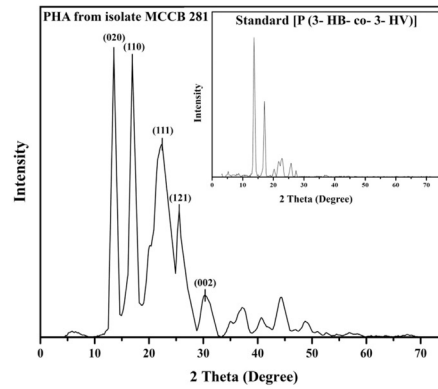


Fig. 7. X-ray diffraction pattern of PHA produced by MCCB 281 and standard [P(3-HB-co-3-HV)] (12 mol% 3-HV).

and the interactive model terms (BC and CD) were significant. The significant variables that influenced PHA yield were glycerol (B), inoculum size (C) and incubation time (D). Glycerol (B) and inoculum size (C) were found to be significant factors that positively correlated PHA production. The response surface plots describing the interactive effect of different process variables are presented in Fig. 5. It was noticed that, the interactive effect of variables BC had negative effect on PHA production. As the inoculum size (C) increased, PHA yield also increased. The increase in concentration of glycerol (B) showed an increase in PHA yield up to a certain limit after which, higher concentrations slightly reduced PHA production (Fig. 5a). A similar trend was observed in PHA production by *Pannonibacter phragmitetus*

ERC8 isolate which showed reduced polymer production at higher glycerol concentrations [44]. Moreover, glycerol concentration higher than 2% showed negative effect on PHA production in *B. firmus* NII 0830 [42]. The interactive effect of CD exhibited positive relationship on PHA yield (Fig. 5b). However, increase in incubation time (D) resulted in reduced PHA yield, whereas increase in inoculum size (C) simultaneously increased PHA yield. In an optimization study for PHA production using acid pre-treated rice straw in *B. firmus* NII 0830, high inoculum concentration (7.0–8.0%, v/v) reported maximum PHA yield [7]. Numerous studies were carried out employing central composite design for PHA optimization in different *Bacillus* spp. using agro-industrial residues [10, 18, 45].

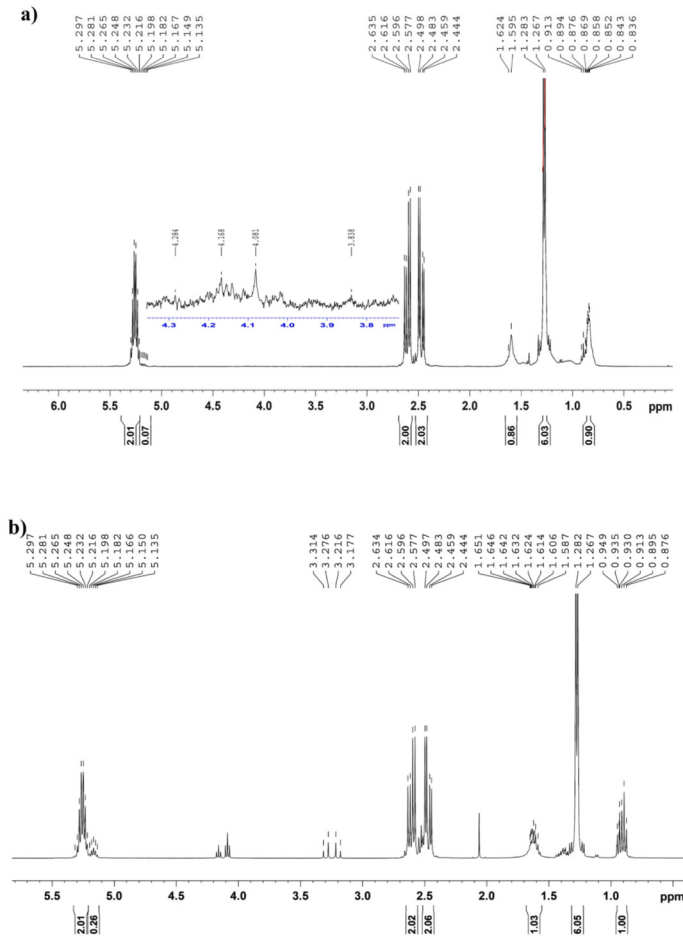


Fig. 8. ¹H NMR spectra of (a) purified PHA from MCCB 281 (b) standard [P(3-HB-co-3-HV)] (12 mol% 3-HV); ¹³C NMR spectra of (c) purified PHA from MCCB 281 (d) standard [P(3-HB-co-3-HV)] (12 mol% 3-HV).

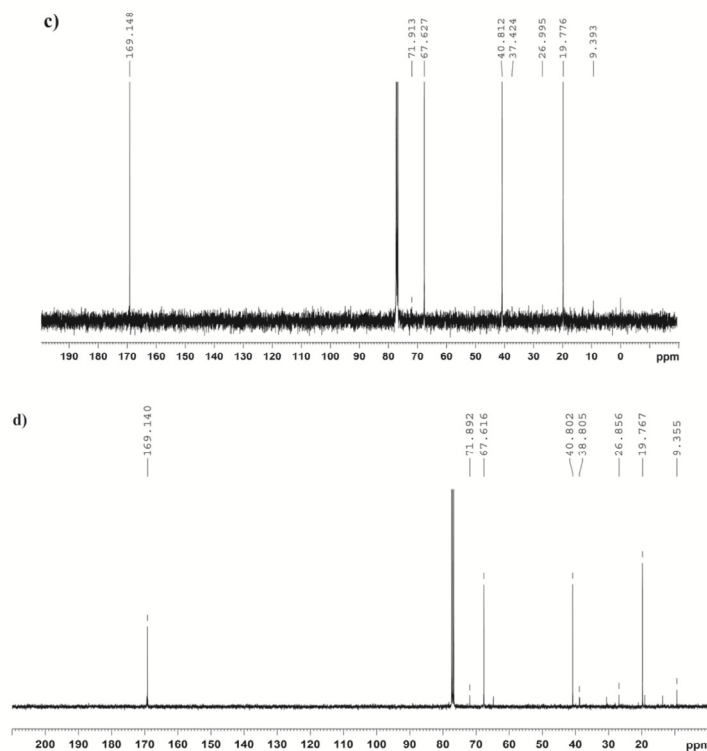


Fig. 8 (continued).

3.6. Validation of the model

The optimized conditions for maximum PHA production in *B. cereus* MCCB 281 were 9.99 g L^{-1} sodium chloride, 4.06% (v/v) glycerol, 8.13% (v/v) inoculum size and 22.86 h incubation time at 30°C . To validate the prediction of the model, experiments were conducted in the optimized conditions and CDW of $3.22 \pm 0.06 \text{ g L}^{-1}$ with a PHA yield of $2.14 \pm 0.08 \text{ g L}^{-1}$ was achieved. There was a good agreement between the predicted and experimental results, thus validating the model. Furthermore, there were 1.5 fold higher PHA yield than un-optimized conditions and PHA yield was increased from 1.44 g L^{-1} to 2.14 g L^{-1} . Also, maximum PHA yield was obtained within shorter incubation time. Similar result was reported in marine *B. megaterium* JK4h strain that showed maximum PHA production within 24 h incubation and 2.61 fold increment in PHA yield following media optimization using CCD [17].

3.7. Fermenter level studies

Batch fermentation for PHA production of MCCB 281 was performed under the optimized culture conditions. A volume of 240 mL of 16 h old culture was inoculated to the production medium (pH 7.0) containing

120 mL of glycerol (4% v/v) as the sole source of carbon and incubated at 30°C . The maximum PHA production of $2.54 \pm 0.07 \text{ g L}^{-1}$, CDW of $3.72 \pm 0.04 \text{ g L}^{-1}$ and PHA content of $68.27 \pm 1.2\%$ (w/w) was observed after 24 h fermentation. Higher biomass yield and PHA production was observed in fermenter studies than shake flask conditions. The PHA yield obtained was comparable with other *Bacillus* spp. such as *B. cereus* SPV [46] and *Bacillus* sp. SV13 [47].

3.8. Characterization of extracted PHA

3.8.1. FTIR

FTIR spectrum of purified PHA showed distinct bands at 1090, 1224 and 1724 cm^{-1} that represented asymmetric stretching of saturated ester linkage (C—O—C) group and carbonyl (C=O) group respectively (Fig. 6). The bands at 1374 and 1451 cm^{-1} corresponded to the C—H bending of symmetric methyl ($-\text{CH}_3$) group. Other strong absorption bands at 2873, 2922, 2969 and 3434 cm^{-1} represented C—H stretching of symmetric methyl ($-\text{CH}_3$), asymmetric methylene ($-\text{CH}_2$), asymmetric methyl ($-\text{CH}_3$) group and hydroxyl ($-\text{OH}$) groups respectively [48]. This pattern was similar to commercial [P (3-HB-co-3-HV)] (12 mol% 3-HV) (Sigma, USA).

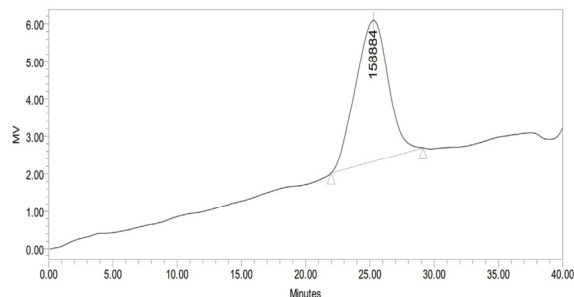


Fig. 9. Gel permeation chromatogram of purified polymer produced by *B. cereus* MCCB 281.

3.8.2. XRD

The physical nature of the purified polymer was deduced by X-ray diffraction (XRD). The characteristic peaks for PHA co-polymer were at $2\theta = 13.5^\circ$, 16.9° , 22.3° , 25.5° and 30.2° corresponding to (020), (110), (111), (121) and (002) reflections respectively (Fig. 7). The polymer showed strong crystalline peaks at $2\theta = 13.5^\circ$ and 16.9° that determine the crystallinity of the polymer [49]. The higher intensities of these peaks indicate higher order of crystallinity of the PHA. The crystallinity of the polymer was calculated to be 42%.

3.8.3. GC-MS

The structure of co-polymer was determined by GC-MS based on the peak areas of ions. In the mass spectrum of methyl 3-hydroxybutyrate, the peak at $43\ m/z$ represented the hydroxyl end of the molecule which occurred due to the cleavage of the bond between C_3 and C_4 (data not shown). The peak at $74\ m/z$ represented the carbonyl end of the molecule which originated due to the cleavage of bond between C_3 and C_4 following McLafferty rearrangement. In the mass spectrum of methyl 3-hydroxyvalerate, the peak at $59\ m/z$ represented the hydroxyl end of the molecule which occurred due to the cleavage at bonds between C_3 and C_4 . The peak at $74\ m/z$ represented the carbonyl end of the molecule due to McLafferty rearrangement. The peak at $103\ m/z$ was caused by α -cleavage between C_3 and C_4 [50]. The result obtained confirmed the presence of methyl esters of hydroxybutyrate (HB) and valerate (HV) units.

3.8.4. NMR

In the 1H NMR spectrum, the characteristic peaks at 0.89 and 1.26 ppm were assigned to the resonance absorption of methyl ($-CH_3$) group from hydroxyvalerate (HB) and hydroxybutyrate (HV) units respectively. The peaks at 1.62, 2.44 and 2.57 ppm represented the methylene ($-CH_2$) group of HV and methylene ($-CH_2$) group of (HV and HB units) respectively. The signals at 5.25 and 5.29 ppm corresponded to methine ($-CH$) group of HB and HV units respectively (Fig. 8). The signals obtained in the spectrum correlated with the previous results [22, 50]. Integration of the area under the peaks at 0.89 and 1.26 ppm in the spectrum confirmed that the polymer was poly(3-hydroxybutyrate-co-3-hydroxyvalerate) [P (3-HB-co-3-HV)] with 13 mol% 3-HV content using the following equation [51].

$$HV\ mol\% = \frac{[Area\ CH_3\ (HV)]}{[Area\ CH_3\ (HV) + Area\ CH_3\ (HB)]} \times 100/3$$

Expansion of the 1H NMR spectral region between 3.0 and 4.5 ppm revealed the presence of additional resonances corresponding to terminal glycerol groups. The region with three resonances at 4.16, 3.80, and 4.28 ppm showed the terminal esterification of glycerol to PHA through the primary hydroxyls (the C_1 or C_3 positions of glycerol). The

resonance at 4.08 ppm corresponded to glycerol end-capping of PHA through the secondary hydroxyl group. The glycerol thus acts as a chain transfer agent resulting in the termination of polymerization, which led to low molecular weight PHA [52].

In the ^{13}C NMR spectrum, the characteristic peaks at 9.3 and 19.7 ppm represents methyl ($-CH_3$) group of HV and HB units respectively. Peaks at 37.4 and 40.8 ppm represents methylene ($-CH_2$) group of HV and HB units and peak at 26.9 ppm corresponded to methylene ($-CH_2$) group of HV unit of PHA co-polymer. Other specific peaks at 67.6 and 71.9 represents methine ($-CH$) group of HB and HV units respectively. The strong signal at 169.1 ppm indicated carbonyl ($-C=O$) group of both HV and HB units [53].

3.8.5. GPC

The molecular mass of PHA co-polymer produced from *B. cereus* MCCB 281 was detected by GPC analysis. The weight average molecular weight (M_w) was 2.56×10^5 Da and number average molecular weight (M_n) was 1.05×10^5 Da with a polydispersity index (PDI) (M_w/M_n) of 2.44 (Fig. 9). The molecular weight was low when compared to *B. thuringiensis* EGU45 utilizing crude glycerol for PHA production [13], but higher than that reported in other *Bacillus* sp. [22, 54]. The low molecular weight of the polymer was due to the glycerol end-capping of PHA as substantiated by the NMR studies.

3.9. PHA nanoparticle synthesis and characterization

PHA nanoparticles were synthesized using oil-in-water emulsion technique. To determine the average particle size and distribution, lyophilized PHA nanoparticles were first suspended in deionized water

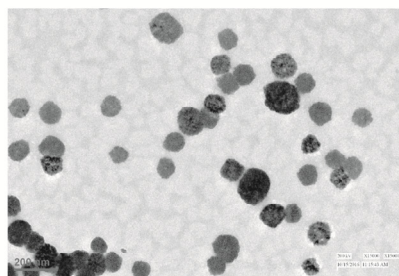


Fig. 10. Transmission electron micrograph of PHA nanoparticles.

and subjected to sonication for 20–30 s before analysis. The average mean particle size of the nanoparticles determined by dynamic light scattering was found to be 179 ± 12.1 nm. The surface charge in terms of zeta potential of PHA nanoparticles was -60.9 mV. The nanoparticles showed a smaller size and good zeta potential which indicated high stability in suspension as justified from previous studies [22, 55]. Size and spherical morphology of synthesized PHA nanoparticles were further confirmed by TEM imaging (Fig. 10).

3.10. Biocompatibility of PHA nanoparticles

Biocompatibility of PHA nanoparticles evaluated by MTT assay in L929 fibroblast cell line demonstrated that no cytotoxicity was observed after incubation with nanoparticles up to a concentration of 1 mg mL^{-1} . The previous studies have also exhibited similar results showing biocompatibility of PHA nanoparticles for effective controlled and targeted drug delivery applications [33, 55]. In addition, the degradation product of PHA, 3-hydroxybutyrate is one of the ketone body present in human blood and tissue which serve as oxidative fuel and lipogenic precursor [56].

4. Conclusion

This study demonstrated the synthesis of biopolymer PHA from a moderate halophile isolate *Bacillus cereus* MCCB 281 utilizing glycerol as sole carbon source. The significant variables that influenced PHA production were glycerol, inoculum size and incubation period. PHA co-polymer with 13 mol% 3-hydroxyvalerate content was produced in presence of glycerol without the addition of precursors. The addition of propionic acid as precursor during fermentation increased valerate content up to 30 mol%. Cell dry weight of 3.72 g L^{-1} and PHA yield of 2.54 g L^{-1} was achieved within 24 h incubation time in the optimized culture conditions in fermenter studies. PHA nanoparticles with particle size 179 nm were synthesized using oil-in-water emulsion method and biocompatibility studies were performed using L929 mouse fibroblast cell line. The results illustrated in this study opens up the potential of utilizing *B. cereus* MCCB 281 for PHA co-polymer synthesis using simple carbon sources for medical applications including tissue engineering and drug delivery.

Acknowledgements

The authors are grateful to Centre for Marine Living Resources and Ecology, Ministry of Earth Sciences, Government of India for the research grant (MoES/CMLRE 10-MLR-TD/09/2012) with which the work was carried out.

Conflict of interest

No conflict of interest declared.

Appendix A. Supplementary data

Supplementary data to this article can be found online at <https://doi.org/10.1016/j.ijbiomac.2018.07.044>.

References

- [1] A.J. Anderson, E.A. Dawes, Occurrence, metabolism, metabolic role, and industrial uses of bacterial polyhydroxyalkanoates, *Microbiol. Rev.* 54 (1990) 450–472. <http://www.pubmedcentral.nih.gov/articlerender.fcgi?artid=372789>.
- [2] A. Steinbüchel, Diversity of bacterial polyhydroxyalkanoic acids, *FEMS Microbiol. Lett.* 128 (1995) 219–228. [https://doi.org/10.1016/0378-1097\(95\)00125-0](https://doi.org/10.1016/0378-1097(95)00125-0).
- [3] A. Anjum, M. Zuber, K.M. Zia, A. Noreen, M.N. Anjum, S. Tabsum, Microbial production of polyhydroxyalkanoates (PHAs) and its copolymers: a review of recent advancements, *Int. J. Biol. Macromol.* 89 (2016) 161–174. <https://doi.org/10.1016/j.ijbiomac.2016.04.069>.
- [4] S. Nakamura, Y. Doi, M. Scandola, Microbial synthesis and characterization of poly(3-hydroxybutyrate-co-4-hydroxybutyrate), *Macromolecules* 25 (1992) 4237–4241. <https://doi.org/10.1021/ma00043a001>.
- [5] E. Akaronye, T. Keshavarz, I. Roy, Production of polyhydroxyalkanoates: the future green materials of choice, *J. Chem. Technol. Biotechnol.* 85 (2010) 732–743. <https://doi.org/10.1002/jctb.2392>.
- [6] J. Choi, S.Y. Lee, Process analysis and economic evaluation for poly(3-hydroxybutyrate) production by fermentation, *Bioprocess Eng.* 17 (1997) 335. <https://doi.org/10.1007/s004490050394>.
- [7] R. Sindhu, N. Silviya, P. Binod, A. Pandey, Pentose-rich hydrolysate from acid pretreated rice straw as a carbon source for the production of poly-3-hydroxybutyrate, *Biochem. Eng. J.* 78 (2013) 67–72. <https://doi.org/10.1016/j.bej.2012.12.015>.
- [8] S.K.S. Patel, P. Kumar, M. Singh, J.-K. Lee, V.C. Kalia, Integrative approach to produce hydrogen and polyhydroxybutyrate from biowaste using defined bacterial cultures, *Bioresour. Technol.* 176 (2015) 136–141. <https://doi.org/10.1016/j.biortech.2014.11.029>.
- [9] S.K.S. Patel, J.-K. Lee, V.C. Kalia, Integrative approach for producing hydrogen and polyhydroxyalkanoate from mixed wastes of biological origin, *Indian J. Microbiol.* 56 (2016) 293–300. <https://doi.org/10.1007/s12088-016-0595-3>.
- [10] S.R. Pandian, V. Deshpak, K. Kalishwarajah, N. Rameshkumar, M. Jeyaraj, S. Gurunathan, Optimization and fed-batch production of PHB utilizing dairy waste and sea water as nutrient sources by *Bacillus megaterium* SRK-3, *Bioresour. Technol.* 101 (2010) 705–711. <https://doi.org/10.1016/j.biortech.2009.08.040>.
- [11] Z.T. Dobroth, S. Hu, E.R. Coats, A.G. McDonald, Polyhydroxybutyrate synthesis on biodiesel wastewater using mixed microbial consortia, *Bioresour. Technol.* 102 (2011) 3352–3359. <https://doi.org/10.1016/j.biortech.2010.11.053>.
- [12] J.M. Naranjo, J.A. Posada, J.C. Higuera, C.A. Cardona, Valorization of glycerol through the production of biopolymers: the PHB case using *Bacillus megaterium*, *Bioresour. Technol.* 133 (2013) 38–44. <https://doi.org/10.1016/j.biortech.2013.01.129>.
- [13] P. Kumar, S. Ray, S.K.S. Patel, J.-K. Lee, V.C. Kalia, Bioconversion of crude glycerol to polyhydroxyalkanoate by *Bacillus thuringiensis* under non-limiting nitrogen conditions, *Int. J. Biol. Macromol.* 78 (2015) 9–16. <https://doi.org/10.1016/j.ijbiomac.2015.03.046>.
- [14] H.W. Tan, A.R. Abdul Aziz, M.K. Aroua, Glycerol production and its applications as a raw material: a review, *Renew. Sust. Energ. Rev.* 27 (2013) 118–127. <https://doi.org/10.1016/j.rser.2013.06.035>.
- [15] F. Yang, M.A. Hanna, R. Sun, Value-added uses for crude glycerol—a byproduct of biodiesel production, *Biotechnol. Biofuels* 5 (2012) 13. <https://doi.org/10.1186/1754-6834-5-13>.
- [16] C. Hermann-Krauss, M. Koller, A. Muhr, H. Fasl, F. Stelzer, G. Brauneegg, Archaeal production of polyhydroxyalkanoate (PHA) co- and terpolyesters from biodiesel industry-derived by-products, *Archaea* 2013 (2013) 241–248. <https://doi.org/10.1155/2013/129268>.
- [17] J.H. Dhangdhariya, S. Dubey, H.B. Trivedi, I. Pancha, J.K. Bhatt, B.P. Dave, S. Mishra, Polyhydroxyalkanoate from marine *Bacillus megaterium* using CSMCRI's dry sea mix as a novel growth medium, *Int. J. Biol. Macromol.* 76 (2015) 254–261. <https://doi.org/10.1016/j.ijbiomac.2015.02.009>.
- [18] P. Sharma, B.K. Bajaj, Production and characterization of poly-3-hydroxybutyrate from *Bacillus cereus* PS 10, *Int. J. Biol. Macromol.* 81 (2015) 241–248. <https://doi.org/10.1016/j.ijbiomac.2015.08.008>.
- [19] S.P. Mohandas, L. Balan, N. Lekshmi, S.S. Cubelio, R. Philip, I.S. Bright Singh, Production and characterization of polyhydroxybutyrate from *Vibrio harveyi* MCCB 284 utilizing glycerol as carbon source, *J. Appl. Microbiol.* (2016) <https://doi.org/10.1111/jam.13359>.
- [20] M. Koller, I. Casser, F. Schmid, G. Berg, Linking ecology with economy: insights into polyhydroxyalkanoate-producing microorganisms, *Eng. Life Sci.* 11 (2011) 222–237. <https://doi.org/10.1002/elsc.201000190>.
- [21] M. Higuchi-Takeuchi, K. Morisaki, K. Toyooka, K. Numata, Synthesis of high-molecular-weight polyhydroxyalkanoates by marine photosynthetic purple bacteria, *PLoS One* 11 (2016), e0160981. <https://doi.org/10.1371/journal.pone.0160981>.
- [22] D. Moorkoth, K.M. Nampoothiri, Production and characterization of poly(3-hydroxybutyrate-co-3-hydroxyvalerate) (PHBV) by a novel halotolerant mangrove isolate, *Bioresour. Technol.* 201 (2016) 253–260. <https://doi.org/10.1016/j.biortech.2015.11.046>.
- [23] D. Tan, Y.-S. Xue, G. Aibaidula, G.-Q. Chen, Unsterile and continuous production of polyhydroxybutyrate by *Halomonas* TD01, *Bioresour. Technol.* 102 (2011) 8130–8136. <https://doi.org/10.1016/j.biortech.2011.05.068>.
- [24] P. Spiekermann, B.H. Rehm, R. Kalscheuer, D. Baumeister, A. Steinbüchel, A sensitive, viable-colony staining method using Nile red for direct screening of bacteria that accumulate polyhydroxyalkanoic acids and other lipid storage compounds, *Arch. Microbiol.* 171 (1999) 73–80. <http://www.ncbi.nlm.nih.gov/pubmed/9914303>.
- [25] A.G. Ostle, J.G. Holt, Nile blue as a fluorescent stain for poly-3-hydroxybutyrate, *Appl. Environ. Microbiol.* 44 (1982) 238–241. <http://www.pubmedcentral.nih.gov/articlerender.fcgi?artid=241995>.
- [26] H.-R. Cheng, N. Jiang, Extremely rapid extraction of DNA from bacteria and yeasts, *Biotechnol. Lett.* 28 (2006) 55–59. <https://doi.org/10.1007/s10529-005-4688-z>.
- [27] N. Saitou, M. Nei, The neighbor-joining method: a new method for reconstructing phylogenetic trees, *Mol. Biol. Evol.* 4 (1987) 406–425. <http://www.ncbi.nlm.nih.gov/pubmed/3447015>.
- [28] J. Felsenstein, Confidence limits on phylogenies: an approach using the bootstrap, *Evolution* 39 (1985) 783. (N. Y.) <https://doi.org/10.2307/2408578>.
- [29] K. Tamura, G. Stecher, D. Peterson, A. Filipski, S. Kumar, MEGA6: molecular evolutionary genetics analysis version 6.0, *Mol. Biol. Evol.* 30 (2013) 2725–2729. <https://doi.org/10.1093/molbev/mst197>.

- [30] J.H. Law, R.A. Slepceky, Assay of poly-beta-hydroxybutyric acid, *J. Bacteriol.* 82 (1961) 33–36. <http://www.pubmedcentral.nih.gov/articlerender.fcgi?artid=279110>.
- [31] S.K. Iahin, Y.K. Chang, S.Y. Lee, Recovery and characterization of poly(3-hydroxybutyric acid) synthesized in *Alcaligenes eutrophus* and recombinant *Escherichia coli*, *Appl. Environ. Microbiol.* 61 (1995) 34–39. <http://www.pubmedcentral.nih.gov/articlerender.fcgi?artid=167258>.
- [32] G. Brauneberg, B. Sonnleitner, R.M. Lafferty, A rapid gas chromatographic method for the determination of poly-β-hydroxybutyric acid in microbial biomass, *Eur. J. Appl. Microbiol. Biotechnol.* 6 (1978) 29–37. <https://doi.org/10.1007/BF00500854>.
- [33] G. Eker, A.M. Kuzmina, A.V. Goreva, E.I. Shshatskaya, N. Hasirci, V. Hasirci, In vitro and transdermal penetration of PHBV micro/nanoparticles, *J. Mater. Sci. Mater. Med.* 25 (2014) 1471–1481. <https://doi.org/10.1007/s10856-014-5169-5>.
- [34] S.P. Valappil, A.R. Boccacini, C. Bucke, I. Roy, Polyhydroxyalkanoates in gram-positive bacteria: insights from the genera *Bacillus* and *Streptomyces*, *Antonie Van Leeuwenhoek* 91 (2007) 1–17. <https://doi.org/10.1007/s10482-006-9095-5>.
- [35] M. Singh, S.K. Patel, V.C. Kalia, *Bacillus subtilis* as potential producer for polyhydroxyalkanoates, *Microb. Cell Factories* 8 (2009) 38. <https://doi.org/10.1186/1475-2859-8-38>.
- [36] F. Masood, F. Hasan, S. Ahmed, A. Hameed, Biosynthesis and characterization of poly(3-hydroxybutyrate-co-3-hydroxyvalerate) from *Bacillus cereus* FA11 isolated from TNT-contaminated soil, *Ann. Microbiol.* 62 (2011) 1377–1384. <https://doi.org/10.1007/s13213-011-0386-3>.
- [37] S.K.S. Patel, M. Singh, V.C. Kalia, Hydrogen and polyhydroxybutyrate producing abilities of *Bacillus* spp. from glucose in two stage system, *Indian J. Microbiol.* 51 (2011) 418–423. <https://doi.org/10.1007/s12088-011-0236-9>.
- [38] S. Porwal, T. Kumar, S. Lal, A. Rani, S. Kumar, S. Cheema, H.J. Purohit, R. Sharma, S.K. Singh Patel, V.C. Kalia, Hydrogen and polyhydroxybutyrate producing abilities of microbes from diverse habitats by dark fermentative process, *Bioresour. Technol.* 99 (2008) 5444–5451. <https://doi.org/10.1016/j.biortech.2007.11.011>.
- [39] S.K.S. Patel, M. Singh, P. Kumar, H.J. Purohit, V.C. Kalia, Exploitation of defined bacterial cultures for production of hydrogen and polyhydroxybutyrate from pea-shells, *Biomass Bioenergy* 36 (2012) 218–225. <https://doi.org/10.1016/j.biombioe.2011.10.027>.
- [40] M. Singh, P. Kumar, S.K.S. Patel, V.C. Kalia, Production of polyhydroxyalkanoate copolymer by *Bacillus thuringiensis*, *Indian J. Microbiol.* 53 (2013) 77–83. <https://doi.org/10.1007/s12088-012-0294-7>.
- [41] S. Ray, R. Sharma, V.C. Kalia, Co-utilization of crude glycerol and biowastes for producing polyhydroxyalkanoates, *Indian J. Microbiol.* 58 (2018) 33–38. <https://doi.org/10.1007/s12088-017-0702-0>.
- [42] S.K. Deepthi, P. Binod, R. Sindhu, A. Pandey, Media engineering for production of poly-β-hydroxybutyrate by *Bacillus firmus* NII 0830, *J. Sci. Ind. Res.* 70 (2011) 968–975.
- [43] G.C. Du, J. Chen, J. Yu, S. Lun, Feeding strategy of propionic acid for production of poly(3-hydroxybutyrate-co-3-hydroxyvalerate) with *Ralstonia eutropha*, *Biochem. Eng. J.* 8 (2001) 103–110. [https://doi.org/10.1016/S1369-703X\(01\)00091-Z](https://doi.org/10.1016/S1369-703X(01)00091-Z).
- [44] S. Ray, V. Prajapati, K. Patel, U. Trivedi, Optimization and characterization of PHA from isolate *Pannonibacter phragmitetus* ERC8 using glycerol waste, *Int. J. Biol. Macromol.* 86 (2016) 741–749. <https://doi.org/10.1016/j.jbiomac.2016.02.002>.
- [45] G. Sathyanarayanan, G. Saibaba, G. Seghal Kiran, J. Selvin, A statistical approach for optimization of polyhydroxybutyrate production by marine *Bacillus subtilis* MSBN17, *Int. J. Biol. Macromol.* 59 (2013) 170–177. <https://doi.org/10.1016/j.jbiomac.2013.04.040>.
- [46] S.P. Valappil, S.K. Misra, A.R. Boccacini, T. Keshavarz, C. Bucke, I. Roy, Large-scale production and efficient recovery of PHB with desirable material properties, from the newly characterised *Bacillus cereus* SPV, *J. Biotechnol.* 132 (2007) 251–258. <https://doi.org/10.1016/j.jbiotec.2007.03.013>.
- [47] W. Suwannasing, T. Imai, P. Kaewkannetra, Cost-effective defined medium for the production of polyhydroxyalkanoates using agricultural raw materials, *Bioresour. Technol.* 194 (2015) 67–74. <https://doi.org/10.1016/j.biortech.2015.06.087>.
- [48] H. Sato, Y. Ando, H. Mitomo, Y. Ozaki, Infrared spectroscopy and X-ray diffraction studies of thermal behavior and lamella structures of poly(3-hydroxybutyrate-co-3-hydroxyvalerate) (PHB-co-HV) with PHB-type crystal structure and PHV-type crystal structure, *Macromolecules* 44 (2011) 2829–2837. <https://doi.org/10.1021/ma102723n>.
- [49] Z. Skrbčić, V. Divjaković, Temperature influence on changes of parameters of the unit cell of biopolymer PHB, *Polymer* 37 (1996) 505–507. [https://doi.org/10.1016/0032-3861\(96\)82922-3](https://doi.org/10.1016/0032-3861(96)82922-3).
- [50] S.V. Reddy, M. Thirumala, S.K. Mahmood, A novel *Bacillus* sp. accumulating poly(3-hydroxybutyrate-co-3-hydroxyvalerate) from a single carbon substrate, *J. Ind. Microbiol. Biotechnol.* 36 (2009) 837–843. <https://doi.org/10.1007/s10295-009-0561-8>.
- [51] S. Bloembergen, D.A. Holden, G.K. Hamer, T.L. Bluhm, R.H. Marchessault, Studies of composition and crystallinity of bacterial poly(β-hydroxybutyrate-co-β-hydroxyvalerate), *Macromolecules* 19 (1986) 2865–2871. <https://doi.org/10.1021/ma00165a034>.
- [52] R.D. Ashby, D.K.Y. Solaiman, T.A. Foglia, Synthesis of short-/medium-chain-length poly(hydroxyalkanoate) blends by mixed culture fermentation of glycerol 1, *Biomacromolecules* 6 (2005) 2106–2112. <https://doi.org/10.1021/bm058005h>.
- [53] Y. Doi, M. Kunioka, Y. Nakamura, K. Soga, Nuclear magnetic resonance studies on poly(β-hydroxybutyrate) and a copolyester of β-hydroxybutyrate and β-hydroxyvalerate isolated from *Alcaligenes eutrophus* H16, *Macromolecules* 19 (1986) 2860–2864. <https://doi.org/10.1021/ma00165a033>.
- [54] P. Plutkun, J.P. Saikia, B.K. Kuniwar, Bio-plastic (P-3HB-co-3HV) from *Bacillus circulans* (MTCC 8167) and its biodegradation, *Colloids Surf. B: Biointerfaces* 92 (2012) 30–34. <https://doi.org/10.1016/j.colsurfb.2011.11.011>.
- [55] F. Masood, P. Chen, T. Yasin, F. Hasan, B. Ahmad, A. Hameed, Synthesis of poly(3-hydroxybutyrate-co-12 mol % 3-hydroxyvalerate) by *Bacillus cereus* FB11: its characterization and application as a drug carrier, *J. Mater. Sci. Mater. Med.* 24 (2013) 1927–1937. <https://doi.org/10.1007/s10856-013-4946-x>.
- [56] S. Cheng, G. Chen, M. Leski, B. Zou, Y. Wang, Q. Wu, The effect of d,l-β-hydroxybutyric acid on cell death and proliferation in 1929 cells, *Biomaterials* 27 (2006) 3758–3765. <https://doi.org/10.1016/j.biomaterials.2006.02.046>.